



University of Bradford eThesis

This thesis is hosted in [Bradford Scholars](#) – The University of Bradford Open Access repository. Visit the repository for full metadata or to contact the repository team



© University of Bradford. This work is licenced for reuse under a [Creative Commons Licence](#).

**LIPID PROFILING OF POLYUNSATURATED FATTY
ACID - TREATED MOUSE BRAIN AND PLASMA**

Investigation into polyunsaturated fatty acid (PUFA)-induced
neuroprotection

ANEST WILLIAMS

PhD

UNIVERSITY OF BRADFORD

2010

Abstract

Pre-treatment with polyunsaturated fatty acids or bioactive lipid mediators has been shown to reduce neuronal injury in rodent models of focal ischaemia, but the molecular mechanisms underlying this neuroprotection are unclear. In this study, we aimed to investigate whether systemic administration of alpha linolenic acid (ALA) leads to changes in the profile of mouse brain phospholipid and bioactive lipid mediators in both mouse brain and plasma within the previously determined neuroprotection time window. Mass spectrometry (MS) and tandem mass spectrometry (MS/MS) allowed us to detect and identify 47 phospholipids in mouse cerebral cortex, including several phospholipid species not previously reported in brain lipidomic studies. These included a phosphatidylethanolamine species with m/z 720 that has been associated with retinal stem cells. No widespread changes in cerebral cortex phospholipid composition were observed following intravenous ALA. Several significant changes in lipid mediators ($P < 0.05$ with two-way ANOVA and post hoc Dunnett's t test) were detected in ALA-treated animals compared to untreated and vehicle-injected animals. Many of the affected lipid mediators are ligands for prostanoid receptors which have been demonstrated to play a role in the development of brain injury following cerebral ischaemia, implying that changes in bioactive lipid mediators or modulation of prostanoid receptors may occur following ALA pre-treatment in mice. This study illustrates the potential of advanced lipidomic analysis as a novel tool for neurochemists.

Key words: mouse, fatty acids, brain, cortex, phospholipid, plasma, tandem mass spectrometry, neuroprotection

Acknowledgements

I would like to thank my supervisors Professor Tihomir Obrenovitch and Professor Anna Nicolaou for their advice and support throughout my time at Bradford. Thanks also to Mr Andrew Healey and to my fellow research students for technical advice and assistance. Many thanks go to friends and family for practical, financial and emotional support, and also to my new employers for their supportiveness during a challenging transition period. Finally, I would like to thank my examiners for their time and effort in reading all of this.

This thesis is dedicated to Marc, in recognition of his patience, support and late night printing services.

Table of Contents

1. Introduction	
1.1. General introduction on lipids and their physiological roles	10
1.2. Fatty acids	10
1.2.1. Structure and nomenclature of fatty acids	10
1.2.2. Biosynthesis of fatty acids	14
1.3. Phospholipids	18
1.3.1. Glycerophospholipids	21
1.3.2. Sphingophospholipids	21
1.4. Cholesterol	21
1.5. Lipid mediators involved in cell signalling	25
1.5.1 The cyclo-oxygenase enzymes and their lipid mediator products	29
1.5.2 The lipo-oxygenase enzymes and their lipid mediator products	32
1.5.3 The cytochrome P450 enzymes and their lipid mediator products	36
1.5.4 Bioactive lipids produced by non-enzymatic (free radical-catalysed) pathways	38
1.6. Polyunsaturated fatty acids and the brain	42
1.6.1. PUFA occurrence and metabolism in the brain	44
1.6.2. PUFA as membrane components	46
1.6.3. PUFA and gene expression	47
1.6.4. PUFA in cell signalling	48
1.6.5. Production of lipid mediators from PUFA	49
1.6.6. Adaptive cytoprotection (Preconditioning and brain tolerance)	50
1.7. Introduction to lipidomics	57
1.7.1. High-performance liquid chromatography	59
1.7.2. Principles of electrospray ionisation	60

1.7.3. Tandem mass spectroscopy (MS/MS)	64
1.7.4. Hybrid analytical techniques	66
1.8. Aims and Objectives	68
2. Materials and Methods	70
2.1. Experimental strategy	70
2.1.1 Use of animals	70
2.1.2. Metabolic inactivation of the brain	72
2.1.3. Tissue storage, processing and analytical issues	85
2.2. Animal treatments	90
2.2.1. Care and welfare of animals	90
2.2.2. Preparation of alpha linoleic acid or vehicle	90
2.2.3. Intravenous injection of alpha linoleic acid or vehicle	91
2.2.4. Sample collection	92
2.3. Lipid extraction	95
2.3.1. Liquid/liquid extraction of phospholipids	95
2.3.2. Solid phase extraction (SPE) of lipid mediators	96
2.4. Lipidomic Analysis	97
2.4.1. ESI-MS/MS of phospholipids	97
2.4.2. ESI-LC-MS/MS analysis of prostaglandins	102
2.4.3. LC-MS/MS analysis of hydroxy fatty acids and other lipid mediators	106
2.5. Data collection and presentation	109
3. Lipidomic analysis of cerebral cortex phospholipids in the mouse	110
3.1. Profiling of phospholipids in mouse cerebral cortex: general scans	110
3.2. Profiling of phospholipids in mouse cerebral cortex: MS/MS analysis	113
3.3. Identification of phospholipid species in mouse cerebral cortex	119
3.3.1. Phosphatidylcholine and sphingomyelin species	119
3.3.2. Phosphatidylethanolamine species	122

3.3.3. Phosphatidylserine species	126
3.3.4. Phosphatidylinositol species	129
3.4. Fragmentation studies of phospholipid species in mouse cerebral cortex	132
3.5. Investigation of changes in cerebral cortex phospholipids produced by ALA 3, 24, 72 and 168 hours after its administration	139
4. Analysis of lipid mediators in mouse cerebral cortex and plasma	153
4.1. Lipid mediator profiling in mouse cerebral cortex and plasma: prostanoid assay	153
4.1.1. Preparation of calibration curves	153
4.1.2. Lipid mediator profiling in naïve mice	163
4.1.3. Effect of ALA treatment	166
4.2. Lipid mediator profiling in mouse cerebral cortex and plasma: hydroxylated fatty acids assay	173
4.2.1. Preparation of calibration curves	173
5. Discussion	180
5.1. Methodology considerations	180
5.1.1. Importance of tissue sampling, storage and processing methods for the validity of lipidomic data	180
5.1.2. Evidence of quality and validity for the lipidomic data obtained in this study	185
5.2. Discussion of analytical findings: phospholipid study	197
5.2.1. Phospholipid profile of naïve mouse cerebral cortex	197
5.2.2. Phospholipid profile of naïve mouse cerebral cortex - potential biological significance	204
5.2.3. Identification of novel phospholipid species in naïve mouse cerebral cortex	208
5.2.4. Effects of alpha linolenic acid treatment on mouse cerebral cortex phospholipid profile	214

5.3. Interpretation of analytical findings: lipid mediators study	223
5.3.1. Prostanoid profiling of naïve mouse cerebral cortex and plasma – potential biological significance	223
5.3.2. Effects of alpha linolenic acid treatment on prostanoid profile of mouse cerebral cortex	227
5.3.3. Effects of alpha linolenic acid treatment on prostanoid profile of mouse plasma	229
5.4. Recommendations for future work	235
5.5 Conclusions	239
Appendix 1.1 Phospholipid analysis in mouse cerebral cortex using MS	266
Appendix 1.2 Phospholipid analysis in mouse cerebral cortex using MS/MS	282
Appendix 2 Profiling of lipid mediator species in mouse cerebral cortex and plasma using LC-MS/MS	320

Table of Figures

Figure 1.1	Shorthand nomenclature of polyunsaturated fatty acids
Figure 1.2	The essential fatty acids
Figure 1.3	Biosynthesis of polyunsaturated fatty acids
Figure 1.4	Structure of glycerol and sphingosine
Figure 1.5	Glycerophospholipid structure
Figure 1.6	Sphingophospholipid structure
Figure 1.7	Cholesterol
Figure 1.8	Cholesterol is a key component of lipid rafts
Figure 1.9	Production of lipid mediators from essential fatty acids
Figure 1.10	Prostaglandin products of dihomo γ – linolenic acid, arachidonic acid and eicosapentaenoic acid
Figure 1.11	Biosynthesis of leukotrienes from polyunsaturated fatty acids
Figure 1.12	Hydroxylation of polyunsaturated fatty acids by lipo-oxygenase enzymes
Figure 1.13	Production of lipoxins from arachidonic acid
Figure 1.14	P450 metabolism of arachidonic acid occurs by three reaction mechanisms
Figure 1.15	A representative isoprostane
Figure 1.16	A representative isofuran
Figure 1.17	Multiple roles of polyunsaturated fatty acids in physiological functions
Figure 1.18	Preconditioning is a time-dependent phenomenon
Figure 1.19	Neuroprotective agents may have direct or prophylactic effects on brain tissue
Figure 1.20	ALA treatment after MCAO resulted in reduced infarct size in mice
Figure 1.21	Schematic diagram of HPLC
Figure 1.22	Schematic of the electrospray ionisation (ESI) interface
Figure 1.23	Tandem mass spectrometry (MS/MS) ion scanning modes
Figure 2.1	Brain metabolic processes can be inactivated by cold, heat or chemical inactivators
Figure 2.2	Selection of brain metabolic inactivation method was carried out by a process of elimination
Figure 2.3	Collection, processing and phospholipid profiling of mouse cerebral cortex
Figure 2.4	Collection, processing and lipid mediator profiling of mouse cerebral cortex

- Figure 2.5 Collection, processing and lipid mediator profiling of mouse plasma
- Figure 2.6 Brain and blood sample collection and preparation for lipid extractions
- Figure 2.7 Phospholipid data analysis between control and different treatment groups at the same timepoints were carried out using one-way ANOVA and post-hoc Dunnett's correction
- Figure 2.8 Lipid mediator data analysis between different treatment and timepoint groups were carried out using one-way ANOVA and post-hoc Dunnett's correction
- Figure 3.1 General ESI-MS scan of a representative sample of mouse cerebral cortex in the ES + mode
- Figure 3.2 General ESI-MS scan of a representative sample of mouse cerebral cortex in the ES – mode
- Figure 3.3 Representative ESI-MS/MS spectrum showing phosphatidylcholine and sphingomyelin species in mouse cerebral cortex tissue
- Figure 3.4 Representative ESI-MS.MS spectrum showing phosphatidylethanolamine species in mouse cerebral cortex tissue
- Figure 3.5 Representative ESI-MS/MS spectrum showing phosphatidylserine species in mouse cerebral cortex tissue
- Figure 3.6 Representative ESI-MS/MS spectrum showing phosphatidylinositol species in mouse cerebral cortex tissue
- Figures 3.7a-b Phosphatidylcholine and sphingomyelin species identified in cerebral cortex samples of naive mice
- Figures 3.8a-b Phosphatidylethanolamine species identified in cerebral cortex samples of naive mice
- Figures 3.9a-b Phosphatidylserine species identified in cerebral cortex samples naive mice
- Figures 3.10a-b Phosphatidylserine species identified in cerebral cortex samples naive mice
- Figure 3.11 MS/MS scan of phosphatidylserine species with m/z 838 identifies its fatty acyl chains as 18:0 and 22:4.
- Figures 3.12a-d Effect of ALA on phospholipid species in mouse cerebral cortex at 3h post- injection
- Figures 3.13a-d Effect of ALA on phospholipid species in mouse cerebral cortex at 24h post- injection

Figures 3.14a-d	Effect of ALA on phospholipid species in mouse cerebral cortex at 72h post- injection
Figures 3.15a-d	Effect of ALA on phospholipid species in mouse cerebral cortex at 168h post- injection
Figure 3.16	Effect of time on phosphatidylcholine and sphingomyelin species in ALA- treated mouse cortex
Figure 3.17	Effect of time on phosphatidylethanolamine species in ALA- treated mouse cortex
Figure 3.18	Effect of time on phosphatidylinositol species in ALA-treated mouse
Figure 3.19	Effect of time on phosphatidylserine species in ALA- treated mouse cortex
Figure 4.1	Representative chromatograms of mixed prostaglandin standards
Figure 4.2	Representative chromatograms of untreated mouse cerebral cortex showing PGE ₂ and PGD ₂
Figure 4.3	Representative chromatograms of untreated mouse plasma showing TXB ₂
Figure 4.4	Effects of ALA on TXB ₂ abundance in mouse cerebral cortex at 3, 24 and 72h after treatment
Figure 4.5	Representative chromatograms of HETE standards
Figures 4.6a-b	Representative chromatograms of untreated mouse cerebral cortex and plasma showing LTB ₄
Figure 5.1	Representative good-quality and poor quality spectra
Figure 5.2	Physiological functions of different phospholipid classes
Figure 5.3	Biosynthesis and metabolism of eicosadienoic acids
Figure 5.4	Members of the prostanoid receptor family have a specific distribution in the body

1. Introduction

1.1. General introduction on lipids and their physiological roles

There is no universal definition of a lipid, but broadly speaking, lipids constitute a diverse group of compounds traditionally characterized by their physicochemical properties, most notably their high solubility in organic compounds such as chloroform and hexane, and their low solubility in water. There is a great variety in the structure and physicochemical properties of lipids. They can be divided into simple lipids, which yield two or fewer products when hydrolysed, and complex lipids that give rise to three or more components when hydrolyzed. Simple lipids include fatty acids and cholesterol. Examples of complex lipids are mono-, di- and tri-glycerides, ceramides, waxes, phospholipids and glycolipids.

1.2. Fatty acids

1.2.1. Structure and nomenclature of fatty acids

The simplest lipids are fatty acids, which are long chain (i.e. acyl chain) monocarboxylic acids. The acyl chain may contain no double bonds in the case of saturated fatty acids (SFA), one double bond if they are

monounsaturated fatty acids (MUFA), or more than one double bond if they are polyunsaturated fatty acids (PUFA). The nomenclature of fatty acids is dependent on the length of the carbon chain and the position and conformation of the C=C double bonds. Systematic prefixes for fatty acids depend on the acyl chain length, as described in Table 1.1.

Table 1.1 Systematic chain length nomenclature of fatty acids

Carbon chain length	Prefix
12	Dodeca -
14	Tetradeca -
16	Hexadeca-
18	Octadeca -
20	Eicosa -
22	Docosa -
24	Tetracosa -

The variety in the number, positions and conformations of double bonds mean that fatty acids exist in many isomeric forms. For example, positional isomers of fatty acids have different locations of double bonds and epimeric fatty acid isomers have differing conformations of groups. A C=C double bond is denoted by Δ , followed by the carbon position of the double bond e.g. Δx indicates that a double bond is located on the x^{th} C atom from the carboxyl group. The rigid nature of the C=C double bond gives rise to *cis* and *trans* isomers of some fatty acids (also known as Z and E isomers, respectively) where the orientation of groups in space differ between two isomers. *Cis* isomers are those where both ends of methyl chain are located on the same

side of the double bond and *trans* isomers have the ends of the methyl chain on opposing sides of the double bond.

The position of the double bond from the methyl carbon end can be denoted by describing a fatty acid as an n-x (or ω-x) fatty acid, where the double bond is on the xth carbon atom from the methyl carbon end of the chain. Hence, n-3 fatty acids have a double bond located at the 3rd carbon atom from the methyl end, n-6 fatty acids have a double bond located at the 6th carbon atom from the methyl end and n-9 fatty acids have a double bond located at the 9th carbon atom from the methyl end. PUFA can also be described using a shorthand form, as in Figure 1.1.

Figure 1.1 Shorthand nomenclature of PUFA

Systematic name **all- *cis* – 9,12,15-octadienoic acid**

Number before colon =
number of C atoms in acyl
chain

Number after colon = number of
C=C double bonds in acyl chain

18 : 3 n-3

Position of double bond
nearest to omega carbon

Shorthand nomenclature of PUFA describes the number of C atoms in its structure, the number of C=C double bonds and the position of the C=C bond furthest away from the COOH group

In addition to systematic nomenclature, many fatty acids have trivial names, which are commonly used in literature. Table 1.2 shows the systematic, trivial and shorthand names of common saturated and unsaturated fatty acids.

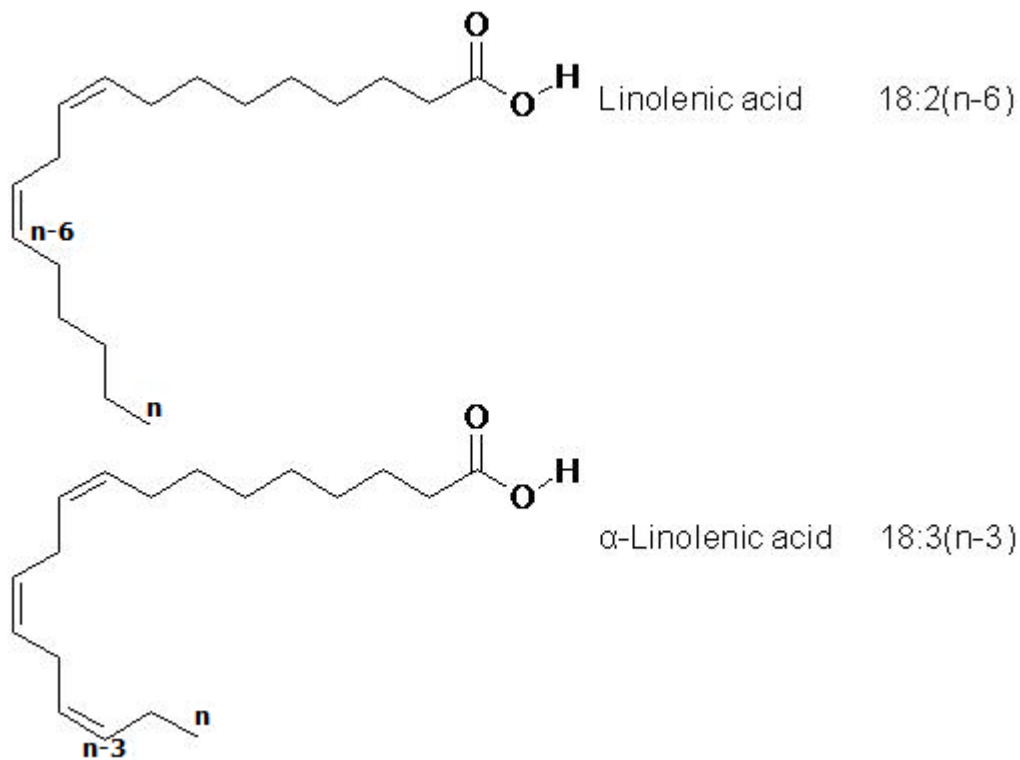
Table 1.2 Nomenclature of long chain fatty acids (adapted from www.cyberlipid.com)

Systematic name	Trivial name	Shorthand
Saturated fatty acids		
Dodecanoic	Lauric	12:0
Tetradecanoic	Myristic	14:0
Hexadecanoic	Palmitic	16:0
Octadecanoic	Stearic	18:0
Omega – 9 fatty acids		
<i>cis</i> 9-octadecenoic	Oleic	18:1(n-9)
All <i>cis</i> 5,8,11-eicosatrienoic	Mead	20:3(n-9)
Omega – 6 fatty acids		
All <i>cis</i> 9,12-octadecadienoic	Linoleic	18:2(n-6)
All <i>cis</i> 6,9,12-octadecatrienoic	γ -Linolenic	18:3(n-6)
All <i>cis</i> 8,11,14-eicosatrienoic	Dihomo- γ -linolenic	20:3(n-6)
All <i>cis</i> 5,8,11,14-eicosatetraenoic	Arachidonic	20:4(n-6)
All <i>cis</i> 7,10,13,16-docosatetraenoic	-	22:4(n-6)
All <i>cis</i> 4,7,10,13,16-docosapentaenoic	-	22:5(n-6)
Omega – 3 fatty acids		
All <i>cis</i> 9,12,15-octadecatrienoic	α -Linolenic	18:3(n-3)
All <i>cis</i> 6,9,12,15-octadecatetraenoic	Stearidonic	18:4(n-3)
All <i>cis</i> 8,11,14,17-eicosatetraenoic	-	20:4(n-3)
All <i>cis</i> 5,8,11,14,17-eicosapentaenoic	-	20:5(n-3)
All <i>cis</i> 7,10,13,16,19-docosapentaenoic	-	22:5(n-3)
All <i>cis</i> 4,7,10,13,16,19-docosahexaenoic	-	22:6(n-3)

1.2.2. Biosynthesis of fatty acids

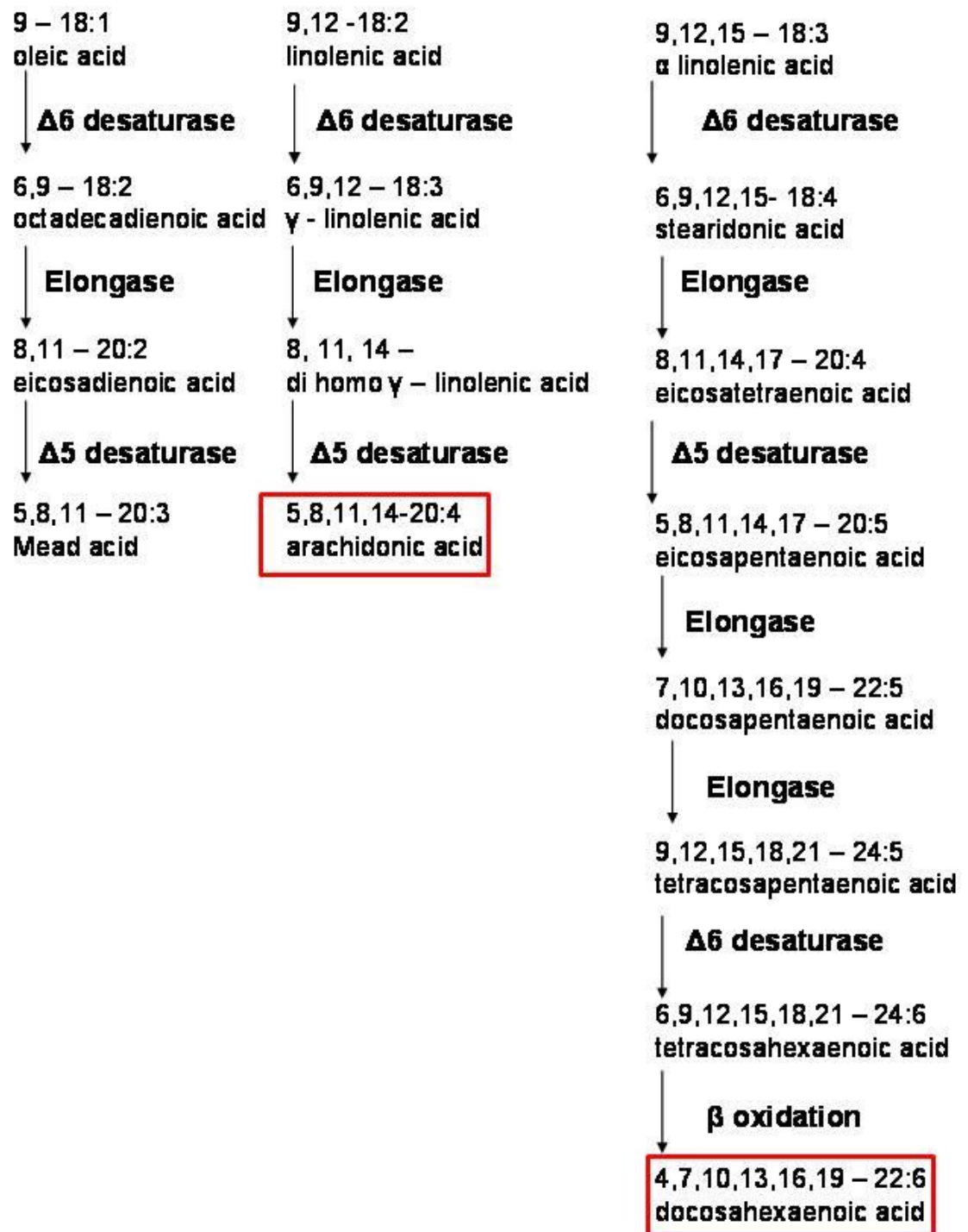
It has long been known that lipids form an essential part of a balanced diet. In the 1920s, Burr and Burr described a deficiency disease in rats when fat was strictly excluded from the diet, which could be cured by addition of a few daily drops of lard (Burr & Burr, 1929). More recent work on dietary lipids led to the use of the term “essential fatty acids” to describe the two polyunsaturated fatty acids (PUFA) linoleic acid (LA) and α -linolenic acid (ALA). The essential fatty acids are so called because they are required by mammals, and yet they cannot be synthesised by mammalian cells (Nicolaou & Kokotos, 2004).

Figure 1.2 The essential fatty acids



Mammals can synthesise long chain saturated fatty acids *de novo* by elongation of a short-chain precursor (typically acetyl CoA) by 2 carbon units until the carbon chain length reaches C16 or C18 (Gurr et al., 2002). Palmitic acid (C16:0) and stearic acid (C18:0) can then be used as a starting point for the production of many other fatty acids using a variety of elongases and desaturases. The biosynthesis of LA and ALA from saturated fatty acids requires a Δ -12 desaturase (also known as ω -6 desaturase) and a ω -3 desaturase respectively (James, 1963; Harris & James 1965). These enzymes can be found in plant cells and cyanobacteria but not in mammalian cells, which means that LA and ALA must be supplied from the diet (Ursin, 2003). Other long-chain PUFA can either be supplied from the diet or biosynthesised from dietary essential fatty acids by the pathways illustrated in Figure 1.3. The biosynthesis of long-chain polyunsaturated n-3 and n-6 PUFA in mammals occurs by two parallel pathways which have ALA and LA as their respective starting points (Sprecher, Luthria et al., 1995; Parker-Barnes, Das et al., 2000; Nakamura & Nara, 2003). LA is the precursor of many important n-6 PUFA, including arachidonic acid (AA), whilst several n-3 PUFA can be synthesised from ALA by animals and humans, including eicosapentaenoic acid (EPA) and docosahexaenoic acid (DHA) (Rapoport et al., 2001; Sinclair & Wesinger, 2004). The synthesis of long-chain PUFA in mammals is a multi-step process involving elongases, desaturases and partial β -oxidation (Sprecher et al., 1995).

Figure 1.3 Biosynthesis of polyunsaturated fatty acids



Biosynthesis of long-chain PUFA from C18 fatty acids is a multi-step process resulting in end products of Mead acid (20:3n-9), arachidonic acid (20:4n-6) and docosahexaenoic acid (22:6n-3). Arachidonic acid and docosahexaenoic acid (boxed in red) are precursors to lipid mediators involved in physiological and pathophysiological cell signalling.

Both $\Delta 5$ -desaturase and $\Delta 6$ -desaturase genes (FADS1 and FADS2, respectively) have been identified and cloned in mammalian cells (Cho et al., 1999a; Cho et al., 1999b). The FADS-2 gene has recently been shown to possess $\Delta 8$ -desaturase activity on both n-6 and n-3 fatty acids in yeast cells transfected with a baboon gene (Park et al., 2009) and $\Delta 8$ -desaturation of 20:2n-6 acid to 20:3n-6 has previously been reported in both rat and human tissue (Albert & Coniglio, 1977; Albert et al., 1979)

Six fatty acid elongase genes (Elovl 1-6) have been identified in rats, mice and humans, which show differential expression in different tissue types and also have different substrate specificity (Wang et al., 2005). Elovl-1 is expressed in many tissue types, including liver, lung, kidney, skin, heart and brain, with a particularly high level expression in CNS myelin. Its substrates are saturated and monounsaturated fatty acids up to a chain length of C₂₆, and its activity is essential for myelination since a reduction in Elovl-1 activity in the CNS results in animal models of myelination deficiency (Tvrdik et al., 2000). Elovl-2 can be found in liver, brain and testes. It elongates C₂₀ – C₂₂ polyunsaturated fatty acids and is believed to be important in the production of long-chain n-3 and n-6 PUFA. Elovl-3 is expressed in skin, sebaceous glands, heart and adipose tissue (Westerberg et al., 2006) and can act on monounsaturated and saturated fatty acids with chain lengths up to C₂₄. Elovl-4 is only expressed in the retina and acts upon very long chain fatty acids (chain length longer than C₂₆). A deficiency of Elovl-4 has been linked to juvenile macular degeneration, and a lack of very long chain phospholipids

in the retinal tissues (McMahon et al., 2007). Elovl-5 has a wide range of substrates, and can elongate most saturated, monounsaturated and polyunsaturated fatty acids in the range of C₁₆ – C₂₂. It is widely-expressed in many tissue types but is most prominent in liver, where it is the most abundant elongase type. Elovl-6 is predominantly found in liver, brain and adipose tissue. It is selective for C₁₂ - C₁₆ saturated and monounsaturated fatty acids and is regulated at transcription level by SBERP1, a key protein in the regulation of hepatic lipid synthesis (Matsuzaka et al., 2002).

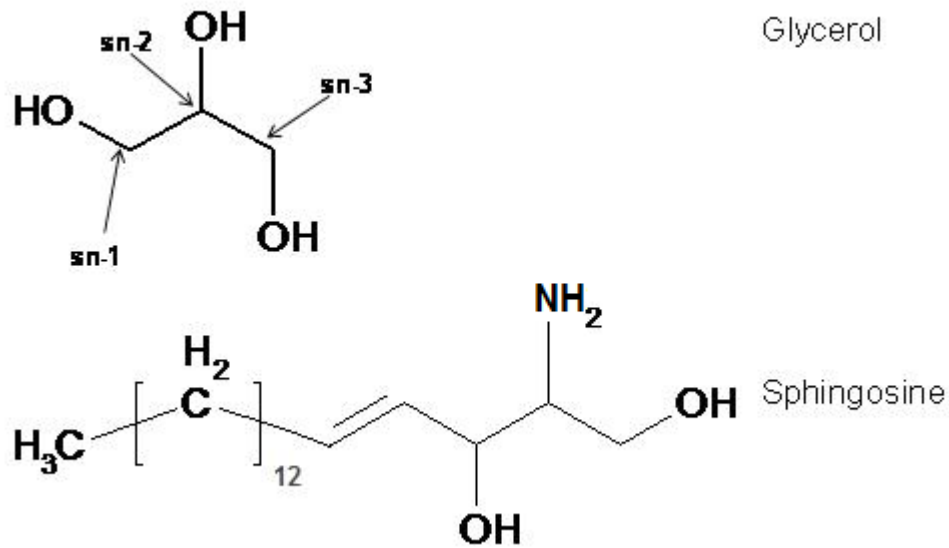
1.3. Phospholipids

Phospholipids are complex lipids, which serve primarily as structural lipids in membranes. Phospholipids can be defined as compounds which consist of:

- (i) a short organic backbone (either glycerol or sphingosine)
- (ii) fatty acid moieties linked to the glycerol or sphingosine backbone by either acyl, alkyl or ether linkages at the *sn*-1 and *sn*-2 position
- (iii) a polar head group at the *sn*-3 position of the backbone

Phospholipids which contain a glycerol backbone are termed glycerophospholipids and those with a sphingosine backbone are called sphingophospholipids.

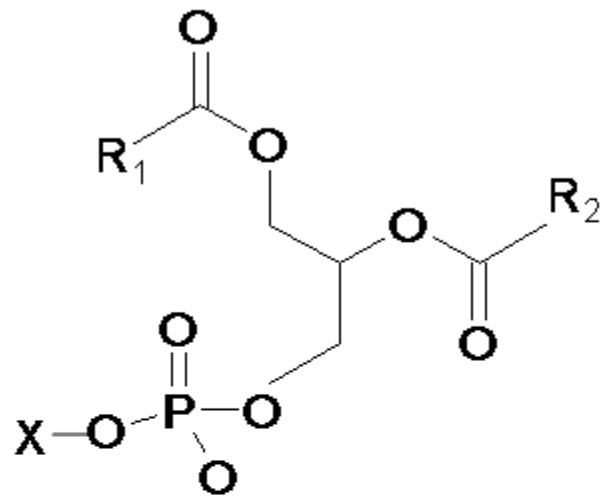
Figure 1.4 Structure of glycerol and sphingosine



1.3.1. Glycerophospholipids

Glycerophospholipids are amphipathic compounds (i.e. contain both a polar and a non-polar moiety in their structure), as they include a glycerol backbone with a polar head group attached to a phosphate unit at the *sn*-3 position, and fatty acid chains at the *sn*-1 and *sn*-2 positions (denoted R_1 and R_2 in Figure 1.5). Further variation in the structure of glycerophospholipids can be introduced by a variety of R groups at the *sn*-1 and *sn*-2 positions. The variety of acyl chain length and unsaturation, as well as the many different possible polar head groups, results in a broad range of glycerophospholipids in biological tissues.

Figure 1.5 Glycerophospholipid structure



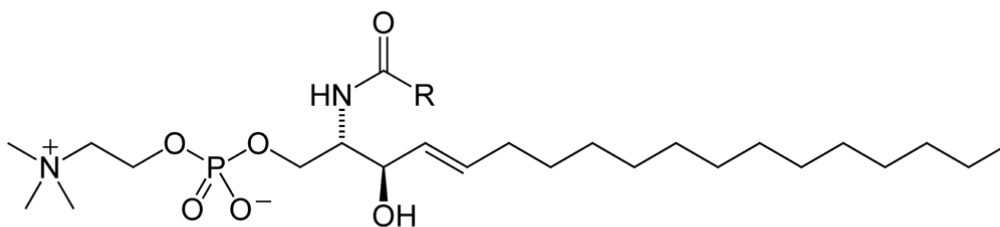
X = polar head group

Polar Head Group	X	Lipid
Hydrogen	—H	Phosphatidic acid
Choline		Phosphatidylcholine
Ethanolamine		Phosphatidylethanolamine
Glycerol		Phosphatidylglycerol
Serine		Phosphatidylserine
Inositol		Phosphatidylinositol

1.3.2. Sphingophospholipids

Sphingophospholipids contain sphingosine, a long-chain hydrophobic molecule, as their backbone, with a phosphate group at the *sn*-3 position and a fatty acid chain at the *sn*-2 position (denoted R in Figure 1.6).

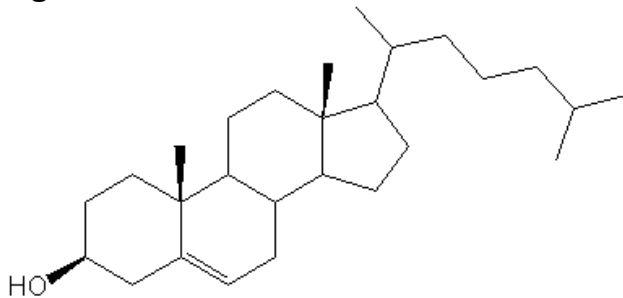
Figure 1.6 Structure of sphingomyelin



1.4. Cholesterol

Cholesterol is a polycyclic compound that is widely found in all animal tissues (Figure 1.7). The fused rings in cholesterol's structure means that the molecule is planar, except for the iso-octyl side chain and the hydroxy and two methyl groups. The hydroxy and methyl groups are arranged in β conformation.

Figure 1.7 Cholesterol



Cholesterol can either be synthesised *de novo* in all eukaryotic cells (except red blood cells), or can be obtained from the diet and transported into cells from the circulation. Uptake of dietary cholesterol from the circulation can occur directly by desorption from the plasma membrane or through receptor – mediated uptake from lipoproteins. The main site of cholesterol biosynthesis is the liver, where it occurs inside the endoplasmic reticulum, but cholesterol biosynthesis also happens in brain peroxisomes. Cholesterol is a major brain lipid but its amphipathic nature (due to the non-polar iso-octyl side chain and the polar hydroxy group in its structure) means that it cannot be readily transported across the tight junctions of the blood–brain barrier. The brain is therefore reliant on intracerebral *de novo* synthesis of cholesterol to fulfil its cholesterol requirements.

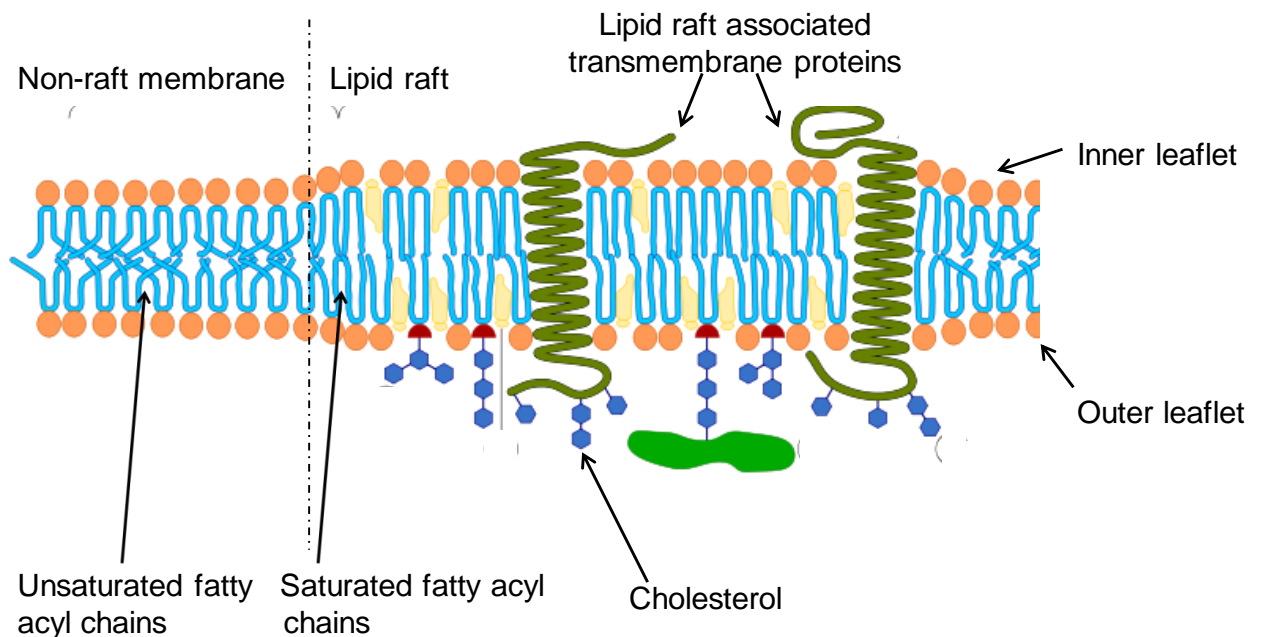
The process of cholesterol biosynthesis from mevalonate is a complex multi–step reaction (McMurry & Begley, 2005). The rate-limiting step in cholesterol biosynthesis is the reduction of 3(S)-Hydroxy-3-methylglutaryl CoA to (R)-mevalonate by HMG-CoA reductase (HMGR), and regulation of HMGR activity and its expression is the primary means of controlling the rate of cholesterol biosynthesis. Cholesterol can directly cause feedback inhibition of HMGR, control HMGR gene expression and the rate of HMGR degradation. In addition, HMGR can be regulated by covalent modification; with phosphorylation of HMGR by AMP-activated protein kinase decreasing its activity.

Cholesterol can interact with membrane phospholipids and sphingolipids to form “lipid rafts”, transient microdomains approximately 100-200nm diameter that are enriched in cholesterol and sphingolipids. Sphingolipids have predominantly saturated fatty acyl chains and the glycerophospholipids located within lipid raft areas are more saturated than in non-raft domains, increasing the efficiency of and the degree of order in fatty acyl chain packing within the raft microdomain. The result is a decreased permeability in lipid raft regions compared to other membrane regions. Membranes which predominantly contain glycerophospholipids are fluid and easily permeable due to loose packing of the phospholipids, which occurs for two reasons. Firstly, some glycerophospholipids contain bulky head groups, which mean that they do not naturally pack together tightly to form a bilayer structure. For example, phosphatidylethanolamines have a conical shape and naturally form a hexagonal phase in aqueous solutions. Secondly, unsaturated C=C bonds cause a kink in the fatty acyl chains and prevent close packing of acyl chains. Many glycerophospholipids contain polyunsaturated fatty acyl chains, which unlike saturated fatty acyl chains cannot be packed tightly together.

Intercalation of cholesterol within lipid rafts also alters the physicochemical properties of the plasma membrane by stabilizing its structure. Hydrophilic interaction between the cholesterol molecule’s hydroxy group and choline-containing phospholipids inside the lipid raft increases the mechanical strength of the membrane without affecting its horizontal flexibility.

Cholesterol can also have an effect on the activity of integral membrane proteins such as ion channels, receptors and enzymes either directly, by binding to them (for example, proteins with sterol-binding domains can be directly modulated by cholesterol), or indirectly, by causing changes in plasma membrane physico-chemical properties that affect the folding and function of the proteins. Many proteins linked to cell signalling have also been found to be enriched in lipid rafts. These include G proteins, MAP kinase, protein kinase C and the p85 subunit of PI 3-kinase.

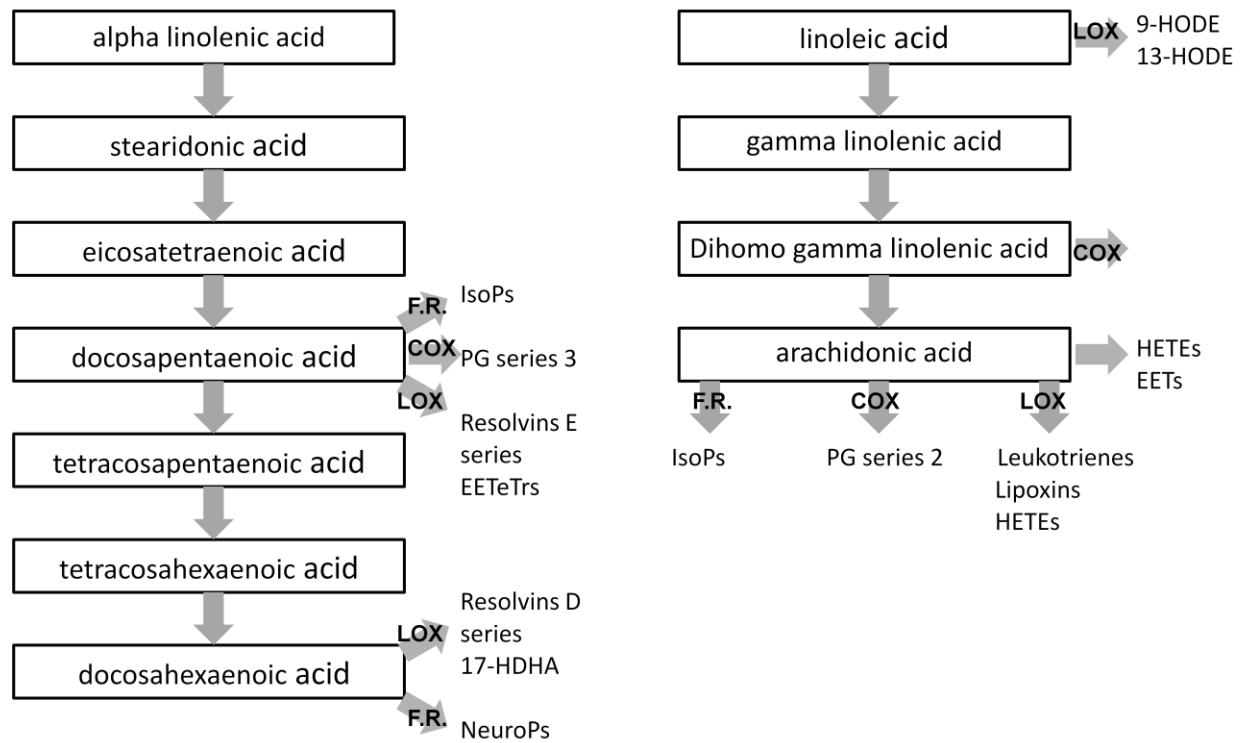
Figure 1.8 Cholesterol is a key component of lipid rafts, which have been implicated in many physiological functions, including cell signalling (adapted from <http://cellbiology.med.unsw.edu.au/units/science/lecture0803.htm>)



1.5. Lipid mediators involved in cell signalling

Eicosanoids are biologically active lipid mediators derived from C₂₀ fatty acids (eicosa = “twenty” in Greek), including prostaglandins (PG), thromboxanes (TX), leukotrienes (LT), lipoxins (LX), isoprostanes (IsoP), isofurans (IsoF) and a host of hydroxy, hydroperoxy and epoxy eicosatrienoic, eicosatetraenoic and eicosapentaenoic acids (Cracowski, 2004; Hong et al., 2003; Parker-Barnes et al., 2000; Serhan et al., 2000; Serhan et al., 2004; Serhan et al., 2006; Zhou & Nilsson, 2001). Eicosanoids are derived from C₂₀ polyunsaturated fatty acids, mainly dihomo-gamma-linoleic (20:3n-6), arachidonic (20:4n-6), and eicosapentaenoic (20:5n-3) acids, through the action of cyclo-oxygenases-1 and 2 (COX-1 and COX-2), lipo-oxygenases (LOX), cytochrome P450 monooxygenases and free radical-catalysed reactions. Analogous compounds can be derived from DHA, such as resolvins, neuroprotectins, neuroprostanes (NeuroP) and neurofurans (NeuroF) (Hong et al., 2003; Moriguchi et al., 2004; Roberts & Fessel, 2004). Figure 1.9 illustrates the wide variety of lipid mediator compounds that can be produced from PUFA by enzymatic and non-enzymatic pathways.

Figure 1.9 Production of lipid mediators from the essential fatty acids can take place by several pathways



COX = cyclo-oxygenase
 EET = epoxyeicosatrienoic acid
 EETeTr = epoxyeicosatetraenoic acid
 F.R. = free radicals
 PG = prostaglandin

HETE = hydroxyeicosatetraenoic acid
 HDHA = hydroxydocosahexaenoic acid
 IsoP = isoprostane
 LOX = lipo-oxygenase
 NeuroP = neuroprotectins

Prostaglandins and thromboxanes are an important class of lipid mediators which are involved in physiological and pathophysiological processes in practically every organ, tissue and cell. They play a role in vasomotor control, regulation of inflammation and the immune response, platelet aggregation and blood clotting, and initiation of labour (Lieberman et al., 2006). PGI₂, PGD₂ and PGE₂ generally favour vasodilation and a decrease in platelet and leukocyte aggregation, and also reduce T cell proliferation and lymphocyte migration, whilst PGF_{2α} causes vasoconstriction, bronchoconstriction and contraction of smooth muscle. The biologically-active TXA₂ shares many functions with PGF_{2α}, causing vasoconstriction, platelet aggregation, bronchoconstriction and lymphocyte proliferation. The biological functions of prostaglandins are mediated through prostanoid-specific receptors and intracellular signalling pathways, whilst their biosynthesis is inhibited by the action of nonsteroidal anti-inflammatory drugs (NSAID) such as ibuprofen and indomethacin on COX enzymes. However, some NSAID such as acetylsalicylic acid (aspirin) can also lead to the modification of COX-2, which leads to biosynthesis of modified eicosanoids which have anti-inflammatory properties, such as the aspirin-triggered lipoxins (Claria & Serhan, 1995).

Leukotrienes are products of LOX and play a role in inflammation processes and in anaphylaxis. LTB₄ acts on immune cells; promoting adhesion and chemotaxis of leukocytes, and aggregation, enzyme release and production of reactive oxygen species in neutrophils. The cysteinyl 4-series LTs (LTC₄, LTD₄ and LTE₄) act on smooth muscle and endothelial cells, causing

bronchoconstriction and increased microvascular permeability (Samuelsson et al., 1987).

Many hydroxy, hydroperoxy and epoxy fatty acids have biological functions affecting vasomotor control or inflammation, with the exception of the diol products of epoxy eicosatrienoic acids (which are biologically inactive). In general, n-3 hydroxy fatty acids are anti-inflammatory or pro-resolution, whilst n-6 compounds are generally vasoactive or pro-inflammatory. The hydroxy derivatives of EPA and DHA known as resolvins and protectins are examples of anti-inflammatory n-3 hydroxy fatty acids, and 20-HETE is an example of a vasoactive n-6 hydroxy fatty acid (Capdevila & Falck, 2002; Serhan et al., 2000).

Isoprostanes are considered reliable markers of oxidative stress status and have been linked to inflammation, ischaemia-reperfusion, cardiovascular disease, reproductive disorders and diabetes (Masoodi & Nicolaou, 2006). They have also been shown to have biological activity, for example, both 8-iso- PGE₂ and 8-iso-PGF_{2α} can modulate platelet aggregation (Roberts & Morrow, 1997). IsoFs are biomarkers of oxidative stress in mitochondria and are produced in significant quantities under conditions of high oxygen pressure (Fessel & Roberts, 2005). Since IsoF production is greater than IsoP production in some tissues (such as brain and kidney), it has been suggested that a combined measure of IsoP and IsoF may be a more accurate measure

of oxidative stress than either of these compounds alone (Fessel & Roberts, 2005).

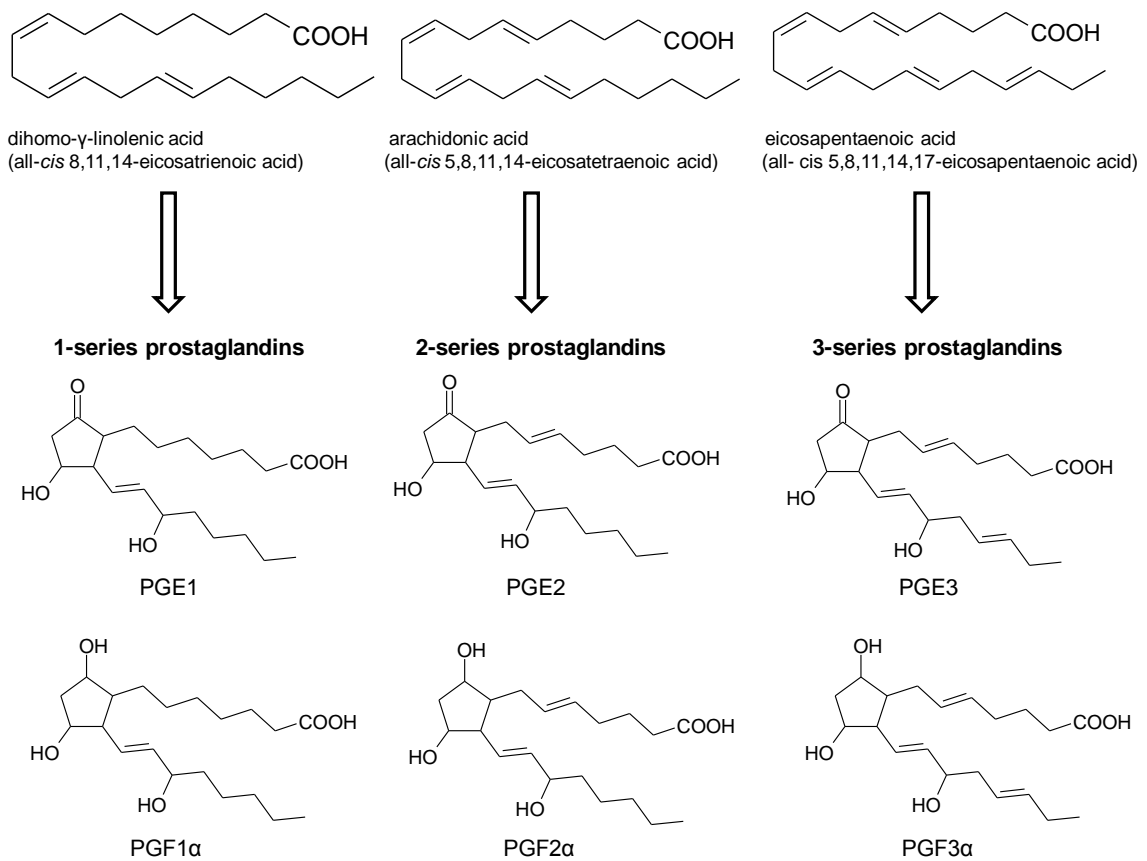
1.5.1 The cyclo-oxygenase enzymes and their lipid mediator products

Two isoforms of cyclo-oxygenase (COX) exist, which differ in tissue expression patterns, pharmacological properties and physiological functions (Morita, 2002, Rouzer & Marnett, 2005). COX-1 is widely acknowledged to be a housekeeping gene, constitutively expressed in many tissue types (Morita, 2002, Rouzer & Marnett, 2005). COX-2 is an inducible gene, which is regulated at the transcription level (Morita, 2002). A splice variant of the COX-1 gene third isoform (COX-3) has also been reported, which has been designated COX-3 (Chandrasekharan et al. 2002; Shafteel et al. 2003). A splice variant of the COX-1 gene has also reported as a third isoform of COX, and designated COX-3 (Chandrasekharan et al., 2002). This splice variant contains intron 1 of the COX-1 gene, which is highly-conserved between mammalian species, including dogs, mice and humans. COX-3 is believed to be constitutive, and gene expression studies have shown the presence of COX-3 mRNA in the majority of tissues in human, rat and mouse brains, with the highest expression observed in endothelial cells of the cerebral cortex (Chandrasekharan et al., 2002; Kis et al., 2004; Shafteel et al., 2003).

The lipid products of COX enzymes are collectively known as prostanoids, and they include prostaglandins, leukotrienes and thromboxanes (Tapiero et

al. 2002). COX enzymes can undergo regiospecific oxidation of dihomo- γ -linolenic acid (DHGLA), AA, or EPA to produce 1-series, 2-series or 3-series PGs respectively, the products differing in structure due to the different number of double bonds in the substrates.

Figure 1.10 Prostaglandin products of dihomo γ – linolenic acid, arachidonic acid and eicosapentaenoic acid (adapted from Nicolaou & Kokotos, 2004)



The PG products of AA and EPA differ considerably in biological activity (Arita et al., 2005; Claria & Serhan, 1995). For example, the PG-2 series synthesised from AA are predominantly pro-inflammatory, whereas the PG-3

series produced from EPA have anti-inflammatory physiological effects (Nicolaou & Kokotos, 2004, Tapiero et al., 2002). The anti-inflammatory properties of PG-3 series compounds have been attributed to the difference of prostaglandin receptor (PG-R) binding to PG-2 series and PG-3 series compounds. PG-3 series compounds generally have a lower affinity to PG-R than PG-2 series compounds and they also do not result in activation of PG-R. The presence of both PG-3 and PG-2 series compounds results in competitive antagonism, where both PG series compete for PG-R binding sites, reducing PG-2 series binding and hence reducing PG-R activation (Bagga et al., 2003; Wada et al., 2007).

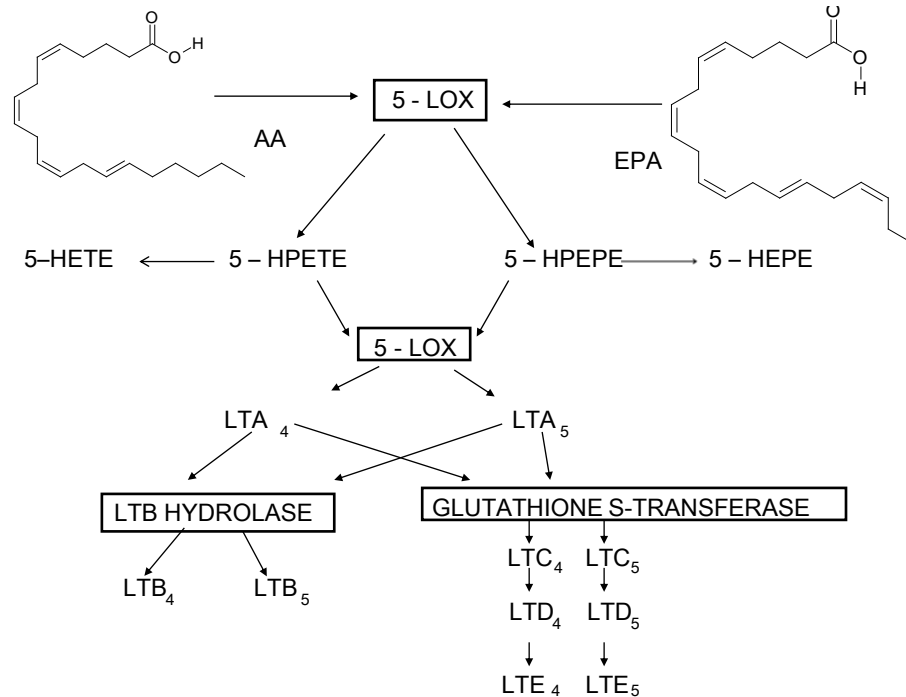
Acetylated COX-2 can also produce hydroxy acids from PUFA, such as 9-hydroxyoctadienoic acid (9-HODE) and 13-hydroxyoctadienoic acid (13-HODE) from LA, 11-hydroxyeicosatetraenoic acid (11-HETE) from AA, 11-hydroxyeicosapentaenoic acid (11-HEPE) from EPA and 13-hydroxydocosahexaenoic acid (13-HDHA) from DHA (Arita et al., 2005). It has been proposed that the acetylation of COX-2 can modify the enzyme's substrate-binding pocket, resulting in production of positional and stereochemical isomers of the previously mentioned HETEs and HEPES (Serhan et al., 2000). COX-2 reduces production of 9-HODE, 11R-HETE, 11R-HEPE and 15R-HEPE and increases that of 15(R)-HETE, 15(R)-HEPE, 18(R)-HEPE and 17(R)-HDHA (Arita et al., 2005, Claria & Serhan, 1995, Serhan et al., 2000). Some of these hydroxy fatty acids, such as 18(R)-HEPE, are bioactive lipids that reduce inflammation and assist in the

resolution of inflammation (Chen & Bazan, 2005, Hong et al., 2003, Lagarde, 2003, Mukherjee et al., 2004). Others can compete with other bioactive compounds for receptor binding positions, resulting in a biological effect. For example, 18(R)-HEPE competes with LTB₄ for binding to human LTB₄ receptor expressed in HEK293 cells, resulting in reduced PMN migration following injury (Serhan et al., 2000).

1.5.2 The lipoxygenase enzymes and their lipid mediator products

LOX enzymes can synthesise a wide range of products which participate in the development or the resolution of inflammation, including hydroperoxy and hydroxy fatty acids, LTs and LXs (Arita et al., 2005; Claria & Serhan, 1995; Hong et al., 2003; Mukherjee et al., 2004). In a similar manner to COX enzymes, LOX enzymes can produce both 4-series and 5-series LTs, which have different physiological functions. The 4-series leukotrienes are pro-inflammatory lipid mediators; LTA₄ is a potent platelet,-aggregating factor and LTB₄ stimulates the chemotaxis and activation of neutrophils. 5-series leukotrienes, however, do not share these properties. LTA₅ inhibits the production of TXA₂, reducing blood clotting, and LTB₅ is a weak chemotactic agent. The 5-series LTs exert their anti-inflammatory effects by directly competing with the 4-series LTs for LT receptor binding.

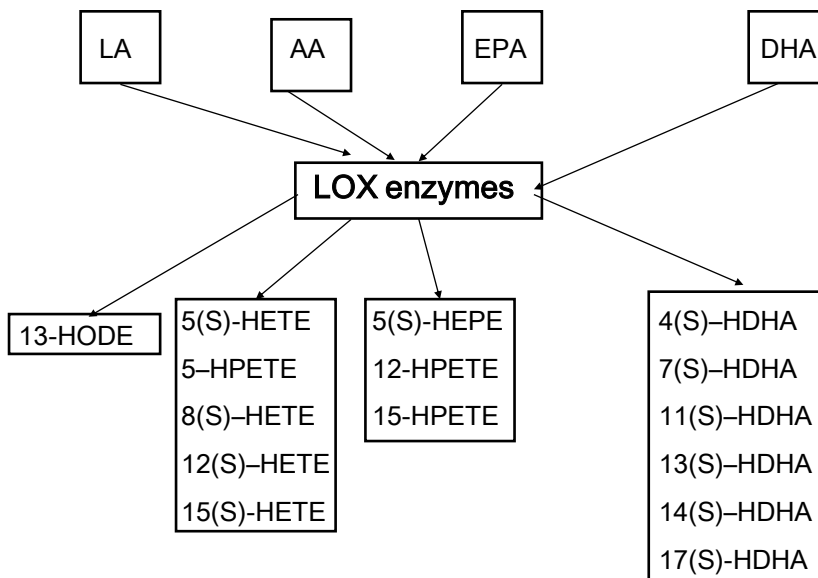
Figure 1.11. Biosynthesis of leukotrienes from polyunsaturated fatty acids by 5- lipoxygenase. Other enzymes (leukotriene B hydrolase and glutathione S-transferase) are responsible for the conversion of leukotriene A to other leukotriene species.



AA= arachidonic acid	LOX= lipo-oxygenase
EPA= eicosapentaenoic acid	LTA= leukotriene A
HEPE= hydroxyeicosapentaenoic acid	LTB= leukotriene B
HETE= hydroxytetraenoic acid	LTC= leukotriene C
HPEPE= hydroxyperoxyeicosapentaenoic acid	LTD= leukotriene D
HPETE= hydroxyperoxytetraenoic acid	LTE= leukotriene E

LOX enzymes can also hydroxylate PUFA in a regiospecific and stereospecific manner, catalysing the oxidation of fatty acids to produce hydroperoxy and/or hydroxy fatty acids (Arita et al., 2005; Brash, 1999; Jisaka et al., 2005; Kuhn et al., 2002; VanRollins & Murphy, 1984). Most of the compounds produced are in the (S) configuration, although a few LOX enzymes which produce (R) products have been recognised (Brash, 1999).

Figure 1.12 Hydroxylation of polyunsaturated fatty acids by LOX enzymes produces a wide range of hydroxy and hydroxyperoxy fatty acids

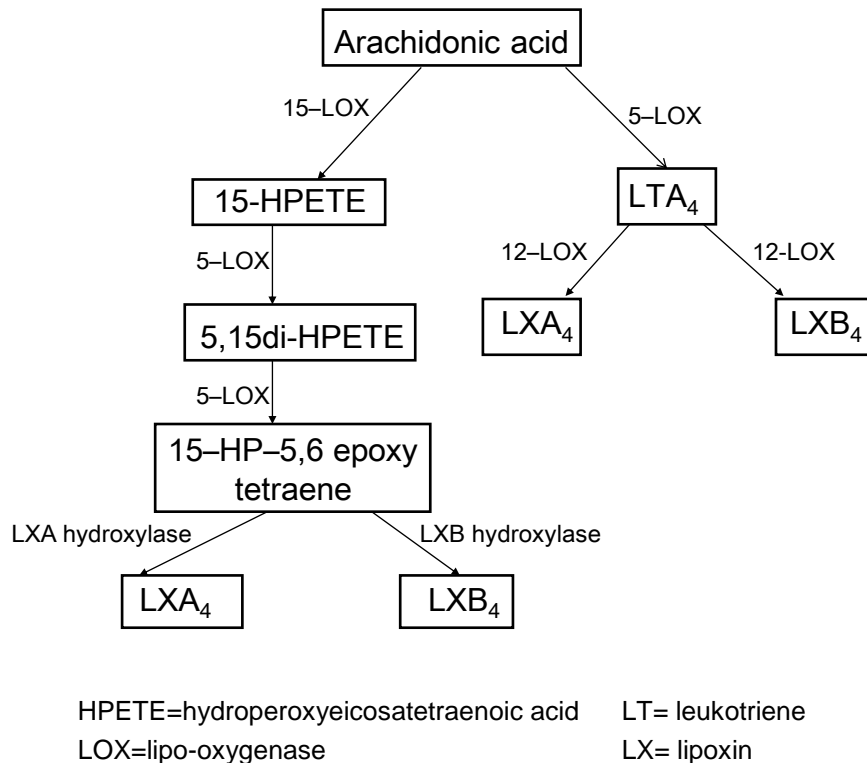


AA= arachidonic acid
 DHA= docosahexaenoic acid
 EPA=eicosapentaenoic acid
 HDHA= hydroxydocosahexaenoic acid
 HEPE= hydroxyeicosapentaenoic acid
 HETE= hydroxyeicosatetraenoic acid
 HPETE= hydroperoxyeicosatetraenoic acid
 HODE= hydroxyoctadienoic acid
 LA= linolenic acid
 LOX= lipo-oxygenase

The term “lipoxin” was introduced to describe anti-inflammatory lipid mediators synthesised from AA by sequential reactions of more than one type of LOX enzymes (Serhan et al. 1984). LX contain three hydroxy groups and are conjugated tetraenes ($\Delta^{6,8,10,12}$). The two LX compounds were designated LXA (5(S),6(R),5(S)-trihydroxytetraeicosanoic acid) and LXB (5(S),15(R),16(S)-trihydroxytetraeicosanoic acid). LXA and LXB can be synthesised by one of two biochemical pathways that require interaction of two different LOX enzymes located in different cell types. One pathway involves interaction of 15-LOX-1 in reticulocytes and 5-LOX in neutrophils

and the other, interaction of 5-LOX in neutrophils and 12-LOX in platelets (see figure 1.13).

Figure 1.13 Production of lipoxins from arachidonic acid is a multiple step process and requires LOX enzymes from different cell types



15-*epi*-lipoxins have also been isolated from cell cultures, which are (R) epimers of LXA and LXB. These compounds arise from the oxidation of 15(R)-HETE produced by acetylated COX-2 enzymes in the manner previously described. The 15-*epi*-lipoxins are also known as aspirin-triggered lipoxins (ATL), and their biosynthesis requires interaction between acetylated COX-2 and 5-LOX. ATL have been shown to be anti-inflammatory. ATL are unstable and have very short half-lives *in vitro* and *in*

vivo, which made their study difficult. However, more stable synthetic analogues of ATL which share their anti-inflammatory properties have been synthesized to allow the study and better understanding of ATL's biological actions (Chiang et al., 2005; Petasis et al., 2005).

1.5.3 The cytochrome P450 enzymes and their lipid mediator products

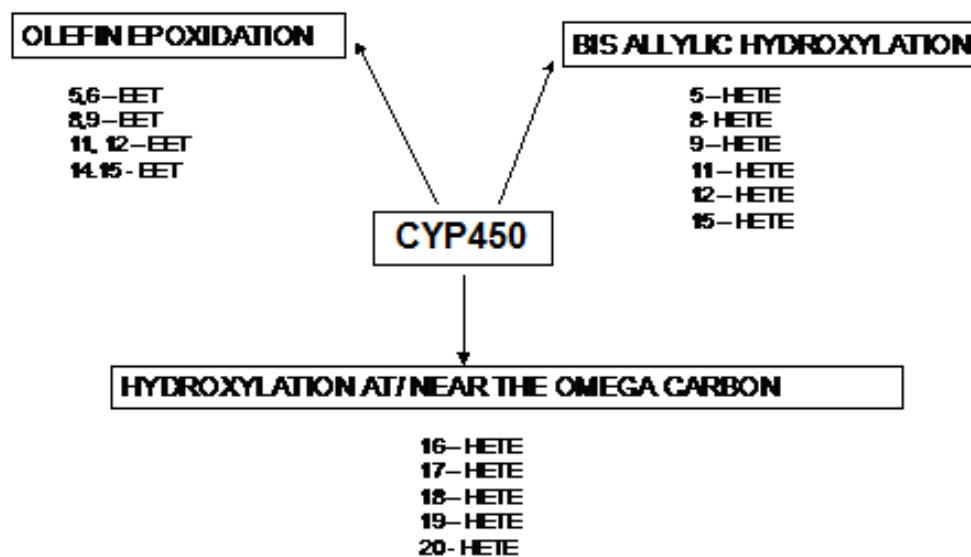
Numerous isoforms of cytochrome P450 monooxygenases exist in plants and mammals, for example, humans have over fifty P450 genes (Lewis, 2004). The P450 monooxygenases involved in oxidation of eicosanoids and PUFA are members of the CYP2 and CYP4 families (Lagarde 2003). Of the PUFA, AA is the most widely acknowledged PUFA substrate for P450 oxidation, but EPA is also an efficient substrate for these enzymes (Barbosa-Sicard et al., 2005). The reactions catalysed by the P450 monooxygenases are based on three main mechanisms (Capdevila et al., 2000), which are:

- i. Bis-allylic hydroxylation of fatty acids (LOX-like reaction mechanism)
- ii. Hydroxylation of fatty acids at or near the ω -position
- iii. Epoxidation of fatty acids

The first mechanism produces hydroxyeicoasatetraenoic acids (HETEs) from AA, the second produces HETEs from AA and hydroxyeicoasapentaenoic acids (HEPEs) from EPA, and the third produces epoxyeicosatrienoic acids

(EETs) from AA and epoxyeicosatetraenoic acids (EETeTrs) from EPA (Barbosa-Sicard et al., 2005; Capdevila et al., 2000; Capdevila & Falck, 2000; Lagarde, 2003).

Figure 1.14 Cytochrome P450 metabolism of arachidonic acid occurs by three reaction mechanisms



EET=epoxyeicosatrienoic acid HETE=hydroxyeicosatetraenoic acid

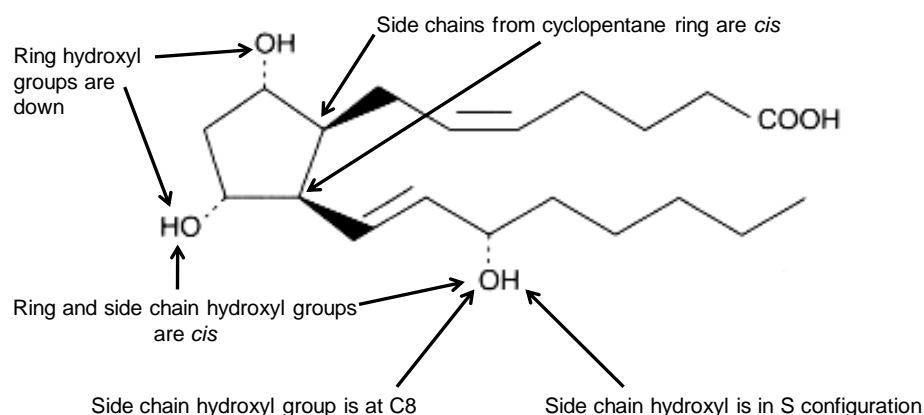
Many of the oxidized PUFA products generated by P450 enzymes are known to possess biological activity, with the exception of the hydrolysed diol products of EETs (Capdevila & Falck, 2002). Most of these compounds have been reported to exert vascular or inflammatory effects, for example, 15-HETE has been reported to vasoconstrict the renal vascular bed (Capdevila & Falck, 2002) and 5,6-EET and 8,9-EET are potent angiogenic agents (Pozzi et al., 2005). Both 5-HETE and 12-HETE have been known to mediate inflammatory effects in the vascular system (Natarajan and Nadler, 2004). However, some lipid mediators have anti-inflammatory effects, such as 18(R)-

HETE (Chiang et al., 2005, Serhan et al., 2000) and 11,12-EET (Arita et al, 2005). In addition, the EETs as a group can alter the flow of ions in the heart and kidney (Lagarde, 2003) and 20-hydroxy-14,15-EET is a high affinity endogenous ligand for PPAR α (Cowart et al., 2001).

1.5.4 Bioactive lipids produced by non-enzymatic (free radical-catalysed) pathways

Isoprostanes (IsoPs) are PG-like compounds derived from AA *in vivo* by nonenzymatic (free radical induced) peroxidation (Roberts & Morrow, 1997, Montine et al., 2004). They can be detected and quantified at physiological levels in tissues or in plasma, urine and other biological fluids and they are considered reliable biomarkers of inflammation (Cracowski, 2004, Cracowski et al., 2005). Initially the isoprostanes were divided into four classes, one to represent each regioisomer formed, but more recently, a nomenclature system based on their structure has been developed (Morrow et al., 1990, Taber et al., 1997).

Figure 1.15 A representative isoprostane (8_c-iso prostaglandin F_{2α}). The nomenclature of isoprostanes is dependent on their structure and is described in detail below.



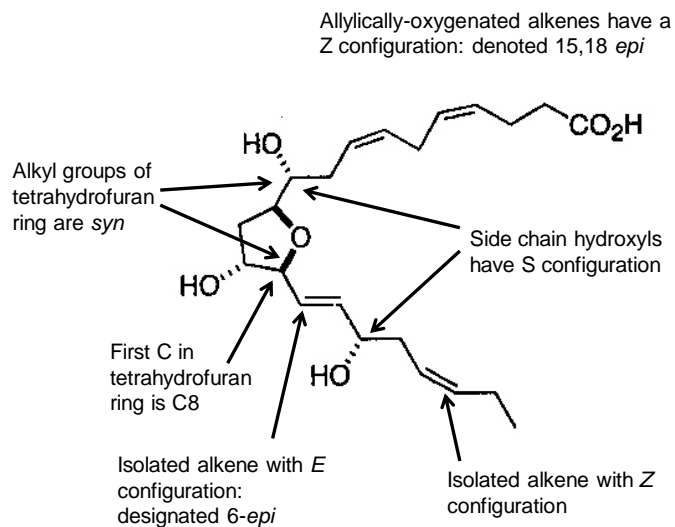
Isoprostane letter	Based on prostaglandin of which it is an epimer (e.g. F ₂ , E ₂ and D ₂)
Number prefix to name	Location of side chain hydroxyl group
Default absolute configuration of side chain hydroxyls	(S) Compound with (R) configuration is denoted as “ <i>ent</i> ” (for enantiomer)
Default absolute configuration of ring hydroxyls	Down (α) Compounds where hydroxyls are in an upwards configuration are denoted as “ <i>ent</i> ”
Position of side chains relative to cyclopentane ring	Normally <i>cis</i> Lower number C is designated as “ <i>epi</i> ” if <i>trans</i> conformation
Position of side chains relative to cyclopentane ring hydroxyls	<i>Cis/trans</i> – subscript <i>c/t</i> is used

IsoPs display potent biological activities. They have a constrictor effect in many vascular beds (including cerebral arterioles and retinal blood vessels) and a bronchoconstrictor effect on human tissue *in vitro* and guinea pig *in vivo* (Cracowski, 2004). *In vitro* experiments have shown increased F₂-IsoP production during oxidation of low-density lipoprotein (LDL), which is a key event in the formation of atherosclerotic plaque (Montuschi et al., 2004). IsoPs may also have a role in the pathology of neurodegenerative diseases where oxidative stress is known to play a part e.g. Alzheimer’s disease, since their formation in membranes may alter membrane biophysical properties, resulting in alteration or impairment of neuronal function, and they have been

suggested as a biomarker of neuronal inflammation (Nourooz-Zadeh et al., 1999; Roberts et al., 1998). Some 3-series isoprostanes can also be produced from eicosapentaenoic acid (Gao et al., 2006). Similarly, the neuroprostanes are free radical-catalysed oxidation products of docosahexaenoic acid (DHA) that are analogous to IsoPs (Moriguchi et al., 2004, Roberts & Fessel, 2004). NeuroPs can be considered as suitable biomarkers of neuronal inflammation owing to the high concentration of DHA in the CNS compared to other regions of the body (Montine et al., 2004).

Isofurans (IsoFs) are compounds similar in structure to IsoPs, but they have a furan ring instead of a cyclopentane ring (Roberts & Fessel, 2004). IsoFs are produced from the peroxidation of AA (Montine et al., 2004) and are more likely to be formed under conditions of oxidative stress or high pO_2 , since the mechanism of their biosynthesis involves attack by oxygen on a double bond of an intermediate compound (Roberts & Fessel, 2004), leading to speculation that production of IsoFs may be a reliable indicator of oxidative stress (Fessel et al., 2003). The nomenclature system of IsoFs is similar to that of the IsoPs (Taber et al., 2004), and is described in Figure 1.16. Neurofurans (NeuroFs) analogous to IsoFs have recently been identified (Taber & Roberts, 2005) and it is conceivable that they may also be suitable biomarkers of CNS inflammation. NeuroPs and NeuroFs share a nomenclature system that is analogous to that of IsoPs and IsoFs.

Figure 1.16 A representative isofuran (*syn 8-cis-6,15,18-epi* isofuran). The nomenclature of isofurans is dependent on their structure and is described in detail below.

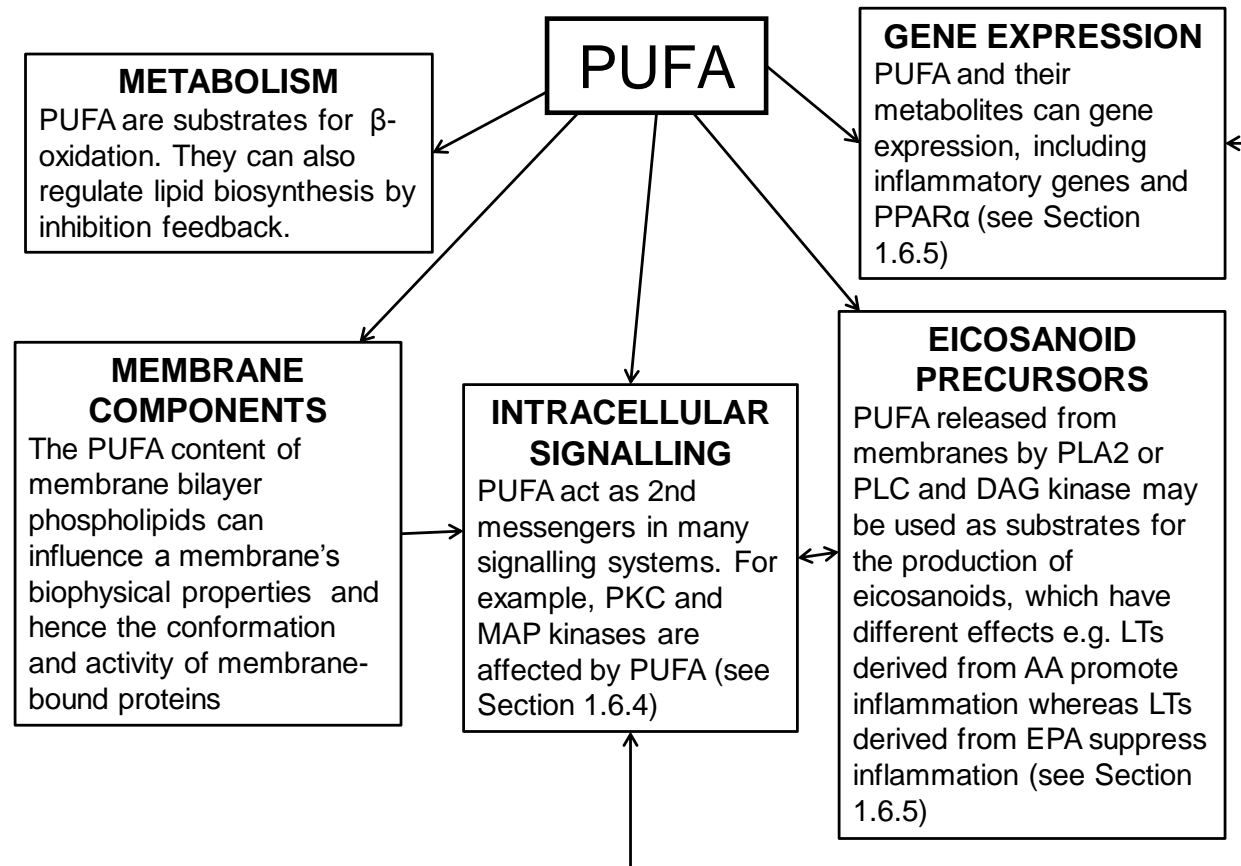


Isofuran number	Number of first C atom in tetrahydrofuran ring
Position of alkyl groups of tetrahydrofuran ring	<i>syn</i> / <i>anti</i> (S/A)
Position of ring hydroxyl relative to adjacent alkyl group	<i>cis</i> / <i>trans</i> (C/T)
Default absolute configuration of side chain hydroxyls	(S) – compounds with an (R) configuration are denoted as “ <i>enti</i> ”
Default geometry of isolated alkenes	<i>Z</i> – compounds with an <i>E</i> configuration are denoted as “ <i>epi</i> ”
Default geometry of allylically – oxygenated alkenes	<i>E</i> – compounds with a <i>Z</i> configuration are denoted as “ <i>epi</i> ”

1.6. Polyunsaturated fatty acids and the brain

Lipids, PUFA in particular, are known to be essential for the development of the brain (Wilson & Sargent, 1993; Uauy et al., 2000; Wainwright, 2002). They may be incorporated into structural lipids, for example, DHA and AA are both important constituents of phospholipids in neuronal membranes (Williard et al., 2001; Zhou & Nilsson, 2001), or used as substrates for the production of lipid mediators that participate in numerous physiological functions (Yehuda et al., 1998; Tapiero et al., 2002). Some of the biological roles of PUFA are outlined in Figure 1.17.

Figure 1.17 Diagram of the multiple roles of PUFA in physiological functions, some of which may be inter-related



AA= arachidonic acid
DAG= diacylglycerol
EPA= eicosapenatenoic acid

MAP= mitogen-activated protein
PKC = protein kinase C
PLA₂= phospholipase A₂

PLC= phospholipase C
PPAR= peroxisome proliferator-activated receptor
PUFA= polyunsaturated fatty acid

1.6.1. PUFA occurrence and metabolism in the brain

It has been estimated that lipids account for over half of the brain's dry weight (Simopoulos, 1991; Calvani & Benatti, 2003). Brain composition analysis has shown that lipids account for more than half of the grey matter, and the majority of grey matter lipids contain PUFA in their structure (Sinclair & Wesinger, 2004).

Tracer studies using carbon-14 radiolabelled PUFA suggest that PUFA can cross the blood–brain barrier (BBB) (Rapoport et al., 2001; Sinclair & Wesinger, 2004). Moreover, rats fed deuterated LA and ALA showed accumulation of the radiolabelled fatty acid in brain and plasma lipids (Liu & Salem, 2007). The kinetics of fatty acid transport from the blood to the brain varies between lipid species, and more than one model has been proposed for the uptake of PUFA by the brain.

The lipophilic nature of fatty acids means that they may be rapidly incorporated into and easily dissociated from membrane structures. This has led to the suggestion by Hamilton (1998) that fatty acids diffuse down a concentration gradient across the BBB. It was proposed that un-ionized fatty acids can slot into the outer leaflet of the BBB, rapidly diffuse through the lipid bilayer, and then dissociate from the inner leaflet of the membrane, the whole process occurring almost instantaneously. Other models of fatty acid

transport have also been proposed, such as active transport using carrier proteins. Work in the 1990s led to the cloning of a family of five proteins known as the fatty acid transporter proteins (FATP1 - 5). It has been suggested that these act as carrier proteins, transporting fatty acids across the BBB using facilitated diffusion or active transport (Schaffer & Lodish 1994; Abumrad et al., 1998; Hirsch et al., 1998). The exact mechanism of fatty acid transport across the BBB has not been elucidated, although a highly-conserved AMP-binding site has led to the suggestion that fatty acids may be actively transported.

It is also possible that different PUFA are uptaken by different mechanisms, for example, plasma AA correlates directly to the amount of AA in brain tissues, whereas plasma DHA does not correlate directly to the amount of DHA in brain tissues (Blank et al., 2002), implying that DHA may be actively uptaken by brain or there may be another source of DHA available. This suggestion has also been echoed by Abumrad and colleagues (1998), who proposed that at high concentrations of free fatty acids, simple diffusion may be the most important transport mechanism, whilst at physiological conditions, the role of FATP is more important than that of diffusion.

Elovl-1, Elovl-2, Elovl-5 and Elovl-6 gene expression have all been demonstrated in the brain, and of these elongases, both Elovl-2 and Elovl-5 are capable of elongating 18:2n-6 and 18:3n-3 to produce C₂₀ and C₂₂ PUFA (Wang et al., 2005). However, biosynthesis of long-chain PUFA in the brain is

not believed to be a significant source of EPA and DHA, despite the presence of fatty acid elongases in the brain (Igarashi et al., 2007). It has been postulated that a signalling system exists for the delivery of DHA to the central nervous system (CNS) from the liver, which could be activated when extra DHA is required in the CNS e.g. following neuronal membrane damage (Scott & Bazan, 1989). Rapoport and colleagues (Igarashi et al., 2007) reported that dietary n-3 PUFA deficiency upregulated elongase and desaturase expression in the liver, but not in the brain, supporting the theory that the liver supplies the majority of the brain's PUFA requirements.

1.6.2. PUFA as membrane components

Phospholipids are a major component of neuronal membranes and they incorporate esterified PUFA in their structures in the *sn*-2 position and sometimes also the *sn*-1 position (Figure 1.3). Insufficiency of PUFA, whether caused by diet or by metabolic disorders (for example, peroxisomal disorders) can result in abnormal fatty acid metabolism. These can result in changes in brain lipid composition (Uauy et al., 2000; Wainwright, 2002; Barcelo-Coblijn et al., 2003; DeMar et al., 2004). Changes in the lipid content of the diet, in particular n-3 PUFA, can alter the phospholipid composition of membranes in many tissues, including the brain (Gerbi et al., 1999; Blank et al., 2002; Barcelo-Coblijn et al., 2003).

Changes in the lipid environment can also influence the functional properties of enzymes that are incorporated into the membrane structure. For example, the Na⁺/K⁺-ATPase α_2 isoenzyme in rats fed a sunflower oil diet (which is low in n-3 PUFA) showed a higher affinity for sodium than in rats fed a soybean oil diet (which is rich in n-3 PUFA) (Gerbi et al., 1999). The biophysical properties of membranes (fluidity, flexibility and permeability) are affected by their phospholipid and cholesterol content (Chen & Bazan, 2005) and changes in the composition or biophysical properties of membranes may lead to changes in receptor conformation and ion channels' activity (Barcelo-Coblijn et al., 2003). Alternatively, some PUFA may be endogenous ligands for ion channels, for instance, AA, DHA and ALA can bind to and activate the TREK-1 K⁺ channel (Lauritzen et al., 2000).

1.6.3. PUFA and gene expression

Many genes have been reported to be affected by changes in dietary lipids, including genes that are involved in cytoskeleton and membrane association, signal transduction, ion channels, metabolism and regulatory proteins (Kitajka et al., 2002; Barcelo-Coblijn et al., 2003). Fatty acids can regulate several genes at transcription level, including peroxisome proliferator-activated receptors (PPARs), of which PPAR α is the most widespread, retinoid X receptor (RXR), sterol regulatory element binding protein (SREBP) and nuclear factor kappa B (NF κ B) (Jump et al., 2005).

Rats fed perilla oil (rich in ALA) or fish oil (rich in DHA and EPA) show differences in gene expression in the brain compared to those fed a standard diet (Kitajka et al., 2002; Barcelo-Coblijn et al., 2003). Animals which received a diet enriched in n-3 fatty acids had an increase in the expression of synucleins, which are involved in synapse formation (Kitajka et al., 2002). The addition of oxidised n-3 fatty acids to *in vitro* cell cultures reduced the expression of pro-inflammatory genes (Mishra et al., 2004). A study on the effects of dietary n-3 fatty acids showed that plasma levels of several inflammatory biomarkers, such as C-reactive protein (CRP), interleukin-6 (IL-6), E-selectin, inflammatory cell adhesion molecule-1 (ICAM-1) and secreted vascular cell adhesion molecule-1 (sVCAM-1) was inversely related to dietary intake of n-3 fatty acids in women (Lopez-Garcia et al., 2004). This lends itself to the suggestion that a deficiency in n-3 fatty acids may lead to increased susceptibility to pathophysiological inflammatory states. Similarly, a high intake of n-3 fatty acids may protect against inflammatory conditions such as cardiovascular disease or cerebrovascular disease.

1.6.4. PUFA in cell signalling

The vast majority of lipids in the brain are esterified and incorporated into complex lipids but the hydrolysis of phospholipids at the *sn*-2 position by phospholipase A₂ (PLA₂) results in the release of PUFA as free fatty acids (FFA), which form a substrate pool for the formation of numerous lipid second

messengers that can regulate and/or interact with intercellular signalling. Some PUFA can themselves affect the synthesis and/or release of neurotransmitters and brain peptides. In addition, the production of bioactive lipid mediators such as prostaglandins, hydroxy-polyunsaturated fatty acids and isoprostanes from FFA may further affect cell signalling mechanisms (Rouzer & Marnett, 2005; Serhan, 2005).

1.6.5. Production of lipid mediators from PUFA

Eicosanoids are well-known for their pro-inflammatory effects but recently it has been pointed out that “not all eicosanoids are bad guys” (Serhan, 2005). Although it has been traditionally held that eicosanoids and their derivatives are pro-inflammatory compounds, both anti-inflammatory and pro-resolution (promoting tissue repair) lipid mediators have been described (Serhan et al., 2000; Hong et al., 2003; Serhan et al., 2004; Sethi et al., 2004; Bannenberg et al., 2005). For example, 18(R)-hydroxyeicosapentaenoic acid (18(R)-HEPE), a metabolite of EPA, reduced the migration of neutrophils following cell injury in HEK 293 cell cultures that express leukotriene (LT) receptors by competing with LTB₄ for binding sites (Serhan et al., 2000). Mouse models of peritonitis showed a reduction in leukocyte infiltration mediated by two metabolites of DHA, 4(S)-hydroxydocosahexaenoic acid and 10(S),17(S)-docosatriene (Marcheselli et al., 2003). The latter also caused a neuroprotective effect in mouse models of focal brain ischemia-reperfusion,

reducing the volume of the infarcted tissue and increasing the strength of electronic signal from the hippocampus following a simulated stroke (Marcheselli et al., 2003). Aspirin-triggered lipoxins (ATL) have also been reported to show anti-inflammatory properties in many rodent models of inflammation, including peritonitis and ischaemia-reperfusion injury of the lung (Bannenberg et al., 2004; Chiang et al., 1999).

1.6.6. Adaptive cytoprotection (Preconditioning and brain tolerance)

Tolerance is an adaptive cytoprotective response initiated in response to a sublethal insult which gives increased resistance to a subsequent potentially lethal insult. The process of inducing tolerance is termed preconditioning. Many types of stimuli have a preconditioning effect, for example, thermal stress, tissue injury, oxidative agents and ischaemia.

Ischaemic preconditioning was first demonstrated twenty years ago by Murry and colleagues (1986), who showed that a short period of ischaemia in canine myocardium led to increased survival after a subsequent prolonged period of ischaemia. This phenomenon has since also been reported in rabbit and swine myocardium, inferring that this phenomenon is common to many mammalian species (Schott et al., 1990; Cohen et al., 1991). A retrospective study on patients admitted to hospital following myocardial infarction showed that patients who had experienced episodes of prodromal angina in the 24

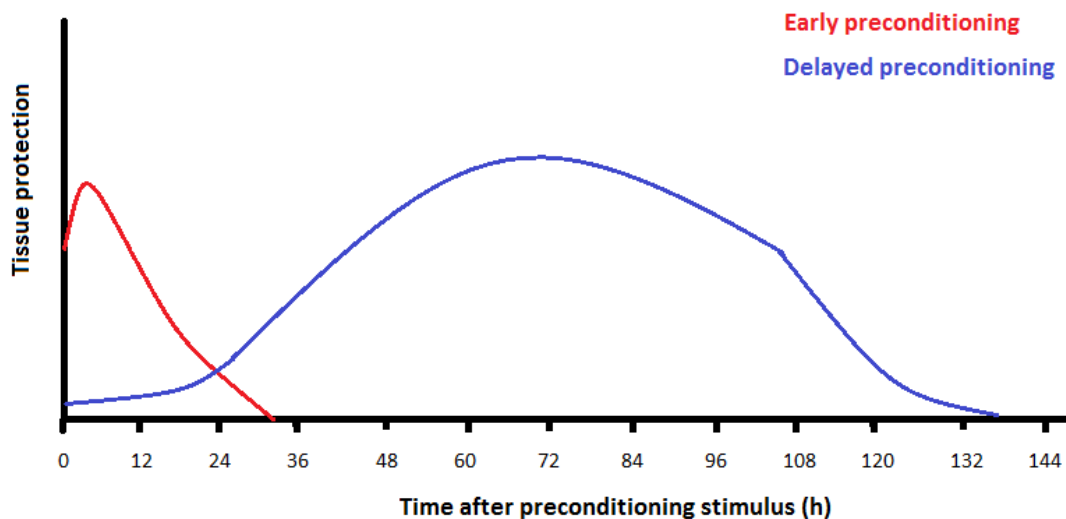
hours prior to myocardial infarction had smaller infarct sizes than those who had not, implying that human myocardium may also be responsive to preconditioning (Ottani et al., 1995). Preconditioning is not unique to the heart, and many other organs, including the brain, have also been reported to be protected by ischaemic preconditioning (Kitagawa et al., 1990; Kitagawa et al., 1991; Liu et al., 1992; Matsushima & Hakim, 1995).

The occurrence of prodromal transient ischaemic attacks (TIA) were linked to less severe strokes and improved outcome in stroke patients (Weih et al., 1999), prompting speculation that ischaemic preconditioning could also occur in the human brain. A later multi-centre study supported this theory by showing that patients who had experienced prodromal TIA had smaller infarct volumes following a stroke than patients with no prior ischaemic events, despite showing a comparable reduction in cerebral blood flow and cerebral blood volume (Wegener et al., 2004). This study demonstrated that the protective effects of prodromal TIA were due to an intrinsic neuroprotective effect rather than alterations in cerebral blood flow caused by enhanced vascularisation.

Preconditioning has a time-dependent effect and only offers temporary protection against a subsequent noxious stimulus. This time frame has been described as the 'window of protection' and has been widely studied in order to assess the potential benefits of preconditioning and also to gain insight into the molecular mechanisms behind preconditioning (and identification of

pharmacological targets). It was found in rodents that two stages of preconditioning exist: 'early preconditioning', which takes effect immediately after the sublethal noxious stimulus and lasts for up to 24 hours, and 'delayed preconditioning', which only develops at least 24 hours after the initial noxious stimulus, peaking approximately 72 hours after the preconditioning event, and lasting for several days in total. Figure 1.18 illustrates the time effect of the two forms of preconditioning.

Figure 1.18 Preconditioning is a time-dependent phenomenon, which exists in two forms: (i) early preconditioning and (ii) delayed preconditioning. Both forms are believed to be the result of different cellular processes (adapted from Dirnagl et al., 2003).

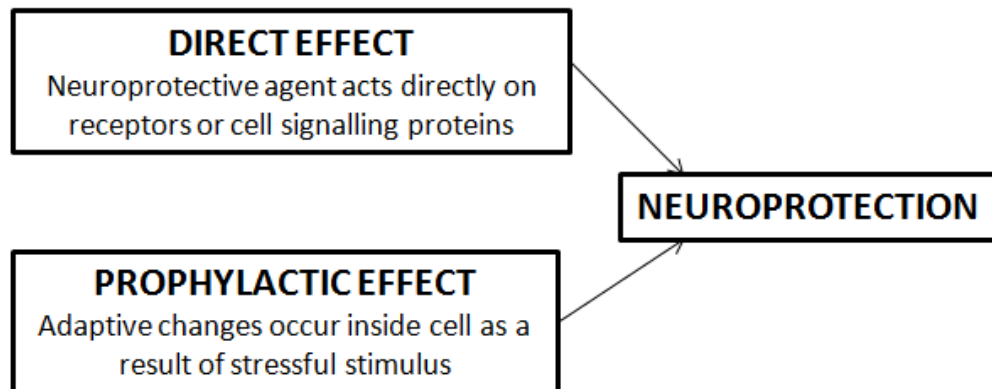


The ability of one type of preconditioning treatment to induce tolerance to other forms of cellular stress is known as cross-tolerance. For example, whole body hyperthermia is neuroprotective against brain ischaemia (Wada et al., 1999). The existence of cross-tolerance opens the possibility of using

different treatments or procedures to induce ischaemic tolerance, of which some may have potential applications in treating human diseases such as heart disease and ischaemic stroke.

Two main strategies have emerged in stroke treatment and the induction of neuroprotection. These are: (a) enhancing direct effects of a neuroprotective agent on pharmacological targets, and (b) induction of prophylactic neuroprotection by causing adaptive changes in cell biology.

Figure 1.19 Neuroprotective agents have been postulated to work by either having direct or prophylactic effects on brain tissue.



Extensive research has been carried out into pharmacological methods of reducing neuronal death after an ischaemic insult, including animal studies on platelet-activating factor (PAF) receptor antagonists and LOX inhibitors (Belayev et al., 2008; Belayev et al., 2009; Jatana et al., 2006) and clinical trials on N-methyl D-aspartate (NMDA) receptor antagonists (Grotta et al.,

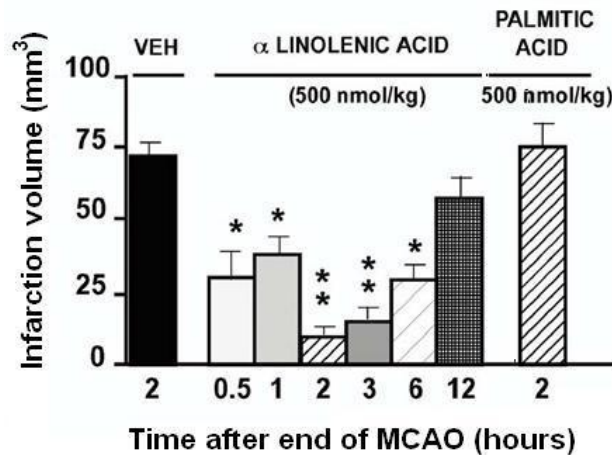
1995; Lees et al., 2000). LOX inhibitors showed a reduction in post-ischaemic inflammation in rodent models of stroke and exerted their actions by preventing the activation of NF κ B and INOS (Jatana et al., 2006). The novel PAF receptor antagonist, LAU-0901 also provided neuroprotection in rodent models of stroke by reducing the inflammatory effects of PAF (Belayev et al., 2008; Belayev et al., 2009). However, despite extensive effort, there has been no success in drug development for a single pharmacological target for stroke treatment.

Prophylactic strategies have not received as much attention, although PPAR α has been pointed out as a potential target for development of anti-ischaemic drugs, due to the ability of PPAR α ligands (e.g. fenofibrate and WY-14643) to reduce infarct size in animal models of ischaemia-reperfusion (Inoue et al., 2003; Lee et al., 2003). Some PUFA, including LA and ALA, are also endogenous ligands of PPAR α , with optimal binding to PPAR α occurs in fatty acids that have chain lengths of C₁₆- C₂₀ and several double bonds in the carbon chain (Forman et al., 1997; Cullingford et al., 1998; Lee et al., 2003). Treatment of animals with PPAR α activators prior to brain ischaemia has been shown to confer a neuroprotective effect which is dependent upon PPAR α activation (Deplanque et al., 2003; Lee et al., 2003; Gelé, 2004). It has been suggested that fibrates exert their effect through a combination of reducing oxidative stress and inflammation, and the modulation of lipid metabolism (Gelé, 2004). It can therefore be deduced that the reduction of

post-ischaemic inflammatory processes results in a better outcome following focal ischaemia in animal models, with animals treated with anti-inflammatory compounds receiving lower infarct volumes and a higher neurological score (Belayev et al., 2008; Belayev et al., 2009; Deplanque et al., 2003; Gelé, 2004; Inoue et al., 2003; Jatana et al., 2006).

PUFA have been reported to exert a neuroprotective effect in rat models of ischaemic stroke and epilepsy (Lauritzen et al., 2000; Blondeau et al., 2002). Intracerebroventricular or intravenous administration of PUFA resulted in increased survival of hippocampal neurons in rats subjected to a period of global forebrain ischaemia or exposure to kainate (Lauritzen et al., 2000; Blondeau et al., 2002). Many n-3 and n-6 PUFA including LA, ALA, AA and DHA were protective, but ALA appeared to be the most efficient of the compounds tested (Lauritzen et al., 2000; Blondeau et al., 2002). Saturated fatty acids did not show a neuroprotective effect on neuronal survival, implying that neuroprotection is specific to PUFA rather than all fatty acids (Lauritzen et al., 2000). A more recent study by the same group showed that neuroprotection was also seen in rats subjected to MCAO. Intravenous injection of one of several n-3 or n-6 PUFA to rats 24 – 96 hours prior to an ischaemic challenge resulted in reduced infarct size and increased neuronal survival compared to vehicle-injected animals (Blondeau et al., 2002). PUFA administration was also neuroprotective in mice, even when administrated after the MCAO period, as seen in Figure 1.20 (Heurteaux et al., 2006; Blondeau et al., 2009).

Figure 1.20 Post-ischaemia ALA treatment of C57/BL6 mice resulted in a statistically significant (* $P < 0.05$, ** $P < 0.01$) reduction in infarct volume following 1h MCAO (from Heurteaux et al., 2006)



Treatment of rats with DHA conjugated to albumin significantly improved their neurological scores 72 hours after MCAO (Rodriguez de Turco et al., 2002; Belayev et al., 2005). This effect was dose-dependent, with a greater improvement seen in rats administered a low dose (0.62mg/kg of DHA–albumin) than in those given a higher dose of 1.25 mg/kg DHA–albumin (Belayev et al., 2005). Lipidomic analysis of the treated rats’ brains showed accumulation of 10,17S–docosatriene in the ipsilateral hemispheres of rats treated with DHA-albumin but not in those rats treated with albumin or saline (Belayev et al., 2005). More recently, the same group unequivocally demonstrated the neuroprotective effects of low or medium intravenous doses of DHA administered shortly after MCAO onset, leading to the theory that DHA could be beneficial to patients after ischaemic stroke (Belayev et al., 2009).

Metabolites of PUFA have also been implicated in neuroprotection, namely the neuroprotectins and resolvins. Intracerebroventricular infusion of the DHA metabolite 10,17S-docosatriene (also known as “neuroprotectin D1” or NPD1), has been reported to reduce the volume of the infarction in mice exposed to focal ischaemia by MCAO, and to improve neurological test scores following MCAO (Marcheselli et al., 2003; Mukherjee et al., 2004; Belayev et al., 2005). As it has been pointed out, inflammation and resolution are not direct opposites, and ‘anti-inflammation’ and ‘pro-resolution’ differ slightly in their meaning (Serhan & Chiang, 2008). The molecular mechanisms behind the neuroprotective effect of NPD1 appear to be its pro-resolution qualities, rather than inhibition of the inflammatory response (Serhan & Chiang, 2008). The resolution of inflammation in rodent models of stroke is promoted by NPD1 through inhibition of neutrophils infiltration into brain tissue, reduction of expression of pro-inflammatory proteins (such as NFkB and COX-2) and apoptotic proteins (such as Bax and Bad), and up-regulation of anti-apoptotic protein expression, such as members of the Bcl family (Marcheselli et al., 2003; Lukiw et al., 2005).

1.7. Introduction to lipidomics

Lipidomics can be defined as the study of all lipid species present in a biological system. It comprises both the identification of lipid species present in the system and the study of their biochemical properties.

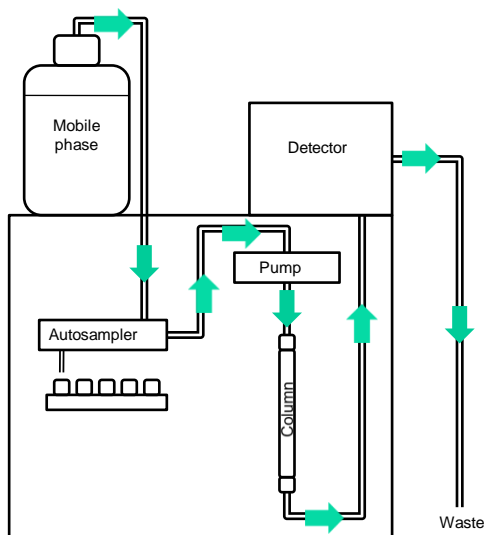
The isolation, localisation, characterization and quantification of known lipid species and the identification of novel lipid molecules in the cell plays a major role in lipidomics (van Meer 2005; Wenk 2005). Advances in lipid analytical techniques during the past twenty years, most notably the development of the electrospray ionisation (ESI) interface, and the increased processing power of online mass spectrometry software, have made it feasible to carry out “shotgun lipidomic” studies, where a broad range of lipid classes in biological samples can be simultaneously investigated (Pulfer & Murphy, 2003; Han & Gross, 2005; Houjou et al., 2005; Taguchi et al., 2005). The use of bioanalytical techniques to study diverse classes of lipids such as glycerophospholipids, sphingophospholipids, eicosanoids, isoprostanes, fatty acids and hydroxy fatty acids is essential for the other part of lipidomics, which is to develop an understanding of the influences of lipids on biological systems, including their roles in membrane architecture, transcriptional and translational modification, cell signalling and interaction between cells (Watson, 2006). Our study will utilise either high-performance liquid chromatography (HPLC) coupled to electrospray ionisation interface tandem mass spectrometry system to identify a variety of lipid mediators in mouse plasma and cerebral cortex, and direct infusion of the analyte to an electrospray ionisation interface tandem mass spectrometry system to identify glycerophospholipids in mouse cerebral cortex tissue.

1.7.1. High-performance liquid chromatography

Liquid chromatography (LC), in particular high-performance liquid chromatography (HPLC) is a popular bioanalytical technique which is widely available. Compounds are separated on the basis of their physicochemical properties, based on their elution time out of an organic-phase packed column back into the more polar mobile phase (or in the case of reverse-phase HPLC, from a polar packed column into a non-polar (organic) mobile phase).

The sample is injected into the mobile phase, which flows through the HPLC equipment and into the column. The sample adsorbs onto the surface of the beads packed into the column and is flushed out of the column by the continuous flow of mobile phase, its constituents separated on the basis of their elution time out of the column. The analyte is passed through a detector (most commonly an ultraviolet (UV) spectrometer, although other detection techniques, such as fluorescence or refractive index measurement, may be used), where an absorption peak is recorded. The detection equipment may be linked to a computer which uses software to calculate the area beneath the chromatogram peak to produce a quantifiable result. Figure 1.21 illustrates a schematic diagram of HPLC, showing its main components and the route the analyte takes through the analytical set-up (shown by arrows).

Figure 1.21 Schematic diagram of HPLC



HPLC is particularly suitable for high-throughput analysis due to its speed and the availability of automated sample injectors. Furthermore, it is a sensitive and accurate analytical method which does not require large samples and does not destroy the sample during analysis; meaning that it can be coupled to other analytical equipment, such as a mass spectrometer, instead of a detector.

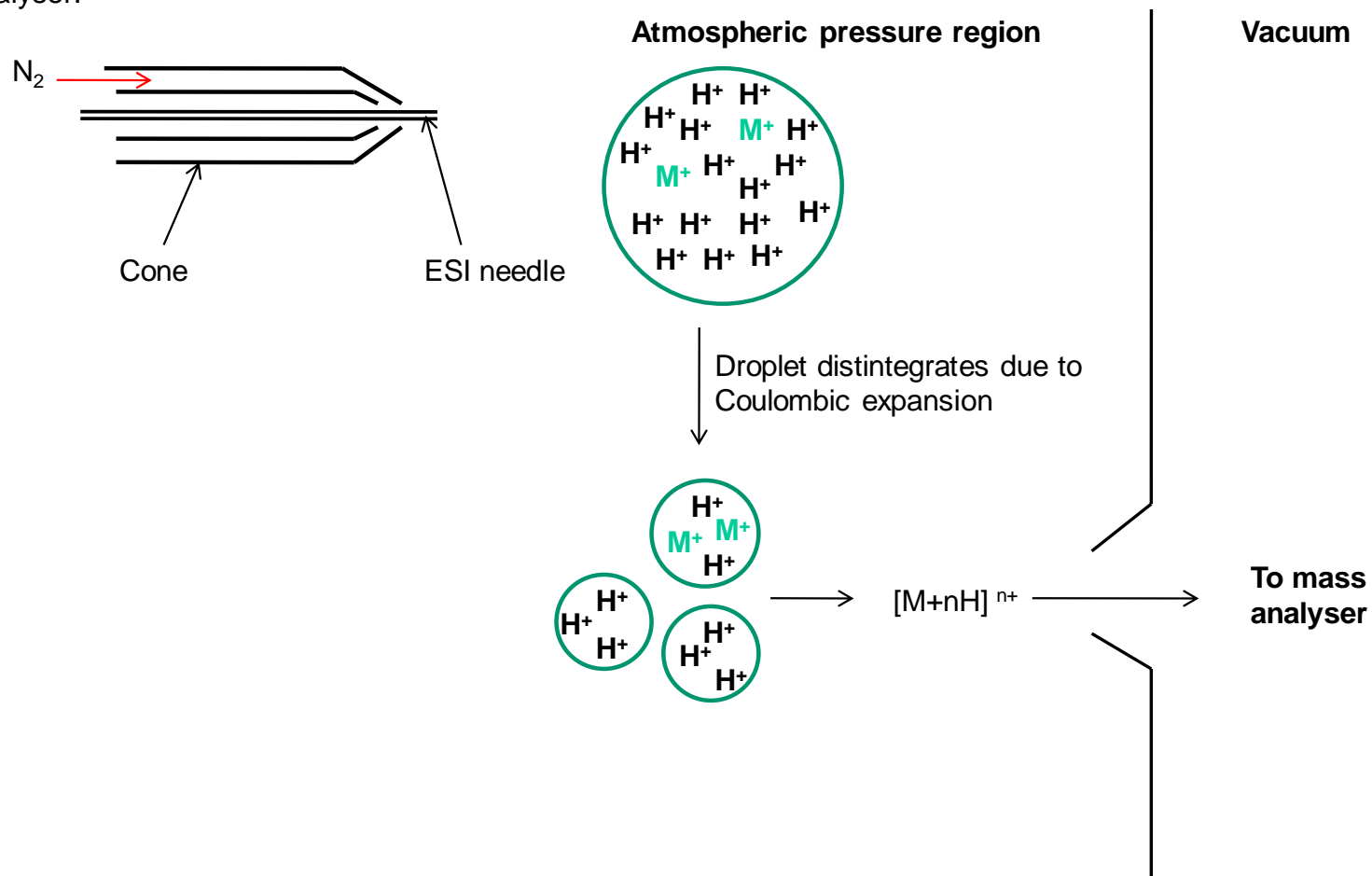
1.7.2. Principles of electrospray ionisation

Electrospray ionization (ESI) is a “soft” ionization technique which allows the production, detection and identification of molecular ions. Biomolecules generally possess complex chemical structures, often with high molecular mass, and they may also be polymers. The ability of ESI to form molecular

ions rather than ion fragments is advantageous for the analysis of biological molecules, since the production of small- sized ion fragments would not give much information on the overall structure of the analysed compound (Hoffman, 2005).

It is essential that compounds to be analysed by ESI-MS are ionized in solution. The sample, dissolved in organic solvent, is introduced to the electrospray needle from a coupled liquid chromatography (LC) system or directly from a syringe pump. The sample comes out of the needle in a fine spray. A potential difference is applied across a cone surrounding the electrospray needle to facilitate the formation of ions inside the sample droplets. An internal heat source is applied to the analyte source and the cone surrounding the electrospray needle to assist the evaporation of solvent, and nitrogen gas is used as a desolvation gas to vaporize the droplets of volatile organic solvent. As the solvent evaporates, the surface tension of the charged droplets increases to such an extent that the highly-charged droplets disintegrate during what is known as “Coulombic expansion” to produce droplets that are much smaller in size. The solvent evaporates from the droplets, leaving behind the ionized analyte.

Figure 1.22 Diagram of the electrospray ionisation (ESI) interface. The sample is dissolved in volatile solvent and injection through a fine needle inside a cone that has a voltage set across it. Large ionized droplets are formed which are reduced in size by evaporation of solvent, assisted by a flow of N₂ gas in the cone. The highly-charged droplet disintegrates as the similar charges repel each other (Coulombic expansion), leaving behind ionized analyte which passes through a vacuum to the analyser.



The formation of ions in solution necessary for ESI-MS may prove difficult for non-polar lipids. However, the formation of lipid species molecular ions in solution can be facilitated by adding ammonium hydroxide to the mass spectrometry solvent. It is alternatively possible to add ammonium sulphate to the mass spectrometry solvent to aid the ionization and separation of acidic lipids (Christie, 2003).

The production of molecular ions rather than ion fragments is advantageous in lipid analysis, since many lipids have a complex chemical structure containing more than one component. For example, sphingophospholipids contain a sphingoid base and fatty acyl chains and glycerophospholipids comprise of a polar head group, glycerol backbone and fatty acyl chains. If only ion fragments of the analysed compound could be recovered, then it would not be possible to calculate the overall structure of many lipid species in a biological sample. ESI-MS produces mainly molecular ions, which provides information on the molecular weight of a species but not on its structure. Phospholipids are difficult to separate using ESI-MS alone because the variation in head group, chain length and saturation of phospholipids means that more than one phospholipid species can have the same molecular weight. In the past, researchers have used chromatography methods coupled to mass spectrometry, for instance, gas chromatography–mass spectrometry (GC-MS) or liquid chromatography–mass spectrometry (LC-MS). However, the recent arrival of electrospray tandem mass spectrometry (ESI-MS/MS) for analysis of biological samples has provided a

highly sensitive method of phospholipid analysis. GC-MS, LC-MS and MS/MS share many advantages: they are high-resolution, sensitive, and rapid (analysis takes minutes), require only a small volume of sample and allow both qualitative and quantitative analysis. However, MS/MS poses an advantage over other methods in that no derivatization of fluorescent lipid products or fatty acid methyl esters (FAME) from fatty acids is necessary.

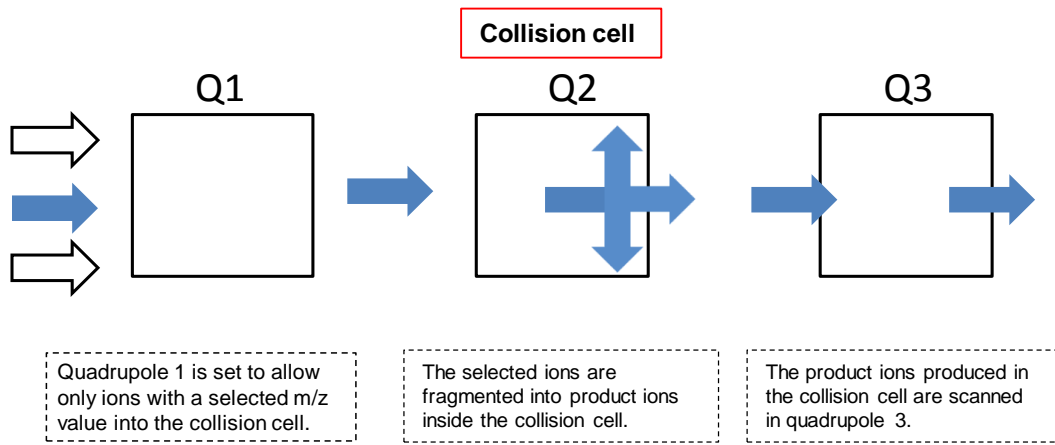
1.7.3. Tandem mass spectroscopy (MS/MS)

Tandem mass spectrometry may be carried out using a triple quadrupole mass spectrometer. A quadrupole consists of four metallic rods, two set at a positive voltage and the other two at a negative voltage. The quadrupole has both electrical and radio voltage components, and the ratio of electrical and radio potential difference determines the mass of the ions which can pass through the quadrupole at the resonance frequency. The first and third quadrupoles in a triple quadrupole mass spectrometer are detection chambers and the second quadrupole is a collision chamber, where high-energy collision of ions leads to fragmentation of ions; this is known as collision-induced dissociation (CID). Figure 1.23 illustrates the three modes of ion scan that can be carried out using tandem mass spectrometry (MS/MS).

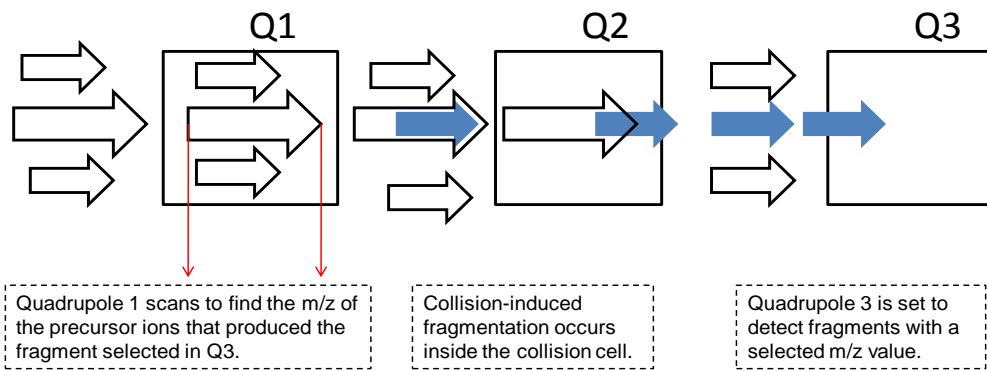
Figure 1.23 Tandem mass spectrometry (MS/MS) ion scanning modes

(Q = quadrupole)

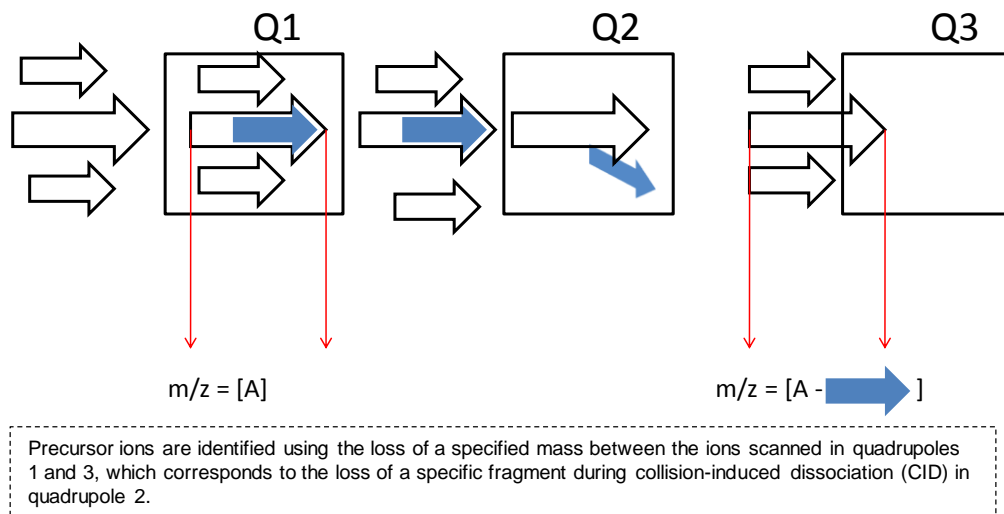
Product ion scanning



Precursor ion scanning



Neutral loss scanning



The use of different settings on quadrupoles 1 and 3 allow three types of ion scan to be carried out using MS/MS:

- a) Product ion scanning, where quadrupole 1 is set to allow only ions with a selected m/z value into the collision cell. The selected ions are fragmented into daughter ions, which are scanned in quadrupole 3.
- b) Precursor ion scanning, where quadrupole 3 is set to detect fragments with a selected m/z value and quadrupole 1 scans to find the m/z of the precursor ions that produce that fragment upon CID in the collision cell.
- c) Neutral loss scanning, where precursor ions are identified using the loss of a specified mass between the ions scanned in quadrupoles 1 and 3, which corresponds to the loss of a specific fragment during CID.

1.7.4. Hybrid analytical techniques

A combination of two or more analytical techniques can be used to produce a hybrid analytical technique (also known as 'hyphenated' analytical techniques due to their shorthand nomenclature) to detect and/or separate compounds from a sample. Over the past 25 years, hyphenated analytical techniques (such as GC-MS and LC-MS) have been developed and become widely used for the analysis of pharmaceutical and biological compounds, including forensic and toxicological analysis. More recently, hyphenated analytical

techniques have been explored as analytical tools to building a molecular profile of biological systems, as seen in proteomics and lipidomics.

Gas chromatography and liquid chromatography are often coupled to another analytical technique because of their ability to analyse a sample without destroying the analyte, and the use of GC and LC coupled to tandem mass spectrometry has been developed over the past twenty years. GC-MS and LC-MS share the advantages of high sensitivity and high specificity, and both methods also provide information-rich detection. The use of a chromatographic method coupled to a mass spectrometer provides information on both the retention time and the fragmentation pattern of a compound, meaning that two compounds which share the same m/z value but have differing retention times can be identified without need for fragmentation studies. Tandem MS coupled to GC or LC offers even higher sensitivity and specificity than MS coupled to one of these methods. For example, HPLC-MS/MS can be used to detect glycerophospholipids and eicosanoids in the picomolar range.

LC-MS offers an additional advantage over GC-MS in that it is not limited to volatile compounds, so compounds with molecular weight of $>500\text{Da}$ can also be analysed using this method. Complex lipids such as glycerophospholipids and ceramides are generally not volatile and tend to have heavier molecular weights. The use of LC-MS for their analysis rather than GC-MS means that derivatization of fatty acid methyl esters (FAME) from glycerophospholipids is

not necessary and that the entire structure of the compound, including information on the positioning of the fatty acyl chain can be determined. LC-MS systems also have lower maintenance requirements than GC-MS systems, which allows continuous analysis of large sample batches.

1.8 Aims and Objectives

Stroke is the third most common cause of death in the United Kingdom and is the most common cause of severe disability (<http://www.stroke.org.uk>). Research efforts in the past were concentrated on the discovery of a pharmacological target which could be blocked in order to reduce neuronal injury following a stroke, but more recent efforts have placed greater emphasis on preventative treatment to make the brain more resistant to the deleterious effects of a reduction in blood supply.

It has been demonstrated that intravenous injections of PUFA can lead to neuroprotective effects in models of ischaemic stroke and epilepsy in rodents (Blondeau et al., 2002, Lauritzen et al., 2000) and that pre-treatment with bioactive lipid mediators can reduce neuronal injury in rodent models of focal ischaemia, but the molecular mechanisms underlying this neuroprotection are unclear.

We speculate that intravenous PUFA treatment may lead to changes in the lipid profile of the mouse. These changes may occur in structural lipids (e.g. glycerophospholipids) or in bioactive lipid mediators (e.g. prostanoids) and may be systemic or limited to the area of protection (i.e. the cerebral cortex). To assess whether intravenous PUFA injection causes changes in the lipidomic profile of the mouse and to determine whether these effects are systemic or localised, we propose to (i) create a profile of cerebral cortex phospholipids in the mouse using mass spectrometry (MS) and tandem mass spectrometry (MS/MS), (ii) investigate whether intravenous fatty acid (ALA) leads to changes in cerebral cortex phospholipid composition at 3, 24, 72 and 168 hours after its administration, (iii) profile lipid mediators (including prostanoids and hydroxy fatty acids) in mouse cerebral cortex and plasma, and (iv) assess the effects of ALA treatment on lipid mediator profiles in mouse cerebral cortex and plasma within the previously determined neuroprotection time window.

2. Materials and Methods

2.1. Experimental strategy

The purpose of this study was to obtain an accurate picture of the lipidomic profile in the living animal. In order to ensure that this result was achieved, we must consider the source of our samples, the methods used for sample collection, sample storage conditions, sample processing methods and analytical methods. This section explores these issues and explains how we developed an experimental strategy for the collection, processing, storage and analysis of tissue and plasma samples that prevented the formation of artefacts from post-mortem metabolic changes and minimised the degradation of glycerophospholipids and lipid mediators.

2.1.1 Use of animals

The growth of three-dimensional brain cell aggregate cultures which contain a mixture of differentiated cell types has been reported using both murine and human tissue (Seeds, 1971; Pulliam et al., 1988). Embryonic cells were used as the source for both of these examples of an *in vitro* model of the developing brain. However, despite developments in cell culture methods and in computer modelling (leading to *in silico* models), a satisfactory model of the

adult brain has not yet been achieved, and as a result, our work necessitates the use of animal models.

Extensive work has been carried out on both the effects of essential fatty acids such as linolenic acid (LA) and α -linolenic acid on rodents and rodent models of brain ischaemia (Lauritzen et al., 2000; Blondeau et al., 2002; Belayev et al., 2005). The neuroprotective effects of PUFA in rat models of ischaemia were demonstrated by Lazundski's group (Lauritzen et al., 2000; Blondeau et al., 2002) and more recent work by the same group also showed a neuroprotective effect of PUFA in mice (Heurteaux et al., unpublished work).

The small size of mice confer them many advantages over rats for our purposes. They are cheaper to acquire and to house than the same number of rats, are easier to kill rapidly and humanely without the use of specialist equipment (e.g. a guillotine), and their smaller-sized brains can be metabolically inactivated more rapidly than the larger rat brains. The small sample size required for lipidomic analysis means it is not necessary to collect a large amount of brain tissue for analytical purposes, and each mouse yielded enough brain tissue to allow both phospholipid analysis and lipid mediator analysis, keeping the number of animals required to a minimum.

The C57/BL6 mouse strain was selected because this is the strain that is commonly used for mouse models of stroke and cerebrovascular disease, and only male mice were used to eliminate the possibility of sex differences. This is also the same strain and sex that were used for the study on the neuroprotective effects of PUFA in mice (Heurteaux et al., unpublished work).

2.1.2. Metabolic inactivation of the brain

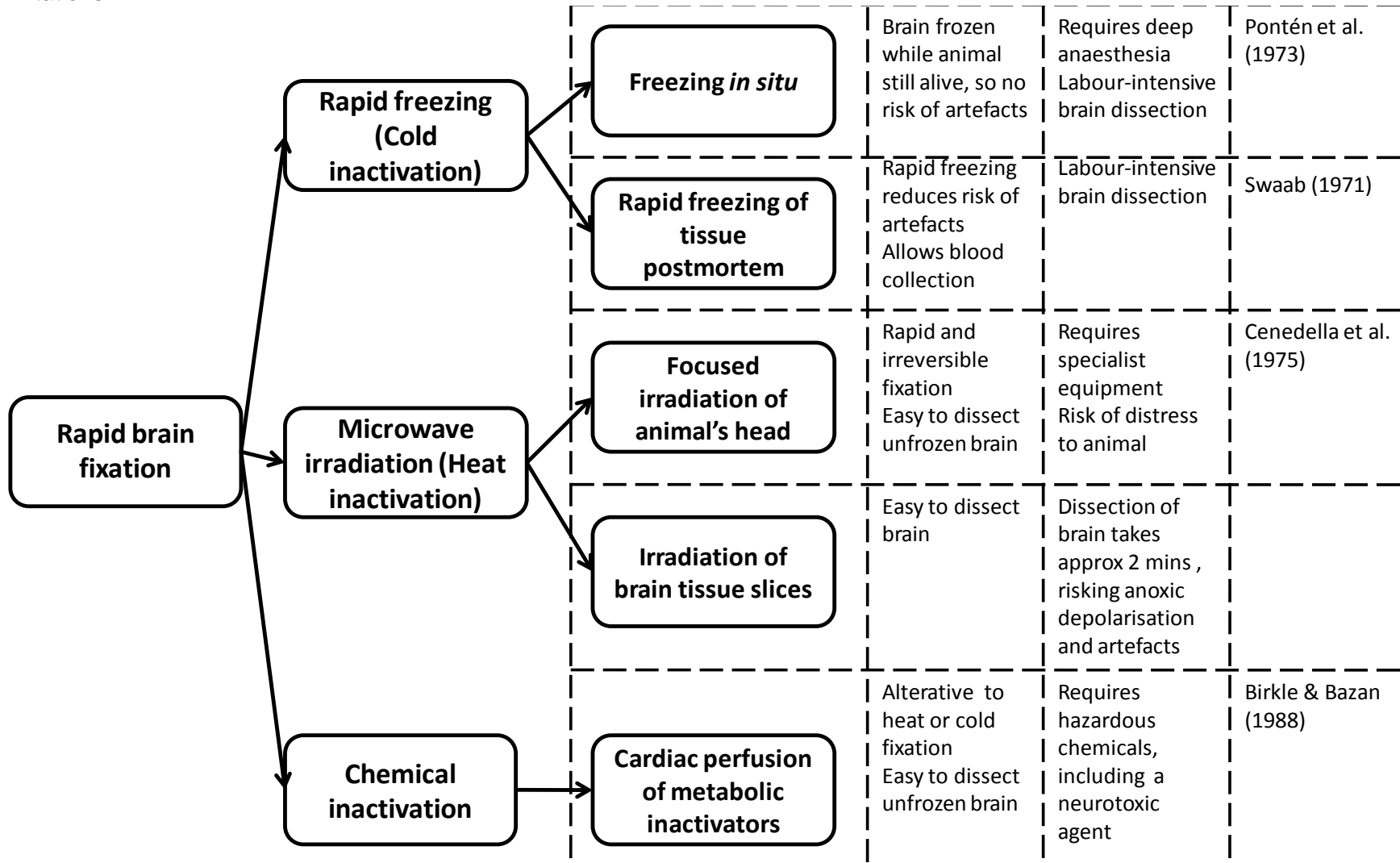
It has been known since the 1970s that rapid post-mortem changes occur in brain lipids (Bazan, 1970), including the autolysis of phospholipids, an increase in free fatty acids, and oxidation of lipids (Lee & Hajra, 1991). Ischaemia leads to failure of ion-exchange pumps, causing anoxic depolarisation. This process leads to a massive influx of Ca^{2+} ions entering the neuronal cell via receptor-linked ion channels. The Ca^{2+} ions activate calcium – dependent phospholipases and kinases, such as phospholipase A_2 (PLA_2), which hydrolyses phospholipids at the sn-2 position. Free fatty acids (FFA) are released from the hydrolysed phospholipids, which serve as a substrate pool for bioactive lipid mediators. As shortly as 90s after cessation of blood supply to the brain, concentrations of FFA and diacylglycerols (DAG) in the brain can rise dramatically whilst the concentration of phospholipids falls (Lee & Hajra, 1991).

In order to ensure that an accurate picture of the living brain's lipidomic profile is obtained, sample collection and processing methods were selected to

result in minimal post-mortem changes and to prevent the formation of artefacts. Metabolic inactivation of the brain (also referred to as fixation of the brain, since the tissue's metabolic status is kept in a fixed state) was used during sample collection, and samples were processed in such a way as to minimise the degradation of glycerophospholipids and lipid mediators.

The brain is known to be a difficult organ to metabolically inactivate, owing to its encasement in bone, high metabolic demands, and susceptibility to rapid changes in metabolic status during ischaemia, in particular following anoxic depolarisation. Two conventional ways of metabolic inactivation of the brain, heating (using microwave irradiation) and cooling (freezing), have been well-documented since the 1970s. More recently, an alternative method of brain metabolic inactivation by inactivation of metabolic processes was reported (Bazan & Birkle, 1988). Figure 2.1 provides a summary of the brain fixation methods available and the advantages and limitations of each fixation method.

Figure 2.1 Brain metabolic processes can be inactivated by cold, heat or chemical inactivators – each method has advantages and limitations



2.1.2.1. Heat inactivation

The most rapid method of brain fixation using heat is focused high-power microwave irradiation. Microwaves are directed onto an unanaesthetised animal's head, causing rapid heating of the brain tissue and leading to the metabolic fixation of the brain and rapid death of the animal. Brain fixation using microwaves prevents all post-mortem metabolic changes and the brain is quickly and irreversibly fixed (Cenedella et al., 1975; Murphy, 2009). It also has the advantage of keeping the tissue's histological structure intact. An alternative to irradiation of the live animal is rapid killing of the animal, dissection of the brain out of the skull and irradiation of tissue slices.

A disadvantage of heat inactivation of brain tissue is that, many naturally-occurring lipids, in particular PUFA, are susceptible to oxidation at high temperatures. This raises the issue of whether PUFA oxidation at high temperatures would occur during microwave irradiation, which could cause the production of hydroxy fatty acids that have bioactive properties themselves, or alternatively lead to the depletion of substrate for production of bioactive lipid mediators. However, previous work on analysis of lipid mediators in the brain did not show an increase in PUFA metabolites in animals killed by microwave irradiation compared to those killed by decapitation (Bazinet et al., 2005; Farias et al., 2008), suggesting that the brief heating of the brain during focussed microwave irradiation does not lead to heat degradation of lipids.

2.1.2.2. Cold inactivation (freezing)

Many methods of brain fixation by cooling are also available, of which the most widely reported is freezing of the brain *in situ*. This method allows the freezing of the surface tissues whilst still allowing blood flow to deeper tissues, preventing ischaemia and anoxic depolarisation occurring in the deeper tissues whilst the surface tissue is being frozen. It has been successfully been used in rats and in mice, as well as larger experimental animals, such as cats (Yang et al., 1983).

There are method variations within *in situ* freezing of the brain, such as “funnel freezing”, carried out by anaesthetizing the animal, making an incision in the skin on the head and pouring liquid nitrogen directly onto the skull (Pontén et al., 1973), “freeze blowing”, where high-pressure airflow through two cranial probes is used to eject brain tissue from a conscious animal into a pre-cooled chamber (Veech et al., 1973) and the “box method”, where a Styrofoam box fitted around an animal’s head is filled with liquid nitrogen and used to rapidly cool the brain (Yang et al., 1983).

Freezing of the brain *in situ* is of particular use in larger animals, where freezing the whole head takes considerably longer than in mice due to larger brain volume and the insulating effect of a thicker skull. The “box method” can

be used to freeze brain surface tissues of even large experimental animals (Obrenovitch et al., 1988).

Another possibility in our study due to the small size of the mouse's brain is to drop the whole animal into liquid nitrogen without the use of anaesthesia. This brings instant death and freezes the brain in under a minute, rapid enough to prevent ischaemic artefacts from occurring (Swaab, 1971). To ensure minimal pain and distress, as required by the Animals (Scientific Procedures) Act 1986, the animal would have to be anaesthetised prior to sacrifice and tissue freezing. However, although blood could be collected from the heart after recovering the animal from the liquid nitrogen, the blood would have undergone haemolysis, meaning that only whole blood could be analysed rather than plasma. An alternative to dropping the whole animal into liquid nitrogen is to sacrifice the anaesthetised animal by decapitation, letting the head fall into a Dewar flask of liquid nitrogen whilst collecting blood into anticoagulant-containing centrifugation tubes on ice. This method allows rapid freezing of the mouse brain, yet still allows easy collection of a blood sample. An advantage of this method over immersion into liquid nitrogen is that the lipid profile of plasma can be analysed, since the blood sample is not frozen and therefore does not haemolyse.

Another option is to anaesthetize and decapitate the mouse, dissect the brain from the head on ice and dropping the dissected tissue into liquid nitrogen to

freeze it. It is possible to dissect the brain from the head in fewer than two minutes and once immersed in liquid nitrogen, the cortex would be expected to freeze in seconds. However, since anoxic depolarisation occurs as shortly as ninety seconds after death, this method may not freeze the brain quickly enough to avoid ischaemic artefact and achieve reliable data.

2.1.2.3. Chemical inactivation

Birkle and Bazan (1988) described an alternative to heat or cold metabolic inactivation of the brain, where cardiac perfusion with a cocktail of metabolic inhibitors and calcium chelators was used to chemically fix brain tissue. Two inhibitors of PLA₂, p-bromophenylacetyl bromide (pBPB) and diisopropyl fluorophosphate (DFP) were used to inactivate PLA₂, ethylditetraacetate (EDTA) was used to chelate free intracellular Ca²⁺ ions and nordihydroguaiaretic acid (NDGA), an antioxidant and an inhibitor of lipoxygenase (LOX), was used to prevent the oxidation of cerebral lipids. The described method could be modified to allow blood collection by cardiac puncture before perfusing the heart with the chemical mixture. The brain retains its histological structure and its dissection from the perfused animal is a rapid and simple process in contrast to the dissection of frozen brain tissue.

2.1.2.4. Selection of a metabolic inactivation method

The importance of selecting an appropriate method of brain fixation to prevent the occurrence of artefacts was illustrated by a study by Farias and

colleagues on LC-MS/MS analysis of brain lipids (Farias et al., 2008). Groups of mice were subjected to one of three brain sample collection methods: (i) focused microwave irradiation of animal's head, followed by dissection of brain (ii) decapitation of animal, followed by dissection of brain, and (iii) decapitation of animal, exposure to the environment for 5 min, followed by focused microwave irradiation and then dissection of the brain. The use of microwave irradiation prior to brain dissection resulted in a significantly lower brain prostaglandin D₂ (PGD₂) concentration compared to the other two sample collection methods but there was no significant difference in brain PGD₂ between the groups of animals that were decapitated, indicating that the fixation process did not stimulate production of brain PGD₂ (Farias et al., 2008). The authors concluded that the elevated level of brain PGD₂ observed in animals not subjected to microwave irradiation was due to ischaemic artefacts, and that microwave fixation was an effective method of preventing artefacts in brain lipid analysis. This study would support our theory that dissection of mouse brain on ice would not be rapid enough to prevent ischaemia-induced metabolic changes in the brain and that an improved method of fixation is required.

Heat fixation using microwave irradiation has been described as a humane method of euthanasia for small rodents if the instrument used is capable of inducing rapid unconsciousness (Animal Procedures Committee report, 2006). High-energy microwave irradiation using powerful equipment can fulfil

this condition, quickly and irreversibly deactivating enzymes in the brain. However, the high temperatures achieved in an animal's brain, even when subjected to only a brief period of microwave irradiation raises the question of whether heat-labile compounds, such as PUFA, would be degraded by the fixation process. The use of high-powered microwave irradiation does not appear to be commonplace, especially in the United Kingdom, and the use of low-power equipment could lead to a slower death, potentially causing distress and suffering to the animal. Therefore, the lack of access in our laboratory to suitably high-powered microwave irradiation equipment effectively precludes the use of microwave irradiation as a method of fixing brain tissue in this study.

Chemical inhibition of brain tissue metabolism initially appears to have many advantages as a brain fixation method. Firstly, no specialist equipment is required for this method, secondly, blood can also be collected unlike as in freezing of the whole animal and thirdly, dissection of the fixed brain is easy and rapid compared to that of frozen tissue. However, this method has the disadvantage of requiring hazardous chemicals, including an acute neurotoxin and a chronic mutagenic agent. Rodent toxicity studies on the anti-cholinesterase DFP have shown a very low LD₅₀ in both rats and mice through oral, inhalation or transdermal routes (www.sciencelab.com/xMSDS-Diisopropyl_Fluorophosphate-9927520). DFP is harmful if absorbed in large quantities through the skin, can cause severe damage to mucosal tissues

including eyes and the respiratory tract and can even be lethal if swallowed (<https://fscimage.fishersci.com/msds/41368>). NDGA is an irritant to mucosal tissues, including the respiratory tract and is potentially harmful if ingested or absorbed through the skin (<http://www.caymanchem.com/msdss/70300>). BPB is also very destructive of mucosal tissues and can be fatal if inhaled.

The toxicity and potential mutagenic properties of some of these chemical metabolic inactivator compounds poses questions as to whether their use can be justified. Although the health risks posed to users of animal laboratory facilities can be minimised by thorough decontamination of the laboratory area and occupational health screening, the use of departmental shared facilities for tissue sectioning means that there is a risk of exposing other personnel to traces of these compounds during the processing of tissue samples. Since there are alternative brain fixation methods available which do not require the use of such hazardous chemicals, the use of chemical inactivators for metabolic inactivation were deemed unacceptable under the School of Life Sciences' COSHH guidelines, and so brain fixation by cardiac perfusion of brain metabolic inhibitors could not be considered for this study.

This essentially leaves freezing as the only available method of brain fixation for this study. Freezing *in situ* involves freezing the outer layers of brain tissue whilst still allowing blood to penetrate the deeper layers of tissue, preventing anoxic depolarisation from occurring in deep tissue layers before they can be

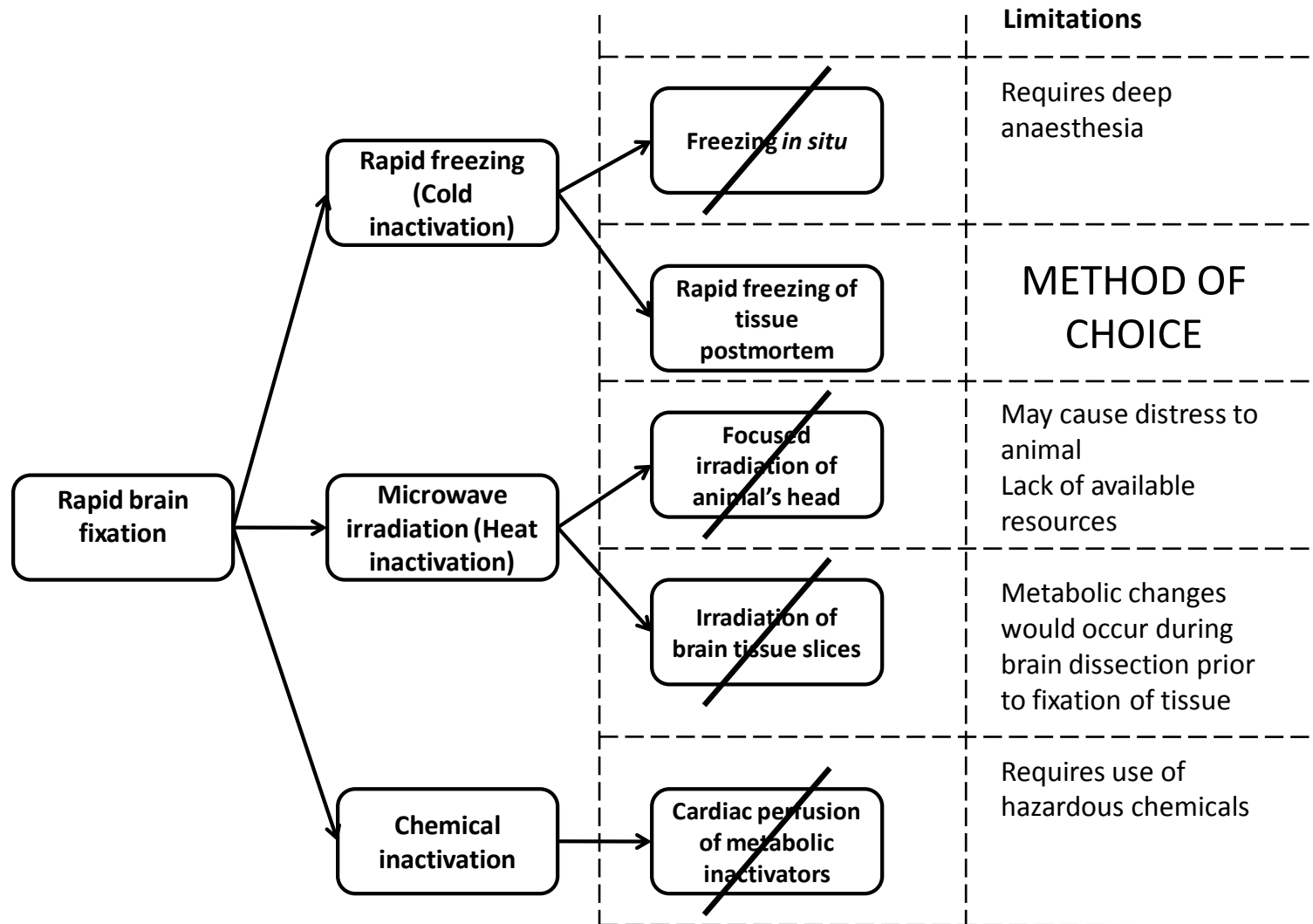
frozen. This method also allows the removal of a blood sample while the brain is being frozen or after the process has been completed.

However, since mice are small enough to be able to freeze the whole head of the animal in under a minute, the brain does not necessarily need to be frozen *in situ* to prevent anoxic depolarisation occurring in deeper brain tissues. The whole animal or the head of an anaesthetised animal could be frozen by immersion in liquid nitrogen instead, removing the need for a complicated experimental set-up as in freezing *in situ*. However, if plasma is to be analyzed, unfrozen blood must be collected, which rules out dropping the whole animal into liquid nitrogen.

Our need for the collection of unfrozen blood and rapid post-mortem freezing of brain tissue means that decapitation can be considered as a method of animal sacrifice. This method allows easy collection of blood from the carotid arteries and if the animal's head is immediately dropped into liquid nitrogen, ensures rapid freezing of the brain before anoxic depolarisation can take place. The dissection of the cerebral cortex out of the frozen head, whilst laborious, is a straightforward process compared to the dissection of frozen cerebral cortex from an animal with its brain frozen *in situ* or the collection of blood from an animal in a stereotactic frame setup for freezing *in situ*.

The following figure illustrates the decision-making process which led to the choice of a method for the collection of blood and brain samples and the fixation of brain tissue. The preferred method was sacrifice of an anaesthetised animal by decapitation, followed by rapid post-mortem freezing of brain tissue. This method requires no specialist equipment, does not involve the use of toxic chemicals and is an efficient method of fixing brain tissue. It also has the advantage of allowing the collection of a blood sample as well as brain tissue from the same animal, reducing the total number of mice required for studies on both brain and plasma lipids, in accordance with the principles of the 3Rs (“Reduce, Refine, Replace”) promoted by the National Centre for the Replacement, Refinement and Reduction of Animals in Research (<http://www.nc3rs.org.uk/>).

Figure 2.2 Selection of brain metabolic inactivation method was carried out by a process of elimination

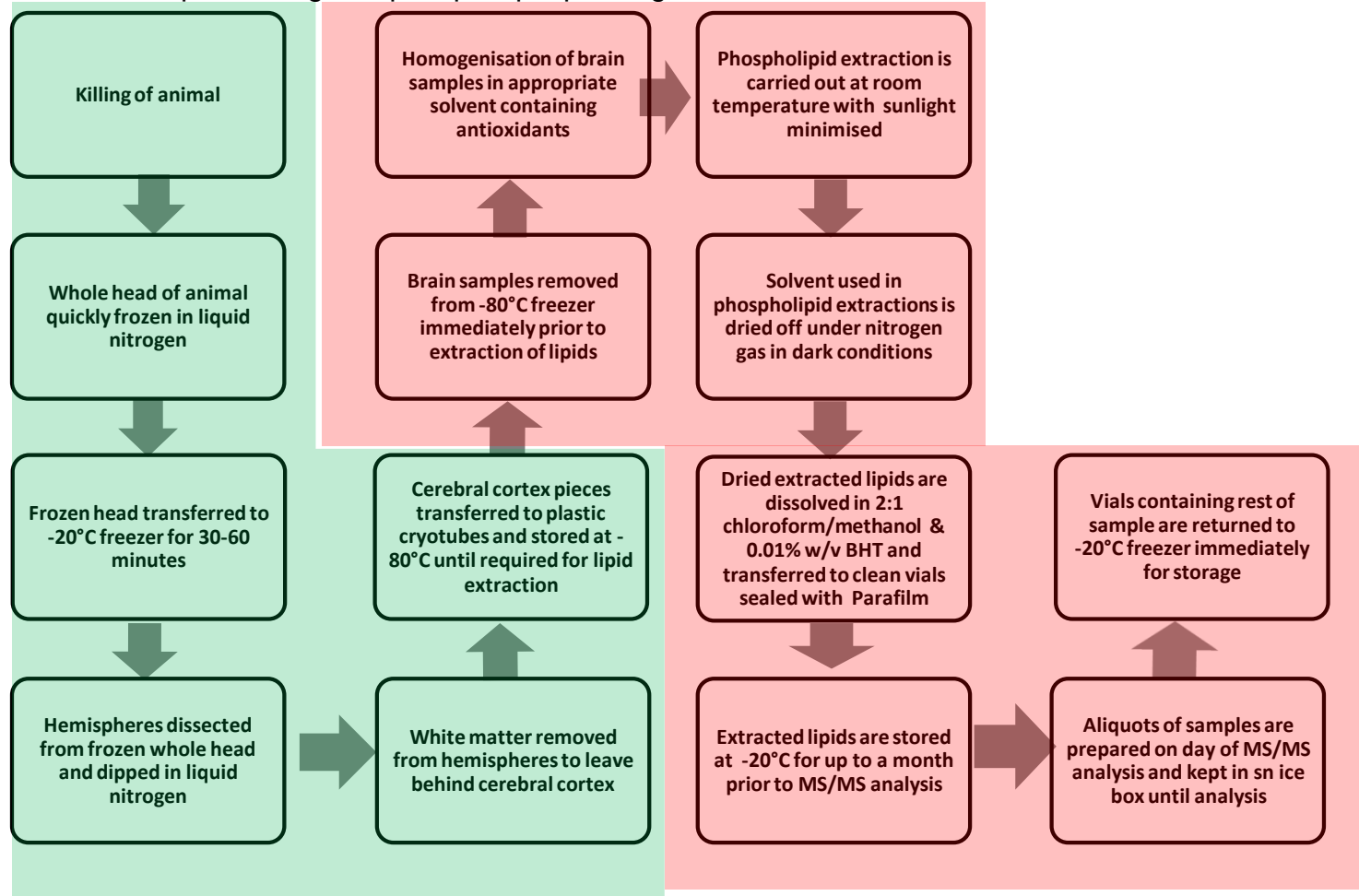


2.1.3. Tissue storage, processing and analytical issues

Care was taken during the extraction process to ensure that minimal degradation of the samples occurred, because lipid mediators are particularly vulnerable to free radical-mediated oxidation upon exposure to UV radiation. Exposure of samples to direct sunlight was minimised using blinds on the laboratory windows and by carrying out extractions earlier during the day (when the sun was not directly upon the west-facing laboratory's windows). Homogenisation of brain samples was carried out on ice and samples were kept on ice at all times unless they were undergoing extraction processes that could not be carried out in an ice box, for example, vortexing, centrifugation and solid phase extraction. During centrifugation, the temperature of the centrifuge was set to 4°C. Extraction solvents were gently dried off under nitrogen gas in a dark environment to prevent oxidation of phospholipids and lipid mediators. Amber glass vials were used to store samples that contained extracted lipid mediators to minimise exposure of eicosanoids to light. Butyl hydroxy toluene (BHT), an antioxidant, was added to the extraction solvents to prevent oxidation and to enable storage of lipids for up to a month at -20°C. However, to minimise the risk of sample oxidation after extraction and before lipidomic analysis, sample extraction was carried out no more than a week prior to analysis where possible. Figures 2.3 – 2.5 illustrate the processes involved the collection, storage, extraction and phospholipid analysis of

mouse cerebral cortex samples, and collection, storage, extraction and lipid mediator analysis of mouse cerebral cortex and plasma.

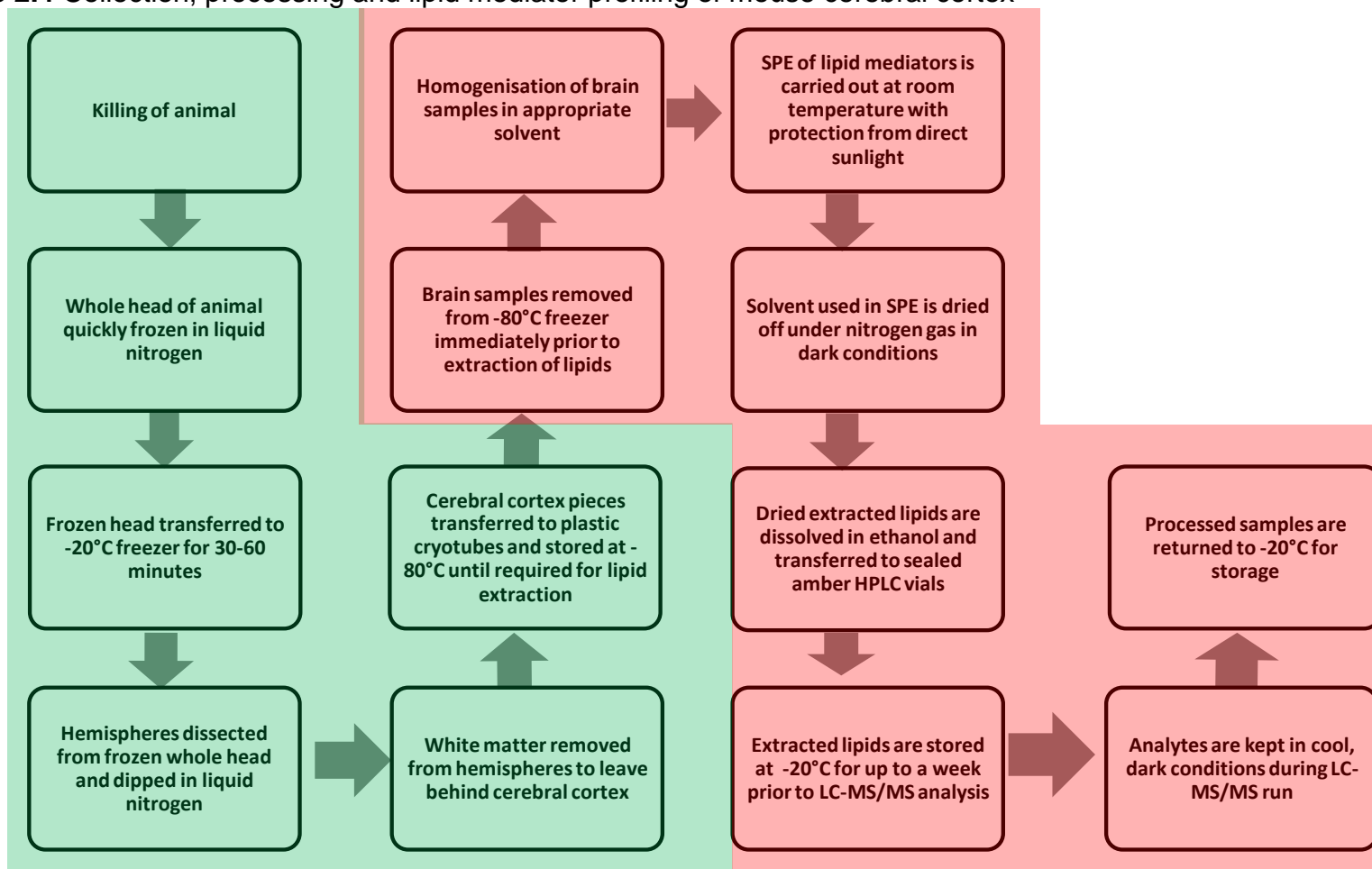
Figure 2.3 Collection, processing and phospholipid profiling of mouse cerebral cortex



Sample collection process shaded in green

Sample analysis process shaded in red

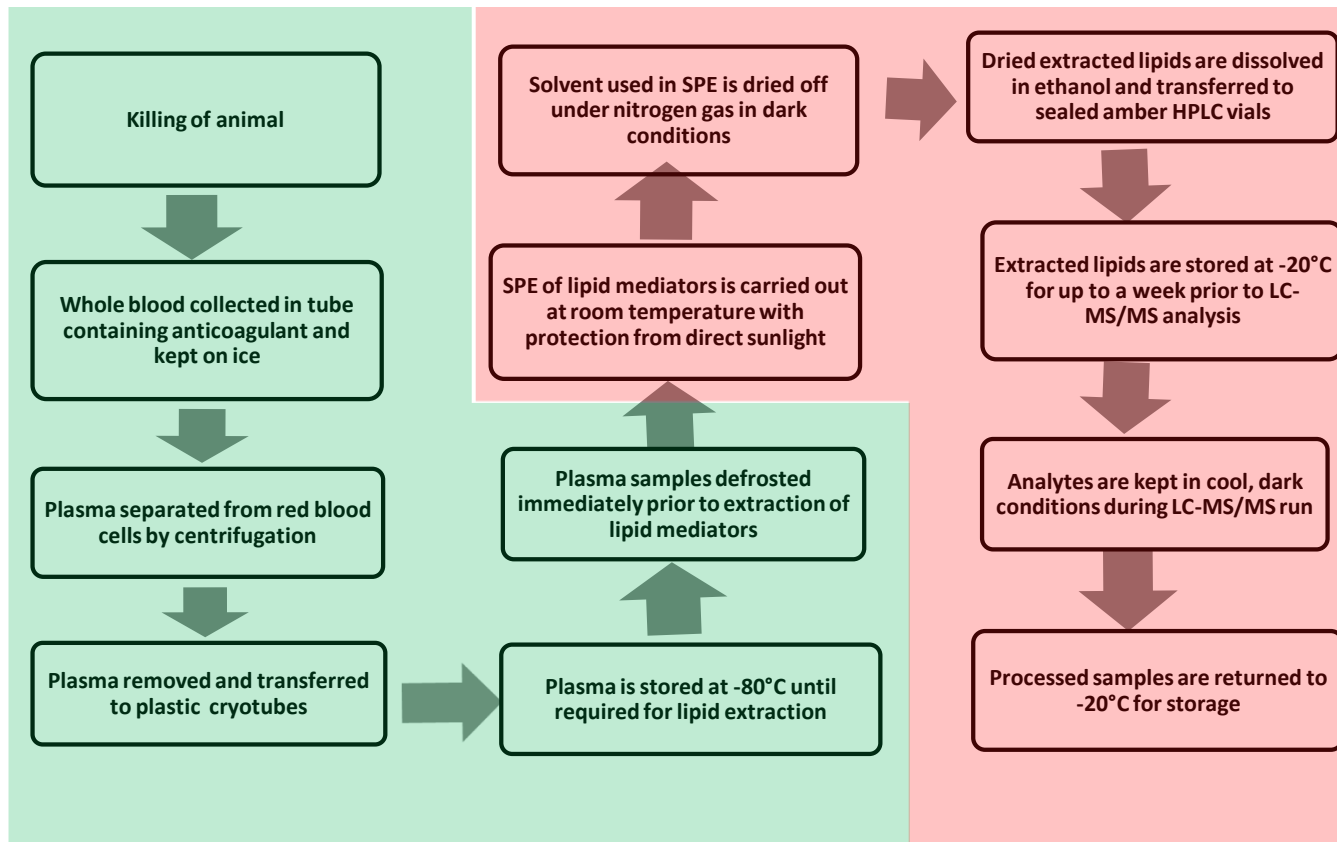
Figure 2.4 Collection, processing and lipid mediator profiling of mouse cerebral cortex



Sample collection process shaded in green

Sample analysis process shaded in red

Figure 2.5 Collection, processing and lipid mediator profiling of mouse plasma



Sample collection process shaded in green

Sample analysis process shaded in red

2.2. Animal treatments

2.2.1. Care and welfare of animals

Young adult male C57/BL6 mice (aged 8 – 16 weeks) obtained from Harlan (Bicester, Oxfordshire, UK) were used throughout. All procedures were carried out in designated premises under Home Office licensing in accordance with the Animals (Scientific Procedures) Act (1986), and with ethical approval from the University ethical review process. Animals were housed in a controlled environment (21 ± 2 °C, 40-60% relative humidity) in consecutive 12 hour cycles of light and dark, and had free access to food and water. All animals were fed on a standard laboratory rodent diet (Harlan Teklad, Bicester, Oxfordshire, UK).

2.2.2. Preparation of alpha linoleic acid or vehicle

α -Linolenic acid (18:3n-3, ALA), like many other PUFA, is thermally labile and is also sensitive to light. Care was taken to minimise exposure of the compound to light, including the selection of amber glass vials were selected for preparation of an ALA solution or vehicle. A 1 M solution of ALA was prepared by dissolving 139 mg of free fatty acid (Sigma-Aldrich, Poole, Dorset, UK) in 0.5ml of ethanol (Fisher Chemicals Ltd, Loughborough, Leicestershire, UK) in an amber glass vial (Sigma-Aldrich, Poole, Dorset, UK). This stock solution was sonicated for two minutes to ensure that all the fatty acid had thoroughly dissolved, then subsequently used to prepare a 50 μ M

ALA solution in 0.9% NaCl, through serial dilution, with an overall dilution factor of 1:20,000. The ALA solution for injection was prepared immediately prior to use in order to ensure that minimal degradation of the compound occurred.

2.2.3. Intravenous injection of alpha linoleic acid or vehicle

The tail vein injections were carried out in a darkened room with a spotlight lamp located next to a purpose-made mouse restrainer (Vet Tech Solutions Ltd, Congleton, Cheshire, UK). Light was concentrated on the area where the mouse entered the restrainer so that exposure of ALA to light could be minimised. The brightness of the light also encouraged the mouse to enter the darker environment of the tube-shaped restrainer.

Male C57/BL6 mice were placed inside a purpose – made restrainer and a local anaesthetic (5% EMLA cream, Astra Pharmaceuticals, Kings Langley, Hertfordshire, UK) was spread over each mouse's tail. The moisture of the EMLA made the tail vein easier to see on the black mice and also caused vasodilation, making the injection process easier for the researcher and less distressing for the mice. 0.0139mg/kg of ALA was injected into the tail vein of the mouse using a disposable syringe (Terumo, Leuven, Belgium) and a 27 gauge winged infusion set (Vygon UK, Cirencester, Gloucestershire, UK). The corresponding vehicle (0.005% v/v ethanol in 0.9% NaCl) was used as controls for drug-treated animals.

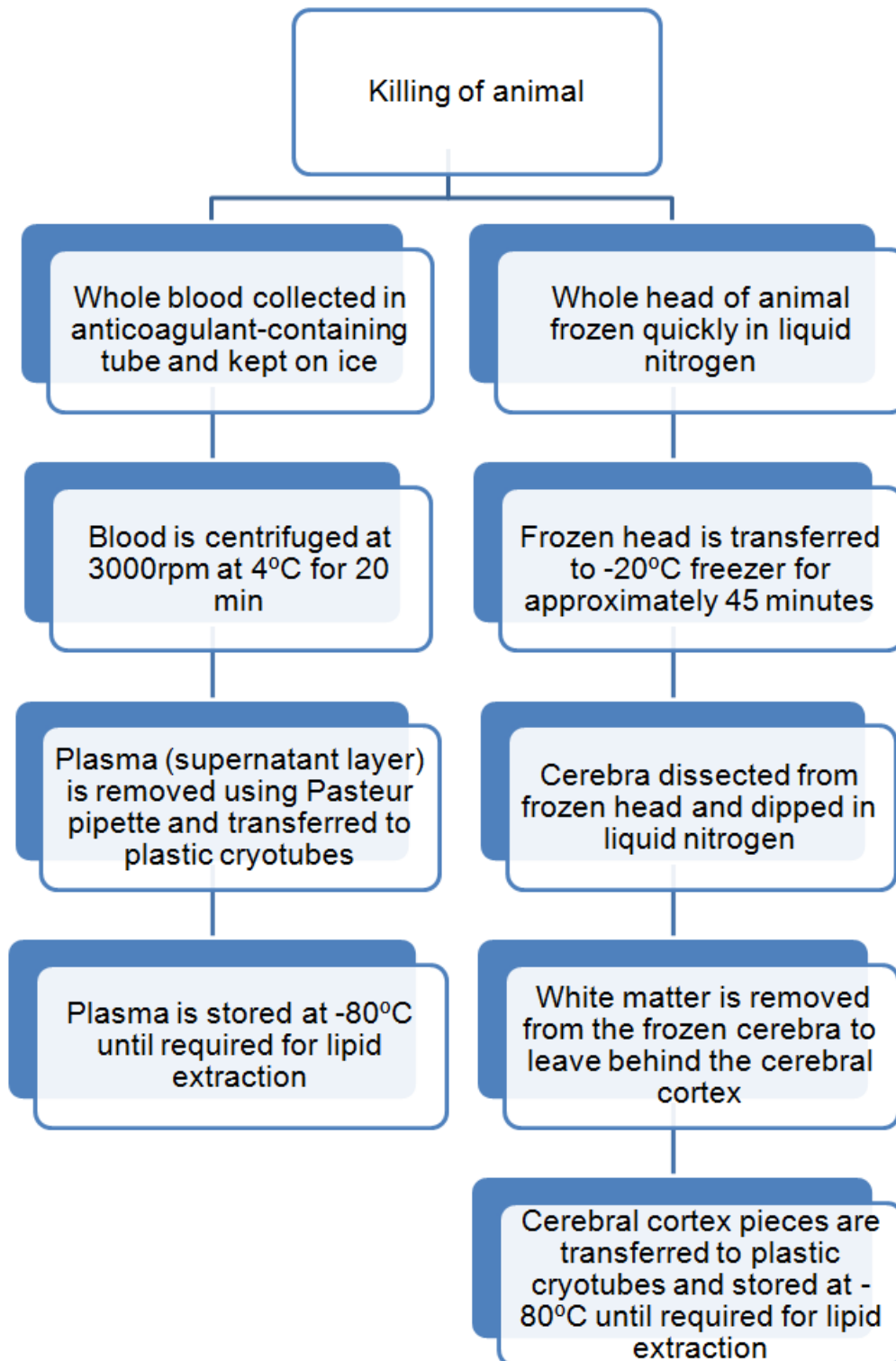
2.2.4. Sample collection

Anaesthesia was induced in the mouse by exposure to 5% halothane in 2:1 N₂O:O₂ for 3 minutes, and the anaesthetized animal was then rapidly killed by decapitation. The head was allowed to fall into a Dewar flask of liquid nitrogen and blood from the severed neck arteries was collected into centrifugation tubes containing an anticoagulant solution of 0.1 ml sodium EDTA in 0.5 M NaOH (both from Sigma-Aldrich, Poole, Dorset, UK) and kept in an ice bucket. The blood samples were centrifuged at 3000 rpm at 4°C for 20 min and the plasma (supernatant layer) was pipetted into cryotubes using glass Pasteur pipettes. Each plasma sample had a volume of approximately 300-400µL and they were stored in plastic cryotubes at -80°C until required for analysis.

The frozen mouse heads were allowed to remain in the liquid nitrogen for approximately 5 minutes after the animal's death, and were then transferred to a -20°C freezer for approximately 45 min to allow their temperature to equilibrate at around -20°C. Once the temperature of the mouse heads had increased sufficiently to make dissection of the brain from the head feasible, they were collected from the -20°C freezer and the cerebra were dissected from the heads in a cooled environment using metal tools that had been cooled by dipping in liquid nitrogen. The dissected-out cerebra were frequently dipped into a small vessel of liquid nitrogen to ensure that they remained frozen throughout the dissection process. Once removed from the

liquid nitrogen, room-temperature tools were used to scoop out the white matter out of the cerebra, leaving behind the cerebral cortex. At optimum dissecting temperature, the consistency of the white matter is that of hard ice cream, whilst the grey matter is frozen solid. The grey matter left behind after dissecting out the white matter was placed in cryotubes that had been cooled by dipping inside the liquid nitrogen vessel and stored at -80°C until extraction. Figure 2.6 demonstrates the different processes undertaken in preparing plasma and cerebral cortex samples for storage prior to lipid extraction.

Figure 2.6 Brain and blood sample collection and preparation for lipid extractions



2.3. Lipid extraction

2.3.1. Liquid/liquid extraction of phospholipids

Phospholipids were extracted from mouse cerebral cortex samples using a modification of the Folch method (Folch et al., 1957). All organic solvents used in this process were purchased from Fisher Chemicals Ltd (Loughborough, Leicestershire, UK) and other chemicals were bought from Sigma-Aldrich (Poole, Dorset, UK). Samples of mouse brain tissue were homogenised in 0.5 ml water and 3 ml of 2:1 v/v chloroform-methanol mixture containing 0.01% BHT. The samples were each vortexed for 5 min, and then centrifuged at 2000 rpm for 5 min at 4°C to separate the aqueous and organic phases. The organic phase was removed and the remainder was re-extracted with 0.5 ml water and 4 ml of 2:1 v/v chloroform-methanol mixture containing 0.01% BHT. Each sample was again vortexed for 5 min and centrifuged at 2000 rpm for 5 min at 4°C. The organic extracts from both cycles of extraction were combined and washed twice with 2 ml of 0.5 KCl in 50% v/v methanol-water. After washing, the combined extracts were dried over anhydrous sodium sulphate and filtered through Pasteur pipettes packed tightly with cotton wool. The filtered extracts were dried gently under a stream of nitrogen gas until no liquid remained, and the residue dissolved in 1ml of 2:1 chloroform-methanol solution with 0.01% w/v BHT added. The vials were then flushed with nitrogen gas and wrapped with parafilm to ensure that the vials containing the extracts were airtight. The extracted sample in storage solvent could be stored at – 20°C or -80°C until required for analysis.

2.3.2. Solid phase extraction (SPE) of lipid mediators

All organic solvents used in this process were purchased from Fisher Chemicals Ltd (Loughborough, Leicestershire, UK) and other chemicals were bought from Sigma-Aldrich (Poole, Dorset, UK). Brain tissue samples were homogenised (approximately 50 up and down strokes) in deionised water using a glass Dounce mini homogeniser with a tight-fitting pestle (Wheaton Micro-homogeniser kit, VWR, Lutterworth, Leicestershire, UK). The tissues were kept on ice during the homogenisation process. The homogenate was adjusted to 15% v/v methanol and a final volume of 3ml. 2.8ml deionised water was added to 200µl aliquots of plasma to achieve a total sample volume of 3ml. 530 µl of methanol and 40µl of 1ng/ml PGB₂-d₄ (Cayman Chemicals, Ann Arbor, MI) dissolved in ethanol were added to each sample. The samples were kept on ice for 30 min, then centrifuged at 3000 rpm for 5 min to remove precipitated proteins. The supernatant was removed to a clean glass vial and pH adjusted to pH 3.0 using 0.025M HCl. The acidified sample was added to SPE cartridges (Strata C18-E, Phenomenex, Manchester, UK) which had been preconditioned with 20ml of methanol, followed by 20ml of deionised water and allowed to pass through drop-wise.

After the samples had run through the cartridges, 20ml of 15% (v/v) methanol was run through the SPE cartridges, followed by 20ml of deionised water and 10ml of hexane. Finally, 10ml of methyl formate was run through the SPE cartridges to extract the lipid mediators and collected in glass extraction

tubes. The extracted eicosanoids were dried under a gentle stream of nitrogen gas until no visible liquid remained. 100µl of ethanol was added to the glass tube, taking care to dissolve the lipid residue thoroughly in the ethanol. The ethanolic solution was transferred to a 100µl glass vial insert that was placed inside a 2ml HPLC amber glass vial (both from Sigma-Aldrich, Poole, Dorset, UK), and then stored at -20°C until required for analysis.

2.4. Lipidomic Analysis

2.4.1. ESI-MS/MS of phospholipids

Analysis of phospholipids was carried out using a triple quadrupole (3Q) mass spectrometer (Quattro Ultima model, Waters, Manchester, UK) with MassLynx 4.0 software. An aliquot of 100µl extracted sample was mixed with 200µl of 70:20:10:3 chloroform: methanol: 10% ammonium hydroxide (aq): water.

General scans of phosphatidylcholine, sphingomyelin and phosphatidylethanolamine species were carried out in ES+ mode and general scans of phosphatidylserine and phosphatidylinositol species in ES – mode, using the instrument parameters described in Table 2.1. The acquisition time for each scan was 24 seconds.

Table 2.1 Instrument parameters for general scanning in ES+ and ES- modes

Instrument (3Q) parameter	ES –	ES +
Polarity	ES –	ES +
Capillary voltage (kV)	2.60	2.30
Cone voltage (V)	55.0	60.0
RF Lens 1	7.6	5.0
Aperture	0.0	0.0
RF Lens 2	1.0	1.0
Source temperature (° C)	80	80
Desolvation temperature (° C)	150	150
Cone Gas Flow (L/hr)	60	60
Desolvation Gas Flow (L/hr)	380	380
LM (Low mass ion) Resolution MS1	14.8	14.8
HM (High mass ion) Resolution MS1	14.5	14.5
Ion Energy	0.5	0.3
Entrance	14	15
Collision Energy (eV)	0	0
Exit	17	20
LM (Low mass ion) Resolution MS2	13.5	13.5
HM (High mass ion) Resolution MS2	13.5	13.5
Ion Energy 2	2.0	0.6
Multiplier (gain)	610	610

In addition to a general scan, two types of fragmentation scans were carried out on each sample: (a) neutral loss scans, where the precursor ions are detected on the basis of a loss of a fragment with a specified m/z value during CID, and (b) precursor ion scans, which reports the m/z value of precursor ions whose fragmentation leads to production of ion fragments with a specified m/z value. The scanning parameters are dependent on the polar

head group of the phospholipid class. Phosphatidylcholines and sphingomyelins are identified through the production of a choline ion (with an m/z of 184) lost from the head group of both classes of phospholipids. Fragmentation of phosphatidylinositol species in the ES- mode results in the production of inositol, which has an m/z value of 241. The loss of ethanolamine from phosphatidylethanolamine species results in the production of a daughter ion with a m/z value 141 less than the parent ion. Similarly, the loss of serine from a phosphatidylserine upon fragmentation of the molecular ion results in a product ion with its m/z value 87 less than the original molecular ion.

Table 2.2 Tandem mass spectrometry parameters for the analysis of phospholipid classes in mouse brain tissue

Phospholipid class	Scanning mode
Phosphatidylcholine	Precursors of m/z 184 (ES+)
Phosphatidylethanolamine	Neutral loss of m/z 141 (ES+)
Phosphatidylinositol	Precursors of m/z 241 (ES-)
Phosphatidylserine	Neutral loss of m/z 87 (ES-)
Sphingomyelin	Precursors of m/z 184 (ES+)

The instrument parameters for fragmentation ion scanning vary slightly according to the class of phospholipid which is to be fragmented, and are detailed in Table 2.3.

Table 2.3 Instrument parameters for phospholipid analysis by tandem mass spectrometry

Instrument parameter	Phosphatidyl choline (PC)	Sphingomyelin (SM)	Phosphatidyl ethanolamine (PE)	Phosphatidyl serine (PS)	Phosphatidyl inositol (PI)
Polarity	ES +	ES +	ES +	ES –	ES –
Capillary voltage (kV)	2.30	2.30	2.30	2.60	2.60
Cone voltage (V)	60.0	60.0	60.0	55.0	55.0
RF Lens 1	7.6	7.6	7.6	5.0	5.0
Aperture	0.0	0.0	0.0	0.0	0.0
RF Lens 2	1.0	1.0	1.0	1.0	1.0
Source temperature (° C)	80	80	80	80	80
Desolvation temperature (° C)	150	150	150	150	150
Cone Gas Flow (L/hr)	60	60	60	60	60
Desolvation Gas Flow (L/hr)	380	380	380	380	380
LM (low mass) 1 Resolution	15.0	15.0	15.0	14.8	14.8
HM (high mass) 1 Resolution	15.0	15.0	15.0	14.5	14.5
Ion Energy 1	0.3	0.3	0.3	0.5	0.5
Entrance	1.0	1.0	1.0	-1	-1
Collision Energy (eV)	30	30	25	25	25
Exit	2.0	2.0	2.0	2.0	2.0
LM (low mass) 2 Resolution	14.0	14.0	14.0	13.5	13.5
HM (high mass) 2 Resolution	14.0	14.0	14.0	13.5	13.5
Ion Energy 2	0.6	0.6	0.6	1.0	1.0
Multiplier (gain)	500	600	600	480	600

Results were quantified by processing spectrometric data from each sample using MassLynx data analysis software, and importation of numerical data into a Microsoft Excel spreadsheet. A macro for Excel developed by collaborators at the University of Southampton (Professor A.Postle and colleagues) was used to calculate the percentage abundance of the phospholipid species detected in each phospholipid class.

The ions detected at above 1% percentage abundance in each phospholipid class using fragmentation scanning were further subjected to precursor ion scans in the negative (ES-) mode to identify the fatty acyl, plasmogen or ether groups that made up the remainder of the phospholipid's structure. A 100µl aliquot of extracted sample was mixed with 200 µl of 70:30 chloroform:methanol with 0.02% formic acid. The formic acid facilitated the production of negative fatty acyl ions from the phospholipid structure. The instrument parameters for this analysis were as described in Table 2.4.

Table 2.4 Instrument parameters for tandem mass spectrometry analysis of phospholipids: identification of fatty acyl chains

Instrument parameter	PC	SM	PE	PS	PI
Polarity	ES –	ES –	ES –	ES –	ES –
Capillary voltage (kV)	2.60	2.60	2.60	2.60	2.60
Cone voltage (V)	55.0	55.0	55.0	55.0	55.0
RF Lens 1	5.0	5.0	5.0	5.0	5.0
Aperture	0.0	0.0	0.0	0.0	0.0
RF Lens 2	1.0	1.0	1.0	1.0	1.0
Source temperature (° C)	80	80	80	80	80
Desolvation temperature (° C)	150	150	150	150	150
Cone Gas Flow (L/hr)	60	60	60	60	60
Desolvation Gas Flow (L/hr)	380	380	380	380	380
LM (low mass) 1 Resolution	14.8	14.8	14.8	14.8	14.8
HM (high mass) 1 Resolution	14.5	14.5	14.5	14.5	14.5
Ion Energy 1	0.5	0.5	0.5	0.5	0.5
Entrance	-1	-1	-1	-1	-1
Collision Energy (eV)	25	30	30	20	20
Exit	2.0	2.0	2.0	2.0	2.0
LM (low mass) 2 Resolution	13.5	13.5	13.5	13.5	13.5
HM (high mass) 2 Resolution	13.5	13.5	13.5	13.5	13.5
Ion Energy 2	1.0	1.0	1.0	1.0	1.0
Multiplier (gain)	500	600	600	480	600

2.4.2. ESI-LC-MS/MS analysis of prostaglandins

ESI-LC-MS/MS analysis was performed on a HPLC pump (model 2695, Waters, Manchester, UK) coupled to an electrospray-interface triple quadrupole mass spectrometer (Quattro Ultima, Waters, Manchester, UK) using MassLynx 4.0 software. Chromatographic analysis was carried out on a C18 column (Luna, 5µm, 150 x 5mm, Phenomenex, Manchester, UK) maintained at ambient temperature. Sample injections were performed using

an autosampler (model number 2690, Waters, Manchester, UK) with the temperature of the sample chamber set at $8 \pm 2^\circ\text{C}$. 200 μl of a 2pg/ μl cocktail of standards in ethanol were prepared containing prostaglandin D₁ (PGD₁), prostaglandin E₁ (PGE₁), prostaglandin F_{1 α} (PGF_{1 α}), 6-keto-prostaglandin F_{1 α} (6-keto-PGF_{1 α}), prostaglandin B₂ (PGB₂), prostaglandin B_{2-d4} (PGB_{2-d4}), prostaglandin D₂ (PGD₂), prostaglandin E₂ (PGE₂), prostaglandin F_{2 α} (PGF_{2 α}), prostaglandin J₂ (PGJ₂) , 15-deoxy- $\Delta^{12,14}$ -prostaglandin J₂ (PGJ₂), prostaglandin D₃ (PGD₃), prostaglandin E₃ (PGE₃), prostaglandin F_{3 α} (PGF_{3 α}), thromboxane B₂ (TXB₂), thromboxane B₃ (TXB₃), 8-iso-PGE₂, 8-iso-PGF_{2 α} , 13,14-dihydro-PGE₁, 13,14-dihydro-PGF_{1 α} , 13,14-dihydro-PGF_{2 α} , 13,14-dihydro-15-keto PGE₁, 13,14-dihydro-15-keto-PGF_{1 α} , 13,14-dihydro-15-keto-PGE₂ and 13,14-dihydro-15-keto-PGF_{2 α} (all purchased from Cayman Chemicals, Ann Arbor, MI).

A range of standard solutions was produced by adding 40 μl of 2ng/ml of the internal standard PGB_{2-d4} and 50 μl , 40 μl , 30 μl , 20 μl , 10 μl or 5 μl of the cocktail of prostanoid standards in ethanol, then diluting with ethanol to produce a final volume of 100 μl . This process produced a range of standard solutions with prostanoid cocktail concentrations of 1pg/ μl , 0.8pg/ μl , 0.6pg/ μl , 0.4pg/ μl , 0.2pg/ μl and 0.1pg/ μl respectively. Calibration lines were set up for each of the prostanoid species in the cocktail of standards using the standard solutions, which were later used during for the quantification of prostanoid species in the biological samples.

The injection volume of the standards was 5 μ l and that of biological samples was 10 μ l. A gradient was set up between Solvent A (45:55:0.02 v/v/v acetonitrile: water: glacial acetic acid) and Solvent B (90:10:0.02 v/v/v acetonitrile: water: glacial acid) with a flow rate of 0.2 ml/min. The gradient was as follows: 100% Solvent A for 0.0 to 8.0 min, ramping to 50% Solvent A and 50% Solvent B from 8.0 to 8.1 min, 50% Solvent A and 50% Solvent B from 8.1 to 12.0 min, ramping to 30% Solvent A and 70% Solvent B from 12.0 to 12.1 min, 30% Solvent A and 70% Solvent B from 12.1 to 20.0 min, ramping from 30% to 100% Solvent A over 20.0 to 20.1 min, remaining at 100% Solvent A from 20.1 to 30.0 min. The mass spectrometer was used in the ES- mode, with the capillary voltage was set to 3500V and the cone voltage set to 35V. The source temperature was set to 120°C and the desolvation temperature to 360°C. Twenty one different MRM transactions were monitored over the course of each run with the collision energy of each transition set as described in Table 2.5.

Table 2.5 Collision energy settings for multiple reaction monitoring (MRM) used for the ESI-LC-MS/MS analysis of prostanoids (Masoodi & Nicolaou, 2006)

Compound	MRM (m/z)	Collision energy (eV)
PGD1	353 → 317	15
PGE1	353 → 317	15
PGF1 α	355 → 311	25
6-keto-PGF1 α	369 → 163	23
PGB2	333 → 175	20
PGB2-d4	337 → 179	20
PGD2	351 → 271	17
PGE2	351 → 271	17
PGF2 α	353 → 193	25
PGJ2	333 → 271	15
Δ 12-PGJ2	333 → 271	15
15-deoxy- Δ 12,14 PGJ2	315 → 271	15
PGD3	349 → 269	15
PGE3	349 → 269	15
PGF3 α	351 → 193	25
TXB2	369 → 169	17
TXB3	367 → 169	15
8-iso-PGE2	351 → 315	15
8-iso-15-keto PGE2	349 → 113	23
8-iso-PGF2 α	353 → 193	25
8-iso-15-keto PGF2 α	351 → 315	15
13,14-dihydro PGE1	355 → 337	15
13,14-dihydro-15-keto PGE1	353 → 335	12
13,14-dihydro PGF1 α	357 → 113	38
13,14-dihydro-15-keto PGF1 α	355 → 193	32
13,14-dihydro-15-keto PGE2	351 → 333	12
13,14-dihydro PGF2 α	355 → 311	30
13,14-dihydro-15-keto PGF2 α	353 → 113	28

2.4.3. LC-MS/MS analysis of hydroxy fatty acids

LC-MS/MS analysis was performed on a HPLC pump (model 2695, Waters, Manchester, UK) coupled to an electrospray-interface triple quadrupole mass spectrometer (Quattro Ultima, Waters, Manchester, UK) using MassLynx 4.0 software. Chromatographic analysis was carried out on a C18 column (Luna, 5 μ m, 150 x 5mm, Phenomenex, Manchester, UK) maintained at ambient temperature. Sample injections were performed using an autosampler (model number 2690, Waters, Manchester, UK) with the temperature of the sample chamber set at 8 \pm 2°C. A cocktail of standards were prepared using 5S,12R,18R-trihydroxy-6Z,8E,10E,14Z,16E-eicosapentaenoic acid (Resolvin E1), 5S,8R,17S-trihydroxy-4Z,9E,11E,13Z,15E,19Z-docosahexaenoic acid (Resolvin D1), 10R,17S-dihydroxy-docosa-4Z,7Z,11E,15Z,19Z-hexaenoic acid (Protectin D1), 9-hydroxy-10E,12Z-octadienoic acid (9-HODE), 13-hydroxy-9Z,11E-octadienoic acid (13-HODE), 5-hydroxy-6E,8Z,11Z,14Z,17Z-eicosapentaenoic acid (5-HEPE), 18-hydroxy-5Z,8Z,11Z,14Z,16E-eicosapentaenoic acid (18-HEPE), 9-hydroxy-5Z,7E,11Z,14Z,17Z-eicosapentaenoic acid (9-HEPE), 8-hydroxy-5Z,9E,11Z,14Z,17Z-eicosapentaenoic acid (8-HEPE), 15-hydroxy-5Z,8Z,11Z,13E,17Z-eicosapentaenoic acid (15-HEPE), 12-hydroxy-5Z,8Z,10E,14Z,17Z-eicosapentaenoic acid (12-HEPE), 5-hydroxy-6E,8Z,11Z,14Z-eicosatetraenoic acid (5-HETE), 8-hydroxy-5Z,9E,11Z,14Z-eicosatetraenoic acid (8-HETE), 11-hydroxy-5Z,8Z,12E,14Z-eicosatetraenoic acid (11-HETE), 15-hydroxy-5Z,8Z,11Z,13E-eicosatetraenoic acid (15-HETE), 12-

hydroxy-5Z,8Z,10E,14Z-eicosatetraenoic acid (12-HETE), 9-hydroxy-5Z,7E,11Z,14Z-eicosatetraenoic acid (9-HETE), Leukotriene B4 (LTB4), 17S-hydroxy-4Z,7Z,10Z,13Z,15E,19Z-docosahexaenoic acid (17S-HDHA) and 12S-hydroxy-5Z,8Z,10E,14Z-eicosatetraenoic-5,6,8,9,11,12,14,15-d8 acid (12-HETE-d8). Protectin D1 and Resolvins E1 and D1 were obtained from the laboratory of C.N. Serhan (Centre of Experimental Therapeutics and Reperfusion Injury, Brigham & Women's Hospital, Boston, MA). All other lipid standards were purchased from Cayman Chemicals (Ann Arbor, MI). A range of standard solutions was produced by adding 40µl of 2ng/ml of the internal standard 12HETE-*d*4 and 50µl, 40µl, 30µl, 20µl, 10µl or 5µl of the cocktail of lipid standards in ethanol, then diluting with ethanol to produce a final volume of 100µl. This process produced a range of standard solutions with lipid cocktail concentrations of 1pg/µl, 0.8pg/µl, 0.6pg/µl, 0.4pg/µl, 0.2pg/µl and 0.1pg/µl respectively. Calibration lines were set up for each of the lipid species in the cocktail of standards using the standard solutions, which were later used during for the quantification of lipid species in the biological samples.

The mass spectrometer was used in the ES- mode, with the capillary voltage was set to 3500V and the cone voltage set to 35V. The source temperature was set to 120°C and the desolvation temperature to 360°C. Analysis was carried out using an isocratic system by mixing two solvents, A and B, at a ratio of 95:5 v/v. Solvent A was 80:20:0.02 v/v/v methanol: water: glacial acetic acid and Solvent B was 45:55:0.02 v/v/v acetonitrile: water: glacial

acetic acid. The injection volume of standards was 5 μ l and that of biological samples was 10 μ l. Twenty different MRM transactions were monitored over the course of each run with the collision energy of each transition set as described in Table 2.6.

Table 2.6 Collision energy settings for MRM transitions of lipo-oxygenase, acetylated COX and P450 enzymes lipid mediator products (Masoodi et al., 2008)

Compound	MRM (m/z)	Collision energy (eV)
9-HODE	295 \rightarrow 171	25
13-HODE	295 \rightarrow 195	25
5-HEPE	317 \rightarrow 115	20
18-HEPE	317 \rightarrow 133	25
9-HEPE	317 \rightarrow 149	20
8-HEPE	317 \rightarrow 155	18
15-HEPE	317 \rightarrow 175	18
12-HEPE	317 \rightarrow 179	20
5-HETE	319 \rightarrow 115	20
9-HETE	319 \rightarrow 123	20
8-HETE	319 \rightarrow 155	20
11-HETE	319 \rightarrow 167	20
15-HETE	319 \rightarrow 175	18
12-HETE	319 \rightarrow 179	20
12-HETE-d8	328 \rightarrow 185	17
LTB4	335 \rightarrow 195	17
17S-HDHA	343 \rightarrow 281	15
RvE1	349 \rightarrow 195	17
PD1	359 \rightarrow 206	15
RvD1	375 \rightarrow 141	15

2.5. Data collection and presentation

The cerebral cortex collected from each mouse was split into two, so that each mouse produced three samples for lipidomic analysis: (i) a plasma sample for lipid mediator analysis, (ii) a cerebral cortex sample for lipid mediator analysis and (iii) another cerebral cortex sample for phospholipid analysis. For each sample type, the mice were divided into three main groups: (a) Control mice, who did not undergo any form of treatment prior to killing and sample collection, (b) PUFA-treated mice, which underwent tail vein injection of 50 μ M ALA solution in 0.9% NaCl prior to killing and sample collection and (c) Vehicle-treated mice, which received a tail vein injection of the corresponding vehicle (0.005% v/v ethanol in 0.9% NaCl) prior to killing and sample collection. Mice in the ALA and the vehicle treatment groups were killed at four different timepoints (3h, 24h, 72h and 168h) following injection with ALA or vehicle.

Statistical analysis was carried out for both phospholipids and lipid mediators between control and treatment groups, and between different treatment groups at the same timepoints using two-way analysis of variance (ANOVA) tests between control and treatment groups with post-hoc Dunnett's correction. A value of $P < 0.05$ between a PUFA-treated group and both control and the corresponding VEH-treated groups was considered statistically significant and a P value of < 0.01 highly significant. All statistical analysis was carried out using SPSS 16.0 for Windows (SPSS Inc, Chicago, IL).

3. Lipidomic analysis of cerebral cortex phospholipids in mice

3.1. Profiling of phospholipids in mouse cerebral cortex: general scans

A general scan of the lipid extract using MS provides an overview of the phospholipid species present. All species that are ionized by the ESI interface, with different mass/charge ratio (m/z) values prominent in the positive and negative ion modes, can be detected with a general scan. The spectrum produced by a general scan provides information on the total ion count, the presence (or absence) of prominent phospholipid species and the relative abundance of lysophospholipid species. This information can be used to determine whether a sample has been extracted, stored and processed in the correct manner. For example, a high ratio of lysophospholipids to phospholipids is indicative of sample degradation. Figures 3.1 and 3.2 shows representative general scan spectra of a tissue sample taken from the cerebral cortex of an untreated (control) mouse in both positive (figure 3.1) and negative (figure 3.2) modes. Although general scans using MS are useful to identify the overall number of C atoms and the number of C=C double bonds present in a phospholipid sample, they can not be used for quantitative analysis. It is for this reason that MS/MS fragmentation scans were used in order to identify which fatty acyl group corresponds to that on the *sn*-1 position and which corresponds to the fatty acyl group on the *sn*-2 position.

Figure 3.1 General ESI-MS scan of a representative sample of mouse cerebral cortex in the ES + mode, where positively-charged $[M+H]^+$ ions are produced

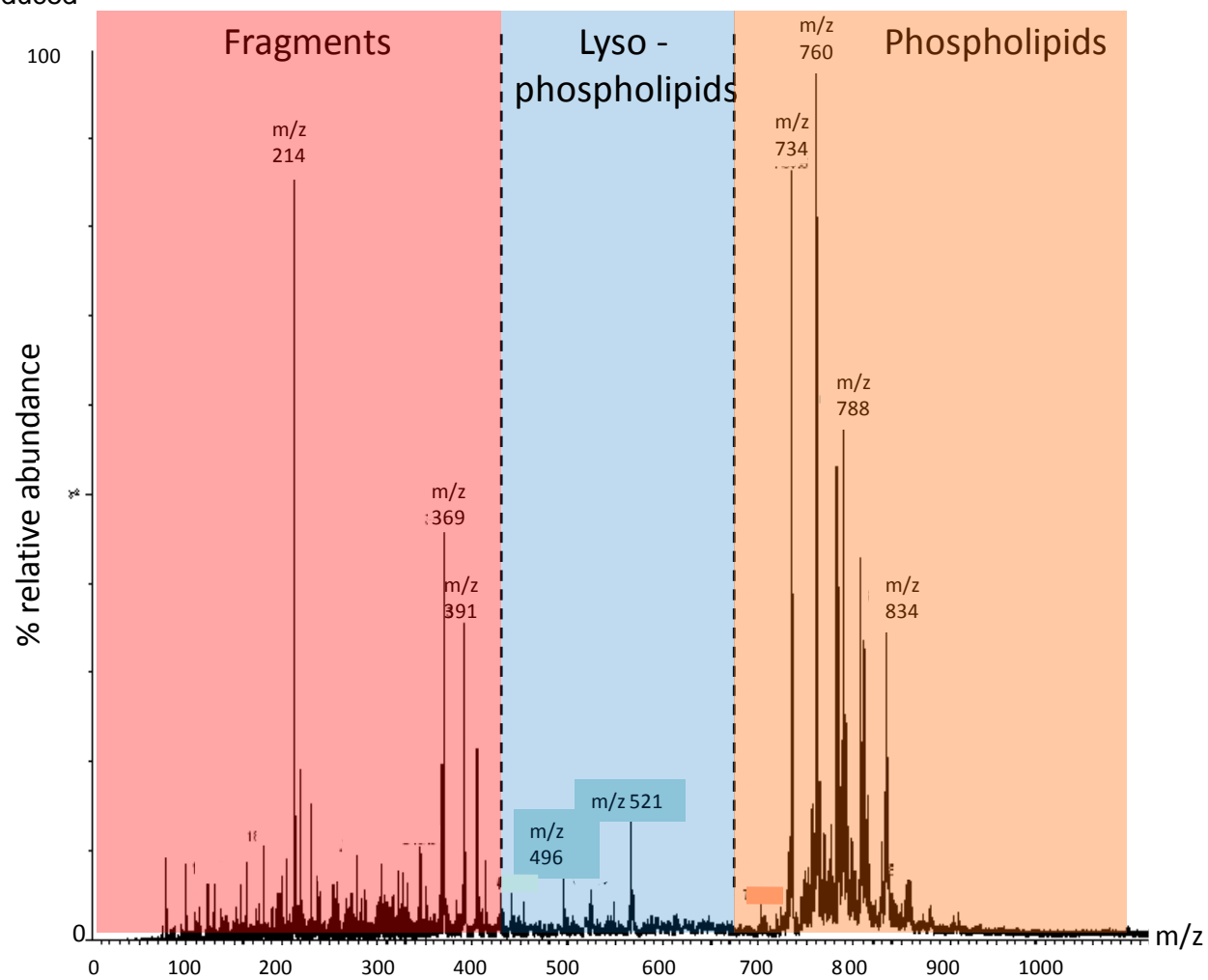
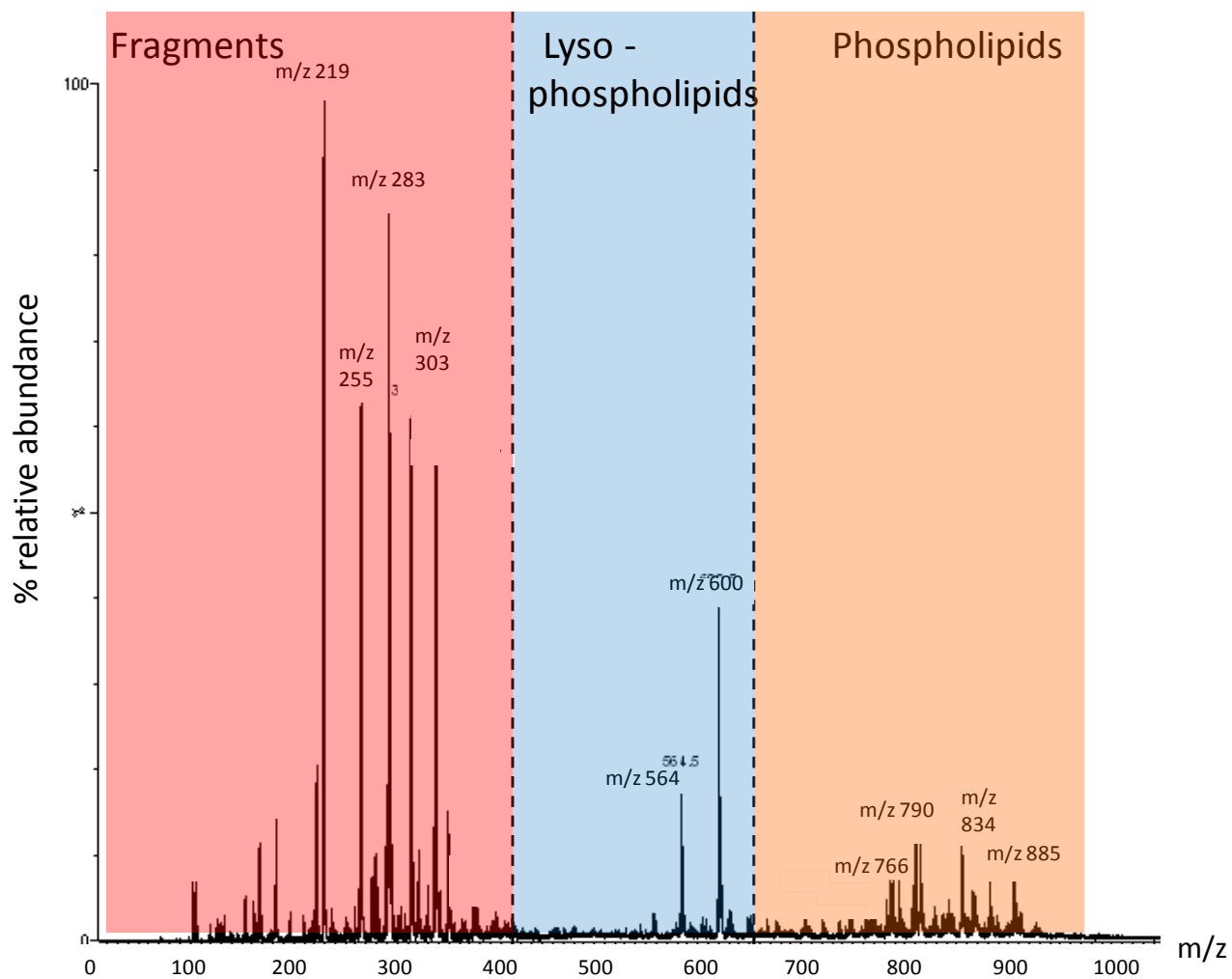


Figure 3.2 General ESI-MS scan of a representative sample of mouse cerebral cortex in the ES – mode, where negatively-charged $[M - H]^-$ ions are produced



3.2. Profiling of phospholipids in mouse cerebral cortex: MS/MS analysis

In addition to a general scan, two types of fragmentation scans were carried out on each sample to identify phosphatidylcholine, sphingomyelin, phosphatidylethanolamine, phosphatidylserine and phosphatidylinositol species. These scans were: (a) neutral loss scans, where the precursor ions are detected on the basis of a loss of an ion fragment with a specified m/z value during collision-induced dissociation (CID), and (b) precursor ion scans, whose fragmentation leads to production of ion fragments with a specified m/z value. The scanning parameters differed according to the polar head group of the phospholipid class to be detected.

Phosphatidylcholines and sphingomyelins were identified through the detection of choline ions (with an m/z of 184) lost from the head group of both classes of phospholipids. Phosphatidylinositol species were identified through the detection of an inositol ion (m/z 241) lost from the head group of this phospholipid class upon fragmentation in the ES- mode. Phosphatidylethanolamine species were detected through neutral loss scanning of 141, where the production of a fragment ion with m/z value 141 less than the parent ion is detected. Similarly, the loss of serine from a phosphatidylserine upon fragmentation of the molecular ion results in a

product ion with its m/z 87 less than the original molecular ion, so phosphatidylserines were detected through neutral loss scanning of m/z 87.

Figures 3.3 – 3.6 show representative spectra of fragmentation scans carried out to identify different classes of phospholipids (namely phosphatidylcholines, sphingomyelins, phosphatidylethanolamines, phosphatidylserines and phosphatidylinositols) in a single tissue sample taken from the cerebral cortex of an untreated (control) mouse.

Figure 3.3 Representative ESI-MS/MS spectrum in the ES+ mode showing phosphatidylcholine (PC) and sphingomyelin (SM) species in mouse cerebral cortex tissue; the scan used is a precursor ion scan of m/z 184

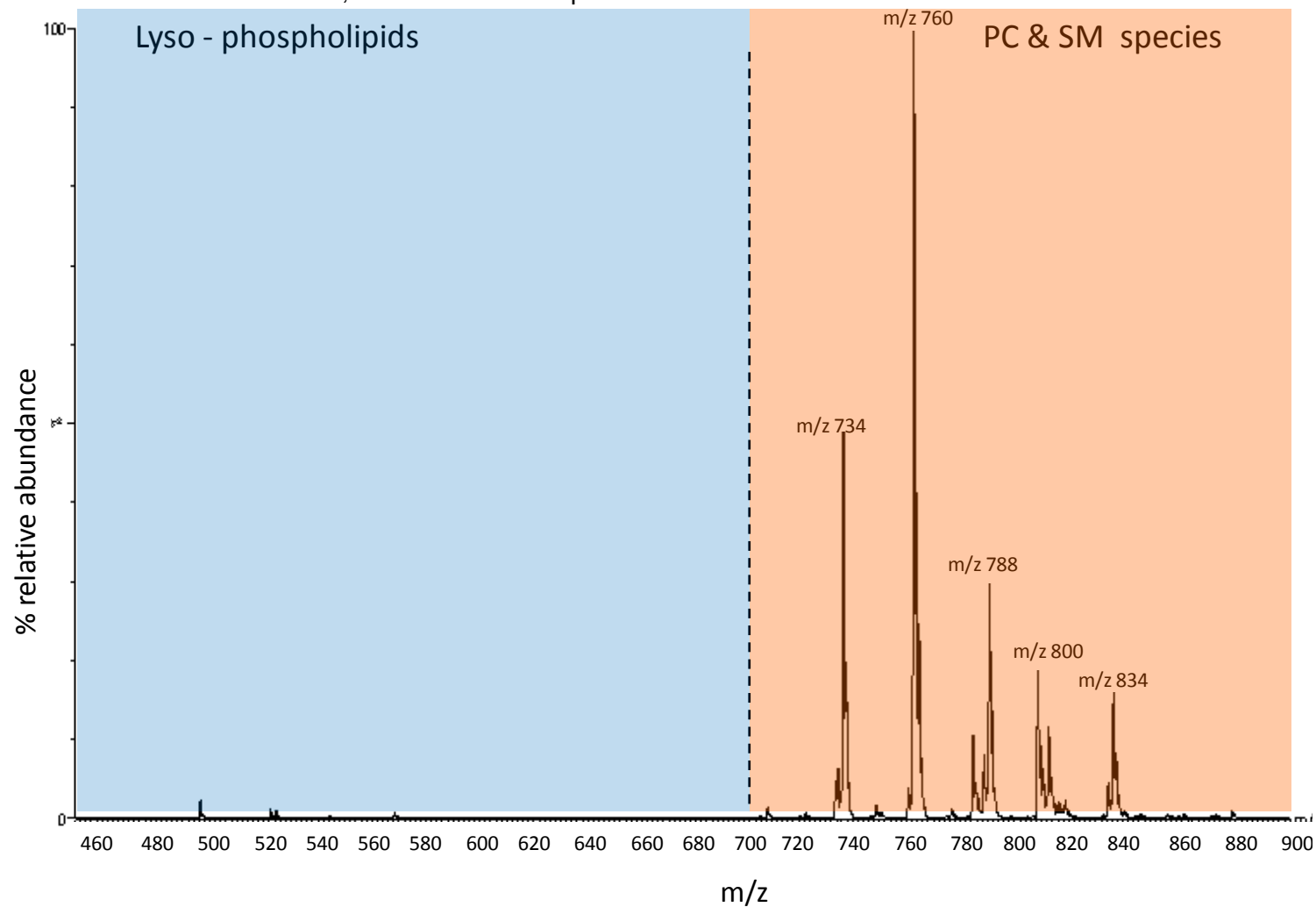


Figure 3.4 Representative ESI-MS/MS spectrum in the ES+ mode showing phosphatidylethanolamine (PE) species in mouse cerebral cortex tissue; the scan used is a neutral loss ion scan of m/z 141.

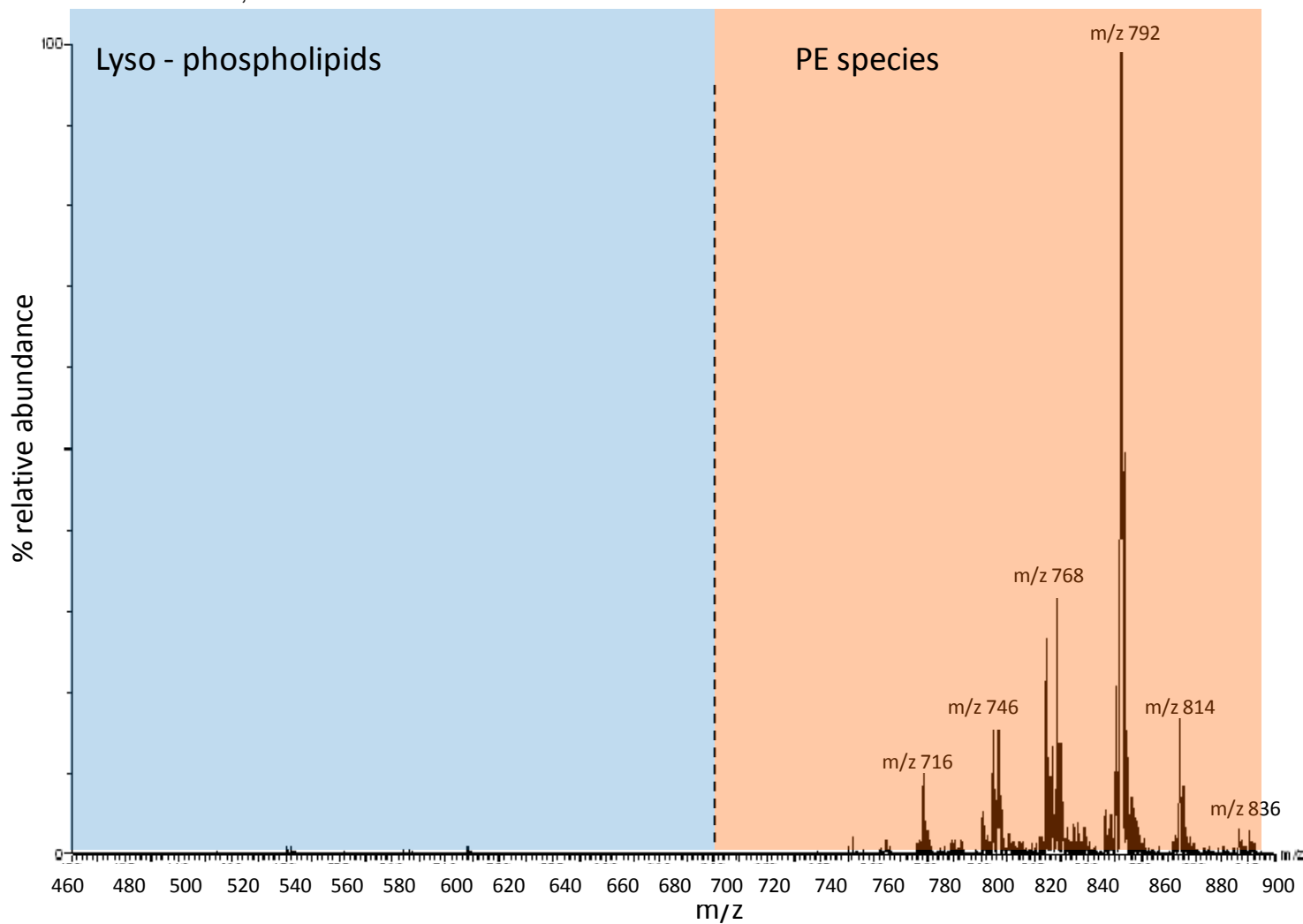


Figure 3.5 Representative ESI-MS/MS spectrum in the ES- mode showing phosphatidylserine (PS) species in mouse cerebral cortex tissue; the scan used is a neutral loss scan of m/z 87.

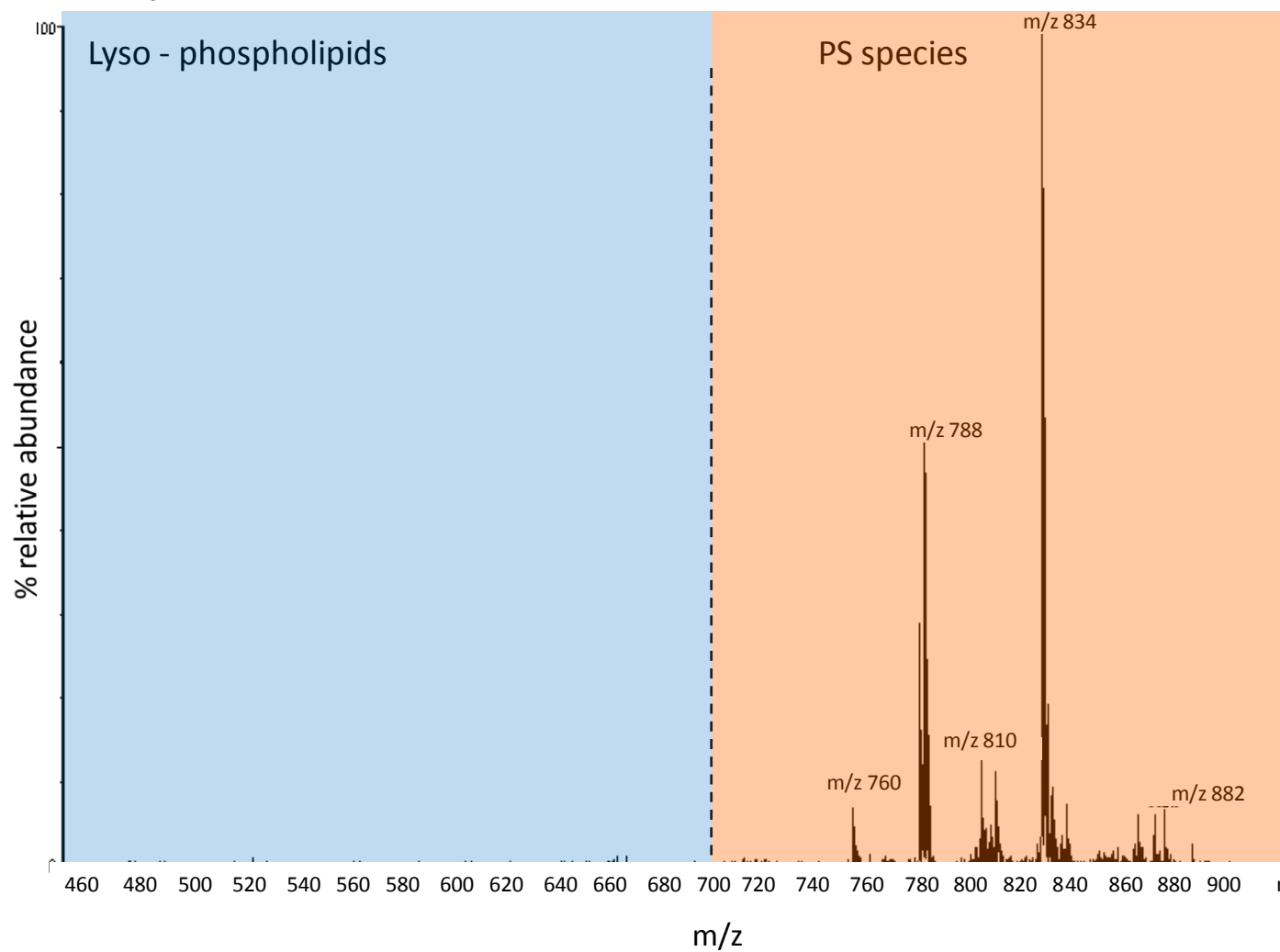
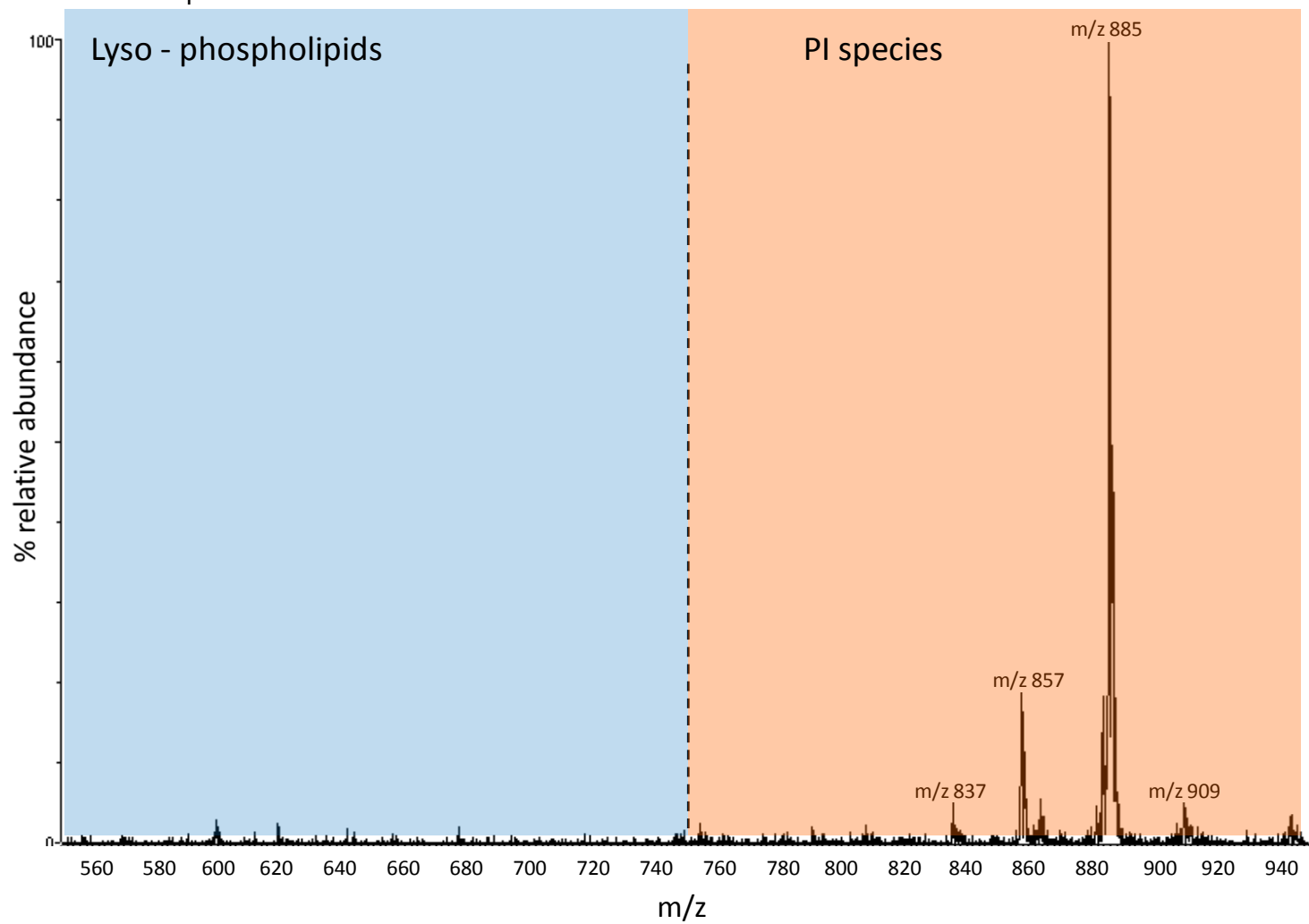


Figure 3.6 Representative ESI-MS/MS spectrum in the ES- mode showing phosphatidylinositol (PI) species in mouse cerebral cortex tissue; the scan used is a precursor ion scan of m/z 241.



3.3. Identification of phospholipid species in mouse cerebral cortex

3.3.1. Phosphatidylcholine and sphingomyelin species

Nineteen phosphatidylcholine (PC) and sphingomyelin (SM) species were identified in individual samples of mouse cerebral cortex using precursor ion scans for the choline headgroup (m/z 184), with the resulting data summarised in figures 3.7a-b.

The majority of choline phospholipid species detected in the mouse cerebral cortex contained saturated and/or monounsaturated fatty acids, with the two most abundant phosphatidylcholines alone accounting for almost half of total choline phospholipids detected in the cerebral cortex of untreated mice. These two species had m/z values of 734 and 760 and were putatively identified using lipid analyser software as PC 32:0 and PC 34:1 respectively. The identities of these compounds in mouse brain were confirmed as PC 16:0/16:1 and PC 16:0/18:0 in the fragmentation study (see section 3.4.)

Highly-unsaturated phosphatidylcholine species contained either arachidonic acid (20:4) or docosahexaenoic acid (22:6), both which are known to be precursors for lipid mediators.

Figure 3.7a Phosphatidylcholine (PC) and sphingomyelin (SM) species identified in cerebral cortex samples of naive mice (n=8), grouped by fatty acyl chain components: docosahexaenoic acid (DHA)/ arachidonic acid (AA)/ monounsaturated fatty acid (MUFA) and saturated fatty acid (SFA)

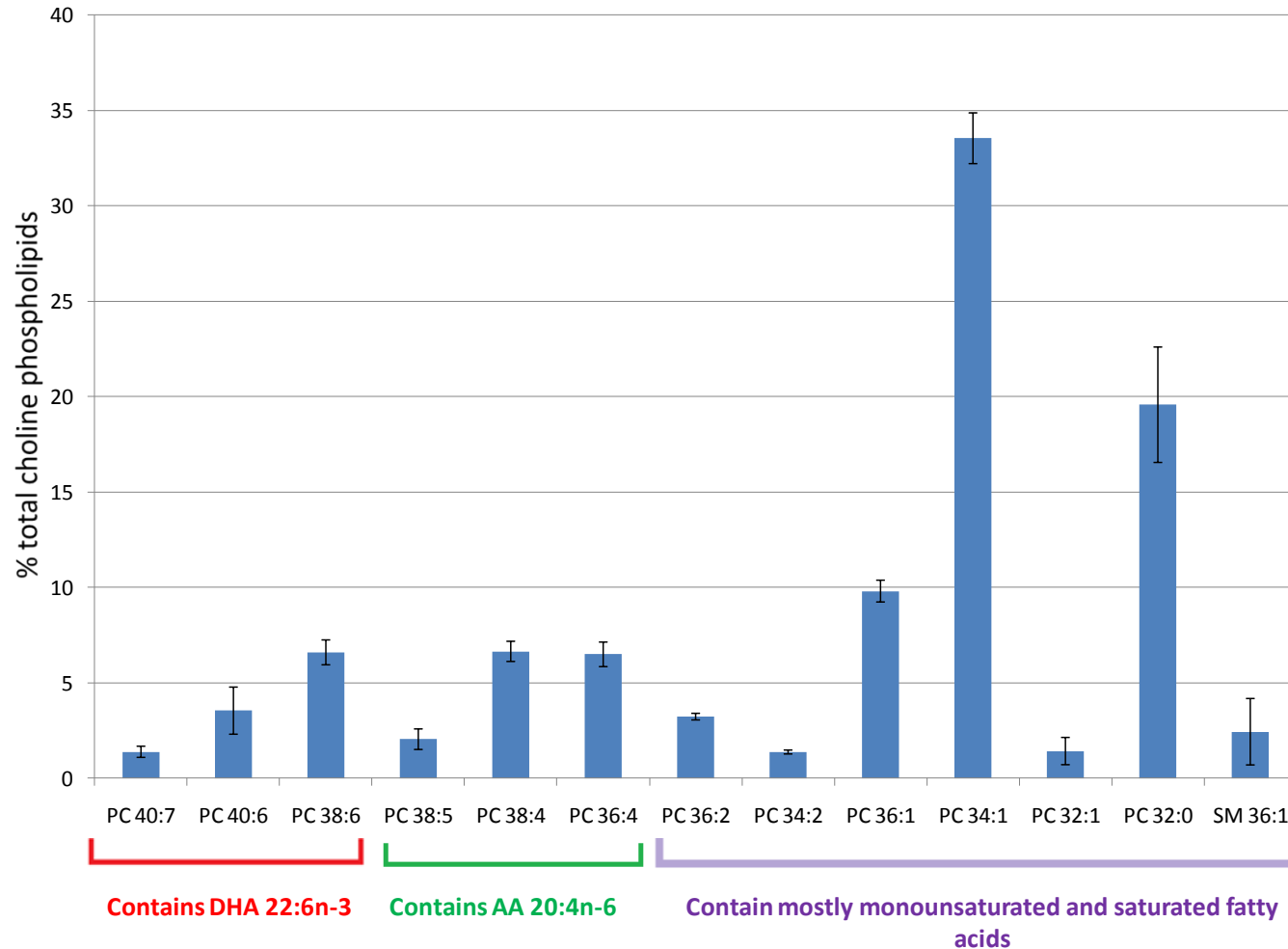
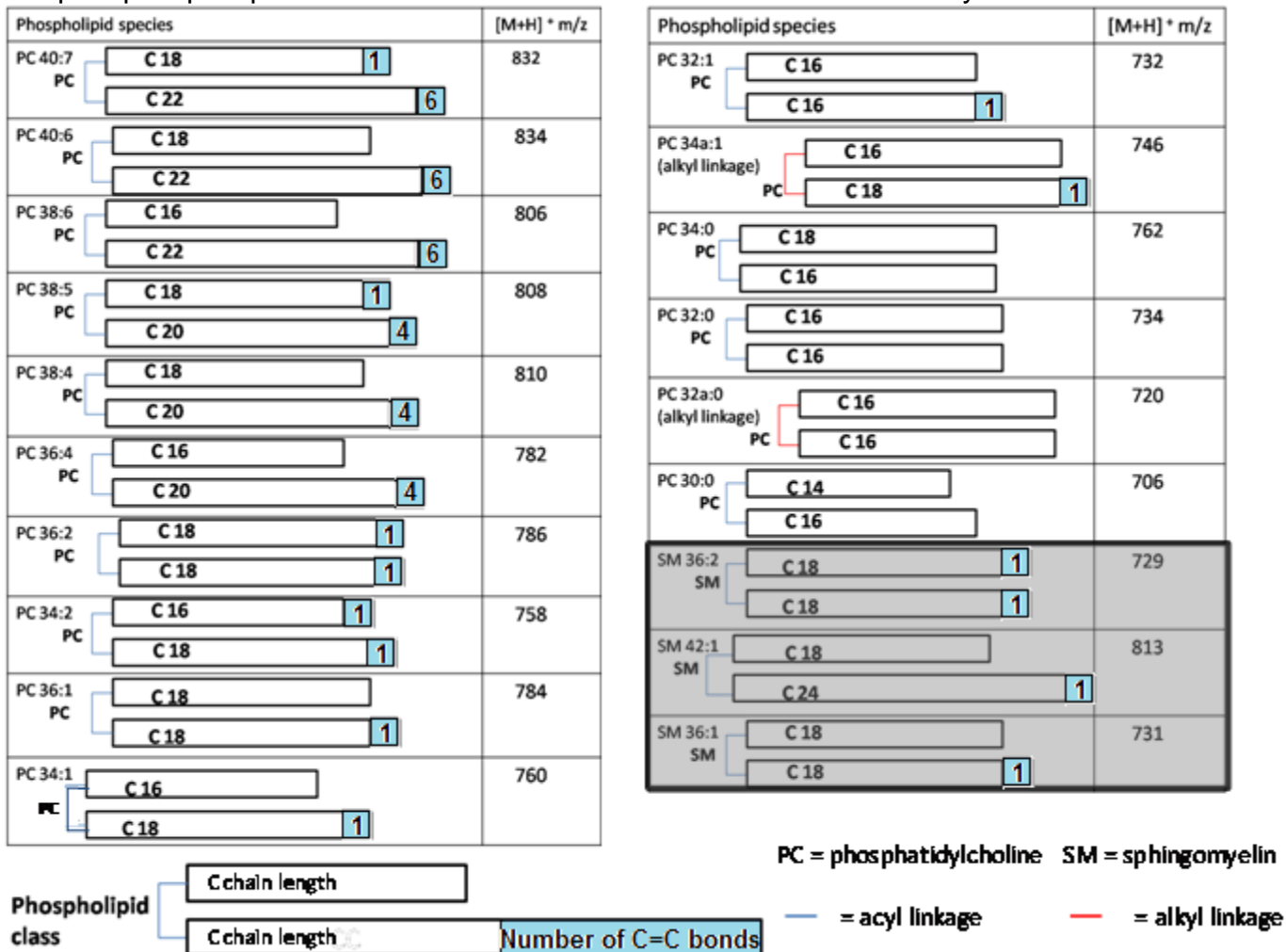


Figure 3.7b Nineteen phosphatidylcholine and sphingomyelin species (including two alkyl-linked PC species) were identified in mouse cerebral cortex samples using precursor ion scans for the choline headgroup (m/z 184). The most abundant choline phospholipid species contained saturated and monounsaturated fatty acids.



3.3.2. Phosphatidylethanolamine species

Many phosphatidylethanolamine (PE) species were identified in mouse cerebral cortex, including some trace species with higher m/z values than those observed in rat brain tissue. As a result, some PE species could not be identified using the lipid analyzer software.

Highly-unsaturated lipids comprise the majority of this phospholipid class in the mouse cerebral cortex. The three most abundant species all contain a PUFA (either arachidonic or docosahexaenoic acid) in their structure, and they account for two thirds of phosphatidylethanolamines in mouse cerebral cortex. The three most abundant phosphatidylethanolamine species detected in mouse cerebral cortex had m/z values of 764, 768 and 792, and were putatively identified using a lipid analyser software calculator as PE 16:0/22:6, 18:1/20:4 and 18:0/22:6 respectively. The identities of these compounds in mouse brain were confirmed using further fragmentation (see section 3.4). In contrast to PC and SM species, phospholipids containing solely saturated or monounsaturated fatty acyl chains are relatively rare in PE species, accounting for under a fifth of all PE species.

..

Figure 3.8a Phosphatidylethanolamine species identified in cerebral cortex samples of naive mice (n=8), grouped by fatty acyl chain components, grouped by fatty acyl chain components: docosahexaenoic acid (DHA)/ arachidonic acid (AA)/tri-enoic and di-enoic/ monounsaturated fatty acid (MUFA) and saturated fatty acid (SFA)

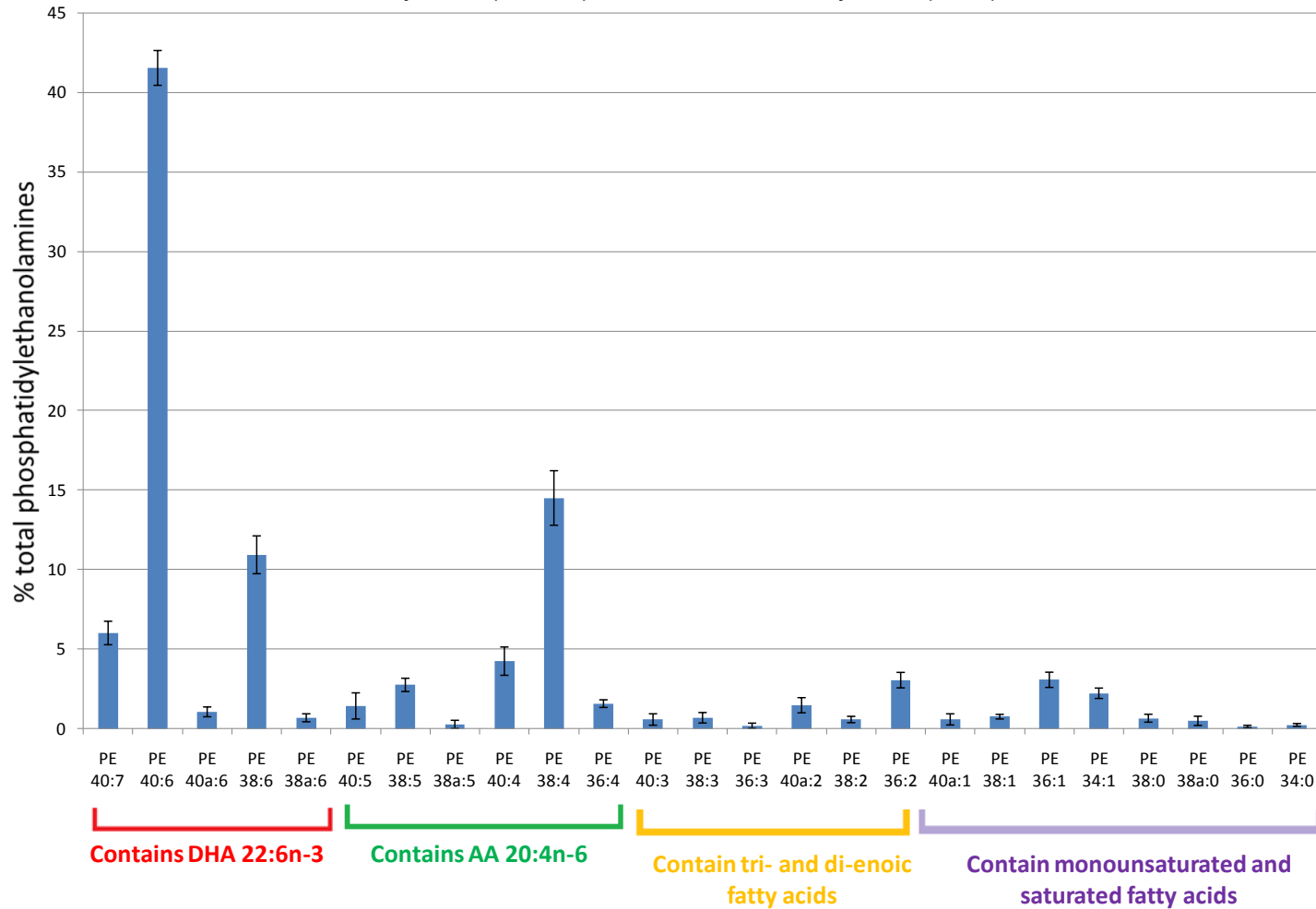


Figure 3.8b – Part I Twenty nine phosphatidylethanolamine species were identified in mouse cerebral cortex samples using neutral loss scans of 141 (equivalent to loss of the ethanolamine headgroup, which has a mass of 141). The most abundant phosphatidylethanolamine species contained arachidonic (20:4) or docosahexaenoic acid (22:6)

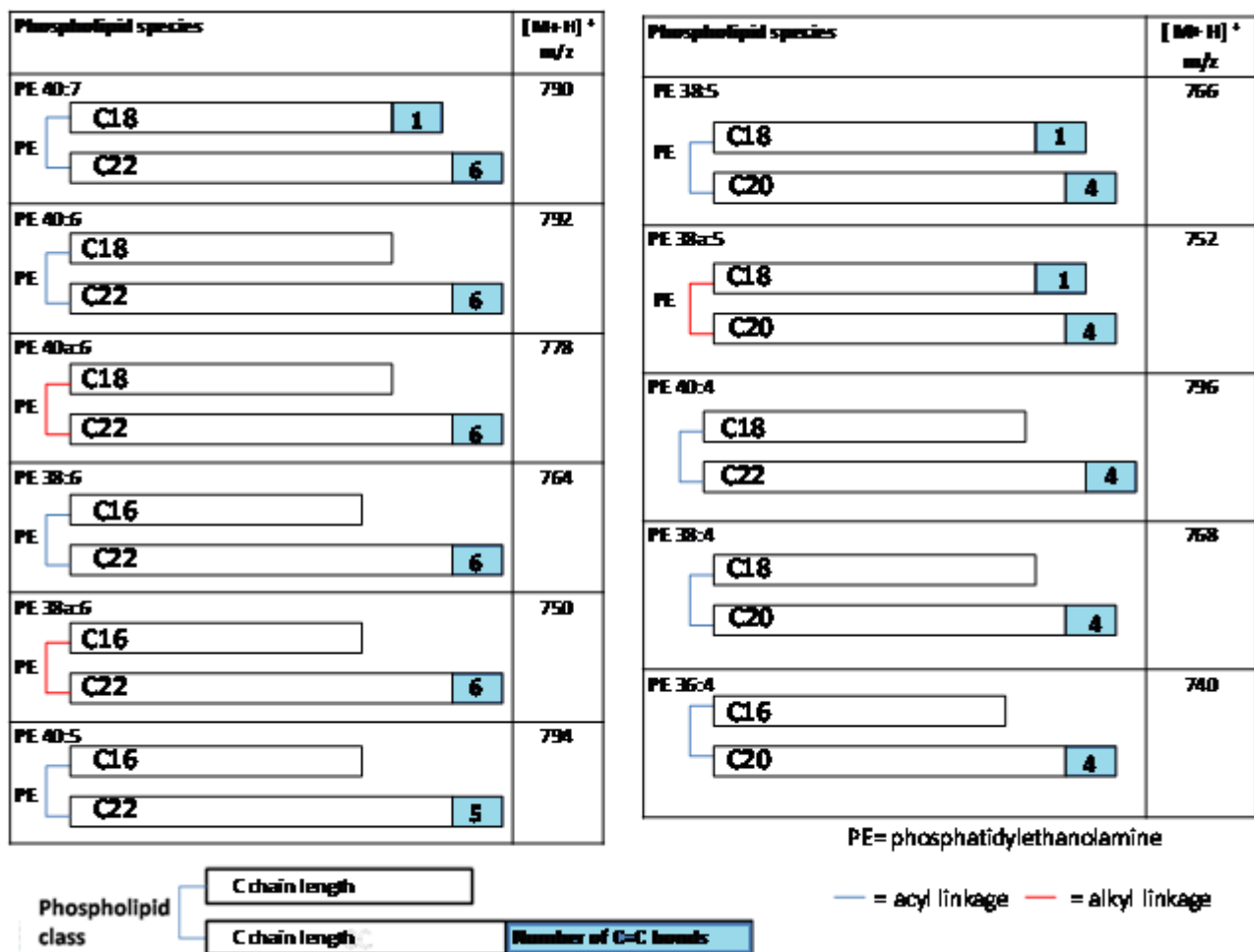


Figure 3.8b – Part II Twenty nine phosphatidylethanolamine species were identified in mouse cerebral cortex samples using neutral loss scans of 141. The most abundant phosphatidylethanolamine species contained arachidonic (20:4) or docosahexaenoic acid (22:6). Some PE species could not be identified using lipid analyzer software

Phospholipid Species	[M+H] ⁺ m/z	Phospholipid species	[M+H] ⁺ m/z
PE44a:3	840	PE42a:1	816
PE42a:3	812	PE40a:1 C18 PE C22 1	788
PE40:3 PE C18 C22 3	798	PE38:1 C18 PE C20 1	774
PE38:3 PE C18 C20 3	770	PE36:1 PE C18 C18 1	746
PE36:3 PE C18 1 C18 2	742	PE34:1 PE C16 C18 1	718
PE42a:2	814	PE38:0 PE C18 C20	776
PE40a:2 PE C18 C22 2	786	PE38a:0 PE C18 C20	762
PE38:2 PE C18 C20 2	772	PE36:0 PE C18 C18	748
PE36:2 C18 C18 2	744	PE34:0 PE C16 C18	720

3.3.3. Phosphatidylserine species

Sixteen phosphatidylserine species were identified in mouse cerebral cortex, including some species with m/z values differing from those observed in rat brain tissue. The two most abundant species in this lipid class accounted for approximately three quarters of all phosphatidylserine species in mouse cerebral cortex, and had m/z values of 788 and 834. The identity of these two phosphatidylserine species, based on the calculations by the lipid analyser software, were 18:0/18:1 for m/z = 788 and 18:0/22:6 for m/z = 834. These identities were confirmed by data from MS/MS analysis (see section 3.4)

Figure 3.9a Phosphatidylserine species identified in cerebral cortex samples of naive mice (n=8), grouped by fatty acyl chain components: docosahexaenoic acid (DHA)/ arachidonic acid (AA)/tri-enoic and di-enoic/ monounsaturated fatty acid (MUFA) and saturated fatty acid (SFA)

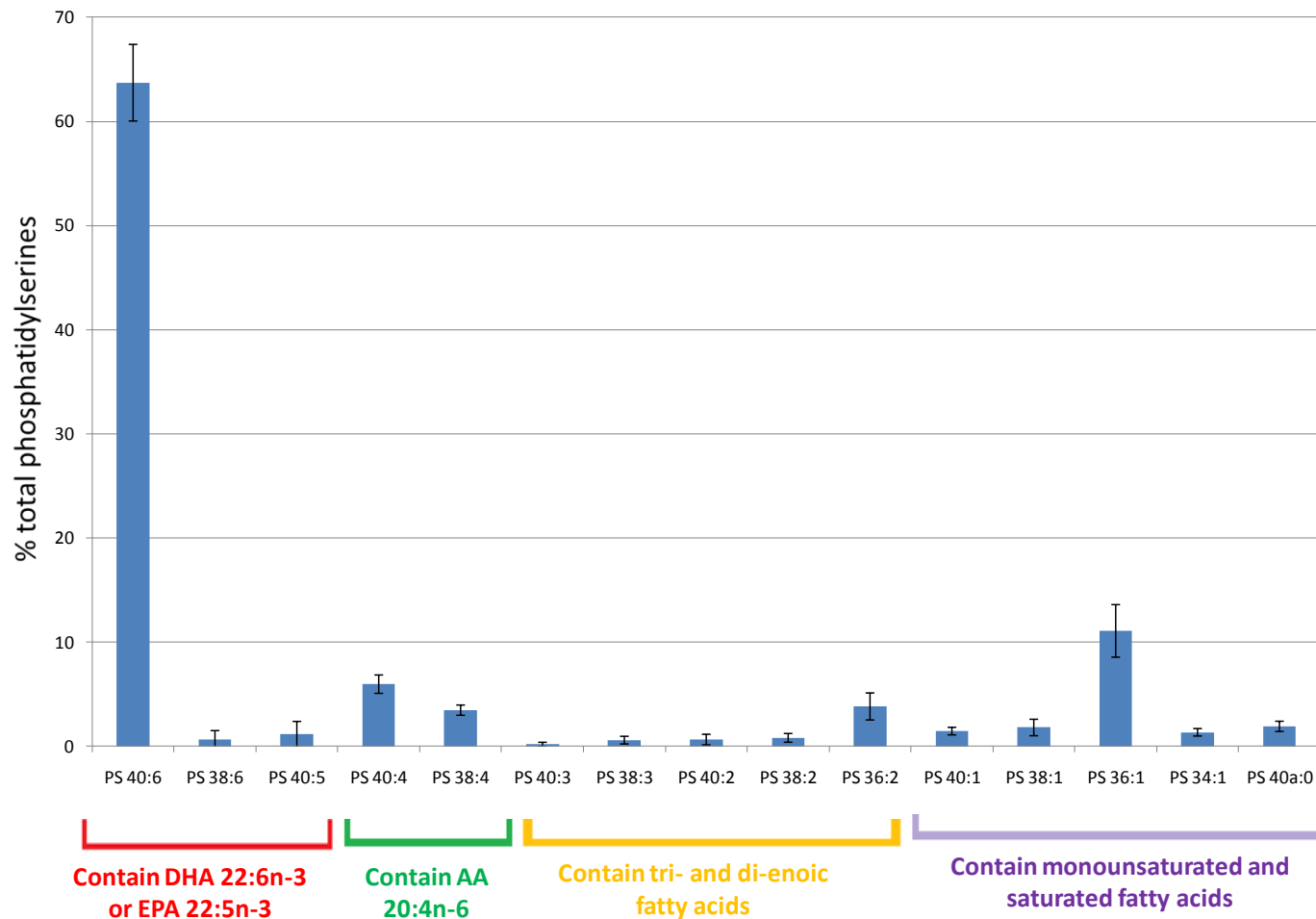
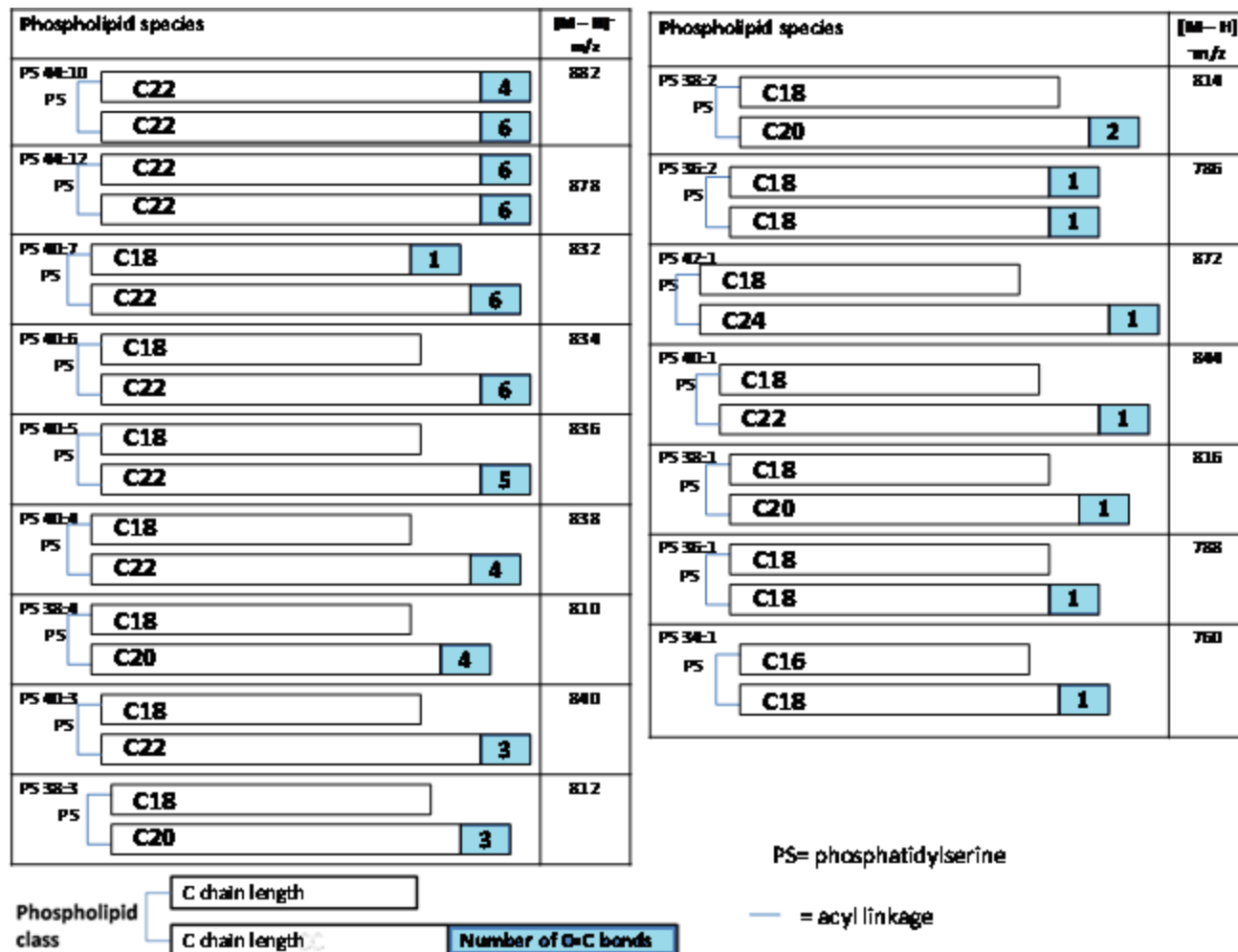


Figure 3.9b Sixteen phosphatidylserine species were identified in mouse cerebral cortex samples using neutral loss scans of 87 (equivalent to loss of the serine headgroup, which has a mass of 87). The most abundant phosphatidylserine species contained either docosahexaenoic acid (22:6) or a monounsaturated fatty acid



3.3.4. Phosphatidylinositol species

The three most abundant phosphatidylinositol species detected in mouse cerebral cortex all contained arachidonic acid (20:4), which has been implicated in cell signalling. The three most abundant PI species had m/z values of 857, 883 and 885 and were putatively identified as 16:0/20:4, 18:1/20:4 and 18:0/20:4 respectively from rat brain data. Data from MS/MS analysis confirmed the putative identities of these phospholipids (see section 3.4).

Figure 3.10a Phosphatidylinositol species identified in cerebral cortex samples of naive mice (n=8), grouped by fatty acyl chain components docosahexaenoic acid (DHA)/ arachidonic acid (AA)/ monounsaturated fatty acid (MUFA) and saturated fatty acid (SFA)

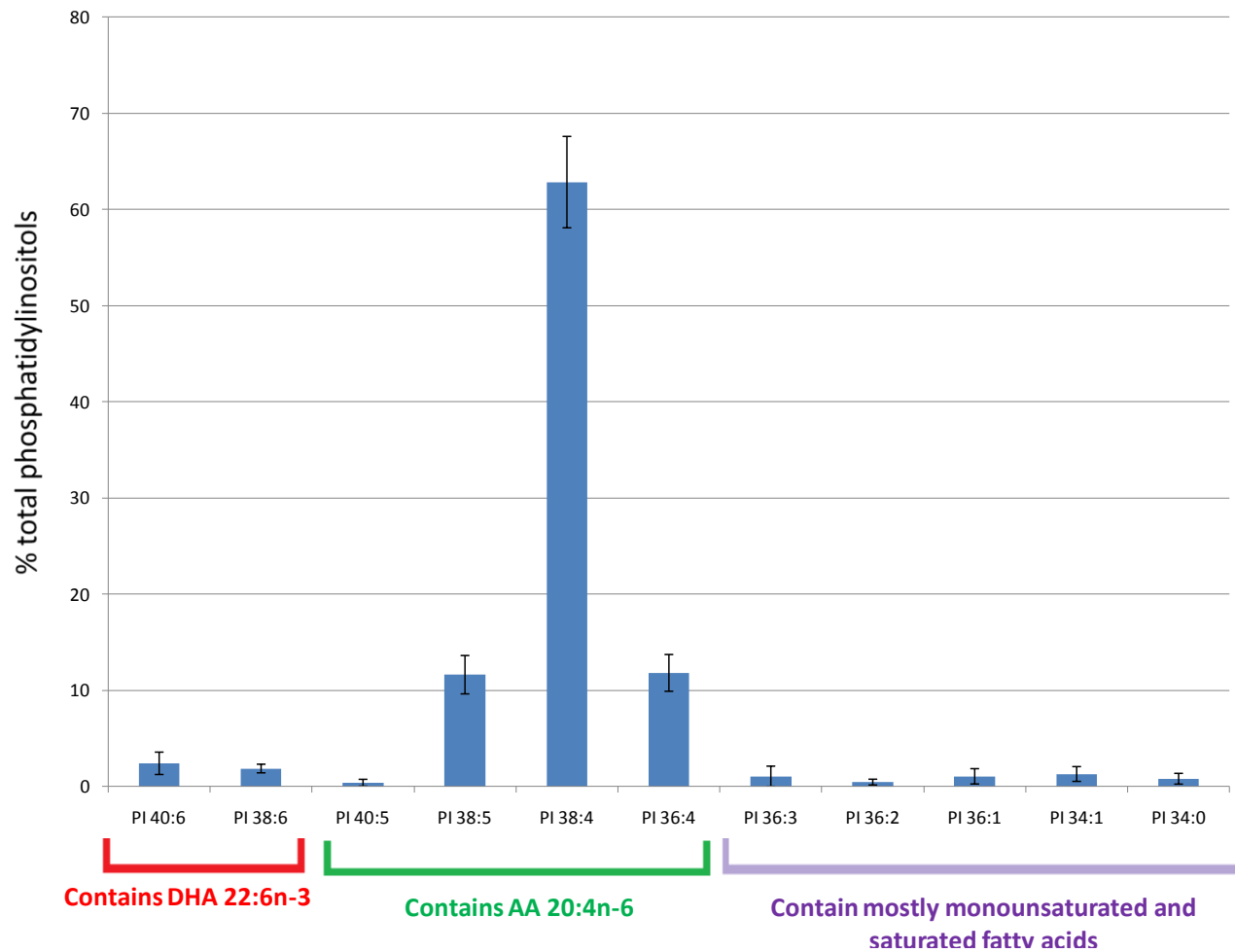
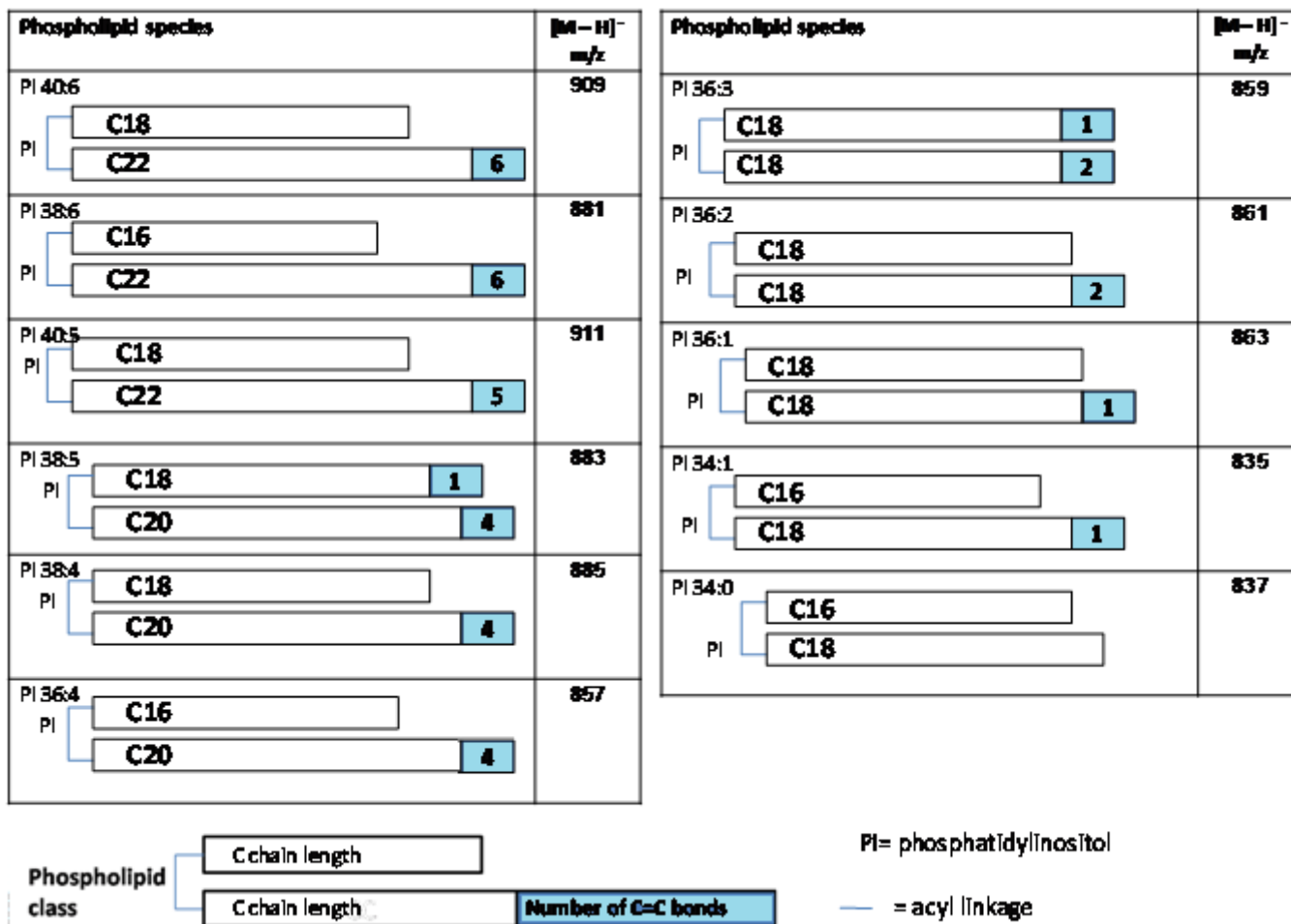


Figure 3.10b Eleven phosphatidylinositol species were identified in mouse cerebral cortex samples using precursor ion scans of m/z 241 (equivalent to loss of the inositol headgroup, which has a mass of 241) The majority of PI in mouse cerebral cortex contained arachidonic acid (20:4)



3.4. Fragmentation studies of phospholipid species in mouse cerebral cortex

Phospholipid ions identified with fragmentation scanning were further subjected to precursor ion scans in the negative (ES-) mode to identify the fatty acyl, plasmogen or ether groups that made up the remainder of the phospholipid's structure. The addition of 0.02% formic acid to the mass spectrometry solvent facilitated the production of negative fatty acyl ions from the phospholipid structure (Esch et al., 2007).

The use of tandem mass spectrometry on the phosphatidylethanolamine, phosphatidylserine and phosphatidylinositol species identified in naïve mouse cerebral cortex sample resulted in the production of negative fatty acyl ions $[R-H]^-$ which can be definitively identified from their m/z values. However, phosphatidylcholine species did not readily form negative ions due to their positively-charged head group despite the addition of 0.02% formic acid to the chloroform/methanol solvent, and so for these lipids, positively-charged ions were used for identification of the fatty acyl chain.

It is generally acknowledged that the fatty acyl group at the sn-2 position gives a stronger signal than that at the sn-1 position, due to the fact that the R group at sn-2 is more easily ionized than that at sn-1 (Han & Gross, 2005; Pulfer & Murphy, 2003; Taguchi et al., 2005). Therefore, if more than one R group is identified on an MS/MS scan, it can be deducted that the R group

with the highest signal is located at the sn-2 position. Figure 3.11 is a representative MS/MS scan of a phosphatidylserine species. This phosphatidylserine species has an m/z of 838 and can be identified as PS 18:0/22:4 from the m/z of the fatty acyl fragments yielded upon MS/MS analysis and the respective signal strength of these two fatty acyl ions.

Tables 3.1–3.4 show the confirmed identities (using MS/MS analysis) of the phospholipid species that had previously been putatively identified in our studies on naïve mouse cerebral cortex using the lipid analyser software.

Figure 3.11 Representative MS/MS scan of a phosphatidylserine species with m/z 838 identifies its fatty acyl chains as 18:0 and 22:4. The positioning of these two R groups can be deduced by looking at the spectrum; in general the R group at *sn*-2 has a stronger signal than that at *sn*-1 due to the fact that cleavage of the *sn*-2 acyl bond is easier than the *sn*-1 acyl bond

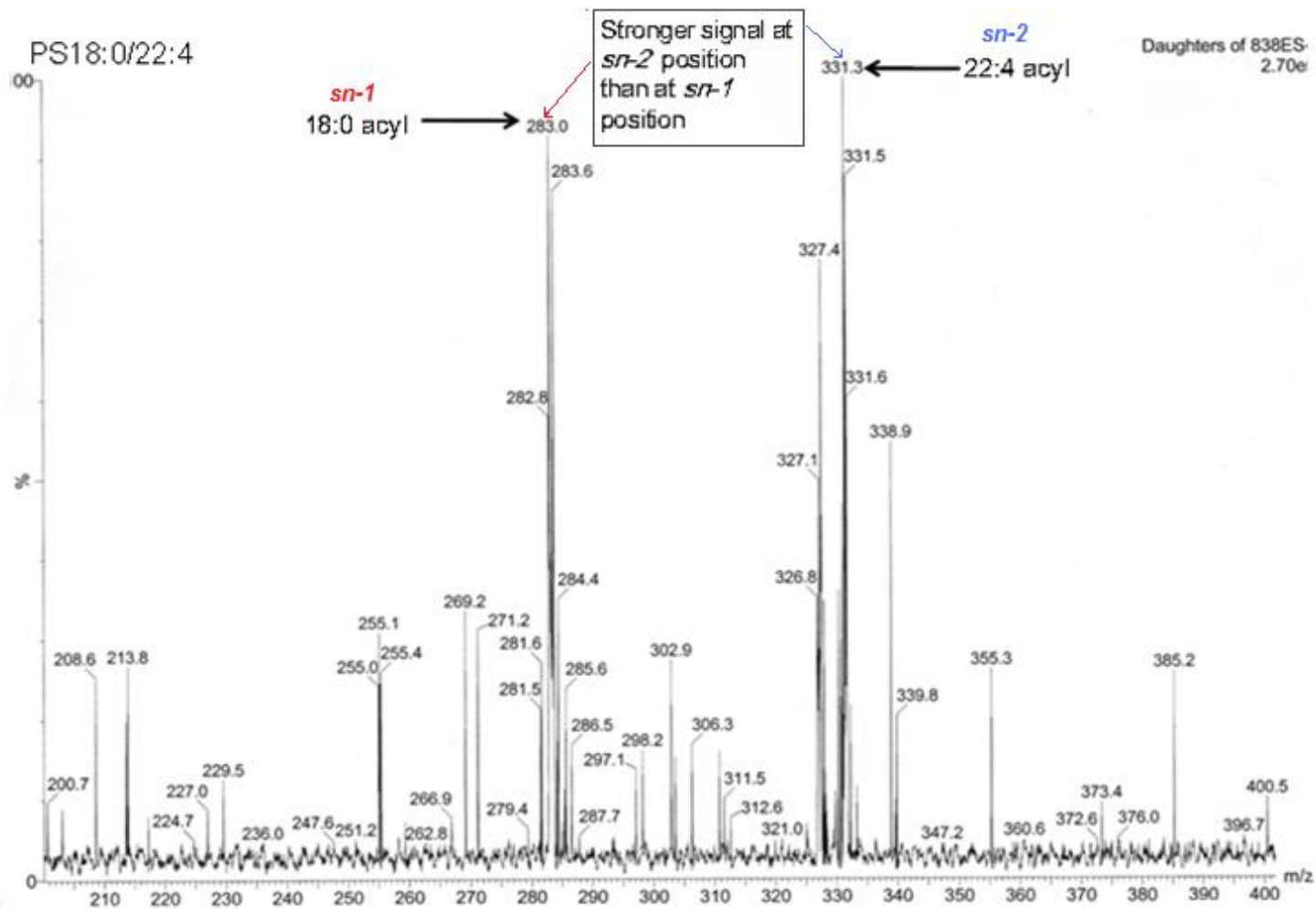


Table 3.1 Phosphatidylcholine and sphingomyelin species identified during MS/MS fragmentation scans of murine cerebral cortex lipid extract

[M+ H] ⁺ m/z	Species	Identity: using ESI-MS data and lipid analyser software	Identity: using ESI-MS/MS data
834	PC40:6	PC18:0/22:6	PC 18:1/ 22:6
832	PC40a:0	PC 18:1/ 22:6	
806	PC38:6	PC16:0/22:6	
810	PC38:4	PC 18:0/20:4	
782	PC36:4	PC16:0/20:4	
814	PC 38:2	PC18:0/20:2	
786	PC36:2	PC18:0/18:2	
758	PC 34:2	PC16:0/18:2	
816	PC 38:1	PC 18:0/20:1	PC16:0/18:1
788	PC 36:1	PC18:0/18:1	
760	PC 34:1	PC16:0/18:1	PC16:0/16:1
746	PC34a:1	PC16:0a/18:1	
732	PC 32:1	PC 16:0/16:1	PC16:0/16:0
734	PC 32:0	PC16:0/16:0	
720	PC32a:0	PC 16:0a/16:0	
706	PC 30:0	PC 14:0/16:0	
729	SM 36:2	SM 18:1/18:1	
813	SM 42:1	SM 18:1/24:0	
731	SM 36:1	SM 18:1/18:0	

Table 3.2 Phosphatidylethanolamine species identified during fragmentation MS/MS scans of murine cerebral cortex lipid extract

$[M+H]^+$ m/z	Species	Identity: using ESI-MS data and lipid analyser software	Identity: using ESI-MS/MS data	$[M-H]^-$ m/z
790	PE 40:7	PE18:1/22:6	PE18:1/22:6	788
792	PE 40:6	PE18:0/22:6	PE18:0/22:6	790
778	PE 40a:6	PE18:0a/22:6	PE18:0/22:4	776
764	PE 38:6	PE16:0/22:6	PE16:0/22:6	762
750	PE 38a:6	PE16:0a/22:6		748
794	PE 40:5	PE18:0/22:5	PE18:0/22:5	792
766	PE 38:5	PE18:1/20:4	PE16:0/22:5 PE18:1/20:4	764
752	PE 38a:5	PE18:1a/20:4		750
796	PE 40:4	PE18:0/22:4	PE18:0/22:4	794
768	PE 38:4	PE18:0/20:4	PE18:0/20:4	766
740	PE 36:4	PE16:0/20:4		738
840	PE44a:3			838
812	PE42a:3			810
798	PE 40:3	PE18:0/22:3	PE18:0/22:3	796
770	PE 38:3	PE18:0/20:3	PE18:0/20:3	768
742	PE 36:3	PE18:1/18:2		740
814	PE42a:2			812
786	PE 40a:2	PE18:0a/22:2		784
772	PE 38:2	PE18:0/20:2		770
744	PE 36:2	PE18:0/18:2	PE16:0/20:2 PE18:1/18:1	742
816	PE42a:1			814
788	PE 40a:1	PE18:0a/22:1		786
774	PE 38:1	PE18:0/20:1		772
746	PE 36:1	PE18:0/18:1	PE18:0/18:1	744
718	PE 34:1	PE16:0/18:1	PE16:0/18:1	716
776	PE 38:0	PE18:0/20:0		774
762	PE 38a:0	PE18:0a/20:0	PE16:1/22:6	760
748	PE 36:0	PE 18:0/18:0		746
720	PE 34:0	PE16:0/18:0	PE16:0/18:0	718

Table 3.3 Phosphatidylserine species identified during fragmentation MS/MS scans of murine cerebral cortex lipid extract

[M – H]⁻ m/z	Species	Identity: using ESI-MS data and lipid analyser software	Identity: from ESI-MS/MS data
882		PS22:4/22:6	
878		PS22:6/22:6	
832	PS 40:7	PS18:1/22:6	PS18:1/22:6
834	PS 40:6	PS18:0/22:6	PS18:0/22:6
836	PS 40:5	PS18:0/22:5	PS18:0/22:5
838	PS 40:4	PS18:0/22:4	PS18:0/22:4
810	PS 38:4	PS18:0/20:4	PS18:0/20:4
840	PS 40:3	PS18:0/22:3	
812	PS 38:3	PS18:0/20:3	PS18:0/20:3 PS18:1/20:2
814	PS 38:2	PS18:0/20:2	
786	PS 36:2	PS18:0/18:2	PS18:1/18:1
872	PS 42:1		PS18:0/24:1
844	PS 40:1	PS18:0/22:1	PS18:0/22:1
816	PS 38:1	PS18:0/20:1	PS18:0/20:1
788	PS 36:1	PS18:0/18:1	PS18:0/18:1
760	PS 34:1	PS16:0/18:1	PS16:0/18:1

Table 3.4 Phosphatidylinositol species identified during MS/MS fragmentation scans of murine cerebral cortex lipid extract

[M – H]⁻ m/z	Species	Identity: using ESI-MS data and lipid analyser software	Identity: from ESI-MS/MS data
909	PI 40:6	PI18:0/22:6	PI18:0/22:6
881	PI 38:6	PI16:0/22:6	PI16:0/22:6
911	PI 40:5	PI18:0/22:5	PI18:0/22:5
883	PI 38:5	PI18:1/20:4	PI18:1/20:4
885	PI 38:4	PI18:0/20:4	PI18:0/20:4
857	PI 36:4	PI16:0/20:4	PI16:0/20:4
859	PI 36:3	PI18:1/18:2	PI16:0/20:3
861	PI 36:2	PI18:0/18:2	PI18:1/18:1
863	PI 36:1	PI18:0/18:1	PI18:1/18:0
835	PI 34:1	PI16:0/18:1	PI16:0/18:1
837	PI 34:0	PI16:0/18:0	PI16:0/18:0

3.5. Investigation of changes in cerebral cortex phospholipids produced by ALA 3, 24, 72 and 168 hours after its administration

The phospholipid profiles of mice given intravenous injections of ALA or vehicle (0.05% volume ethanol) 3 hours, 24 hours, 3 days (72 hours) and 1 week (168 hours) prior to sample collection were analysed using strictly the same MS/MS procedure. A general scan of each species was used to gain an overall picture of the species present in each sample. Following general scanning of each sample, neutral loss scans for 87 (PS species) and 141 (PE species) and precursor ion scans for 184 (PS and SM species) and 241 (PI species) were carried out on each sample to detect individual classes of phospholipids. The following graphs (figures 3.12 – 3.15 a-d) compares the brain phospholipid profile of naïve mice (CTL) compared to mice treated with vehicle (VEH) or α -linolenic acid (ALA) at four separate timepoints (3, 24, 72 and 168 hours after tail vein injection). The effect on each phospholipid class at each timepoint is shown in separate graphs. Statistically significant ($P < 0.05$) changes were observed in three phospholipid species three hours after fatty acid treatment and in two phospholipid at 24 hours after fatty acid injection. Species affected at $t=3$ hours were a sphingomyelin with m/z 813 and phosphatidylethanolamine species with m/z 742 and m/z 746. At 24 hours, a phosphatidylethanolamine with m/z 786 and phosphatidylserine with m/z 812 were affected. None of the species affected at either of these timepoints contained fatty acyl groups that were based on fatty acid substrates known to participate in the production of bioactive lipid mediators,

suggesting that changes in brain glycerophospholipid composition do not play a major role in the development of neuroprotection following PUFA treatment in rodent models of ischaemia.

In addition, the temporal effect of ALA treatment on the phospholipid composition of the cerebral cortex was assessed using statistical analysis software (results shown in Figures 3.16–3.19). No significant differences ($P < 0.05$) were seen between the brain phospholipid composition of naïve mice and mice treated with α -linolenic acid at any of the four tested timepoints ($t = 3\text{h}, 24\text{h}, 72\text{h}, 168\text{h}$ post-injection), agreeing with our theory that changes in brain glycerophospholipid composition can not explain the neuroprotective effects of PUFA treatment in rodent models of ischaemia.

Figure 3.12a Effect of ALA on phosphatidylcholine and sphingomyelin species 3h post- injection (n=8 for CTL, n=4 for ALA and VEH groups, error bars \pm SD.)

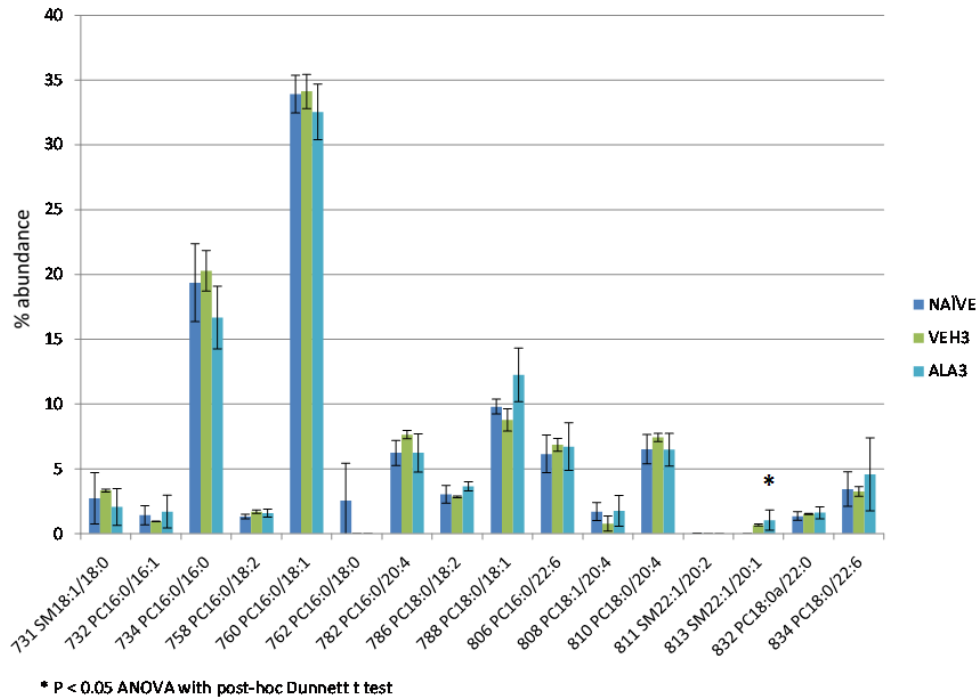


Figure 3.12b Effect of ALA on phosphatidylcholine and sphingomyelin species 24h post- injection (n=8 for CTL, n=4 for ALA and VEH groups, error bars \pm SD)

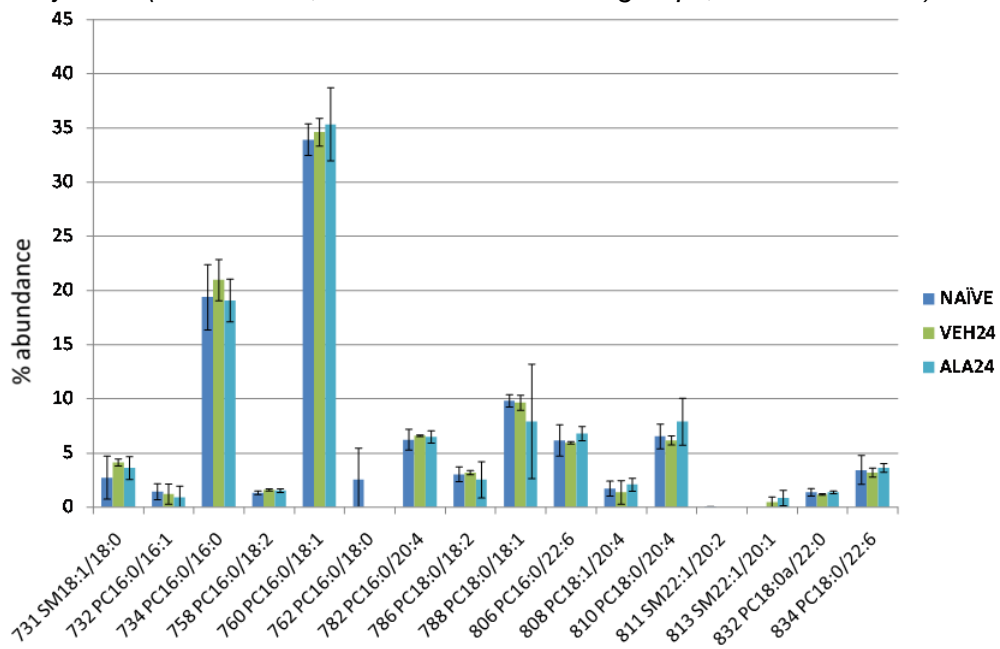


Figure 3.12c Effect of ALA on phosphatidylcholine and sphingomyelin species 72h post- injection (n=8 for CTL, n=4 for ALA and VEH groups, error bars \pm SD)

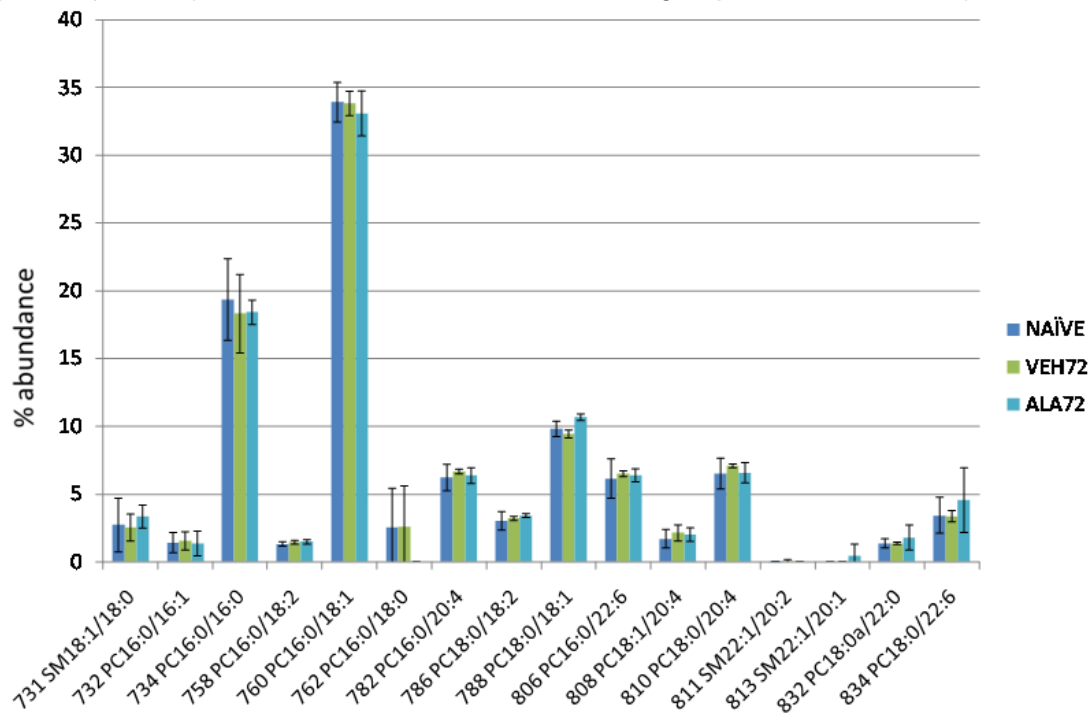


Figure 3.12d Effect of ALA on phosphatidylcholine and sphingomyelin species 168h post- injection (n=8 for CTL, n=4 for ALA and VEH groups, error bars \pm SD)

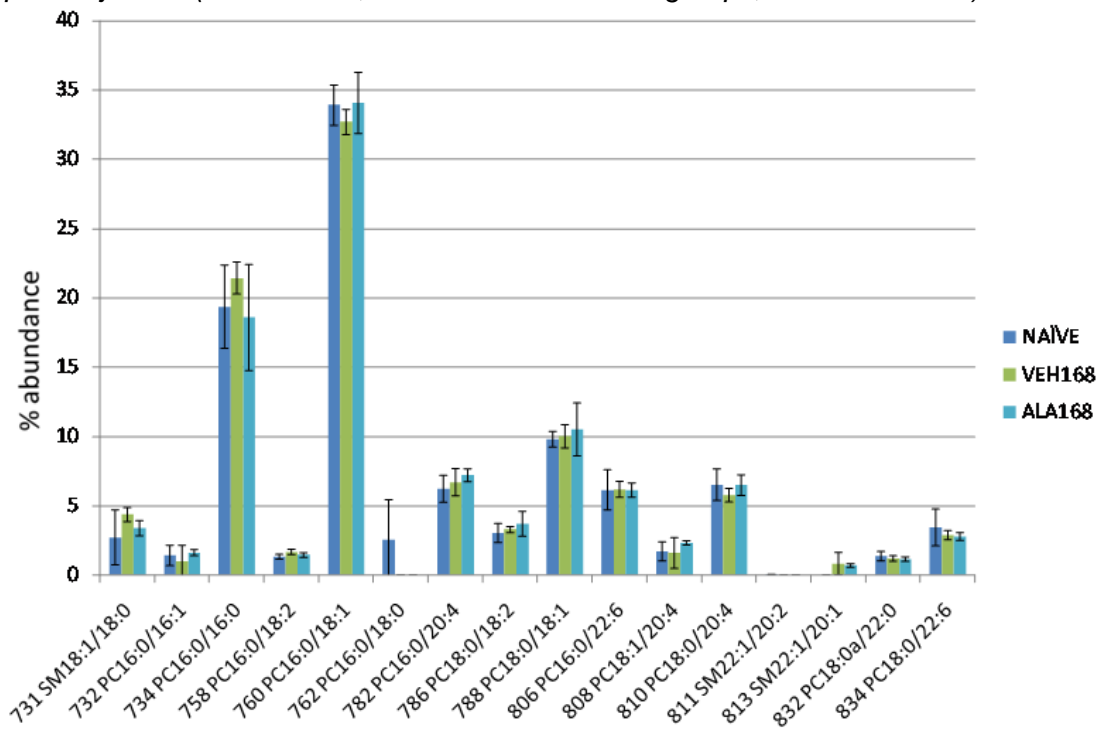


Figure 3.13a Effect of ALA on phosphatidylethanolamine species 3h post- injection (n=8 for CTL, n=4 for ALA and VEH groups, error bars \pm SD)

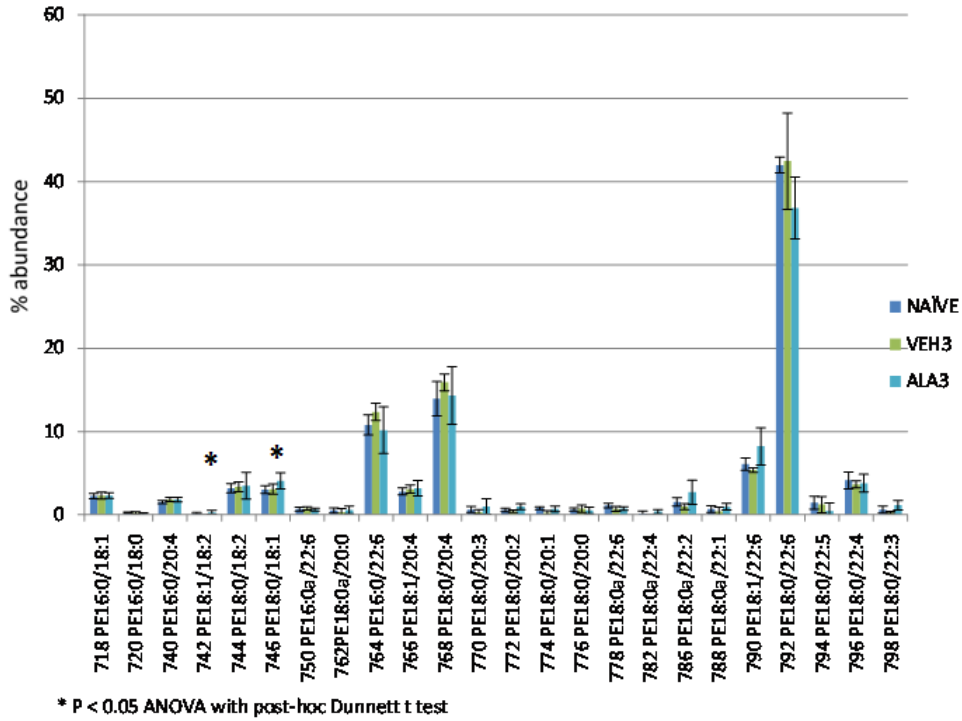


Figure 3.13b Effect of ALA on phosphatidylethanolamine species 24h post- injection (n=8 for CTL, n=4 for ALA and VEH groups, error bars \pm SD)

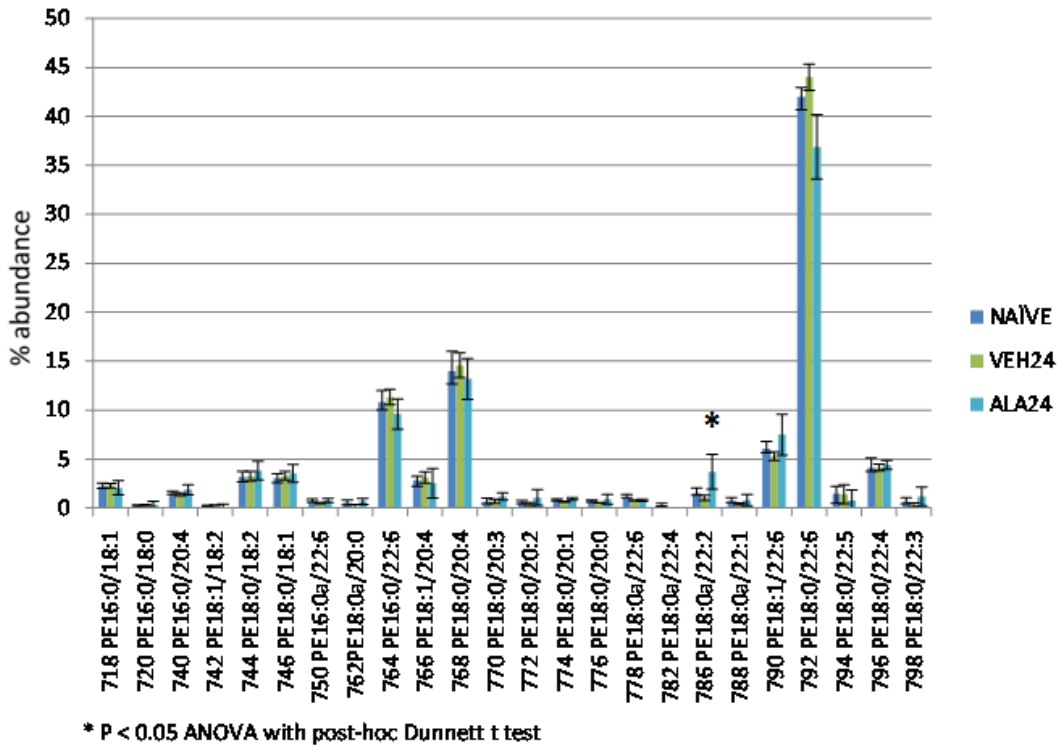


Figure 3.13c Effect of ALA on phosphatidylethanolamine species 72h post- injection (n=8 for CTL, n=4 for ALA and VEH groups, error bars \pm SD)

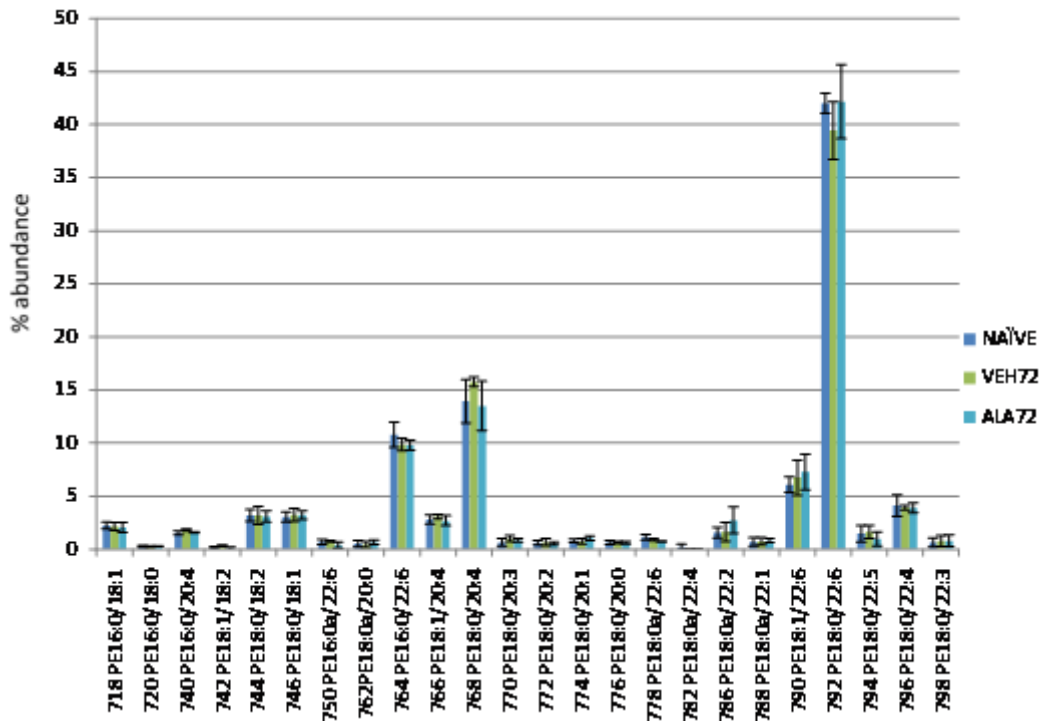


Figure 3.13d Effect of ALA on phosphatidylethanolamine species 168h post- injection (n=8 for CTL, n=4 for ALA and VEH groups, error bars \pm SD)

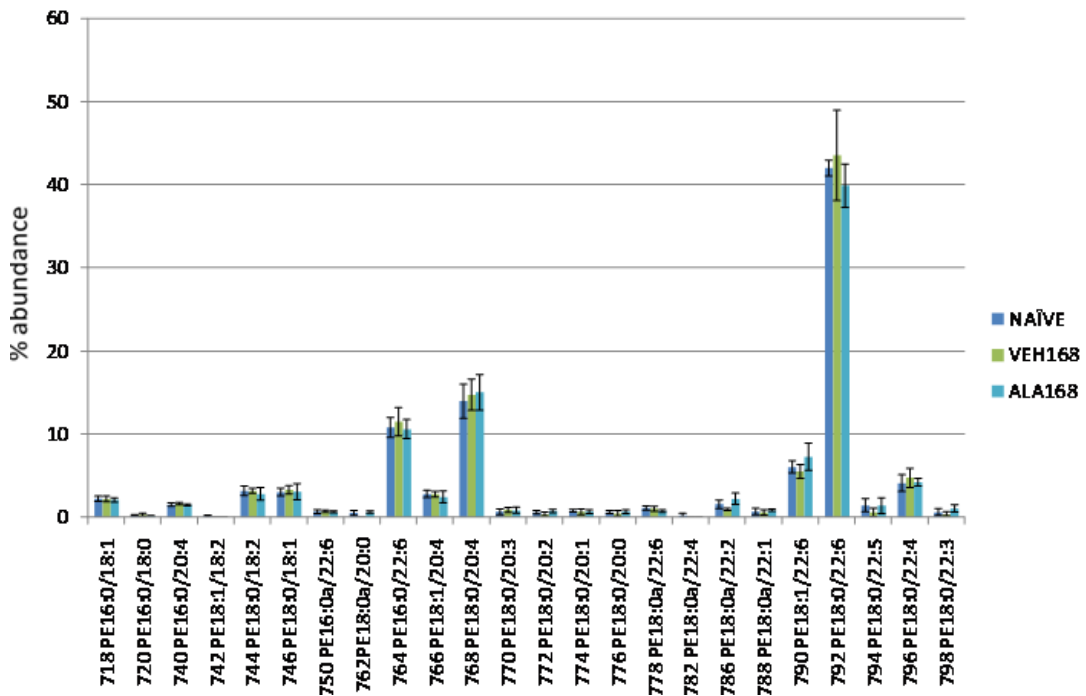


Figure 3.14a Effect of ALA on phosphatidylinositol species 3h post- injection (n=8 for CTL, n=4 for ALA and VEH groups, error bars \pm SD)

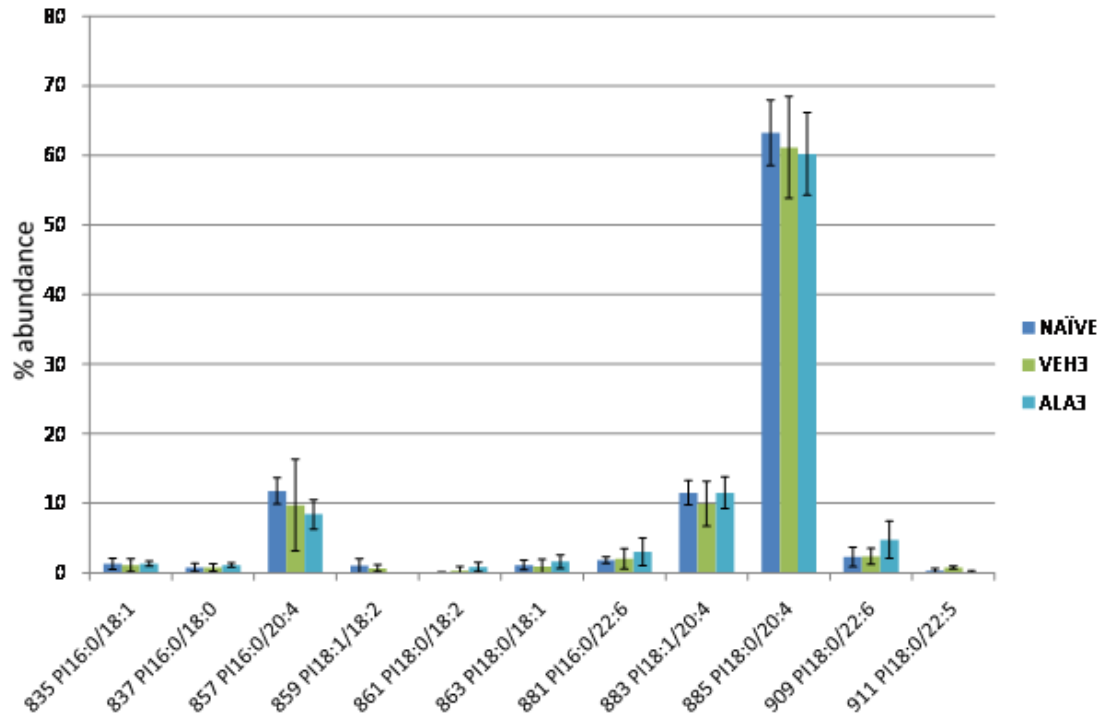


Figure 3.14b Effect of ALA on phosphatidylinositol species 24h post- injection (n=8 for CTL, n=4 for ALA and VEH groups, error bars \pm SD)

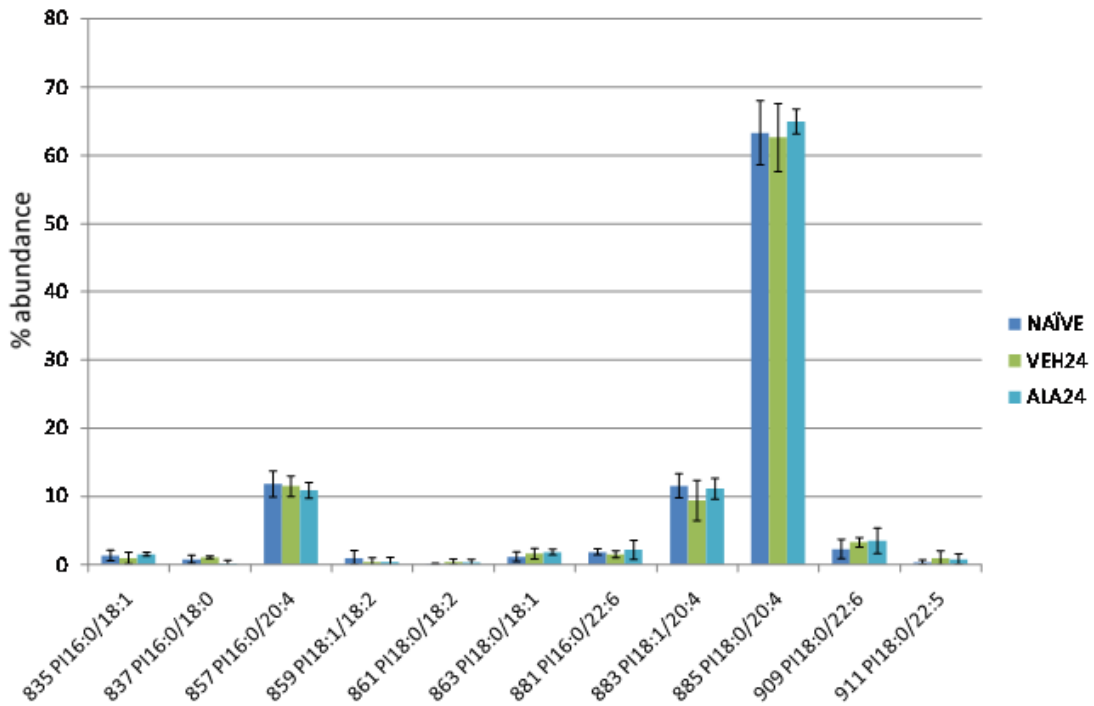


Figure 3.14c Effect of ALA on phosphatidylinositol species 72h post- injection (n=8 for CTL, n=4 for ALA and VEH groups, error bars \pm SD)

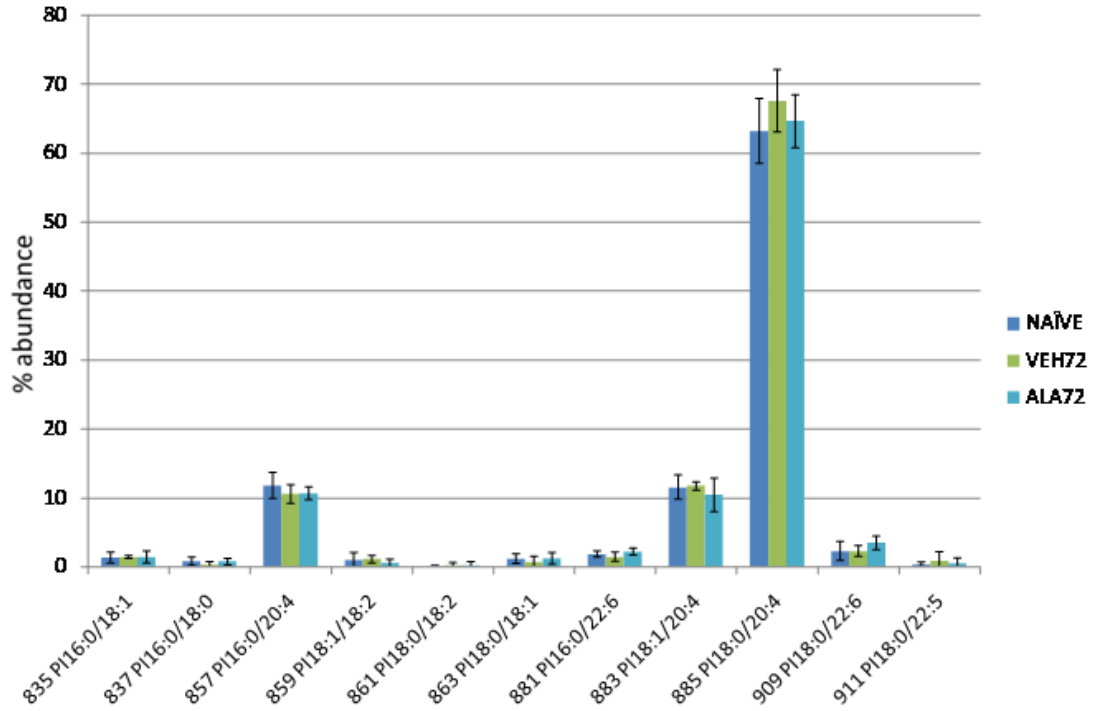


Figure 3.14d Effect of ALA on phosphatidylinositol species 168h post- injection (n=8 for CTL, n=4 for ALA and VEH groups, error bars \pm SD)

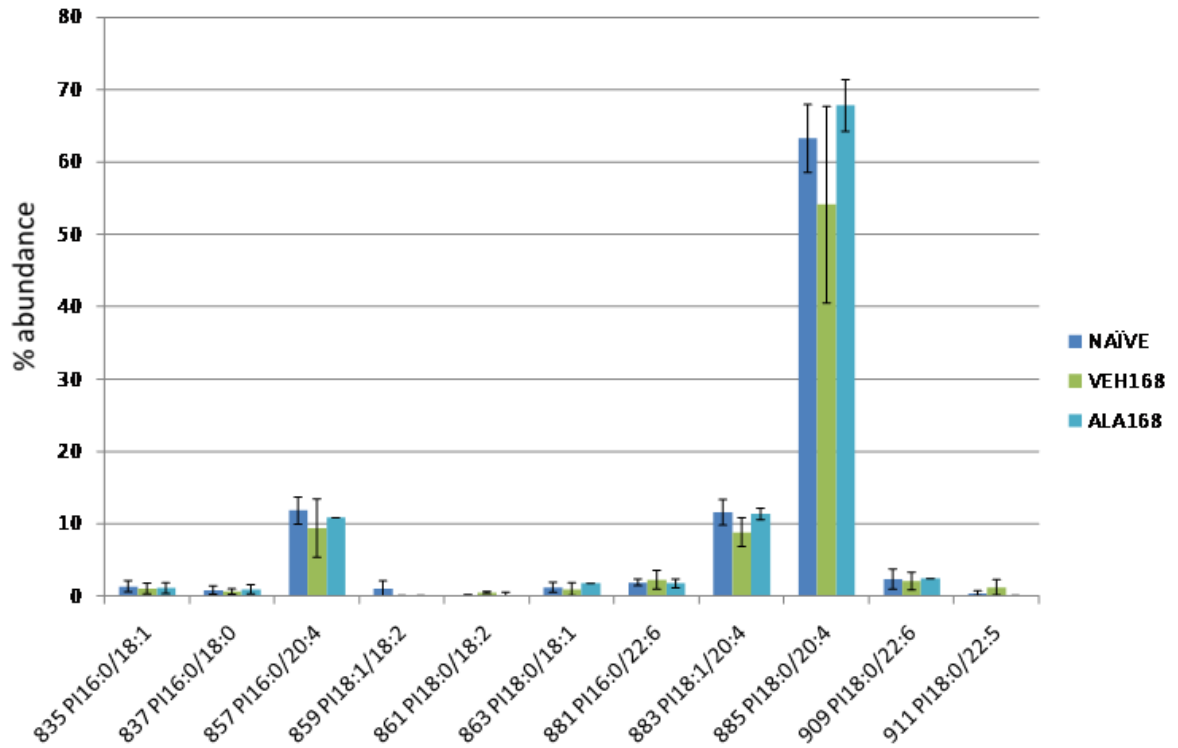


Figure 3.15a Effect of ALA on phosphatidylserine species 3h post- injection (n=8 for CTL, n=4 for ALA and VEH groups, error bars \pm SD)

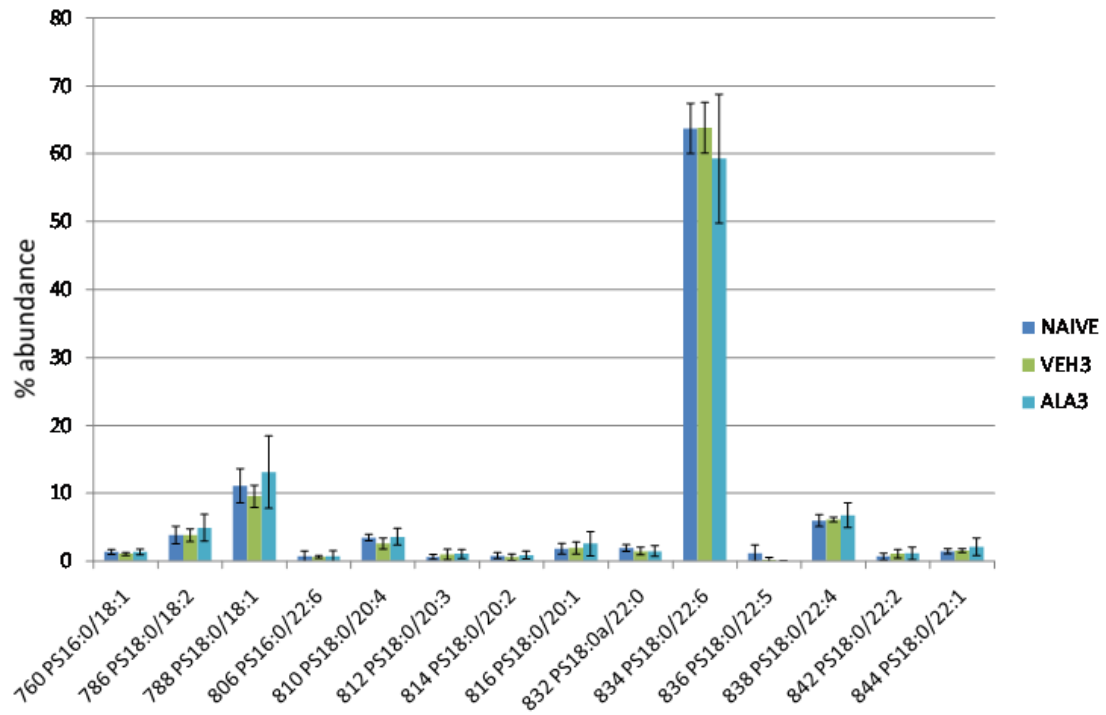
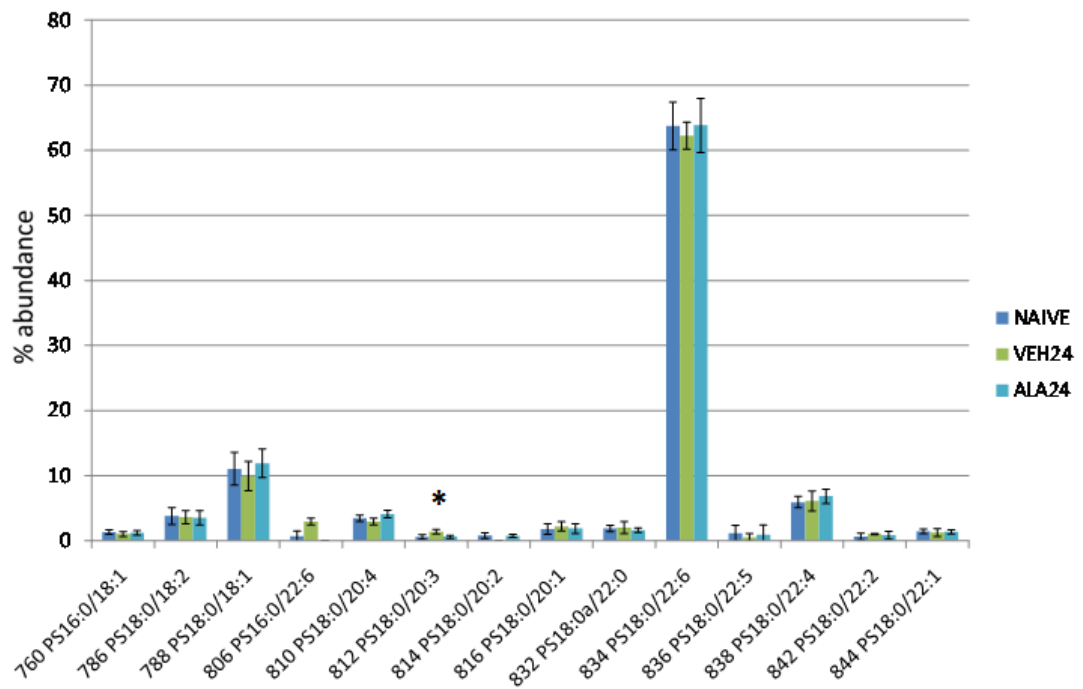


Figure 3.15b Effect of ALA on phosphatidylserine species 24h post- injection (n=8 for CTL, n=4 for ALA and VEH groups, error bars \pm SD)



* P < 0.05 ANOVA with post-hoc Dunnett t test

Figure 3.15c Effect of ALA on phosphatidylserine species 72h post- injection (n=8 for CTL, n=4 for ALA and VEH groups, error bars \pm SD)

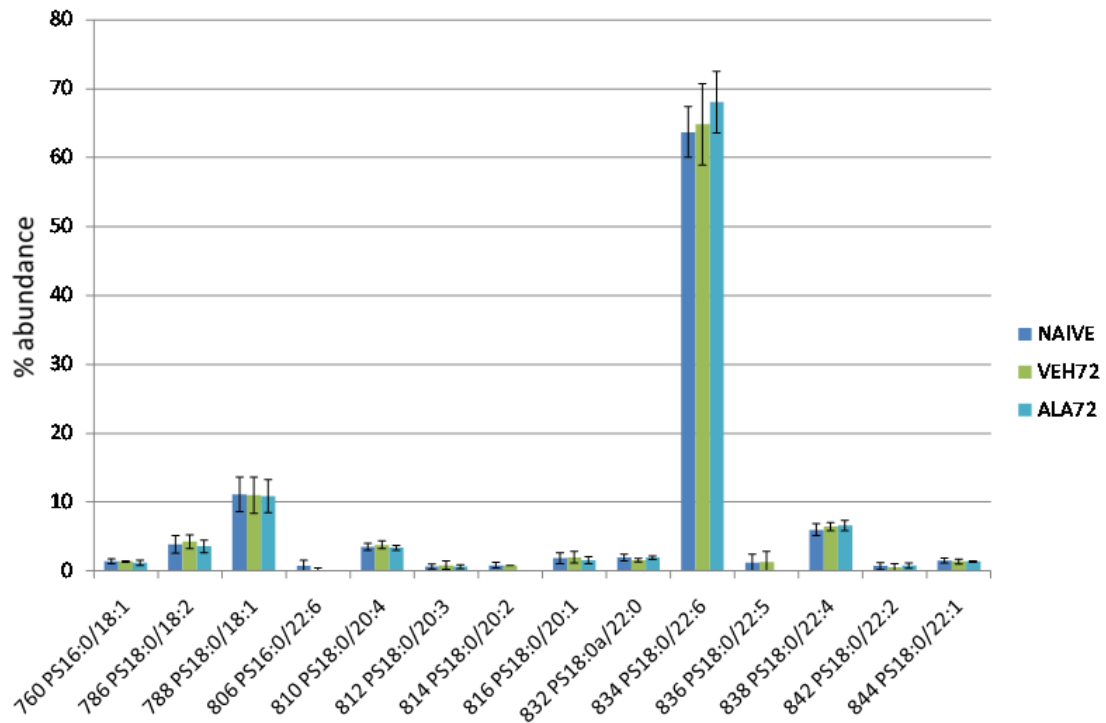


Figure 3.15d Effect of ALA on phosphatidylserine species 168h post- injection (n=8 for CTL, n=4 for ALA and VEH groups, error bars \pm SD)

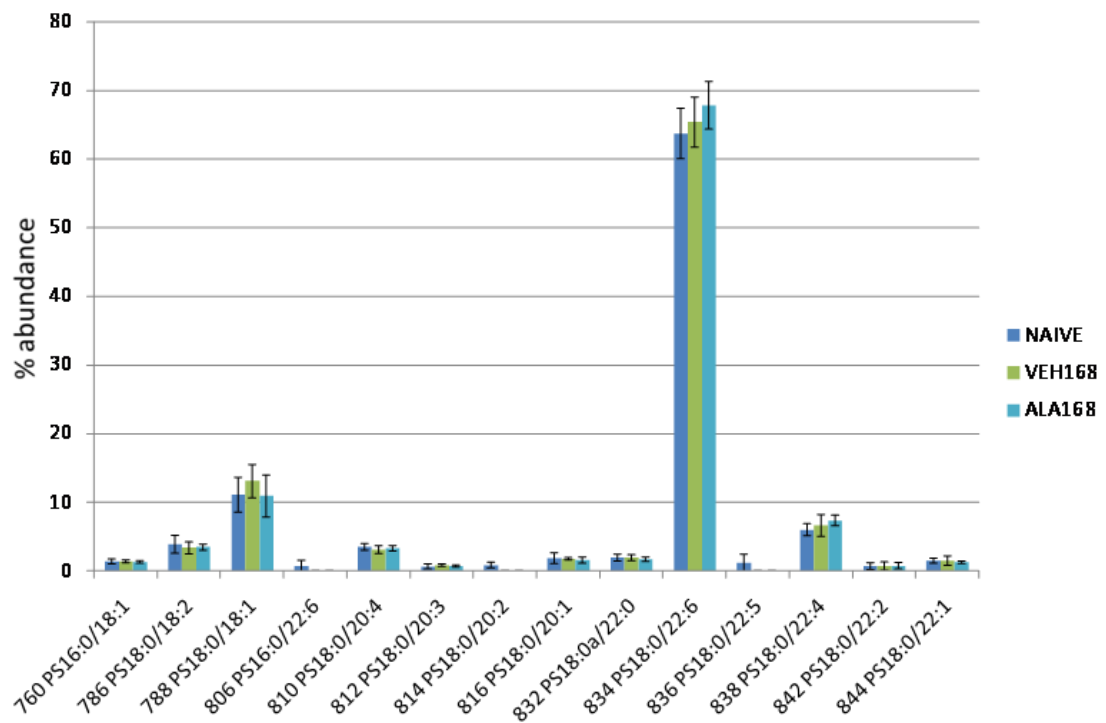


Figure 3.16. Temporal effect of ALA treatment on choline phospholipid species in mouse cortex, error bars \pm SD.

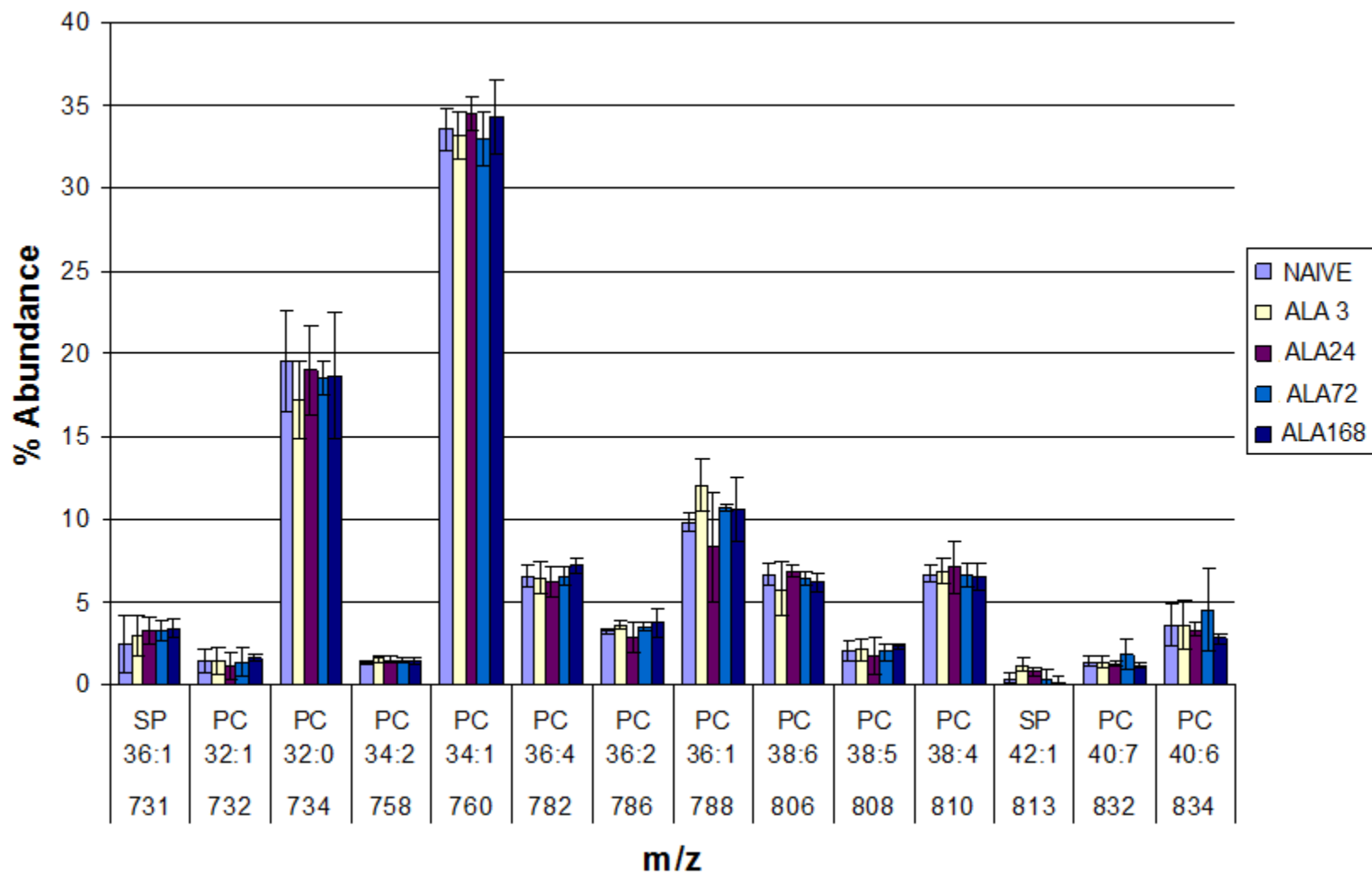


Figure 3.17 Temporal effect of ALA treatment on phosphatidylethanolamine species in mouse cortex, error bars \pm SD.

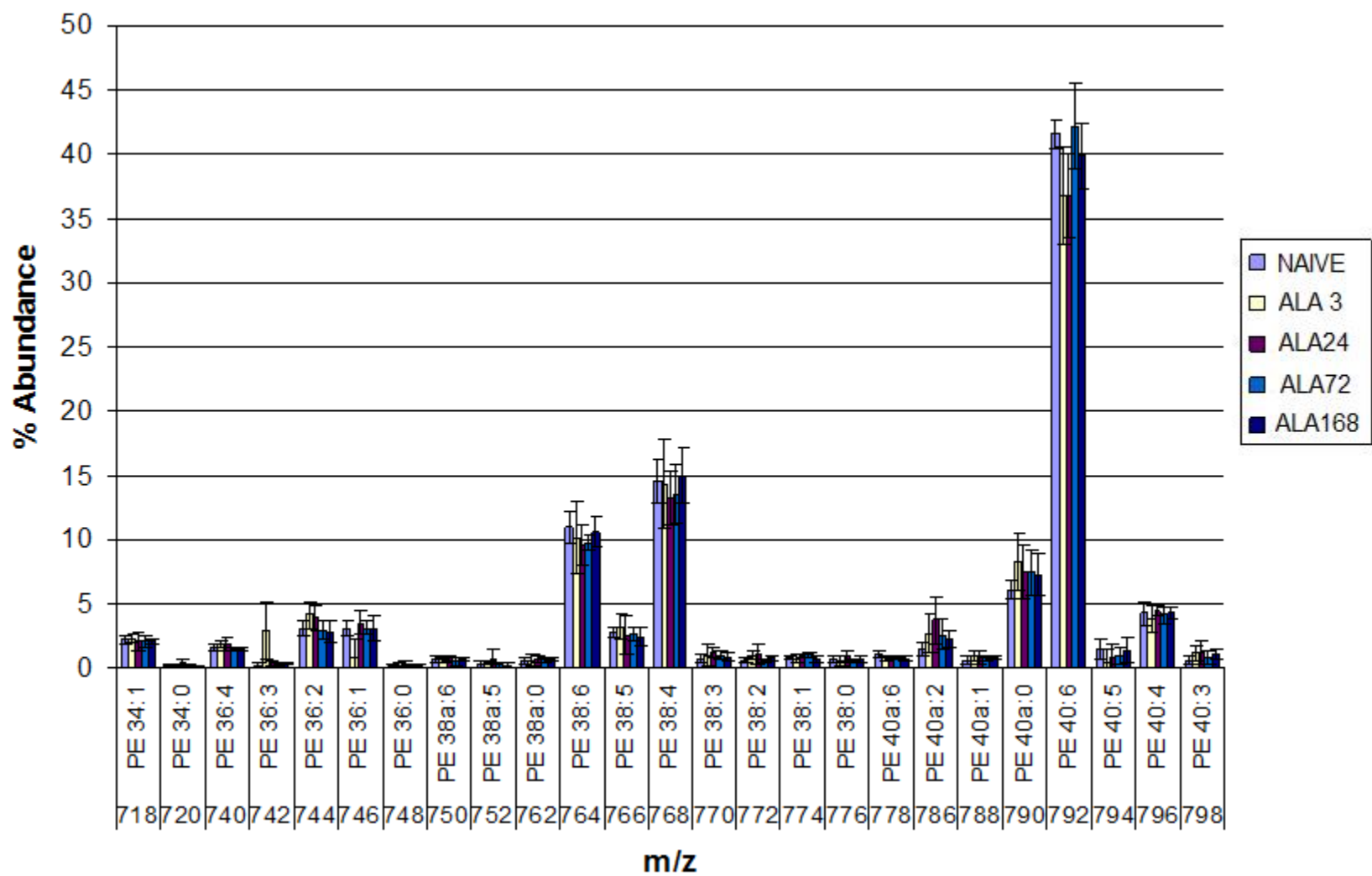


Figure 3.18 Temporal effect of ALA treatment on phosphatidylinositol species in mouse cortex, error bars \pm SD.

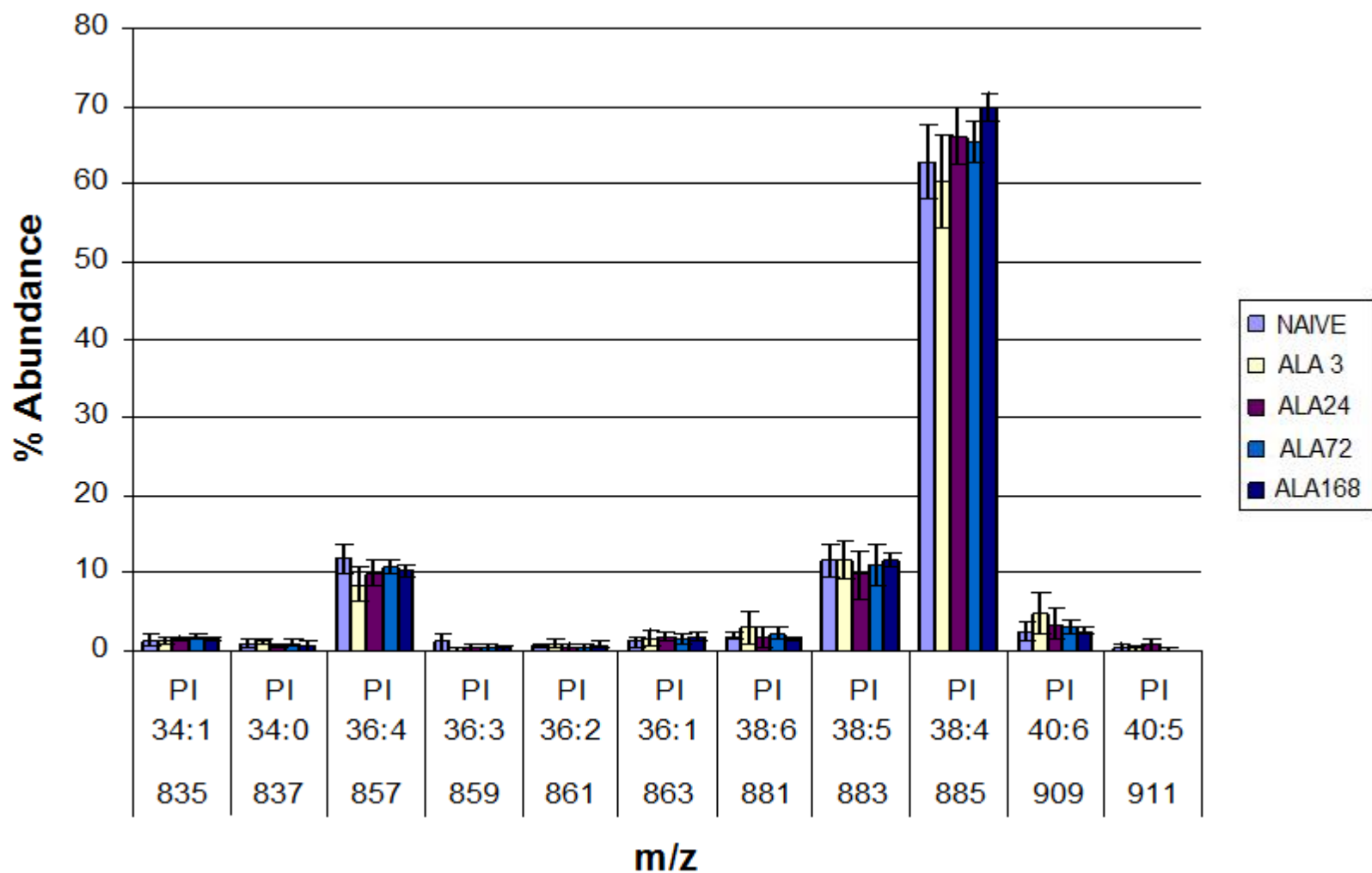
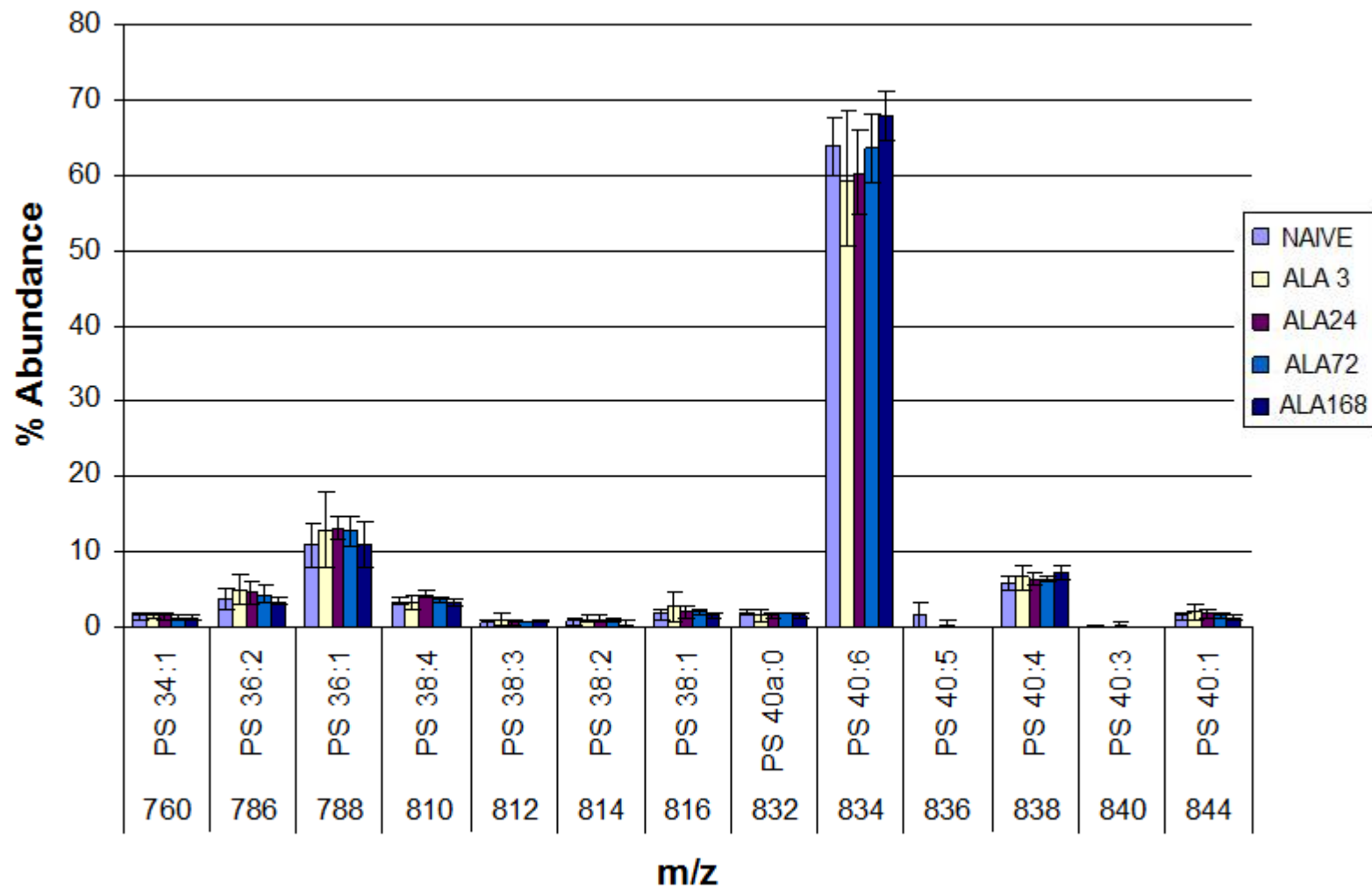


Figure 3.19 Temporal effect of ALA treatment on phosphatidylserine species in mouse cortex, error bars \pm SD.



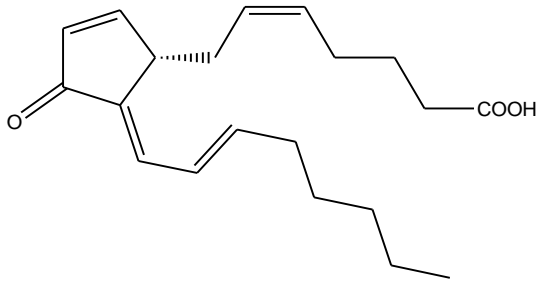
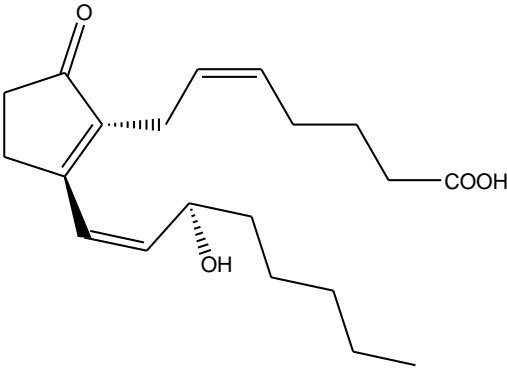
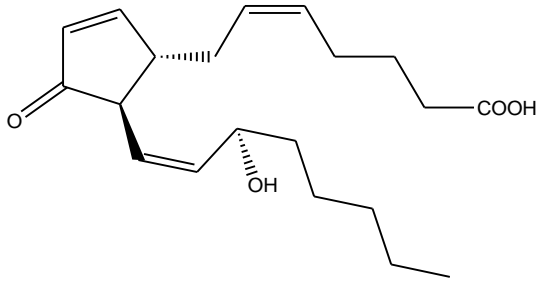
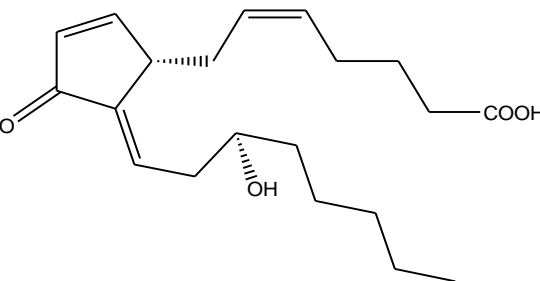
4. Analysis of lipid mediators in mouse cerebral cortex and plasma

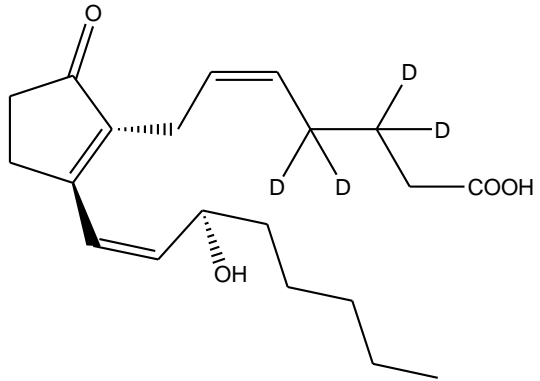
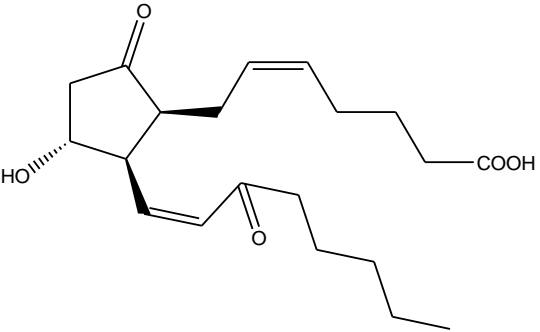
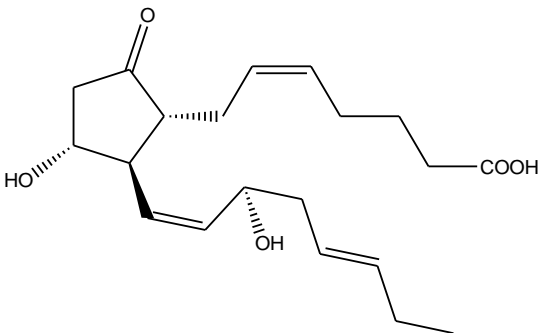
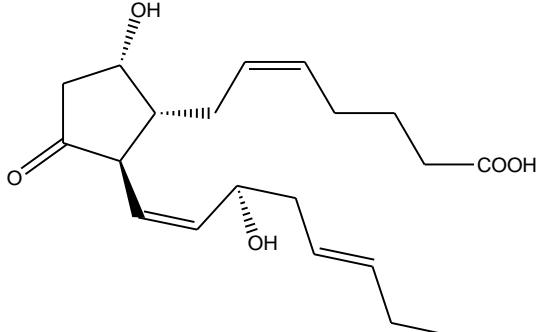
4.1. Profile of prostanoids in mouse cerebral cortex and plasma

4.1.1. Preparation of calibration curves

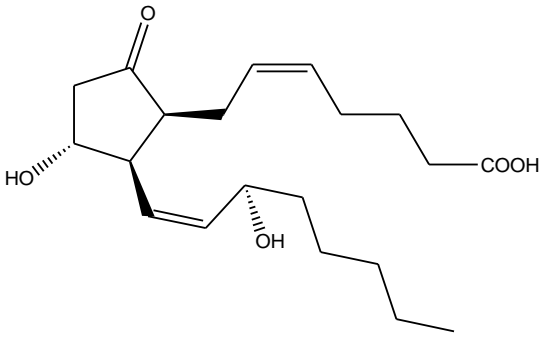
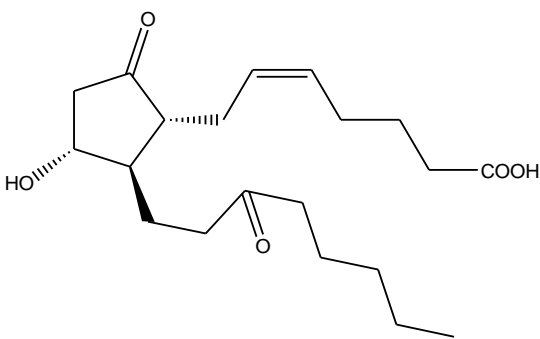
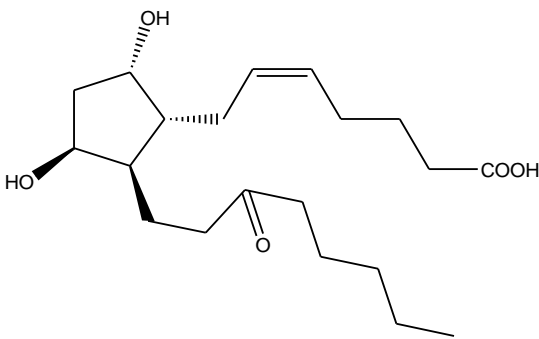
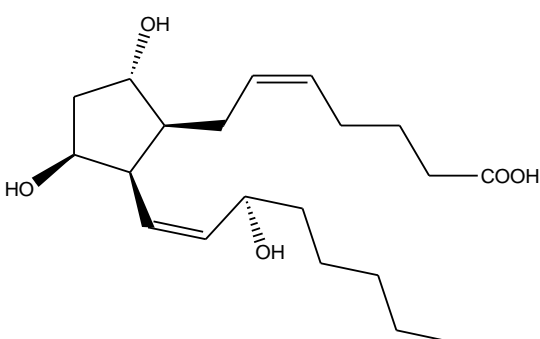
Twenty seven prostanoids were combined into a cocktail of standards, which was diluted into a series of mixed standard solutions containing 200, 160, 120, 80, 40 and 20ng/ml of each prostanoid. Calibration curves were prepared using the diluted standards. Table 4.1 shows the MRM transitions and approximate retention times of each of the compounds in the cocktail of standards.

Table 4.1 Prostanoid standards used for quantification analysis using multiple-reaction monitoring (MRM). Isobaric species can be separated on the basis of their different retention times in the reverse-phase HPLC column (Masoodi et al., 2006).

Species	Mol. wt. of [M-H] ⁻	Structure of species	Transition m/z	Approx. retention time (min)
15-deoxy- Δ 12,14-PGJ ₂	315		315>271	18.10
PGB ₂	333		333>175	9.98
PGJ ₂	333		333>271	9.17
Δ 12-PGJ ₂	333		333>271	9.80

Species	Mol. wt. of [M-H] ⁻	Structure of species	Transition m/z	Approx. retention time (min)
Internal Standard (PGB ₂ -d ₄)	337		337>179	9.96
8-iso-15-keto PGE ₂	349		349>113	5.68
PGE ₃	349		349>269	3.85
PGD ₃	349		349>269	4.09

Species	Mol. wt. of [M-H] ⁻	Structure of species	Transition m/z	Approx. retention time (min)
PGF _{3α}	349		351>193	3.30
PGE ₂	351		351>271	4.47
PGD ₂	351		351>271	5.18
8-iso-15-keto PGF _{2α}	351		351>315	4.09

Species	Mol. wt. of [M-H] ⁻	Structure of species	Transition m/z	Approx. retention time (min)
8-iso-PGE ₂	351	 <p>The structure shows a cyclopentane ring with a ketone group at C1 and a hydroxyl group at C2 (dashed). At C3, there is a propyl chain with a double bond at C4 and a hydroxyl group at C5 (dashed). At C5, there is a heptyl chain with a double bond at C6 and a carboxylic acid group at C7.</p>	351>315	4.47
13,14-dihydro-15-keto-PGE ₂	351	 <p>The structure shows a cyclopentane ring with a ketone group at C1 and a hydroxyl group at C2 (dashed). At C3, there is a propyl chain with a double bond at C4. At C5, there is a heptyl chain with a double bond at C6, a ketone group at C7, and a carboxylic acid group at C8.</p>	351>333	6.98
13,14-dihydro-15-keto-PGF _{2α}	353	 <p>The structure shows a cyclopentane ring with a hydroxyl group at C2 (dashed) and another hydroxyl group at C3 (wedged). At C4, there is a propyl chain with a double bond at C5. At C6, there is a heptyl chain with a double bond at C7, a ketone group at C8, and a carboxylic acid group at C9.</p>	353>113	8.12
8-iso-PGF _{2α}	353	 <p>The structure shows a cyclopentane ring with a hydroxyl group at C2 (wedged) and another hydroxyl group at C3 (dashed). At C4, there is a propyl chain with a double bond at C5 and a hydroxyl group at C6 (dashed). At C6, there is a heptyl chain with a double bond at C7 and a carboxylic acid group at C8.</p>	353>193	3.38

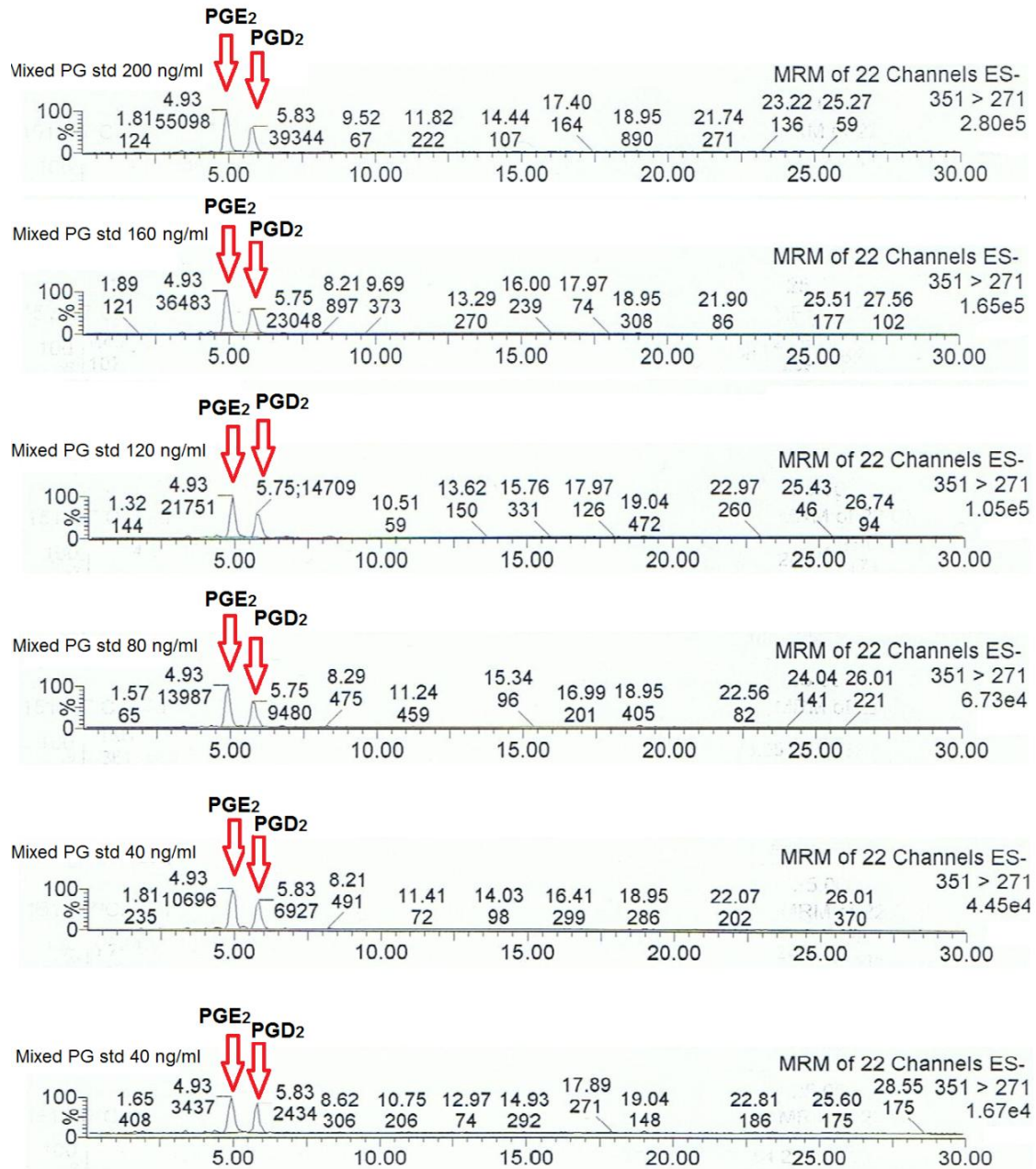
Species	Mol. wt. of [M-H] ⁻	Structure of species	Transition m/z	Approx. retention time (min)
PGF _{2α}	353		353>193	3.77
PGE ₁	353		353>317	4.47
PGD ₁	353		353>317	4.79
13,14-dihydro-15-keto PGE ₁	353		353>335	7.61

Species	Mol. wt. of [M-H] ⁻	Structure of species	Transition m/z	Approx. retention time (min)
13,14-dihydro-15-keto-PGF _{1α}	355		355>193	6.67
PGF _{1α}	355		355>311	3.69
13,14-dihydro-PGF _{2α}	355		355>311	4.79
13,14-dihydro-PGE ₁	355		355>337	5.41

Species	Mol. wt. of [M-H] ⁻	Structure of species	Transition m/z	Approx. retention time (min)
13,14-dihydro-PGF _{1α}	357		357>113	4.94
TXB ₃	367		367>169	3.06
6-keto PGF _{1α}	369		369>163	2.83
TXB ₂	369		369>169	3.46

Each of these 22 MRM channels yielded a chromatogram, on which the compounds undergoing that specific transition could be detected. Figure 4.1 illustrates representative chromatograms generated from the transition 351>271. This transition can detect two compounds with different column retention times: PGE₂, which has a retention time of approximately 4.9 min, and PGD₂, which has a slightly longer retention time of approximately 5.8 min.

Figure 4.1 Analysis of mixed prostaglandin standards following the transition m/z 351 > 271. Both PGE₂ (retention time ≈ 4.9 mins) and PGD₂ (retention time ≈ 5.8 mins) can be simultaneously detected. Integration of the peaks obtained can be used to produce calibration lines for these two prostanoids.



4.1.2. Lipid mediator profiling in naïve mice

Out of the twenty seven prostanoid species that could be detected by this ESI/LC-MS/MS assay, twenty five species were detected in samples of mouse cerebral cortex and eighteen were detected in samples of mouse plasma.

The most prominent prostanoid species in the cerebral cortex of untreated mice, each accounting for more than 10% of total prostanoids were PGE₂, PGD₂, 6-keto-PGF_{2α}, PGF_{2α} and PGE₁. The most prominent prostanoid species in the plasma of untreated mice, each accounting for more than 10% of total prostanoids, were 15-deoxy-Δ12,14-PGJ₂, PGB₂ and TXB₂. The prostanoid species detected in untreated mouse cerebral cortex and plasma are listed in Tables 4.2 and 4.3.

Table 4.2 Table showing % total of prostanoids in naïve mouse cerebral cortex

Prostanoid species	% total prostanoids in naïve mouse cerebral cortex (n=6)
	MEAN ± SD
PGD ₂	33.65 ± 29.33
PGF _{2α}	25.22 ± 25.09
6-keto PGF _{2α}	14.04 ± 13.20
PGE ₁	12.32 ± 19.55
PGE ₂	10.54 ± 14.06
PGD ₁	2.00 ± 4.91
TXB ₂	1.75 ± 4.28
Δ12-PGJ ₂	1.19 ± 2.31
PGB ₂	0.73 ± 1.78
15-deoxy-Δ12,14-PGJ ₂	0.66 ± 1.06
13,14-dihydro-PGF _{2α}	0.21 ± 0.51
13,14-dihydro-15-keto PGE ₂	0.08 ± 0.14

Table 4.3 Table showing % total of prostanoids in naïve mouse plasma

Prostanoid species	% total prostanoids in naïve mouse plasma (n=6)
	MEAN ± SD
15-deoxy- Δ 12,14-PGJ ₂	33.25 ±
TXB ₂	31.90 ±
PGB ₂	22.35 ±
8-iso-PGF ₂	8.41 ±
PGE ₂	2.01 ±
Δ 12-PGJ ₂	1.12 ±
PGF _{2α}	0.96 ±

Figure 4.2 shows representative chromatograms acquired from analysis of naïve mouse cerebral cortex tissue. The transitions shown include the m/z 351>271 transition, which is used to detect both PGD₂ and PGE₂, and the m/z 351>315 transition, which detects 6-keto PGF_{2 α} . These three compounds are amongst the most abundant prostanoid species detected in our study on naïve mouse cerebral cortex.

Figure 4.3 shows representative chromatograms acquired from analysis of naïve mouse plasma. The transitions shown include the m/z 369>269, which is used to detect TXB₂. This compound is amongst the most abundant prostanoid species detected in our study on naïve mouse plasma.

Figure 4.2 Representative chromatograms acquired from analysis of cerebral cortex tissue taken from a naïve mouse. The transition m/z 351 > 271 shows two well-separated peaks, which are indicative of PGE_2 (retention time 4.44 min) and PGD_2 (retention time 5.09 min). The transition m/z 351 > 315 shows a distinctive peak for 6-keto $PGF_{2\alpha}$ with a retention time of 5.09min.

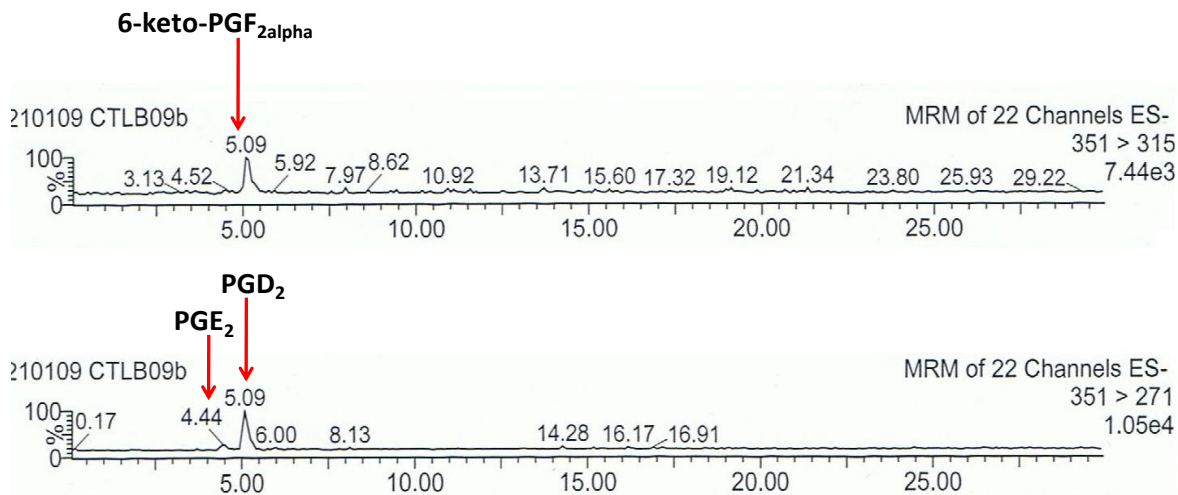
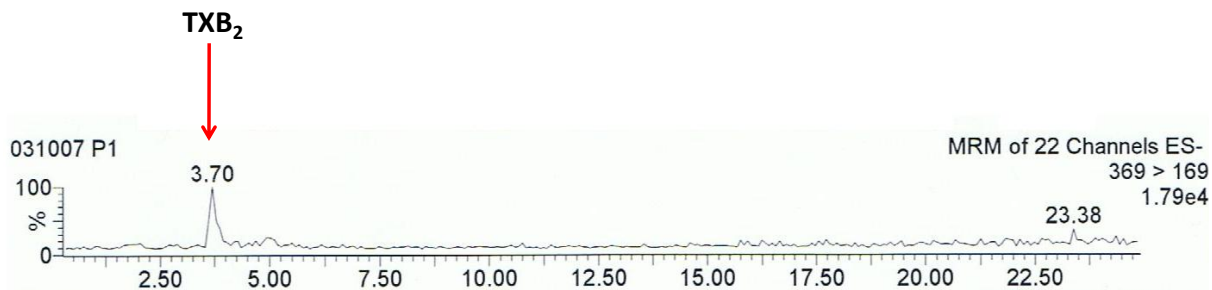


Figure 4.3 Representative chromatogram acquired from analysis of plasma collected from a naïve mouse. The transition m/z 369 > 169 shows a defined peak at 3.70 min, which corresponds to TXB_2 .



4.1.3. Effect of ALA treatment

Mice which underwent different treatments had some similarities in the identities of the most abundant prostanoid species. For example, PGE₂ and PGD₂ accounted for more than 10% of total prostanoid species in the cerebral cortex of mice in the VEH3, VEH24 and ALA3 treatment groups. 6-iso-15-keto PGF_{2α} was prominent in both the VEH3 and VEH168 groups and 8-iso-PGE₃ in the VEH3, ALA3 and ALA24 groups. Other prominent prostanoid species were PGB₂ in the VEH72 and ALA168 groups, PGF_{2α} in the VEH72 and VEH168 groups, 15-deoxy-Δ^{12,14}-PGJ₂ in the ALA72 and ALA168 groups, and TXB₂ in the ALA3, ALA24 and ALA72 groups.

Details of the abundance of prostanoid species detected in samples of mouse cerebral cortex and mouse plasma collected at various timepoints from animals divided into different treatment groups are shown in Tables 4.4 and 4.5 respectively.

Table 4.4 Table showing the % abundance of prostanoids detected in samples of mouse cerebral cortex collected at various timepoints from animals divided into different treatment groups (CTL= naïve/untreated mice, VEH3= intravenous vehicle at 3h post-injection, ALA3= intravenous α -linolenic acid at 3h post-injection, VEH24= intravenous vehicle at 24h post-injection, ALA24= intravenous α -linolenic acid at 24h post-injection VEH72= intravenous vehicle at 72h post-injection, ALA72= intravenous α -linolenic acid at 72h post-injection, VEH168= intravenous vehicle at 168h post-injection, ALA168= intravenous α -linolenic acid at 168h post-injection, N/D= not detected)

	CTL n=6		VEH3 n=6		ALA3 n=7		VEH24 n=6		ALA24 n=4		VEH72 n=6		ALA72 n=4		VEH168 n=6		ALA168 n=6	
	MEAN	SD	MEAN	SD	MEAN	SD	MEAN	SD	MEAN	SD	MEAN	SD	MEAN	SD	MEAN	SD	MEAN	SD
PGD ₂	33.65	29.33	12.28	6.23	26.26	15.17	76.32	39.70	51.61	5.19	N/D	N/D	N/D	N/D	12.04	8.76	N/D	N/D
PGF _{2α}	25.22	25.09	3.83	9.39	5.80	13.62	5.59	10.40	N/D	N/D	22.90	32.61	N/D	N/D	17.31	8.53	N/D	N/D
6-keto PGF _{2α}	14.04	13.20	11.71	2.05	2.58	2.71	N/D	N/D	N/D	N/D	3.58	5.59	N/D	N/D	24.09	24.53	N/D	N/D
PGE ₁	12.32	19.55	17.25	9.48	N/D	N/D	N/D	N/D	N/D	N/D	N/D	N/D	N/D	N/D	N/D	N/D	N/D	N/D
PGE ₂	10.54	14.06	14.18	5.68	17.15	18.86	2.12	5.19	N/D	N/D	N/D	N/D	N/D	N/D	N/D	N/D	N/D	N/D
PGD ₁	2.00	4.91	4.84	5.97	N/D	N/D	N/D	N/D	N/D	N/D	N/D	N/D	N/D	N/D	6.89	3.43	N/D	N/D
TXB ₂	1.75	4.28	3.99	2.62	11.80	4.97	N/D	N/D	10.80	4.37	N/D	N/D	48.27	6.74	10.22	8.66	N/D	N/D
Δ 12-PGJ ₂	1.19	2.31	N/D	N/D	0.42	1.12	N/D	N/D	N/D	N/D	5.46	4.27	N/D	N/D	N/D	N/D	4.07	3.16
PGB ₂	0.73	1.78	N/D	N/D	N/D	N/D	N/D	N/D	N/D	N/D	94.44	59.53	N/D	N/D	N/D	N/D	60.55	42.41
15-deoxy- Δ 12,14-PGJ ₂	0.66	1.06	N/D	N/D	3.93	6.06	N/D	N/D	2.89	5.78	3.18	4.11	45.81	7.65	N/D	N/D	29.00	37.42
13,14-dihydro-PGF _{2α}	0.21	0.51	N/D	N/D	N/D	N/D	N/D	N/D	N/D	N/D	N/D	N/D	N/D	N/D	N/D	N/D	N/D	N/D
13,14-dihydro-15-keto PGE ₂	0.08	0.14	N/D	N/D	N/D	N/D	N/D	N/D	N/D	N/D	N/D	N/D	N/D	N/D	10.60	5.80	N/D	N/D
8-iso-PGE	N/D	N/D	13.15	3.33	22.81	10.50	1.43	3.49	34.65	4.64	N/D	N/D	N/D	N/D	10.71	5.66	N/D	N/D
13,14-dihydro-15-keto PGE ₁	N/D	N/D	5.75	3.10	N/D	N/D	N/D	N/D	N/D	N/D	N/D	N/D	N/D	N/D	N/D	N/D	N/D	N/D
8-iso-15-keto PGE ₂	N/D	N/D	3.11	2.65	N/D	N/D	N/D	N/D	N/D	N/D	N/D	N/D	N/D	N/D	1.68	2.62	6.39	15.64
PGF _{1α}	N/D	N/D	2.36	3.65	N/D	N/D	N/D	N/D	N/D	N/D	N/D	N/D	N/D	N/D	1.53	3.76	N/D	N/D
TXB ₃	N/D	N/D	2.26	3.50	2.75	4.74	N/D	N/D	N/D	N/D	N/D	N/D	N/D	N/D	1.64	4.02	N/D	N/D
6-keto PGF _{1α}	N/D	N/D	1.98	3.23	N/D	N/D	N/D	N/D	N/D	N/D	N/D	N/D	N/D	N/D	0.94	2.30	N/D	N/D
PGD ₃	N/D	N/D	1.65	2.58	N/D	N/D	N/D	N/D	N/D	N/D	N/D	N/D	N/D	N/D	N/D	N/D	N/D	N/D
PGE ₃	N/D	N/D	0.98	2.41	N/D	N/D	N/D	N/D	N/D	N/D	6.80	11.63	N/D	N/D	N/D	N/D	N/D	N/D
13,14-dihydro-15-keto PGF _{2α}	N/D	N/D	0.68	1.66	1.26	3.35	N/D	N/D	N/D	N/D	N/D	N/D	N/D	N/D	1.81	2.82	N/D	N/D
13,14-dihydro-15-keto PGF _{1α}	N/D	N/D	N/D	N/D	0.99	2.61	N/D	N/D	N/D	N/D	N/D	N/D	N/D	N/D	N/D	N/D	N/D	N/D
8-iso-PGF _{2α}	N/D	N/D	N/D	N/D	0.91	2.40	N/D	N/D	N/D	N/D	N/D	N/D	5.91	10.24	N/D	N/D	N/D	N/D
PGF _{3α}	N/D	N/D	N/D	N/D	0.11	0.29	N/D	N/D	N/D	N/D	N/D	N/D	N/D	N/D	N/D	N/D	N/D	N/D

* In the presence of PGE₂, the estimation of 8-iso-PGE₂ is not reliable

Table 4.5 Table showing the % abundance of prostanoids detected in samples of mouse plasma collected at various timepoints from animals divided into different treatment groups (CTL= naïve/untreated mice, VEH3= intravenous vehicle at 3h post-injection, ALA3= intravenous α -linolenic acid at 3h post-injection, VEH24= intravenous vehicle at 24h post-injection, ALA24= intravenous α -linolenic acid at 24h post-injection VEH72= intravenous vehicle at 72h post-injection, ALA72= intravenous α -linolenic acid at 72h post-injection, VEH168= intravenous vehicle at 168h post-injection, ALA168= intravenous α -linolenic acid at 168h post-injection, N/D= not detected).

Prostanoid species	CTL n=7		VEH3 n=6		ALA3 n=7		VEH24 n=6		ALA24 n=6		VEH72 n=6		ALA72 n=6		VEH168 n=6		ALA168 n=6	
	MEAN	SD	MEAN	SD	MEAN	SD	MEAN	SD	MEAN	SD	MEAN	SD	MEAN	SD	MEAN	SD	MEAN	SD
15-deoxy- Δ 12,14-PGJ ₂	41.46	27.57	16.52	20.54	35.81	19.23	18.44	6.58	11.04	14.40	18.39	7.55	N/D	N/D	30.54	30.79	N/D	N/D
PGB ₂	20.48	29.80	49.75	35.46	18.73	30.75	63.69	11.61	35.41	42.86	61.97	16.72	7.89	12.56	N/D	N/D	N/D	N/D
Δ 12-PGJ ₂	0.96	2.54	13.13	23.85	1.49	2.93	8.81	2.60	2.93	3.72	9.14	6.81	N/D	N/D	N/D	N/D	2.05	5.02
8-iso-15-keto PGE ₂	N/D	N/D	1.66	4.07	3.99	7.04	N/D	N/D	N/D	N/D	N/D	N/D	N/D	N/D	N/D	N/D	N/D	N/D
PGE ₃	N/D	N/D	1.40	3.43	N/D	N/D	N/D	N/D	N/D	N/D	N/D	N/D	N/D	N/D	N/D	N/D	N/D	N/D
PGF _{3α}	N/D	N/D	N/D	N/D	N/D	N/D	N/D	N/D	28.18	48.14	N/D	N/D	N/D	N/D	N/D	N/D	N/D	N/D
PGE ₂	N/D	N/D	N/D	N/D			N/D	N/D	9.12	22.02	N/D	N/D	57.16	31.02	N/D	N/D	64.11	28.10
PGD ₂	N/D	N/D	N/D	N/D	0.46	1.23	N/D	N/D	10.05	20.10			5.04	9.17	14.50	29.28	7.13	11.10
6-keto PGF _{2α}	N/D	N/D	N/D	N/D	0.74	1.95	N/D	N/D	10.13	20.26	1.74	4.27	N/D	N/D	N/D	N/D	N/D	N/D
8-iso-PGE ₂	N/D	N/D	N/D	N/D	4.61	12.19	N/D	N/D	0.69	1.38	5.78	14.15	N/D	N/D	N/D	N/D	N/D	N/D
13,14-dihydro-15-keto PGE ₂	N/D	N/D	N/D	N/D	N/D	N/D	N/D	N/D	N/D	N/D	N/D	N/D	7.53	15.15	N/D	N/D	2.88	7.05
8-iso-PGF _{2α}	7.21	19.08	N/D	N/D	N/D	N/D	N/D	N/D	0.20	0.52	N/D	N/D	11.68	10.25	N/D	N/D	7.34	6.36
PGF _{2α}	0.82	2.17	N/D	N/D	15.48	26.13	9.07	15.46	1.65	4.37	0.76	1.87	1.15	2.83	13.20	32.33	N/D	N/D
PGE ₁	N/D	N/D	N/D	N/D	N/D	N/D	N/D	N/D	N/D	N/D	N/D	N/D	0.74	1.81	N/D	N/D	N/D	N/D
PGD ₁	N/D	N/D	N/D	N/D	N/D	N/D	N/D	N/D	N/D	N/D	N/D	N/D	1.78	4.36	4.47	10.95	1.67	4.10
PGF _{1α}	N/D	N/D	0.87	2.01	N/D	N/D	N/D	N/D	0.19	0.51	N/D	N/D	7.04	8.00	N/D	N/D	4.66	3.88
TXB ₂	27.34	38.61	N/D	N/D	18.70	20.08	N/D	N/D	N/D	N/D	2.21	5.42	N/D	N/D	37.30	30.99	2.38	5.84

* In the presence of PGE₂, the estimation of 8-iso-PGE₂ is not reliable

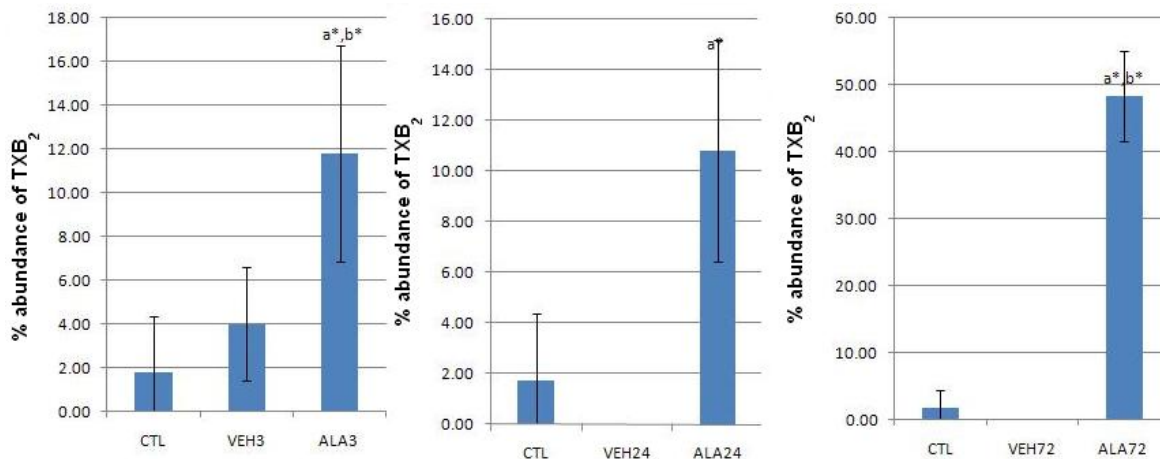
Statistical analysis of the percentage abundance of prostanoids between the different treatment groups at each timepoint was carried out using one-way ANOVA tests with post-hoc Dunnett's t tests. A P value of <0.05 was considered statistically significant, and a P value of <0.01 highly significant.

Table 4.6 shows significant differences in the percentage abundance of prostanoids in cerebral cortex tissue samples of mice undergoing vehicle or ALA injection compared to naïve (untreated) mice in prostanoid species. Significant differences in the abundance of several prostanoids were seen at one or two timepoints but only one prostanoid species significantly increased in the cerebral cortex of mice at three timepoints after ALA injection. The effects of ALA at 3h, 24h and 72h post-injection on the cerebral cortex abundance of TXB₂ are shown in figure 4.4.

Table 4.6 Statistical analysis of prostanoid abundance in cerebral cortex tissue of mice undergoing different treatments showed significant differences in the % abundance of several prostanoid species after VEH or ALA injection.

Time after injection (h)	VEH vs CTL (*P<0.05, ** P<0.01)		Both VEH and ALA vs CTL (*P<0.05, ** P<0.01)				ALA vs VEH (*P<0.05, ** P<0.01)			
		CTL	VEH		CTL	VEH	ALA	VEH	ALA	
3		CTL	VEH					VEH	ALA	
	8-iso-15-keto PGE ₂	NOT DETECTED	3.11 ± 2.65*				TXB ₂	3.99 ± 2.62	11.80 ± 4.97**	
	13,14-dihydro-15-keto PGF _{2α}	NOT DETECTED	0.66 ± 1.66*							
	PGF _{2α}	25.22 ± 25.09	3.83 ± 9.39*							
24					CTL	VEH	ALA		VEH	ALA
				6-keto PGF _{2α}	14.04±13.20	11.71±2.05*	2.58±2.71*	TXB ₂	NOT DETECTED	10.80 ± 4.37**
				PGD ₂	33.65 ± 29.33	76.32 ± 39.70 *	51.61±5.19*			
72		CTL	VEH					VEH	ALA	
	PGB ₂	0.73 ± 1.73	NOT DETECTED*				15-deoxy-Δ ^{12,14} -PGJ ₂	NOT DETECTED	3.83 ± 6.06*	
							TXB ₂	NOT DETECTED	48.27 ± 6.74**	
168		CTL	VEH		CTL	VEH	ALA			
	13,14-dihydro-15-keto PGE ₂	0.08 ± 0.14	10.60 ± 5.80*	PGF _{2α}	25.22 ± 25.09	3.83 ± 9.39*	NOT DETECTED*			

Figure 4.4 Mice injected with α -linolenic acid (ALA) showed a significant difference in TXB₂ abundance in cerebral cortex tissue samples at 3h, 24h and 72h post-injection compared to vehicle- injected (VEH) or naïve (CTL) mice.



** P < 0.01 one-way ANOVA with post-hoc Dunnett's t test

Table 4.7 shows significant differences in the percentage abundance of prostanoids in plasma samples of mice undergoing vehicle or ALA injection compared to naïve (untreated) mice in prostanoid species. There were fewer species displaying significant differences in their abundance between naïve and treated mice, with only three species showing significant difference at 72h post-ALA injection. These species were 15-deoxy- Δ 12,14-PGJ₂, PGE₂ and PGF_{1 α} . Of these species, only one showed significant differences at more than one timepoint post-ALA injection.

Table 4.7. Statistical analysis of prostanoid abundance in plasma of mice undergoing different treatments showed significant differences in the % abundance of three prostanoid species after VEH or ALA injection.

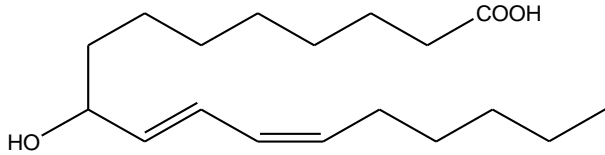
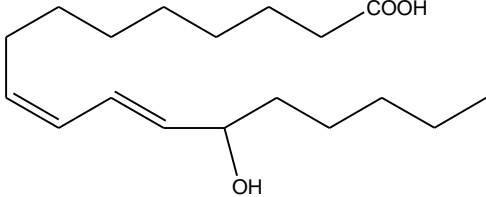
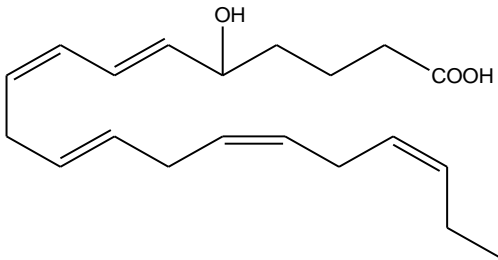
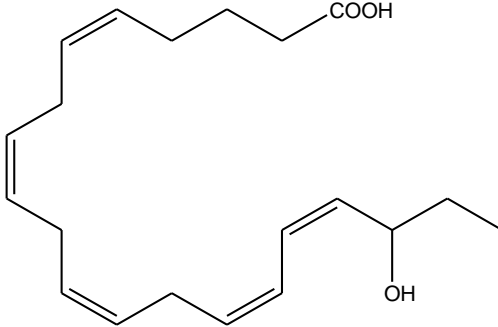
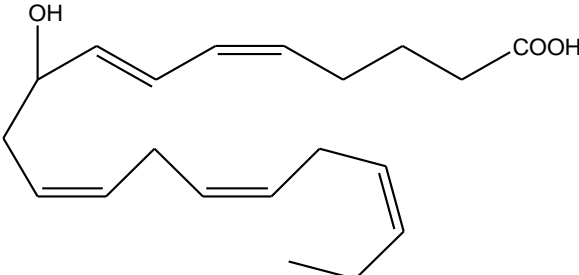
Time after injection (h)	VEH vs CTL (*P<0.05, ** P<0.01)		Both VEH and ALA vs CTL (*P<0.05, ** P<0.01)	ALA vs VEH (*P<0.05, ** P<0.01)		
		CTL		VEH		VEH
3						
24	15-deoxy- Δ 12,14-PGJ ₂	41.46 ± 27.57	16.52 ± 20.54*			
72					VEH	ALA
	15-deoxy- Δ 12,14-PGJ ₂				18.39 ± 7.55	NOT DETECTED*
	PGE ₂				NOT DETECTED	57.16 ± 31.02*
168					VEH	ALA
	15-deoxy- Δ 12,14-PGJ ₂				16.52 ± 20.54	NOT DETECTED*

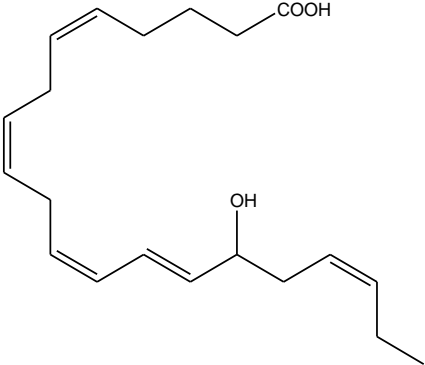
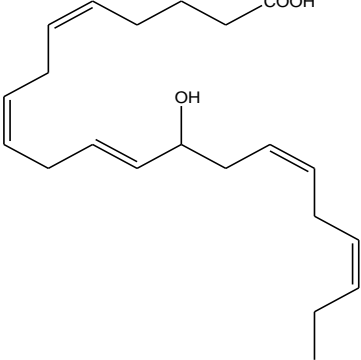
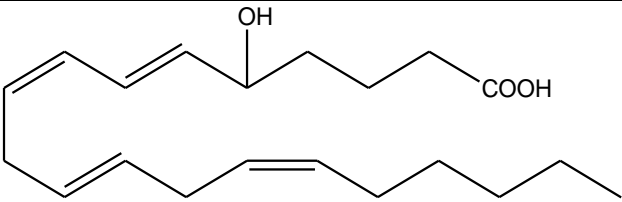
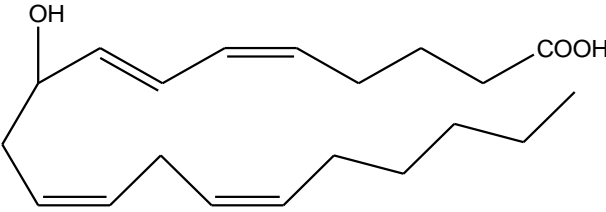
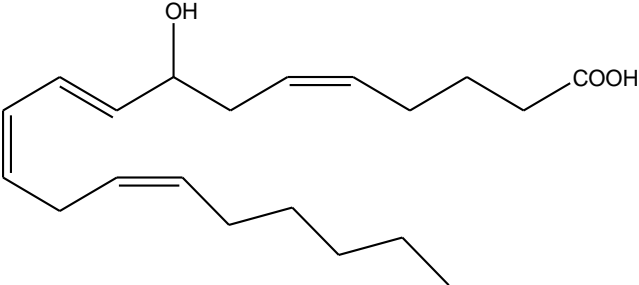
4.2. Hydroxy fatty acids profiles in mouse cerebral cortex and plasma

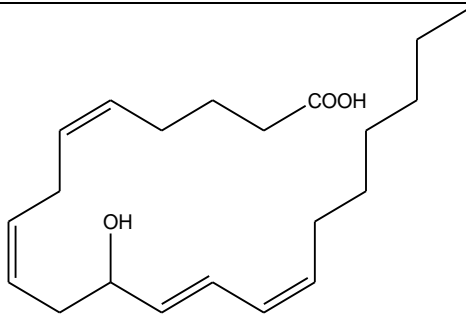
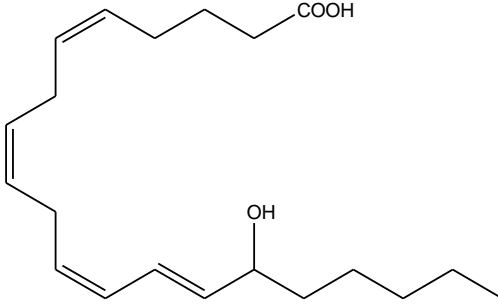
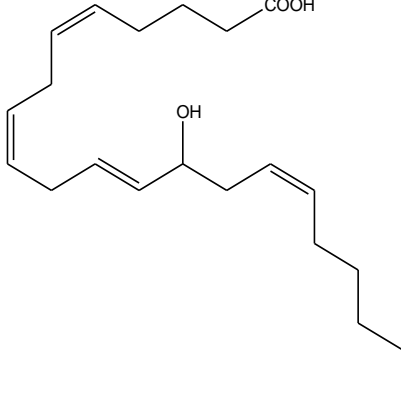
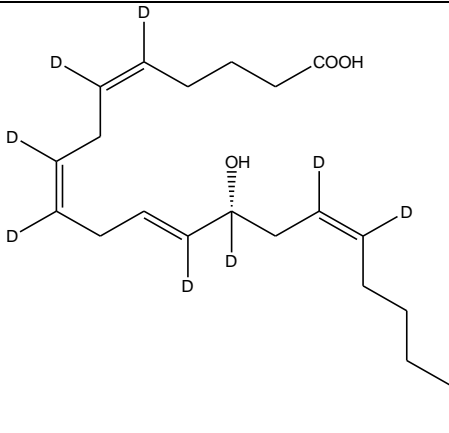
4.2.1. Preparation of calibration curves

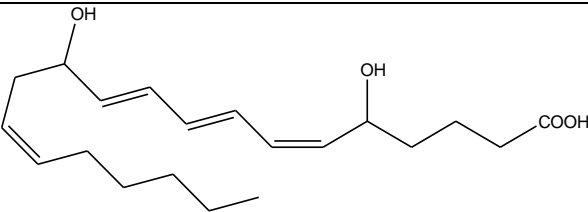
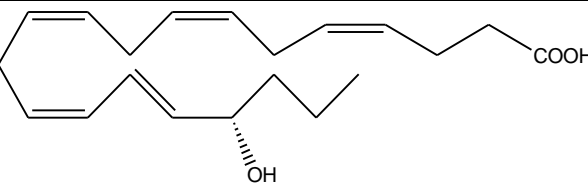
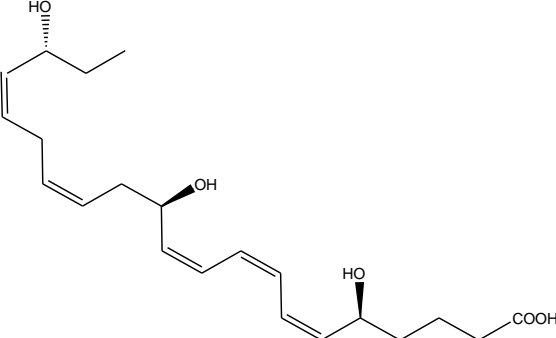
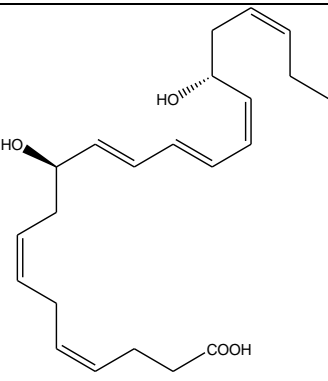
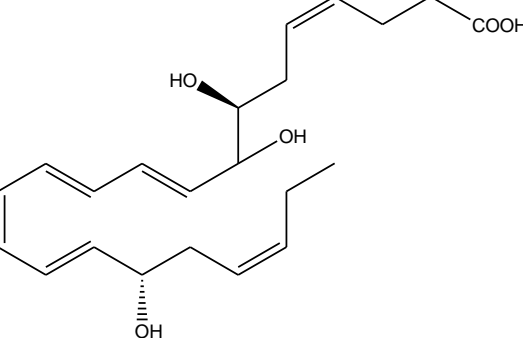
Twenty two standards were combined into a cocktail of hydroxy fatty acids, which was diluted into a series of standard solutions containing 160, 120, 80 and 40 pg/μl. Calibration curves were prepared using diluted standards. Table 4.8 records the transitions and approximate retention times of each of the compounds in the cocktail of standards.

Table 4.8 Hydroxy fatty acid standards used for quantification analysis using multiple-reaction monitoring (MRM). Isobaric species can be separated on the basis of their different retention times in the reverse-phase HPLC column (Masoodi et al., 2008).

Species	Mol. wt. of [M-H] ⁻	Structure of species	Transition m/z	Approx. retention time (min)
9-HODE	295		295>171	16.99
13-HODE	295		295>195	16.91
5-HEPE	317		317>115	16.58
18-HEPE	317		317>133	12.56
9-HEPE	317		317>149	15.35

Species	Mol. wt. of [M-H] ⁻	Structure of species	Transition m/z	Approx. retention time (min)
15-HEPE	317		317>175	13.54
12-HEPE	317		317>179	14.61
5-HETE	319		319>115	24.94
9-HETE	319		319>123	23.06
8-HETE	319		319>155	21.42

Species	Mol. wt. of [M-H] ⁻	Structure of species	Transition m/z	Approx. retention time (min)
11-HETE	319		319>167	19.94
15-HETE	319		319>175	18.55
12-HETE	319		319>179	21.25
12-HETE-d8	328		328>185	20.51

Species	Mol. wt. of [M-H] ⁻	Structure of species	Transition m/z	Approx. retention time (min)
LTB4	335		335>195	7.80
17S-HDHA	343		343>281	19.61
RvE1	349		349>195	2.57
PD1	349		359>206	6.90
RvD1	375		375>141	3.62

Each MRM channel yielded a chromatogram, on which the compounds undergoing that specific transition could be detected. Figure 4.5 illustrates a representative chromatogram of the transition m/z 335 > 195 for each of the diluted standard solutions. The same transition was also used in biological samples collected from mice in different treatment groups (naïve (CTL), and injected with α -linolenic acid (ALA) or vehicle (VEH) at various timepoints).

Figure 4.5 Representative chromatograms of lipid mediator standards for transition m/z 335 > 195. Leukotriene B4 (LTB₄) has a retention time of approx 7min.

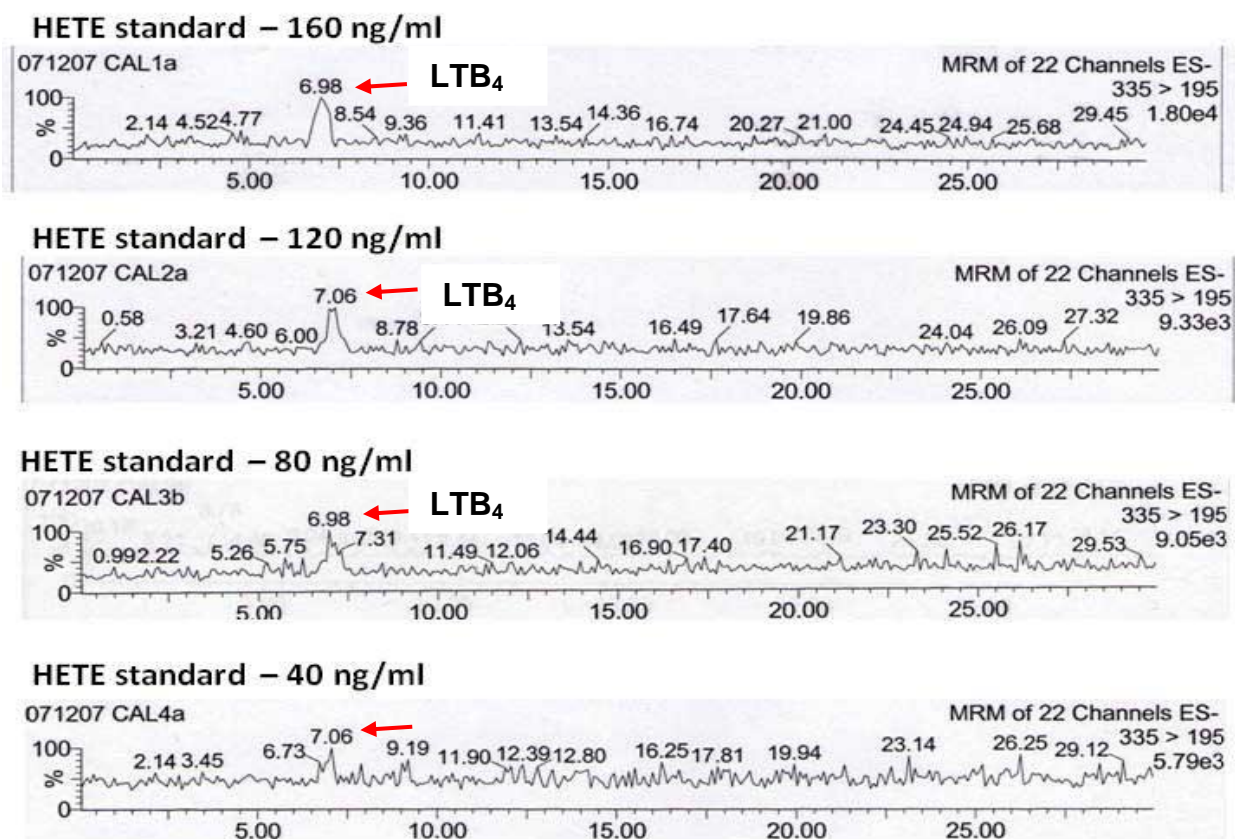
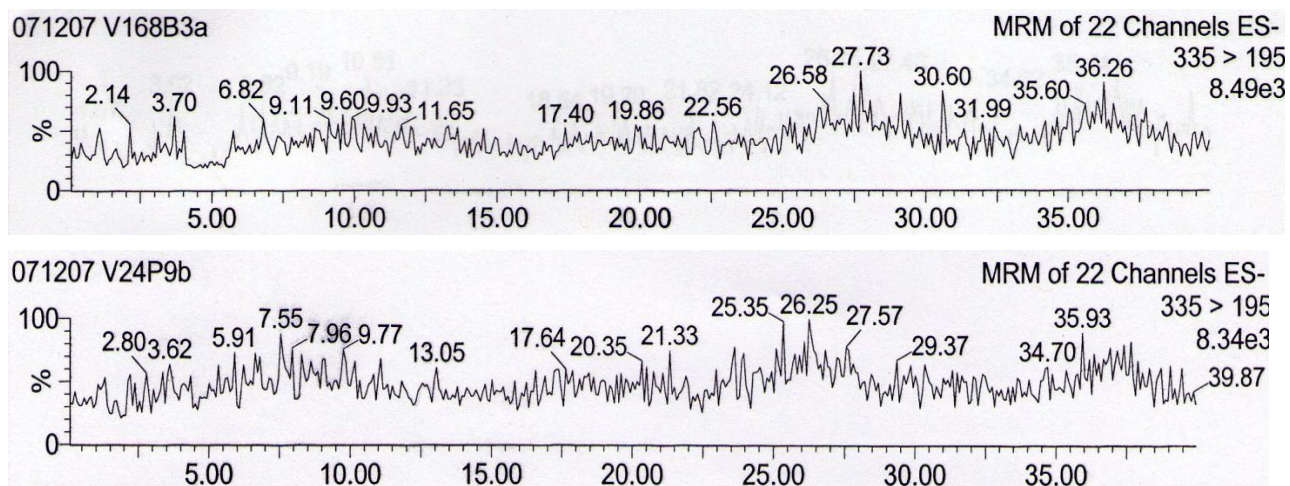


Figure 4.6 shows representative chromatograms of the transition m/z 335>195 in cerebral cortex tissue and plasma respectively. In comparison to the standard solutions, there is a high level of background noise and there are no clearly defined peaks at approximately 7min, indicating that the compound was not present.

Figure 4.6 Representative chromatogram of transition m/z 335>195 for mouse cerebral cortex (upper) and plasma (lower) samples. Note the absence of clearly defined peaks, indicating no compound was present.



5. Discussion

5.1. Methodology considerations

5.1.1. Importance of tissue sampling, storage and processing methods for the validity of lipidomic data

The methods used for tissue sampling, sample storage and sample processing are important, and must be considered carefully in order to avoid artefacts, and to ensure that the lipidomic profile generated is an accurate representation of that in the living brain. Rapid post-mortem changes in brain lipids can occur, with changes observed as shortly as 90 seconds after death (Lee & Hajra, 1991)

Hydrolysis of phospholipids decreases their concentration as they are converted to lysophospholipids and free fatty acids (FFA), The hydrolysis of phospholipids, whether it is mediated by calcium-dependent phospholipases, UV irradiation, heat or plasticizers, leads to increased levels of free fatty acids (FFA), which serve as a substrate pool for bioactive lipid mediators, and lysophospholipids (Lee & Hajra, 1991). Tissue trauma can lead to the release of polyunsaturated fatty acids from the *sn*-2 position of phospholipids, providing another potential source of lipid mediators (Lee & Hajra, 1991). A

rapid killing method was chosen to minimize the risk of tissue trauma, and the tissue was frozen within seconds of death to avoid phospholipid hydrolysis by calcium-activated phospholipases.

It has also been proposed that the metabolism of free fatty acids released upon post-mortem ischaemia could lead to artificially elevated concentrations of eicosanoids, isoprostanes and docosanoids in samples of brain tissue unless tissue enzymes were inactivated, for example, by use of microwave irradiation (Farias et al, 2008). It has been reported that even a 1-minute post-mortem incubation of mouse brain could result in significant production of artifact PGE, and PGD₂ (Golovko & Murphy, 2008). Previous lipidomic studies by our group used a different sample collection method, where an anaesthetized animal was decapitated and the brain dissected from an unfrozen skull kept on ice. However, since this sample collection method may not successfully inactivate brain enzymes, it can be asked whether all the prostaglandins detected in these brain samples were formed before death, or were they caused by post-mortem oxidation of free fatty acids released during brain ischaemia. Since the use of microwave irradiation to kill the mice could not be considered in this study for ethical and practical reasons, our method of brain tissue sample collection and dissection by rapidly freezing the cerebral cortex and keeping it frozen throughout the dissection process was a feasible alternative method of inactivating brain enzymes.

The process of dissecting a frozen brain is time-consuming, requiring approximately 20 minutes for dissection of the cortical grey matter from the whole head of the mouse. Extensive care was taken to ensure that the mouse brains were kept frozen during brain dissection, in order to minimize the risk of phospholipid degradation and lipid mediator oxygenation. Once dissected, samples of mouse cerebral cortex were stored at -80°C inside sealed cryogenic vials that had been pre-cooled with liquid nitrogen. These storage conditions have previously been used by our group to store samples of rodent brain and plasma for up to three years, with good recovery of phospholipids, prostaglandins and hydroxy fatty acids (Masoodi & Nicolaou, 2006; Little et al., 2007; Masoodi et al., 2008).

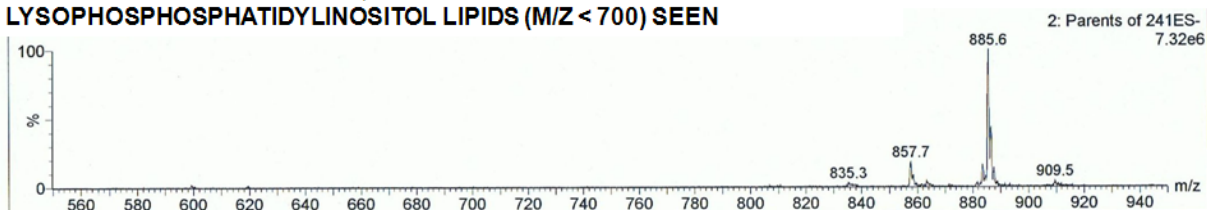
Successful extraction of phospholipids from tissue samples requires both (i) the removal of phospholipids from the tissue pellet into the organic solvent phase, and (ii) the complete removal of the aqueous phase, which contains proteins and water-soluble metabolites. The incomplete extraction of lipids from the biological sample into the organic phase would lead to low ion counts, whilst the presence of proteins and water-soluble proteins in the extracted sample would lead to a low signal-to-noise ratio and the possibility of broad and non-specific peaks in the spectrum. Table 5.1 illustrates the effects of phospholipid extraction quality on MS/MS data quality.

Table 5.1 The quality of MS/MS data is highly-dependent on the phospholipid extraction process, which can be verified by inspecting specific criteria of the resulting spectra

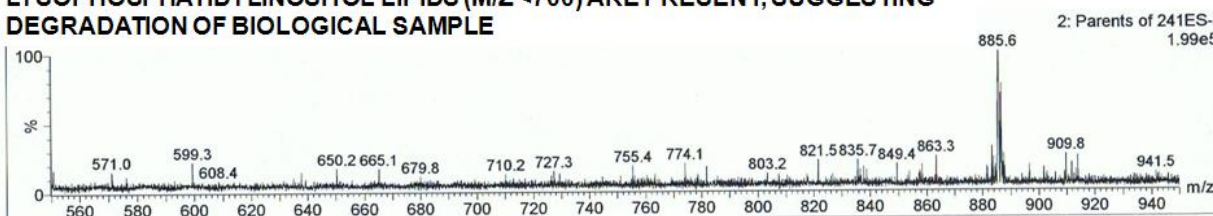
Good quality extraction	Bad quality extraction
High signal-to-noise ratio	Low signal-to-noise ratio
Spectrum contains narrow and well-defined peaks	Spectrum contains broad peaks
High ion count (> 1×10^7 for general scans, $>1 \times 10^4$ for fragmentation scans, depending on species)	Low ion count (< 1×10^6 for general scans, $>1 \times 10^3$ for fragmentation scans, depending on species)

Figure 5.1 Representative diagrams of a high-quality spectrum (above) and a poor-quality spectrum (below). A high signal-to-noise ratio and a good ion count is indicative of successful phospholipid extraction, whilst an unsuccessful extraction will show a low signal-to-noise ratio, undefined peaks and a low ion count.

HIGH-QUALITY SPECTRUM: OBSERVE CLEARLY-DEFINED PEAKS WITH A LOW LEVEL OF NOISE, A HIGH ION COUNT AND NO LYSOPHOSPHATIDYLINOSITOL LIPIDS (M/Z < 700) SEEN



POOR-QUALITY SPECTRUM: HIGH LEVEL OF BACKGROUND NOISE AND PEAKS ARE NOT VERY CLEAR AND SHARP; A LOWER ION COUNT IS OBSERVED AND LYSOPHOSPHATIDYLINOSITOL LIPIDS (M/Z < 700) ARE PRESENT, SUGGESTING DEGRADATION OF BIOLOGICAL SAMPLE



The solid phase extraction of lipid mediators is performed using reversed phase SPE cartridges, and is dependent upon hydrophobic interactions between the silica beads packed inside the cartridge and the compounds to be extracted. The successful extraction of eicosanoids is dependent on adequate conditioning or priming of the SPE cartridge, appropriate pH adjustment of the sample to be analysed, correct washing of the packing and the elution of the compounds of interest. The total ion count for each sample can be used to deduce whether extraction of lipid mediators from the raw samples was successfully carried out. A low ion count indicates inadequate or unsuccessful extraction of lipid mediators, which could be explained by a number of reasons. For example, insufficient or inadequate priming of the SPE cartridges means that the silica-coated beads in the cartridge are not thoroughly wetted prior to addition of the sample. As a result, the lipid mediators might not be able to interact with the silica in the cartridge, and would be expelled from the cartridge before the addition of the elution solvent. Similarly, inaccurate pH adjustment of the biological sample prior to SPE could damage the cartridges by stripping away the silica on the surface of the beads, or reduce the binding of lipid mediators to the SPE cartridge. Eicosanoids are protonated and soluble in water at a low pH, so careful pH adjustment to pH 3.5 is crucial to avoid flushing out the eicosanoids from the SPE cartridge when rinsing with water. Finally, slow running of each solvent through the cartridge is crucial for successful extraction of eicosanoids. Each solvent should also be run very slowly (ideally drip-wise) through the SPE cartridges. Running solvents through cartridges at too rapid a pace runs a risk

that lipid mediators might be forcibly flushed out of the cartridge during the washing process.

The methods used for the extraction purification, separation and detection of prostaglandins and other lipid mediators in this study were based on extensive previous work carried out by other members of our group (Masoodi & Nicolaou, 2006;; Masoodi et al., 2008; Nicolaou et al., 2009). Similar methods have also been used by other research groups, with successful extraction of lipid mediators (Marchellesi et al., 2003; Farias et al., 2008). However, previous studies carried out by our group used a different sample collection method, which may have influenced the lipid mediator profile obtained because of post-mortem metabolic changes.

5.1.2. Evidence of quality and validity for the lipidomic data obtained in this study

Phospholipid study

The spectra obtained from general scans of the samples showed mass/charge (m/z) values that corresponded to the lipid species in the standards, which had been stored at $-20\text{ }^{\circ}\text{C}$ in glass vials, sealed with parafilm and kept in a dark environment. There was also only a low percentage abundance of lysophospholipids detected in all samples, indicating that the extent of phospholipid degradation had also been

minimized during sample collection and storage (Christie, 2003). Previous studies on brain phospholipids produced similar data on the number and m/z values of phospholipid species detected using MS in samples of rodent brains (Bang et al. 2007; Little et al. 2007; Hicks et al. 2006), suggesting that the sample collection, storage and extraction methods used in this study did not result in degradation of phospholipids before analysis.

Spectra obtained from general scans and from the fragmentation spectra for phosphatidylcholine, sphingomyelin, phosphatidylinositol, phosphatidylserine, and phosphatidylethanolamine species all had a satisfactorily high ion count, indicating that phospholipid extraction was successfully carried out from the cerebral cortex tissue samples. The ion counts for phosphatidylinositol species tended to be rather lower than those for other phospholipid classes but this trend was observed for all samples, and the ion count for phosphatidylinositol standards were also lower than for other phospholipid classes. Since the phospholipid standards had not been exposed to UV radiation or to plasticizers during their storage, they would not be expected to show oxidative degradation. It can therefore be deduced that the lower ion count for phosphatidylinositol species was not caused by degradation of the sample or by inadequate sample extraction. Possible explanations for the lower ion counts observed for phosphatidylinositol species are that there may be a lower abundance of phosphatidylinositol lipids in the biological samples, or that these lipids are not as easy to ionize as the other phospholipid classes, resulting in a smaller signal under similar ionization conditions. This

is confirmed by literature (Wenk et al., 2003), with phosphatidylinositol species being considered minor phospholipids in brain tissue, where the majority of phospholipids comprise of phosphatidylethanolamines and phosphatidylserines (Christie, 2008; Vance & Vance, 2008). The lack of a highly polarized centre in the structure of inositol (in comparison to the acidic properties of serine, and the basic properties of choline, sphingosine and ethanolamine) could also account for the lower ion counts of phosphatidylinositols compared to the other phospholipid classes across all samples, despite optimization of the mass spectrometry conditions for each phospholipid class.

Initial identification of the fatty acyl chains of phospholipids was based on the development of lipid analyzer software using samples of whole rat brain (Little, 2006; Little et al., 2007). Scans were carried out to detect phospholipid species in each class, and data from the fragmentation spectra of each detected species was used to calculate the most likely combination of fatty acyl chains for a phospholipid species with a certain m/z value. However, there is a possibility that there are inter-species differences in brain phospholipid composition, so in order to definitively identify the fatty acyl chains of each phospholipid species in the mouse brain, it is necessary to fragment each detected species in each phospholipid class using tandem mass spectrometry. The second part of this study used MS/MS to fragment each phospholipid species which had a percentage abundance of above 1%

in a fragmentation scan, in order to definitively identify the most abundant phospholipid species.

The number of phospholipid species identified using MS/MS in this study differed considerably from earlier studies (Bang et al. 2007; Little et al. 2007; Hicks et al. 2006), although the number of species identified using MS general, precursor/fragment ion and neutral loss MS scans which were specific for different phospholipid classes (i.e. parent ion scan of m/z 184 for phosphatidylcholines and sphingomyelins, neutral loss scan of m/z 141 for phosphatidylethanolamines, parent ion scan of m/z 241 for phosphatidylinositol lipids and neutral loss scan of 87 for phosphatidylserines) were comparable in number to a previous study by our group on whole rat brain (Little, 2006). Of all studied phospholipid classes, this is most notable for choline phospholipid species, where only four choline lipid species were successfully identified using MS/MS in this study, compared to over a dozen in earlier work using similar equipment and experimental methods (Little et al., 2007). This is in stark contrast to the part of this study that used MS and lipid analyser software to identify phospholipids, where sixteen phosphatidylcholine and three sphingomyelin species were identified in mouse cerebral cortex (described in further detail in Chapter 3.3.1).

The fact that a similar number of choline lipids were identified in the MS part of this study as in previous work suggests that the reason for the discrepancy

in choline lipids identifiable using MS/MS was not due to a shortage of phospholipids in the extracted biological samples. Also, the method of sample collection in this study was developed in order to ensure that the hydrolysis of phospholipids caused by activation of PLA₂ during post-mortem brain ischaemia was minimal. The low level of lysophospholipids observed during MS analysis of all phospholipid classes confirms that this was the case, and so we can rule out the possibility that incorrect sample collection, processing and extraction is the reason behind the low number of choline phospholipids identified using MS/MS in this study.

However, there is a possibility that degradation of the extracted samples occurred after initial MS analysis and prior to MS/MS analysis. The extracted samples were stored at -20°C for some months between initial MS analysis and the MS/MS study, but the vials in which they were stored were sealed with parafilm and the extraction solvent also had added anti-oxidant (0.01% w/v BHT) in order to prevent oxidation or hydrolysis of sample lipids. Degradation of the extracted samples in between MS and MS/MS analysis is an unlikely explanation for the lesser number of choline phospholipids identified in this study using MS/MS, since the number of species identified using MS/MS in other phospholipid classes was comparable in this study to other work (see Section 5.2.1. Tables 5.2a-d for details).

A more likely cause of the lack of identifiable choline phospholipids using MS/MS is that the experimental parameters had not been optimized to

generate fatty acyl anions from these positively-charged phospholipids. Higher collision energy was selected for MS/MS analysis in other lipidomic studies on phospholipids, with collision energies of >40eV being common (Bang et al., 2007; Hicks et al., 2006; Brügger et al., 2006). An attempt was made to facilitate the production of fatty acyl anions by the addition of formic acid to the sample dissolution solvent, and also increasing the collision energy from an initial 25eV to 30eV. The purpose of this work was to confirm the identity of a molecular ion with a certain m/z by fragmenting it and studying the fatty acyl ions liberated from the molecular ion. In order to ensure that the fatty acyl ions were indeed produced from the correct molecular ion rather than from a higher m/z parent ion which had partially degraded to form an intermediate ion with the m/z of interest, the collision energy was set as to allow the molecular ion to still be present. It was considered that further increasing the collision energy would result in excessive fragmentation of the molecular ion, which may have increased the amount of information on the side chain structures of the lipid species by producing fatty acyl ions, but this would have been at the expense of information on the molecular ion's m/z value. Despite an attempt to further optimize the production using formic acid to promote the production of $[M+CH_3COO]^-$ adduct anions, only limited success was achieved on identifying choline phospholipids using MS/MS in this study.

In contrast, the number of phosphatidylethanolamine species detected using MS/MS in the ES- mode was comparable to that observed in previous studies

using MALDI tandem mass spectrometry, nanoflow LC-MS/MS and ESI-MS/MS (Bang et al. 2007; Little et al. 2007; Hicks et al. 2006), suggesting that the analytical techniques used in this study were sensitive enough to enable detection and identification of phosphatidylethanolamine, phosphatidylinositol and phosphatidylserine species in mouse cerebral cortex samples.

It has been previously noted that differences exist in the phospholipid composition of white matter and grey matter (Carrie et al., 2000; Xiao et al., 2005). Our samples were essentially composed of grey matter, but samples of whole brain tissue containing both white and grey matter were used for the lipid analyzer software. A phospholipid species present at high percentage abundance in the white matter may mask the presence of another species with the same m/z value, but a different fatty acyl chain composition, found at a lower concentration in the grey matter. The use of MS/MS to identify the fatty acyl chains of each phospholipid species eliminates this possibility.

Lipid mediator study

The sensitivity of the analytical method is such that it is essential to ensure that both the column and the ESI source of the mass spectrometer are clean prior to starting LC-MS/MS analysis. To avoid a high level of background noise, thorough flushing out of the HPLC column is crucial, and to ensure that this was achieved, the HPLC column was flushed overnight prior to set-up of

calibration line runs. The signal-to-noise ratio was generally acceptable in most biological samples, although some samples displayed a high level of noise, implying that the extraction process was not successful in these samples. In order to avoid deterioration of data quality, any samples with a high noise-to-signal were discarded and the chromatograms were not used for lipid mediator profiling.

The internal standard for the mixed prostaglandin assay (d_4 -PGB₂) was detectable in each cocktail of standards and in each biological sample, indicating that the analytical equipment was set up in a satisfactory manner. It can also be deduced from the consistent peak area of the internal standard that the methods used in this study for storage and processing of samples did not result in their degradation. However, since the internal standard was not added to the samples prior to the extraction and purification process, it is possible that breakdown of prostaglandins may have occurred during sample collection and storage. The use of cold inactivation to instant freezing (freeze clamping) to inhibit all tissue enzymes can reasonably be expected to have prevented enzyme-mediated oxidation of lipid mediators. However, prostaglandins can also be oxidized by a non-enzymatic (free-radical) catalysed reaction, which may have occurred during to some extent during tissue storage at -80°C . A methodology study on brain prostanoid analysis reported that prostaglandin mass in brain powder stored at -80°C was reduced 2- to 4-fold within 4 weeks (Golovko & Murphy, 2008) and it was suggested that tissue samples should be immediately extracted and stored in

solvent with added antioxidant. The samples in this study were stored as pieces of tissue rather than as a powder, therefore would be less exposed to oxygen and UV radiation (which both generate free radicals), but the possibility that the levels of prostaglandins in the cerebral cortex tissue on the outer surface may have been reduced by the auto-oxidation of prostanoids can not be discarded. The difference in sample collection methods used between this study and previous work carried out by our group may also have influenced the levels of prostanoids detected in the analysed samples.

The data obtained in this study showed that the retention times of the peaks of both the standard solutions and biological samples were similar to those described in previous studies by our group. It is well known that even slight changes in mobile phase composition or pH can have a considerable effect on the retention time of compounds, with shifts of ± 1 minute in retention times not being uncommon. The similar retention times observed in both the PG assay standards and biological samples indicate consistency between the standard solutions and the biological samples in terms of eluent pH, column temperature and mobile phase composition. The absence of shunting and shifting of LC peaks observed in biological samples, as well as the clear and sharp shape of the peaks, also indicate good quality data was collected on prostaglandin species in this study.

A high degree of variability in brain and plasma prostanoid composition both within treatment groups and between different sample groups was seen in our

study, with some eicosanoid species being detected in some tissue samples within a treatment group, but not in other samples. This suggests that the assay we used is close to the limit of detection of lipid mediators, which means that slight variations in the abundance of species between two samples could result in detection in one sample and non-detection in the other.

Genotyping of human volunteers has showed a high degree of genetic variation in the genes encoding prostaglandin synthase and receptor proteins, with over 20 allelic varieties of PGE synthase and prostanoid receptors observed in a sample of fewer than a hundred individuals (Bigler et al., 2007). Of these genotypes, several changes in amino acid sequence were observed, leading the authors to conclude that there is a wide variation in prostaglandin-related enzymes between individuals. However, the inbred mouse strain used in this study (C57/BL6) is a well-established strain which is renowned for its genetic homozygosity (<http://www.sanger.ac.uk>), suggesting that genetic variation between individual animals is unlikely to be a major cause of the variability in lipid mediators within and between treatment groups.

Differences in the levels of stress between individual mice may have led to differences in stress hormones and as a result, differences in inflammatory status in the mice. Chronic stress caused by in-cage fighting (male C57/BL6 mice that are not littermates frequently fight when kept in the same cage) or acute stress caused by exposure to other stressors such as bright light,

handling, insertion into the tube restrainer or the injection process may vary from individual to individual, just as humans vary in their perception of stress. The pro-inflammatory effects of chronic stress should not be underestimated, since some groups of animals were housed together for up to three weeks between the acclimatization, injection and sample collection process, and visible signs of fighting were seen on some mice in the form of tail scratches.

The HETE assay internal standard (d_8 -12(S)-HETE) was absent in some of the standards when setting up calibration curves for this assay, leading to delays between extraction of the samples and running of the assay while fresh standards were prepared. The same biological samples were used for both the PG and the HETE assay, with both assays being run back-to-back and the internal standard (as well as other standards used for set-up of calibration curves) for the HETE assay were stored under the same conditions as those used for calibration curves in the PG assay. However, the extreme sensitivity of hydroxy fatty acids to photo-oxidation and their susceptibility to auto-oxidation compared to prostanoid species means that that it is possible that the sample storage conditions used for the extracted, dried and reconstituted samples in this study may have been accountable for the low levels of hydroxy fatty acids detected in biological samples.

Farias and co-workers (2008) reported the formation of prostanoid and docosanoid artefacts in rat brains subjected to global post-mortem ischaemia compared to control animals that were killed using high-powered microwave

irradiation focused on the head. Animals which were decapitated and incubated at 37°C for 5 minutes showed clear peaks for several hydroxy, di-hydroxy and tri-hydroxy fatty acids, including 5-HETE, 12-HETE, resolvin D1 (RvD1) and neuroprotectin D1 (NPD1). These lipid mediators were however not detectable in the brains of control animals, which had been killed by microwave irradiation. In contrast, the same lipid mediators were all prominent in a study by our group on rat brains, where the animals were killed by decapitation and their unfrozen brains dissected on ice, prompting the question of whether these species were caused by post-mortem artefacts rather than their presence in the living brain. This theory is supported by earlier work on post-ischaemia prostaglandin production in rodent brains (Spagnulo et al., 1979; Bosisio et al., 1976).

In addition to the low signal-to-noise ratio, some of the peaks obtained for biological samples in the HETE assay also showed slight tailing. Tailing can occur as a result of column overload, but this is an unlikely scenario in our study, since the injection volume for biological samples was only 5µL. Tailing can also occur because of polar interactions between the hydrophobic C₁₈ phase and an acidic component, which is the more probable cause in this case. A possible method of eliminating tailing in this instance would be to use a polar C₁₈ phase, or to lower the pH of the eluent. The use of a polar C₁₈ phase for the HETE assay would necessitate the use of two different columns for the mixed prostaglandin and HETE assays, increasing the cost and time requirements of the analytical work by eliminating the possibility of running

both assays back-to-back. A more suitable alternative would be to use a suitable buffer in the mobile phase used for the HETE assay to ensure that the pH of the eluent did not drop low enough to cause tailing.

5.2. Discussion of analytical findings: phospholipid study

5.2.1. Phospholipid profile of naïve mouse cerebral cortex

The majority of phospholipid species identified using MS and MS/MS in this study had also previously been identified in previous studies on mouse and rat brain, suggesting inter-species similarities in brain phospholipid composition.

Two novel species which had previously not been reported using either MS or MS/MS were identified in our study. These species were (i) a phosphatidylethanolamine with m/z 720, identified as PE 16:0-18:0 using MS/MS and (ii) a long-chain fatty acyl phosphatidylserine with m/z 872, identified as PS 18:0-24:1 using MS/MS. Although other PE species of comparable chain length were identified in other lipidomic studies on rodent phospholipids, PE 16:0-18:0 is usually linked to retinal phospholipids, most notably retinal stem cells, having been described as a “signature glycerophospholipids” of this cell type (Li et al., 2007). Very long-chain fatty acyl phospholipids with a chain length of $\geq C_{24}$ are usually linked with white matter and retinal tissues (Scott & Bazan, 1987; Suh & Clandinin, 2005),

prompting the question of whether these phospholipids could have been derived from contamination of the tissue samples. Our selected dissection method of cracking open the frozen skull along the central fissure and scooping out the cerebra whole does not lend itself to this possibility of retinal tissue being incorporated into the sample, and the absence of other very long chain phospholipid species in other phospholipid classes also suggests that contamination of cerebral cortex samples by white matter is also an unlikely source of PS 18:0-24:1. It can therefore be concluded that these two phospholipid species, although not detectable in lipidomic studies on whole mouse or rat brains, are enriched in grey matter compared to the rest of the brain.

Some differences in the identities of the fatty acyl, alkyl or ether chains identified during fragmentation of phospholipid species were also observed between this study and previous work. The phosphatidylethanolamine with m/z 744 was identified as PE 16:0-20:2 and PE 18:1-18:1 rather than the PE 18:0-18:2 species observed in studies on mouse and rat whole brain (Bang et al., 2007; Hicks et al., 2006; Little et al., 2007). Another instance where a 20:2 species is featured in cerebral cortex lipids is the discovery of a PS species with m/z 812 which has the structure PS 18:1-20:2, as well as the more PS 18:0-20:3 species with the same m/z value that has previously been reported in brain lipidomic studies (Bang et al., 2007; Hicks et al., 2006; Little et al., 2007).. The presence of several novel phospholipids with a 20:2 component identified in this study implies that the grey matter may be enriched in 20:2,

which would appear to be an otherwise rare fatty acyl component of brain phospholipids.

Finally, differences in the structure of phosphatidylinositol species identified in this study were observed compared to previous work. The phosphatidylinositol with m/z 861 had an identity of 18:1-18:1 rather than the PI 18:0-18:2 species described by Hicks and co-workers (2006) and the phosphatidylinositol with m/z 863 was identified as 18:1-18:0, not 18:0-18:1 as reported by the same authors (Hicks et al., 2006). Since these are minor changes and only account for a small fraction of phosphatidylinositols, they can be assumed to not be of crucial importance.

The phospholipid species that were identified using MS/MS in our study are listed in Tables 5.2a-d, with differences highlighted.

Table 5.2a Comparison of the phosphatidylcholines identified using MS/MS in mouse brain tissue in this study against previous literature; all differences are highlighted

		Little et al. (2007)	Hicks et al. (2006)	Bang et al. (2007)	This study
m/z	Species (no. of C atoms: no. of C=C bonds)	RAT WHOLE BRAIN	MOUSE WHOLE BRAIN	MOUSE WHOLE BRAIN	MOUSE CEREBRAL CORTEX
706	30:0		14:0-16:0	14:0-16:1	
732	32:1	16:0-16:1	16:0-16:1	16:0-16:1	16:0-16:1
734	32:0	16:0-16:0	16:0-16:0	16:0-16:0	16:0-16:0
746	34:0	16:0p-18:0			
756			16:1-18:2		
758	34:2	16:0-18:2	16:0-18:2	16:0-18:2	
760	34:1	16:0-18:1	16:0-18:1	16:0-18:1	16:0-18:1
762	34:0	16:0-18:0	16:0-18:0	16:0-18:0	
780			16:0-20:5	18:4-18:1	
			18:2-18:3		
782	36:4	16:0-20:4	16:0-20:4	16:0-20:4	
			18:2-18:2		
784	36:3		18:1-18:2	18:1-18:2	
			16:0-20:3	16:0-20:3	
786	36:2	18:0-18:2	18:0-18:2	18:1-18:1	
				18:0-18:2	
788	36:1	18:0-18:1	18:0-18:1	18:0-18:1	
790			18:0-18:0	18:0-18:0	
802			18:2-20:5		
804	38:7				
806	38:6	16:0-22:6	16:0-22:6	16:2-22:6	
			18:2-20:4		
808	38:5	18:1-20:4	18:1-20:4	18:1-20:4	
			16:0-22:5	16:0-22:5	
			18:0-20:5	18:0-20:5	
810	38:4	18:0-20:4	18:0-20:4	16:0-22:4	
			18:1-20:3	18:1-20:3	
				18:0-22:4	
812			18:0-20:3	18:0-20:3	
814	38:2		18:1-20:1	18:0-20:2	
826			18:0-21:3		
830			18:2-22:6		
832	40:7	18:1-22:6	18;1-22;6	18:1-22:6	18:1-22:6
834	40:6	18:0-22:6	18;0-22;6	18:0-22:6	
836	40:5		18;0-22;5	18:0-22:5	
838	40:4		18;0-22;4	18:0-22:4	
840				18:0-22:3	
Species identified (n)		14	33	29	4
Species matching this study (m)		4	4	4	4

Table 5.2b Comparison of the phosphatidylethanolamines identified using MS/MS in mouse brain tissue in this study against previous literature; all differences are highlighted. (*ES- mode was used in our MS/MS work on PE species; molecular ions identified in this work were $[M-H]^-$ ions and had $m/z = [M+H]^+ m/z \text{ values} - 2$)

m/z	Species (no. of C atoms: no. of C=C bonds)	Little et al. (2007) RAT WHOLE BRAIN	Hicks et al. (2006) MOUSE WHOLE BRAIN	Bang et al. (2007) MOUSE WHOLE BRAIN	This study MOUSE CEREBRAL CORTEX*
716	34:2		16:0-18:2		
718	34:1	16:0-18:1	16:0-18:1	18:0-16:1	16:0-18:1
720	34:0				16:0-18:0
738	36:5		16:0-20:5		
740	36:4	16:0-20:4	16:0-20:4	16:0-20:4	16:0-20:4
742	36:3		16:0-20:3		
			18:1-18:2		
744	36:2	18:0-18:2	18:0-18:2	18:0-18:2	16:0-20:2
					18:1-18:1
746	36:1	18:0-18:1	18:0-18:1	18:0-18:1	18:0-18:1
762	38:7	16:1-22:6		16:1-22:6	16:1-22:6
764	38:6	16:0-22:6	16:0-22:6	16:0-22:6	16:0-22:6
766	38:5	18:1-20:4	18:1-20:4	18:1-20:4	18:1-20:4
			16:0-22:5		16:0-22:5
768	38:4	18:0-20:4	18:0-20:4	18:0-20:4	18:0-20:4
			18:1-20:3		
770	38:3	18:0-20:3	18:0-20:3		18:0-20:3
772	38:2	18:1-20:1	18:1-20:1		
774	38:1	18:0-20:1			
784			18:0-21:3		
786	40:9	18:3-22:6			
788		18:2-22:6	18:2-22:6	18:2-22:6	
790	40:7	18:1-22:6	18:1-22:6	18:2-22:5	18:1-22:6
792	40:6	18:0-22:6	18:0-22:6	18:0-22:6	18:0-22:6
794	40:5	18:0-22:5	18:0-22:5		18:0-22:5
796	40:4	18:0-22:4	18:0-22:4	18:0-22:4	18:0-22:4
798		18:0-22:3			18:0-22:3
812				20:4-22:6	
836				22:6-22:6	
	ether lipids				
750	38:5	18;1p-20;4			
754	38:3	18;0p-20;3			
778	40:5	18;0p-22;4			18;0p-22:4
Species identified (n)		22	21	14	18
Species matching this study (m)		12	12	10	18

Table 5.2c Comparison of the phosphatidylinositols identified using MS/MS in mouse brain tissue in this study against previous literature; all differences are highlighted.

		Little et al. (2007)	Hicks et al. (2006)	Bang et al. (2007)	This study
m/z	Species (no. of C atoms: no. of C=C bonds)	RAT WHOLE BRAIN	MOUSE WHOLE BRAIN	MOUSE WHOLE BRAIN	MOUSE CEREBRAL CORTEX
833	34:2		16:2-18:2	16:1-18:1	
835	34:1	16:0-18:1	16:0-18:1	16:0-18:1	16:0-18:1
837	34:0		16:0-18:0		16:0-18:0
855			16:0-20:5		
			18:2-18:3		
857	36:4	16:0-20:4	16:0-20:4	16:0-20:4	16:0-20:4
			18:2-18:2		
859	36:3	18:1-18:2	18:1-18:2		16:0-20:3
			16:0-20:3		
861	36:2		18:0-18:2		18:1-18:1
863	36:1		18:0-18:1		18:1-18:0
865	36:0		18:0-18:0		
877	38:8		18:2-20:5		
881	38:6	18:2-20:4	16:0-22:6	18:2-20:4	16:0-22:6
			18:2-20:4	16:0-22:6	
883	38:5	18:1-20:4	18:1-20:4	18:1-20:4	18:1-20:4
			16:0-22:5	18:0-20:5	
			18:0-20:5		
885	38:4	18:0-20:4	18:0-20:4	18:0-20:4	18:0-20:4
			18:1-20:3		
887	38:3	18:0-20:3	18:0-20:3	18:0-20:3	18:0-20:3
889	38:2	18:0-20:2	18:1-20:1		
905	40:8		18:2-22:6		
907	40:7	18:1-22:6	18:1-22:6		
909	40:6	18:0-22:6	18:0-22:6	18:0-22:6	18:0-22:6
911	40:5		18:0-22:5		18:0-22:5
913	40:4		18:0-22:4		
Species identified (n)		10	27	10	12
Species matching this study (m)		6	9	7	12

Table 5.2d Comparison of the phosphatidylserines identified using MS/MS in mouse brain tissue in this study against previous literature; all differences are highlighted.

		Little et al. (2007)	Hicks et al. (2006)	Bang et al. (2007)	This study
m/z	Species (no. of C atoms: no. of C=C bonds)	RAT WHOLE BRAIN	MOUSE WHOLE BRAIN	MOUSE WHOLE BRAIN	MOUSE CEREBRAL CORTEX
760	34:1		16:0-18:1	16:0-18:1	16:0-18:1
762	34:0		16:0-18:0	16:0-18:0	
780	36:5		16:0-20:5		
			18:2-18:3		
782	36:4		16:0-20:4		
			18:2-18:2		
784	36:3		18:1-18:2		
			16:0-20:3		
786	36:2	18:0-18:2	18:1-18:2	18:1-18:1	18:1-18:1
788	36:1	18:0-18:1	18:0-18:1	18:0-18:1	18:0-18:1
790	36:0	18:0-18:0	18:0-18:0	18:0-18:0	
804	38:7	18:2-20:5	18:2-20:5		
806	38:6		16:0-22:6	16:2-22:6	
			18:2-20:4		
808	38:5		18:1-20:4	18:1-20:4	
			16:0-22:5		
810	38:4	18:0-20:4	18:0-20:4	18:0-20:4	18:0-20:4
			18:1-20:3		
812	38:3		18:0-20:3	18:0-20:3	18:0-20:3
					18:1-20:2
814	38:2	18:0-20:2	18:1-20:1	18:0-20:2	
816	38:1	18:0-20:1		18:0-20:1	18:0-20:1
826			18:0-21:3		
830	40:8		18:2-22:6	18:2-22:6	
832	40:7	18:1-22:6	18:1-22:6	18:1-22:6	18:1-22:6
834	40:6	18:0-22:6	18:0-22:6	18:0-22:6	18:0-22:6
836	40:5	18:0-22:5	18:0-22:5	18:0-22:5	18:0-22:5
838	40:4	18:0-22:4	18:0-22:4	18:0-22:4	18:0-22:4
840	40:3	18:0-22:3		18:0-22:3	
842	40:2	18:0-22:2			
844	40:1	18:0-22:1		22:0-18:1	18:1-22:0
854	42:10			20:4-22:6	
856	42:9			20:3-22:6	
862	42:6			20:0-22:6	
				18:0-24:6	
872	42:1				18:0-24:1
878	44:12			22:6-22:6	
880	44:11			22:5-22:6	
882	44:10			22:4-22:6	
Species identified (n)		14	26	25	13
Species matching this study (m)		7	8	8	13

5.2.2. Phospholipid profile of naïve mouse cerebral cortex – potential biological significance

The vast majority of highly-unsaturated phospholipids detected in cerebral cortex tissue of naïve mice contained either arachidonic acid (denoted by 20;4 in Tables 5.2a-d) or docosahexaenoic acid (denoted by 22;6 in Tables 5.2a-d). Phospholipids containing arachidonic acid in their structure account for 14% of choline phospholipids, 18% of phosphatidylethanolamines, 9% of phosphatidylserines and 75% of phosphatidylinositols. In contrast, phospholipids containing docosahexaenoic acid in their structure account for 11% of choline phospholipids, 60% of phosphatidylethanolamines, 64% of phosphatidylserines and 4% of phosphatidylinositols.

Phosphatidylcholines make up a very high proportion of the outer leaflet of the plasma membrane and are also the principal phospholipids in plasma, where they are an essential component of high-density lipoproteins. The existence of phospholipases C and D specific for phosphatidylcholines suggest that diacylglycerols released from phosphatidylcholine may have a role in cell signalling (Vance & Vance, 2008). However, the majority of phosphatidylcholines are unsaturated or monounsaturated fatty acids, which yield diacylglycerols with much lower biological activity than highly unsaturated fatty acids, such as arachidonic acid (Christie, 2008). As a result, diacylglycerols formed from phosphatidylcholines would not be expected to show as much biological activity as those derived from phosphatidylinositols.

The plasmalogen form of phosphatidylcholine may also have a signalling function, with phospholipase A₂ activity releasing arachidonic acid (a substrate for eicosanoid production) from the *sn*-2 position of plasmogen phosphatidylcholine species containing releasing this fatty acid (Gora et al., 2006).

Phosphatidylethanolamines are concentrated on the inner leaflet of the plasma membrane, along with phosphatidylserines. The ability of phosphatidylethanolamines to hydrogen bond to proteins through its ionizable amine group means that they exert a lateral pressure that can stabilize membrane proteins in their optimum conformations (Vance and Vance, 2008). Their cationic head group also neutralizes the negative charges on the anionic head groups of phosphatidylserines. Phosphatidylethanolamines do not naturally form a lipid bilayer due to their conical shape, and the high percentage of phosphatidylethanolamine species which contain highly-unsaturated fatty acyl groups also means that membranes formed by this phospholipid class are highly-fluid. Phosphatidylethanolamines are involved in membrane fusion and fission, and can serve as a biosynthetic precursor for anandamide, an endocannabinoid neurotransmitter (Christie, 2008).

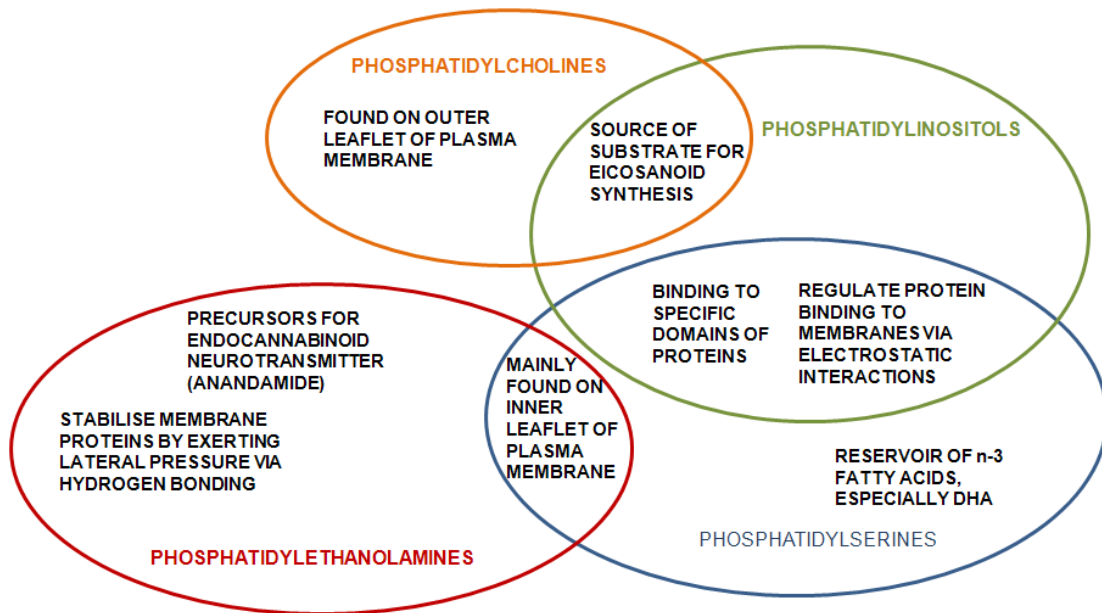
In addition to functioning as negatively charged building blocks of membranes, inositol phospholipids can regulate the binding of proteins via non-specific electrostatic interactions with proteins, or through specific binding to 'PH' domains of cellular proteins (Christie, 2008). They can also participate

in cell signaling through one of two ways. Firstly, they are the main source of inositol diacylglycerols (produced by phospholipase C) that act upon protein kinase C enzymes, which in turn control several key cell functions, including differentiation, proliferation, metabolism and apoptosis. Secondly, they are the primary source of the arachidonic acid required for the biosynthesis of eicosanoids, including prostaglandins (Farooqui & Horrocks, 2006; Vance & Vance, 2008). Phosphatidylinositols containing arachidonic acid account for three quarters of all phosphatidylinositol species, and of these, *sn*-1-stearoyl-*sn*-2-arachidonoyl-glycerophosphorylinositol (18;0-20;4), is by far the most common. The hydrolysis of *sn*-1-stearoyl-*sn*-2-arachidonoyl-glycerophosphorylinositol (18;0-20;4) by phospholipase A₂ releases arachidonic acid from the *sn*-2 position, producing substrate for the production of eicosanoids (Farooqui & Horrocks, 2006). The reverse reaction also occurs, which is a means by which free arachidonic acid and eicosanoid levels can be regulated.

Phosphatidylserines are located entirely on the inner leaflet surface of the plasma membrane and other cellular membranes, although this distribution is disturbed during platelet activation and cell apoptosis (Martin et al., 1995). It is believed that a receptor on the surface of macrophages and other scavenger cells may recognize the phosphatidylserine and remove the apoptotic cells (Vance & Vance, 2008). A high concentration of phosphatidylserine in a region of a cellular membrane also results in an accumulation of negative surface charge, to which poly-cationic proteins can

bind. Some proteins also contain specific phosphatidylserine-binding domains, with which they can dock to membrane lipids, with the result that certain proteins can be re-directed from one target membrane to another (Christie, 2008). The ratio of *n*-3 to *n*-6 fatty acids in brain and retina phosphatidylserines is very much higher than in most other phospholipid classes and DHA accumulation has been shown to be important in the development and function of these tissues (Scott & Bazan, 1987; Birch et al., 2010). It has also been suggested that phosphatidylserine may also act as a reservoir of DHA production for neuroprotection in neuronal tissue (Bazan, 2009), and the fact that almost two thirds of phosphatidylserines in mouse cerebral cortex contained DHA would seem to agree with this theory, although it has not been confirmed.

Figure 5.2 Different phospholipid classes have different biological functions, some of which overlap. For example, both plasmogen phosphatidylcholines and acyl phosphatidylinositols are rich sources of 20:4(*n*-6) when hydrolysed by PLA₂, releasing a substrate for biosynthesis of many bioactive lipid mediators.



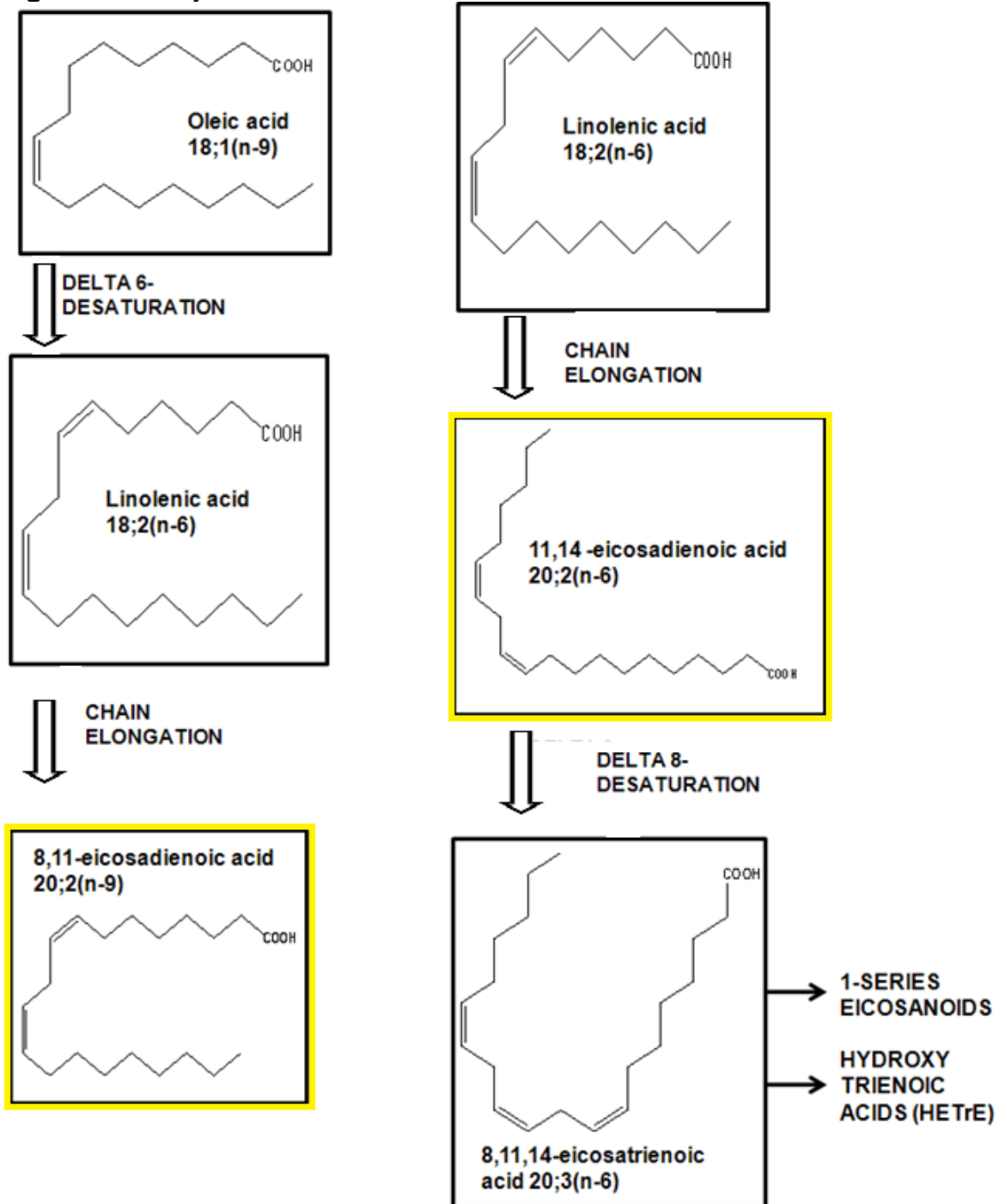
5.2.3. Identification of novel phospholipid species in naïve mouse cerebral cortex

Our study detected several phospholipid species in mouse cortex which had previously not been reported in lipidomic studies on whole mouse or rat brains. These lipid species were PE 16;0-18;0, PE16;0-20;2, PE18;1-18;1, PI 18;1-18;1, PS 18;1-20;2 and PS 18;0-24;1. The fatty acyl chains in the majority of these species are derived from either saturated fatty acids or from a monounsaturated fatty acid (oleic acid). However, two of the novel species detected in our studies contained an eicosadienoic acid (20:2) fatty acyl chain.

Two eicosadienoic acid species have been previously been recorded in mammalian tissue. These are (i) 8, 11-eicosadienoic acid (20:2n-9), which is commonly derived from oleic acid by Δ -6 desaturation followed by chain elongation, and (ii) 11, 14- eicosadienoic acid (20:2n-6), which is commonly derived from linolenic acid by chain elongation (Beermann et al., 2005; Diau et al., 2003; Li et al., 2007). Eicosadienoic acid generally has a low prevalence in body tissues, although it can be detected using advanced analytical methods. For example, 8,11-eicosadienoic acid has been detected at low concentrations (<1% of all fatty acids) in the retina of infant baboons (Diau et al., 2003), and 11,14-eicosadienoic acid has been found amongst phosphatidyl-ethanolamine and phosphatidylserine species of human erythrocyte phospholipids (Beermann et al., 2005). 11,14-eicosadienoic acid

is widely considered a 'dead-end product' i.e. one which is not converted into other long-chain fatty acids, although it has recently been shown to be a substrate of the FADS-2 gene product (Park et al., 2009). Its role as a substrate for Δ -8 desaturation by the FADS2 gene product has led to speculation that 20:2(n-6) may play a part in the production of eicosanoids derived from 20:3(n-6), such as prostaglandins E₁ and F_{1 α} , thromboxane B₁ and hydroxy-eicosatrienoic acids (Park et al., 2009). Yeast cells transfected with the baboon FADS2 gene showed Δ -8 desaturation activity on both n-6 and n-3 fatty acids, including the conversion of 20:2n-6 to 20:3n-6 and of 20:3n-3 to 20:4n-3 (Park et al., 2009). Δ 8-desaturation of 8,11-eicosadienoic acid to 11,14-eicosadienoic acid (20:2n-6 to 20:3n-6) has previously been reported in both rat and human tissue (Albert & Coniglio, 1977; Albert et al., 1979) and polymorphisms in the FADS2 gene have been linked to changes in the lipid profile of human serum and erythrocyte phospholipids of heart patients, including eicosadienoic acid (Malerba et al., 2008). Figure 5.3 illustrates the biosynthesis and metabolism of both eicosadienoic acid species, and the bioactive lipid products to which they can give rise.

Figure 5.3 Biosynthesis and metabolism of eicosadienoic acid



Novel phosphatidylethanolamine species with m/z 720 (PE 16:0-18:0)

The PE species with m/z 720 (PE 16:0-18:0) has previously been identified as a 'signature glycerophospholipid' of rat retinal stem cells in a lipidomic study using ESI-MS/MS (Li et al, 2007), and by extension this lipid species may also be present in other neural stem cells. The presence of the novel phospholipid species PE 16:0-18:0 (1-palmitoyl 2-stearoyl phosphatidylethanolamine) is consistent with the emerging hypothesis that neural stem cells are present in the cerebral cortex. Neural stem cells have previously been identified and located in three regions of the brain in adult rodents, namely: (i) the ventricular and subventricular zone, (ii) the hippocampus, and (iii) tissue connecting the lateral ventricles and the olfactory bulb (Li et al., 2007). These three regions all contain grey matter (Bear et al., 2001) and so tissue from them may have been included in the samples of mouse cerebral cortex that were subjected to phospholipid extraction and analysis.

The low prevalence of this species in the cerebral cortex tissue samples is in accordance with the theory that this phospholipid is primarily present in neural stem cells, although the prevalence of PE 16:0-18:0, although low, accounted for >1% of total cortex phosphatidylethanolamines, which may not be expected from a cell population which is located in only small, discrete brain regions. It has not been documented in literature that neural stem cells have a widespread presence in the cerebral cortex, although the detection of the

neural stem cell 'signature glycerophospholipid' PE 16:0-18:0 in mouse cerebral cortex by this study might imply that neural stem cells may be more numerous or account for a greater proportion of the cerebral cortex than initially expected.

It has been suggested that stem cell therapy may provide a manner in which neuronal damage mediated during cerebral ischaemia could be reversed (Liu et al., 2009). Latent stem cells located in the hippocampus have also been reported to be activated by neural excitation (Walker et al., 2008) and neural progenitor cells in the subventricular zone showed an increase in proliferation rate following stroke in mice (Zhang et al., 2004). More recently, Lai and co-workers (2008) showed functional differentiation of neural progenitor cells in the subventricular zone following a simulated stroke in animals, supporting the possibility of stem cell therapy for stroke. Delivery of neural stem cells to the infarct site can be successfully carried out by injecting scaffold particles made of poly(D,L,lactic-co-glycolic) acid (PLGA) with neural stem cells into the ventricles (Bible et al., 2009), although it has not been clarified whether this strategy would provide long-term success. Our study also supports the theory that neural stem cells are already present in the cerebral cortex under physiological conditions, and that these cells may be involved in neuronal repair following an ischaemic challenge.

Novel phosphatidylserine species containing a very long chain fatty acid (PS 18:0-24:1)

We also detected and identified a novel PS species containing a very long chain fatty acid (PS 18:0-24:1). There is generally an absence of PS species containing fatty acyl chains longer than C22 in other lipidomic studies on whole mouse or rat brain. However, Bang and colleagues also recorded a C24 fatty acyl chain in their analysis of whole mouse brain, where PS18:0-24:6 was identified (Bang et al., 2007). Very long chain fatty acid phospholipids (chain length $\geq C_{24}$) have been identified in retinal tissue, where there is an abundance of phospholipids containing very long chain fatty acids, and 24:1n-9 (nervonic acid) has also been associated with myelin (Martinez & Mougan, 2004). The method of brain dissection used in our studies, where the skull was cracked open along the central fissure and the cerebra scooped out of the frozen head before further dissection and removal of the white matter was carried out, means that it is highly unlikely that mouse eye tissue was accidentally incorporated into the sample. The careful removal of white matter from the cerebra, and the fact that no common myelin lipids (22:1 and 24:1) were detected in any other phospholipid classes, also implies that contamination of cerebral cortex samples with white matter is an unlikely source of this PS species. It can therefore be concluded that murine grey matter contains a small, yet detectable, amount of longer-chain fatty acyl chains within structural phospholipids.

Phosphatidylserine 18:1-20:2 species with m/z 812

Our fragmentation study identified two PS species with an m/z of 812, identified as PS 18;1-20;2 and PS 18;0-20;3, in contrast to previous studies which only found one PS species with this m/z value (PS 18;0-20;3). Although in the past, eicosadienoic acid was widely considered a 'dead-end, its recently discovered role as a substrate for Δ -8 desaturation by the FADS2 gene product has led to speculation that 20:2(n-6) may play a part in the production of eicosanoids derived from 20:3(n-6), such as prostaglandins E₁ and F_{1 α} , thromboxane B₁ and hydroxy-eicosatrienoic acids (Park et al., 2009). The 1-series prostaglandins have been reported to exert an anti-inflammatory effect by direct competition for binding with the pro-inflammatory 2-series prostaglandins, and this competitive effect partially blocks the activation of prostanoid receptors.

5.2.4. Effects of alpha linolenic acid (ALA) treatment on mouse cerebral cortex phospholipid profile

Intravenous injection of ALA did not produce widespread changes in the fatty acid composition of phospholipid and sphingomyelin species in mouse cerebral cortex. No significant differences in the percentage abundance of phosphatidylcholine and sphingomyelin species were observed at any timepoint between ALA-treated, vehicle-treated or naïve mice. Similarly, there were no differences in the abundance of phosphatidylinositol species at 24, 72 or 168 hours following ALA or vehicle treatment, phosphatidylserine species at 3, 72 and 168 hours after ALA or vehicle injection, or in

phosphatidylethanolamine species at 3 and 168 hours after ALA or vehicle injection. However, there were discrete changes in the relative abundance of a few phospholipid species at different time points (see Table 5.3).

Table 5.3. Discrete changes were observed in the relative composition of phospholipid species in cerebral cortex in ALA- treated mice ($P < 0.05$ ANOVA with post-hoc Dunnett t test, control group = naïve mice). R1 and R2 fatty acyl chains were definitively identified using MS/MS.

Phospholipid species				Timepoint affected	Change in phospholipid abundance
Phospholipid class	m/z of [M–H] ⁻ ion	R1	R2		
SM	813	18:0	24:1	3	+1.04%
PE	740 [†]	18:1	18:2	3	+ 0.01%
PE	744 ^{††}	18:0	18:1	3	+ 1.38%
PE	784 ^{†††}	18:0a*	22:0*	24	+0.67%
PS	812	18:0	20:3	24	-0.308%

[†] [M+ H]⁺ m/z value of 742

^{††} [M+ H]⁺ m/z value of 746

^{†††} [M+ H]⁺ m/z value of 786

* Data from studies on rat brain

These changes were:

- (i) An increase in the the relative abundance of the sphingomyelin species with m/z 813 at 3 hours. This species was identified as SM 18:0/24:1 using MS/MS data.

- (ii) An increase in the relative abundance of the phosphatidylethanolamine species with m/z 742 (identified as PE18:1/18:2 by MS/MS), at 24 hours after ALA injection.
- (iii) An increase in the abundance of the phosphatidylethanolamine species with m/z 746 at 72h post-ALA injection. This species was identified as PE18:0/18:1 using MS/MS data.
- (iv) An increase in the abundance of the phosphatidylethanolamine species with m/z 786 at 72h post-ALA injection. This species was identified as PE18:0a/22:0 using MS/MS data.
- (v) A decrease in the relative abundance of the phosphatidylserine species with m/z 812 at 24 hours. This species was identified as PS18:0/20:3 using MS/MS

It had been expected that ALA treatment of mice would lead to either (a) direct effects on brain lipid composition, whereby ALA or n-3 fatty acids derived from ALA would be incorporated into brain phospholipids, or (b) indirect effects, where changes in the homeostasis of lipids in the brain or in the biosynthesis of lipids lead to neuroprotection.

However, despite the use of appropriate statistical analysis to determine whether changes in phospholipid composition were statistically significant or not, the large number of phospholipids detected in the mouse cerebral cortex (75 species detected at >1% abundance in mouse cerebral cortex samples using MS, and 47 phospholipids definitively identified using MS/MS) and the

fact that none of the differences observed were significant at the $P < 0.01$ level, means that it is possible that the changes observed were due to chance. Indeed, probability theory would suggest that at least three of these five significant changes are likely to be due to chance rather than an actual difference in cerebral cortex composition.

Previous studies have shown a direct effect by a single dose of essential fatty acid on brain and plasma lipids. A tracer study on rats fed single 20mg doses of deuterated LA and ALA (Liu & Salem, 2007) showed accumulation of radiolabelled LA and ALA metabolites over a 25-day period. The animals showed only minimal accumulation of radiolabelled ALA itself in the brain, but its metabolites did gradually accumulate in the brain, with maximum concentrations of 20:5n-3, 22:5n-3 and 22:6n-3 in the brain reached at 8h, 96h and 600h after ALA dosing. LA could be incorporated more readily into the brain than ALA, with its concentration in the brain peaking 8h after dosing. However, the metabolites of LA accumulated in the brain at a comparable rate to those of ALA metabolites, with 20:3n-6, 20:4n-6, 22:4n-6 and 22:5n-6 reaching maximal concentrations at 96h, 240h, 600h and 168h respectively, following the radiolabelled lipid dose. Both 22:4n-6 and 22:6n-3 differed from the other PUFA metabolites studied in that they appeared to still be continuously accumulating in the brain at the end of the experiment, and so we cannot be certain whether their concentrations in the brain would increase further had an additional timepoint been included in the experiment. This study demonstrates the far-reaching effects of even a single dose of essential

fatty acid on lipid accumulation in the brain. The same study also examined the plasma concentrations of n-3 and n-6 lipids following dosing of LA and ALA and reported peaks of 18:3n-3 at 4h, and 20:5n-3, 22:5n-3 and 22:6n-3 at 96h. Maximum plasma concentration of 18:2n-6 and 18:3n-6 was reached at 8h, 20:3n-6 and 20:4n-6 at 24h and 22:4n-6 and 22:5n-6 at 96h. The length of time required to reach peak plasma concentrations of many of these PUFA metabolites correspond to the “window of neuroprotection” (Dirnagl & Hallenbeck, 2004; Blondeau et al., 2002; Lauritzen et al., 2000) in preventative stroke therapy, which means that the production of neuroprotective compounds from essential fatty acids or their metabolites is a possibility.

Pawlosky and colleagues (2001) carried out a tracer study following the metabolic fate of radiolabelled ALA in the plasma of human volunteers. Plasma concentrations of radiolabelled ALA, EPA and DHA were measured at time intervals between 0 – 120 hours after ingestion of a meal containing radioactive ALA. Plasma concentrations of ALA, EPA and DHA peaked at approximately 10, 40 and 72 hrs after intake of radioactive ALA respectively. Once again, elevated plasma concentrations of EPA and DHA coincide with the “window of neuroprotection” (Dirnagl & Hallenbeck, 2004), which means that the production of neuroprotective PUFA metabolites from substrates available in the circulation cannot be discounted.

Several metabolites of ALA have bioactive properties themselves, or are precursors to lipid mediator compounds, including pro-resolution and/or neuroprotective polyhydroxylated derivatives of EPA and DHA such as the resolvins and neuroprotectins (Chen & Bazan, 2005, Hong et al., 2003, Marcheselli et al., 2003, Mukherjee et al., 2004, Serhan et al., 2000). For example, 10,17S-docosatrienoic acid, a metabolite of DHA, is produced by many cell types including microglia and Th2 helper T cells (Levy et al., 2007) under a range of pathophysiological conditions, including rodent models of ischaemia (Hong et al., 2003). 10,17S-docosatrienoic acid has been shown to reduce inflammation in a mouse model of asthma by reducing the production of pro-inflammatory lipid mediators (Levy et al., 2007; Serhan et al., 2002). Direct intra-cerebroventricular infusion of 10,17S-docosatrienoic acid resulted in the reduction in infarct size in mice subjected to MCAO in comparison to untreated controls (Belayev et al., 2005; Marcheselli et al., 2003; Mukherjee et al., 2004), implying that the neuroprotective effects of PUFA seen in rodent models of ischaemic stroke may be mediated by PUFA metabolites rather than the injected PUFA itself. If this is the case, then the composition of the free fatty acid pool in brain or plasma may be of more importance than the phospholipid composition.

However, changes in brain phospholipid and free fatty acid homeostasis have been reported in mice subjected to hypoxic preconditioning. A study reported changes in the amounts of four phospholipid classes and several fatty acids in mice subjected to one run of hypoxia compared to untreated mice and mice

subjected to repeated runs of hypoxia (Duan et al., 1999). Phospholipid classes were detected using thin layer chromatography, while FFA were derivatised to fatty acid methyl esters (FAME) and analysed using gas chromatography. It was noted that levels of choline phospholipids (PC and SM) were decreased and those of PE and PS lipids were increased in mice that underwent one run of hypoxia compared to mice in the control group. All of these changes, except for the decrease in SM, were counter-acted in mice subjected to a higher number of hypoxic runs. In addition, free fatty acid levels were increased in mice subjected to one run of hypoxia compared to control mice, but near-control levels of fatty acids were detected in the group of mice that had undergone four periods of hypoxia.

It is plausible that repeated runs of hypoxia lead to no detectable changes in FAME because the preconditioning process invokes an adaptive cytoprotective response upon subsequent exposure to harmful stimulus, reducing influx of calcium ions, minimizing the activation of PLA₂ and subsequent autolysis of membrane phospholipids. Some free fatty acids released from structural phospholipids by PLA₂ activity, such as arachidonic acid, are substrates for the production of pro-inflammatory lipid mediators. For example, prostaglandins, which are produced from arachidonic acid, have neurotoxic effects (Farooqui & Horrocks 2006) and inhibitors of prostaglandin production are known to have a neuroprotective effect in animal models of stroke (Ahmad et al., 2009). As a result, the inhibition of free fatty acid release

by the inhibition of PLA₂ would be expected to be neuroprotective, since it reduces the amount of substrate available for prostaglandin synthesis.

The release of the free fatty acids located at the *sn*-2 position of the majority of the phospholipid species which were increased in ALA-treated mice would not result in additional substrate for the production of bioactive lipid mediators. The two exceptions are to this rule are the phosphatidylethanolamine with *m/z* 742 (identified as PE 18:1/18:2 using MS/MS) and the phosphatidylserine with *m/z* 812 (identified as PS 18:0/20:3) using MS/MS. The hydrolysis of PE18:1/18:2 would release linolenic acid from the *sn*-2 position, which is a precursor for the pro-inflammatory hydroxy octadienoic (HODE) acids 9-HODE and 13-HODE or can alternatively be metabolised to produce arachidonic acid, which can then be converted either enzymatically or by free radical-catalysed reactions into a wide range of bioactive lipid mediators, including prostaglandins, thromboxanes and hydroxy fatty acids. Work using radioactive tracers showed long-term accumulation of radiolabelled LA and ALA metabolites in rat brain tissue following a single dose of deuterated LA and ALA (Liu & Salem, 2007, which provides support for the possibility that an increase in PE18:1/18:2 may lead to the production of LA and its metabolites upon instigation of the phospholipase A2 signalling cascade. However, the length of time required for metabolites of LA to accumulate in the brain during tracer studies means that it is unlikely that any neuroprotective effect caused by a change in brain

phospholipids can be attributed to the production of long-chain LA-derived metabolites.

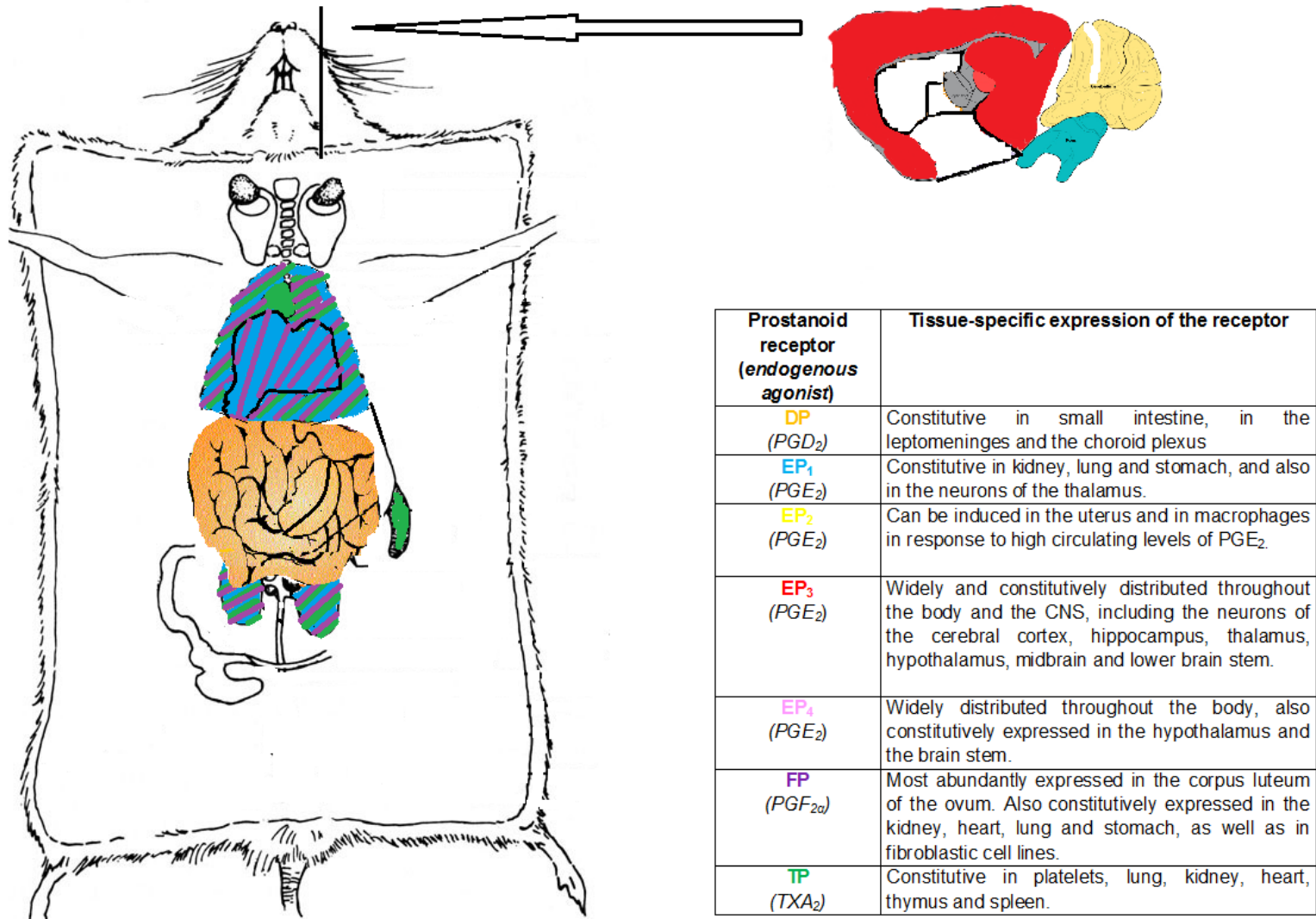
Preconditioning has been defined as a procedure where a noxious stimulus near to but below the threshold of damage is applied to a tissue (Dirnagl et al., 2009), following the principles of the adage “what doesn’t kill one makes one stronger”. However, it can be assumed that the threshold at which tissue injury would occur may differ from region to region of the brain, or from individual to individual. For instance, age may be a factor which affects the threshold at which tissue damage occurs upon a noxious stimulus. Research on elderly stroke patients showed that patients who had experienced transient ischaemic attacks (TIA), commonly known as “mini-strokes”, did not show improved neurological outcome compared to patients of the same age who had not experienced TIA prior to an ischaemic stroke (Della Morte et al., 2008), leading to the question whether differences in age could lead to differences in susceptibility in brain injury, meaning that even TIA could cause tissue damage in the elderly rather than acting as a noxious stimulus below the threshold of tissue injury. Stroke is rare in young adults, but 1,000 people under the age of 30 suffer a stroke every year in the UK, which means that the development of ischaemic tolerance through preconditioning warrants investigating, even if it is suggested that it is a phenomenon which only occurs in young adults.

5.3. Interpretation of analytical findings: lipid mediators study

5.3.1. Prostanoid profiling of mouse cerebral cortex and plasma – potential biological significance

Prostaglandins, isoprostanes and thromboxanes act upon members of a family of prostanoid receptors conserved from rodents to humans (Narumiya & FitzGerald, 2001; Narumiya et al., 1999). They can be activated under both physiological and pathophysiological conditions by a range of bioactive lipids, many of which were identified in mouse plasma and cerebral cortex samples in this study. Each member of the prostanoid receptor family has a specific distribution in the body and their expression varies between tissue types, as shown in Figure 5.4 (Narumiya et al., 1999).

Figure 5.4 Members of the prostanoid receptor family have a specific distribution in the body



Members of the prostanoid receptor family have been shown to play roles in the development of ischaemia-reperfusion injury, and the fact that fatty acid treatment of mice led to significant changes in several lipid mediator species that can act upon these receptors, lends itself to the possibility that fatty acid neuroprotection is mediated by the modulation of prostanoid receptor activity. Table 5.5 summarizes the changes observed in lipid mediators in both mouse cerebral cortex and plasma, and also which prostanoid receptors are affected by the lipid mediators in question.

Table 5.5 Fatty acid (ALA) treatment caused significant differences in the abundance of lipid mediators in both cerebral cortex and plasma, of which some can activate prostanoid receptors. Prostanoid receptors may play a role in the development of tissue injury in animal models of ischaemia.

Prostanoid changes in CEREBRAL CORTEX	RECEPTOR BINDING?	ROLE OF RECEPTOR ACTIVATION IN ANIMAL MODELS OF ISCHAEMIA
15-deoxy- Δ 12,14-PGJ ₂ INCREASED at 72h	PPAR γ ?	Unknown
TXB ₂ REDUCED at 3h, 24h and 72h	TP (via its biologically active precursor TXA ₂)	Increases blood flow in models of myocardium ischemia
Prostanoid changes in PLASMA	RECEPTOR BINDING?	ROLE OF RECEPTOR ACTIVATION IN ANIMAL MODELS OF ISCHAEMIA
15-deoxy- Δ 12,14-PGJ ₂ REDUCED at 72h and 168h	PPAR γ ?	Unknown
PGE ₂ INCREASED at 72h and 168h	EP1 EP2 EP3 EP4	Knockout reduces neuronal death in <i>in vitro</i> ischaemia model (Saleem et al., 2007) and blockade of EP ₁ receptor results in reduced infarct volume & better neurological function in mouse model of focal ischaemia (Abe et al., 2009) Increased neuronal death in EP2 ^{-/-} tissues compared to wild-type controls, and blockade of EP ₂ receptors resulted in increased infarct size (McCullough et al., 2004) Knockout EP3 ^{-/-} mice showed a reduced infarct volume following MCAO compared to wild-type animals (Saleem et al., 2009) Activation of EP ₄ protects against ischaemia-reperfusion injury in rat hearts (Xiao et al., 2004).
PGF _{3α} INCREASED at 24h	FP	Blockade reduces neuronal injury (Saleem et al., 2009)

5.3.2. Effects of alpha-linolenic acid treatment on the prostanoid profile of mouse cerebral cortex

There were several differences in the prominent prostanoid species detected in mouse cerebral cortex of animals in different treatment groups. Table 5.6 shows the most abundant prostanoid species (i.e. have a percentage abundance of >10% in the tissue sample) in naïve mice (CONTROL) and animals subjected to α -linolenic acid (ALA) or vehicle (VEH) injection at various timepoints (3h, 24h, 72h and 168h post-treatment).

Table 5.6 Differences in prominent lipid mediator species (i.e. comprise of >10% abundance of all prostanoids) in mouse cerebral cortex samples of animals from various treatment groups and time points.

Treatment group	Most prominent prostanoid species (>10 % of total prostanoids)									
CONTROL		PGD ₂	PGE ₂		PGE ₁	PGF _{2α}	6-keto PGF _{2α}			
VEH3		PGD ₂	PGE ₂	8-iso-PGE ₂	PGE ₁		6-keto PGF _{2α}			
VEH24		PGD ₂								
VEH72	PGB ₂					PGF _{2α}				
VEH168						PGF _{2α}	6-keto PGF _{2α}			
ALA3		PGD ₂	PGE ₂	8-iso-PGE ₂						TXB ₂
ALA24		PGD ₂		8-iso-PGE ₂						TXB ₂
ALA72	PGB ₂					PGF _{2α}				TXB ₂
ALA168	PGB ₂							15-deoxy-D12,14-PGJ ₂		

Several significant differences ($P < 0.05$, two-way ANOVA and post-hoc Dunnett's t-test) were observed between the eicosanoid composition of cerebral cortex in ALA-treated animals compared to naïve mice or those injected with vehicle. Here, we will outline these differences and consider the biological significance of these changes.

Increase in 15-deoxy- Δ 12,14-PGJ₂

The percentage abundance of 15-deoxy- Δ 12,14-PGJ₂ was increased in ALA-treated mice compared to VEH-injected or naïve (CTL) animals 72h following ALA administration. This compound has been identified as an activator of the PPAR γ receptor, and has been reported to reduce angiogenesis in tumour cells and to inhibit the expression of many inflammatory proteins such as iNOS, COX-2 and NF κ B *in vitro* and *in vivo* (Powell, 2003; Sasaguri & Miwa, 2004). However, these anti-inflammatory effects have only been observed at micromolar concentrations, considerably higher than the usual physiological range of prostaglandins (Bell-Parikh et al., 2003), prompting doubts whether 15-deoxy- Δ 12,14-PGJ₂ is of biological importance or whether it should be regarded as only a metabolite of PGD₂. If the latter is the case, then the increase in 15-deoxy- Δ 12,14-PGJ₂ at 72h post-injection in the cerebral cortex of ALA-treated animals compared to VEH-injected or naïve animals, can be viewed as a reflection of the levels of PGD₂ in the cerebral cortex and plasma.

Reduction in TXB₂

TXB₂ levels in ALA-treated animals were reduced at 3h, 24h and 72h compared to vehicle-injected or naïve animals. TXB₂ is not itself a bioactive lipid, but a stable and physiologically inactive metabolite of TXA₂ (which is synthesized *in vivo* from PGH₂ and has a very short half-life). The short half-life of TXA₂ means that it can't be detected in its active form in tissue samples, but TXB₂ is a reliable indicator of TXA₂ concentration and activity in biological systems. The biological functions of TXA₂ include vasoconstriction, platelet aggregation and bronchoconstriction, and its effects are mediated via a specific thromboxane (TP) receptor. The reduction in TXB₂ in mouse cerebral cortex at 3h, 24h and 72h following ALA injection could result in decreased activity of the TP receptor during this time period, owing to a reduction in the rate of production of TXA₂, the biologically active precursor of TXB₂. However, this reduction may be counter-acted by an increase in 8-iso-PGE₂ binding to TP receptors. These two seemingly counter-productive changes in the concentration of TP receptor ligands imply that changes in TP receptor activity may not be the most important factor in the development of fatty acid-induced neuroprotection

5.2.3. Effects of alpha-linolenic acid treatment on the prostanoid profile of mouse plasma

There were some differences in the prominent prostanoid species detected in mouse plasma of animals in different treatment groups. Table 5.7 shows the

most abundant prostanoid species (i.e. have a percentage abundance of >10% in the sample) in naïve mice (CONTROL) and animals subjected to α -linolenic acid (ALA) or vehicle (VEH) injection at various timepoints (3h, 24h, 72h and 168h post-injection).

Table 5.7 Differences in prominent lipid mediator species (i.e. comprise of >10% abundance of all prostanoids) in mouse plasma samples of animals from various treatment groups and time points.

Treatment group	Most prominent prostanoid species (>10 % of total prostanoids)									
CONTROL	PGB ₂								15-deoxy-D12,14-PGJ ₂	TXB ₂
VEH3	PGB ₂							D12-PGJ ₂	15-deoxy-D12,14-PGJ ₂	
VEH24	PGB ₂		PGE ₂					D12-PGJ ₂		
VEH72	PGB ₂								15-deoxy-D12,14-PGJ ₂	
VEH168		PGD ₂		PGE ₁	PGF _{3α}				15-deoxy-D12,14-PGJ ₂	TXB ₂
ALA3	PGB ₂					PGF _{2α}			15-deoxy-D12,14-PGJ ₂	TXB ₂
ALA24			PGE ₂		PGF _{3α}				15-deoxy-D12,14-PGJ ₂	
ALA72			PGE ₂				8-iso-PGF _{2α}			
ALA168	PGB ₂		PGE ₂							

Several significant differences ($P < 0.05$, two-way ANOVA and post-hoc Dunnett's t-test) were observed between the eicosanoid composition of plasma in ALA-treated animals compared to naïve mice or those injected with vehicle. These differences could in turn lead to modulation of prostanoid receptor activity in the mouse, leading to systemic effects.

Reduction in 15-deoxy- Δ 12,14-PGJ₂

The percentage abundance of 15-deoxy- Δ 12,14-PGJ₂ was decreased in ALA-treated mice compared to vehicle-injected or naïve animals at 72h and 168h following ALA administration. Although this lipid species has been identified as a PPAR γ ligand and found to play a role in certain animal models of inflammation, such as asthma, the lack of information on the actions of 15-deoxy- Δ 12,14-PGJ₂ within the physiological concentration range of prostaglandins has led to doubts as to whether this species is of any biological importance, or whether it should be regarded solely as a metabolite of PGD₂. The decrease in 15-deoxy- Δ 12,14-PGJ₂ at 72h and 168h post-ALA injection may then reflect a drop in circulating PGD₂, and the biological functions of this species should be considered. Although previous lipidomic studies by our group have found considerable amounts of PGD₂ in the brain, the distribution of the DP receptor does not reflect an important role in the CNS and to date, there is a lack of information on the role, if any, that the DP receptor plays in the development of post-ischaemic injury.

Increase in PGE₂

Plasma PGE₂ concentration is also elevated in ALA-treated mice at 72h and 168h compared to untreated or vehicle-injected mice. It is plausible that the elevated levels of circulating PGE₂ in the plasma following ALA treatment may lead to modulation of one or more of the EP receptor subtypes, which in turn mediates a neuroprotective effect upon ischaemic challenge.

Both EP₂ and EP₄ have protective effects in rodent models of ischaemia (McCullough et al., 2004; Xiao et al., 2004) but the EP₁ and EP₃ receptors were both implicated in the development of ischaemia-reperfusion injury in mouse models of focal cerebral ischaemia (Saleem et al., 2007; Abe et al., 2009; Saleem et al., 2009).

Transgenic animals lacking the EP₁ receptor gene (EP1^{-/-}) displayed a higher rate of cerebral blood flow during MCAO than wild-type animals and neuronal cultures from EP1^{-/-} mice also showed greater resistance to oxidative stress than wild-type neurons (Saleem et al., 2007), leading to speculation that the EP₁ receptor is a potential pharmacological target for the treatment of ischaemic stroke. These deductions were confirmed by a more recent study on the use of the selective EP₁ receptor antagonist SC51089 in a mouse model of focal ischaemia. This compound proved to be neuroprotective in both male and female C57/BL6 mice over a wide time window (Abe et al., 2009). Infarct volume was significantly reduced in drug-treated mice compared to control animals, and performance in neurological tests was also

better in drug-treated mice than in controls, leading to speculation that the EP₁ receptor is a potential pharmacological target for the treatment of ischaemic stroke (Abe et al, 2009). Another transgenic animal study showed that EP₃ receptor knockout (EP3^{-/-}) mice also showed a reduced infarct volume in knockout mice following MCAO compared to wild-type animals (Saleem et al., 2009).

All four EP receptor subtypes can be found in the rodent brain, but the most abundant subtype in the brain is the EP₃ receptor, which is widely-distributed in the CNS, including the neurons of the cerebral cortex and hippocampus. These two areas of the brain are particularly vulnerable to tissue damage following a period of ischaemia, which implies that the EP₃ receptor in particular may have a role to play in the development of neuronal injury in stroke. It is possible that the increase in plasma PGE₂ results in down-regulation of the activity of all EP receptor subtypes, which has the positive effect of preventing EP₃ receptor activation in the brain and subsequent neuronal injury following an ischaemic episode. Alternatively, there is the possibility that increased activity of the EP₁ and EP₃ receptor in the brain caused by a temporary period of elevated plasma PGE₂ following ALA treatment acts as a noxious stimulus, leading to the development of ischaemic tolerance.

Increase in PGF_{3α}

The relative abundance of PGF_{3α} was increased in ALA-treated mice compared to untreated animals or those injected with vehicle at 24h following treatment. PGF_{3α} is a 3-series analogue of the biologically active compound PGF_{2α}, which regulates vasoconstriction through its action upon the FP receptor and also plays a key role in both physiological and pathophysiological control of smooth muscle contraction. PGF_{3α} is a partial agonist of the FP receptor, competing directly with its more biologically active 2-series analogue for FP binding space (Wada et al., 2007). The increase in PGF_{3α} at t=24h in ALA-treated animals may have resulted in decreased activation of the FP receptor by the partial agonist effects of PGF_{3α} on this receptor reducing the biological effects mediated by PGF_{2α} through the FP receptor. The FP receptor has been reported to contribute to brain injury in a mouse model of focal ischaemia and blocking FP receptor activity results in a reduction in neuronal injury (Saleem et al., 2009), implying that this prostanoid receptor also plays a role in ischaemia- reperfusion injury. The increase in plasma PGF_{3α} 24h after PUFA injection may contribute to protection against tissue damage in the event of an ischaemic challenge by partially blocking the deleterious effects of FP receptor activation.

5.4. New issues emerging from this study

Methodological issues

The refinement of the methodology for the HETE assay (for example, the use of a buffer or more refined pH adjustment during the extraction process) in order to produce sharper peaks which had minimal tailing would provide increased information on the fatty acids. The lack of detected HETEs in this study compared to earlier work by our group may have been due to differences in sample collection, but there is a possibility that extracted samples may have degraded during storage prior to analysis. The risk of UV degradation or oxidation of HETEs could be eliminated by storage of extracted samples that are to undergo LC-MS/MS analysis of HETEs and other related compounds at -80°C in a non-polar solvent with added antioxidant. The addition of resolvins and the neuroprotectins to the MRM channels studied would also make the assay for hydroxy fatty acids more comprehensive, and provide a clearer picture of whether these neuroprotective compounds are endogenously produced following intravenous PUFA administration.

Total tissue changes vs. redistribution(s) within the tissue

Our chosen analytical methods only permitted the analysis of lipids of the whole tissue rather than at a cellular or sub-cellular level, meaning that the possibility of redistribution of phospholipid species between different cellular

components, or extracellular changes in brain lipids cannot be ruled out. There is also a possibility that statistically significant changes in bioactive lipids may have occurred in discrete brain cell populations which were not detectable at a whole tissue level. This possibility is particularly important when considering changes in the concentration of bioactive lipid mediators in the brain, where the levels of relevant species may only be elevated or depressed in specific areas of the brain, for instance, perhaps those areas which are most vulnerable to injury following brain ischaemia.

Are changes in brain phospholipid composition the most important?

Fatty acyl chains containing highly-unsaturated fatty acids in phospholipids are regarded as a potential pool of substrates for enzymes such as cyclo-oxygenase and lipo-oxygenase. However, these highly-unsaturated fatty acids within the phospholipid structure can only be made available for these enzymes by hydrolysis at the *sn*-2 position, which is tightly regulated by calcium-dependent enzymes. Under normal physiological conditions, the rate of free fatty acid production by PLA₂ is counteracted by phospholipid synthesis from diacylglycerols and fatty acids, and the amount of free fatty acids in the brain remains low. However, the biological actions of hydrolysed or oxidised PUFA products such as 10,17S-docosatrienoic acid are apparent even at low concentrations (Belayev et al. 2005, Marcheselli et al. 2003, Mukherjee et al. 2004), implying that even a small change in the production of certain PUFA metabolites could have an effect in rodent models of ischaemic stroke. If this is the case, then the composition of the free fatty acid pool in

brain or plasma may be of more importance than the phospholipid composition.

A study using GC or GC-MS to investigate free fatty acid composition of mouse cerebral cortex and plasma would show whether PUFA injection has a significant effect on the free fatty acid pool in the circulation, or a more local effect on the free fatty acid pool in the brain. This work could provide insight into whether the production of neuroprotective PUFA metabolites in the brain prior to an ischaemic event could account for the neuroprotective effects of intravenous PUFA prior to or immediately after focal ischaemia in rodents.

Assessing the inflammatory status of the animal following fatty acid treatment

It is also unclear whether the process of intravenous PUFA injection exerts its neuroprotective effects through “true preconditioning”, where exposure to cellular stress results in the development of tolerance to other stressful stimuli i.e. cross-tolerance, or by modulation of the post-ischaemic inflammatory cascade. A method of investigating whether intravenous PUFA results in inflammation following its administration would be to study the expression of known biomarkers of inflammation in mice undergoing PUFA treatment. For example, the presence of systemic inflammation in mice could be detected by studying the expression levels of C-reactive protein or interleukin-6 in plasma. Similarly, localised inflammation of the brain could be assessed by immunoblotting for inflammatory protein biomarkers such as interleukin-6 or

NFκB in brain tissues. An alternative method of assessing brain inflammation would be to develop and run a GC-MS or an LC-MS/MS assay for F₃-isoprostanes and F₄-neuroprostanes, which are 20:5n-3 and 22:6n-3 analogues of F₂-isoprostanes. F₄-neuroprostanes have been suggested as biomarkers of brain inflammation in neurodegenerative diseases such as Alzheimer's disease (Montuschi et al., 2004; Roberts & Fessel, 2004). A significant increase in the level of neuroprostanes in mice treated with PUFA compared to those undergoing vehicle administration would imply that PUFA administration is a stress event, and that PUFA neuroprotection is a form of "true preconditioning". Alternatively, the development of an assay for isofurans or neurofurans, which are both indicative of oxidative stress, would provide information on whether the administration of PUFA causes tolerance to ischaemic conditions through cellular adaptation caused by prior exposure to cellular stress.

Expression and function of bioactive lipid receptors

This study showed changes in the relative composition of some bioactive lipid mediators in both plasma and cerebral cortex samples, but the results of these changes on the expression and the functional activity of receptors in both the brain and the circulatory system have not been assessed. The observed increases in plasma PGE₂ and PGF₃ creates potential for a further study on the expression of the EP1, EP3 and FP receptors in brain tissue and also on the functional activity of these receptors following fatty acid treatment.

Detection and quantification of neural stem cells in adult mice

The detection of a glycerophospholipid which is exclusively linked to neural stem cells in the cerebral cortex of adult mice leads to questions as to whether enrichment of neural stem cells could result in a more favourable neurological outcome following MCAO due to self-repair of the ischaemia-damaged tissue. Several methods of neural stem cell enrichment have been described in literature, including exercise, social contact, BDNF and DN-3 agonists. The presence of the signature phospholipid PE 16:0;20:0 may provide a method in which to quantify the relative population of neural stem cells in enriched compared to non-enriched animals.

5.5 Conclusions

Advanced lipidomic analysis – A new powerful tool for neurochemistry

Our study detected several phospholipid species in mouse cortex which had previously not been reported in lipidomic studies on whole mouse or rat brains (see section 5.2.3.). The fatty acyl chains at both *sn*-1 and *sn*-2 in the majority of these newly identified species are derived from either saturated fatty acids or from the monounsaturated fatty acid, oleic acid. However, two of the novel species identified in our study contained an eicosadienoic acid (20:2) fatty acyl chain at the *sn*-2 position. They were identified using MS/MS as PE16;0-20;2 and PS 18;1-20;2. The phosphatidylethanolamine with *m/z* 720 (identified as PE 16:0-18:0 using MS/MS) has been described as a

'signature glycerophospholipid' of rat retinal stem cells, but had not been previously detected in whole brain lipidomic studies. In other terms, lipidomic analysis allowed us to demonstrate the presence of a neural stem cell lipid in the cerebral cortex.

We also detected and identified a novel PS species containing a very long chain fatty acid (PS 18:0-24:1), typical of retinal tissue (where fatty acyl chains $\geq C_{24}$ are common) and myelin (a rich source of 24:1). The method of brain dissection used in our studies precludes the accidental incorporation of eye tissue into the biological samples and the absence of common myelin lipids from other phospholipid classes implies that no contamination of cerebral cortex samples with white matter occurred. It can therefore be concluded that murine grey matter contains a small, yet detectable, amount of longer-chain fatty acyl chains within structural phospholipids.

How ALA treatment may induce adaptive cytoprotection in the CNS (i.e. brain preconditioning)?

Structural changes in the plasma membrane are unlikely to have a central role

No widespread changes in the phospholipid composition of mouse cerebral cortex were observed following ALA treatment, suggesting that structural changes in the plasma membrane are not the cause of fatty acid-induced

neuroprotection in mouse models of focal ischaemia. However, the discrete changes observed in cerebral cortex lie within the “window of neuroprotection”, which lends itself to the theory that changes in the composition of brain phospholipids could lead to changes in cell signalling, in particular the inflammatory cascade mediated by *sn*-2 hydrolysis of structural brain phospholipids that leads to release of free fatty acids which serve as substrates for bioactive lipid mediator compounds.

Interactions with inflammatory signalling pathways

The majority of the phospholipid species changed in their relative abundance in ALA-treated mice contained fatty acyl or fatty alkyl groups derived from unsaturated or monounsaturated fatty acids. These lipids, in contrast to highly-unsaturated fatty acids, generally do not give rise to bioactive lipid compounds when released from the *sn*-2 position by phospholipid hydrolysis. However, changes observed in eicosadienoic acid-containing species could lead to an increase in the rate of production of eicosatrienoic acid, which is a substrate for the production of 1-series prostaglandins and hydroxytrienoic acids. These lipids can directly compete with the more biologically active 2-series prostaglandins and hydroxytetraenoic acids respectively, partially blocking pro-inflammatory cell signalling pathways.

A potential role for prostanoid receptors in the development of ischaemic preconditioning was confirmed by work on lipid mediator profiling in fatty-acid

treated mouse cerebral cortex and plasma. Significant changes were observed in the composition of eicosanoid species in the cerebral cortex and plasma of ALA-treated mice compared to vehicle-injected or naive mice. Observed changes in lipid mediators in ALA-treated cerebral cortex were a decrease in TXB₂ at 3h, 24h and 72h. The systemic effects of ALA administration differed from localized effects on cerebral cortex prostanoids, with the most notable differences being increases in plasma PGF_{3α} at 24h and in plasma PGE₂ at 72h and 168h after injection.

The pharmacological activities of isoprostanes such as 8-iso-PGE₂ have not been confirmed, although it has been suggested that isoprostanes could activate both the thromboxane receptor as well as specific isoprostane receptors. Activation of the TP receptor by 8-iso-PGE₂ could result in increased cerebral blood flow through vasodilation, which may at least in part counter-act the harmful effects of focal cerebral ischaemia. Cerebral blood flow could be assessed using a laser Doppler probe to confirm this theory. However, no cloning studies on isoprostane receptors have been reported to date and the effect of isoprostane receptors on the development of neuroprotection or neuronal injury in models of ischaemia remains unknown.

A reduction in TXB₂ would appear to counteract the effects of TP receptor activation caused by an increase in 8-iso-PGE₂, but it is possible that a reduction in the rate of production of TXA₂ (the biologically active precursor of TXB₂) results in upregulation of the TP receptor. However, on the whole, the

seemingly counter-productive changes in the concentration of TP receptor ligands imply that changes in TP receptor activity may not be the most important factor in the development of fatty acid-induced neuroprotection.

The increase in plasma PGE₂ at 72h and 168h in ALA-treated animals compared to vehicle-injected or naïve mice also supports the theory that fatty acid-induced neuroprotection is mediated by effects on the inflammatory cascade. Many subtypes of EP prostanoid receptors which are activated by PGE₂ have been linked to animal models of ischaemia, most notably the EP1 and the EP3 receptor, both which have been shown to have a deleterious effect on post-ischaemia rodent brain. Knockout studies on these genes showed that EP1^{-/-} mice and EP3^{-/-} mice both showed a smaller infarct volume after MCAO compared to wild-type mice and pharmacological blockade of either receptor had a neuroprotective effect. A prolonged increase in the levels of circulating PGE₂ may result in down-regulation of this receptor, or alternatively, the presence of high levels of PGE₂ may act as a cellular stress event, resulting in the development of cross-tolerance. The lack of an obvious phenotype in EP1^{-/-} and in EP3^{-/-} mice may point towards these two EP receptor subtypes as a possible pharmacological target for stroke therapy.

Finally, the increase in PGF_{3α} observed in mouse plasma after ALA injection suggests that FP receptor activity is modulated following ALA injection. PGF_{3α} binds to the same prostanoid receptor as its 2-series analogue, but has a

lower rate of biological activity than the corresponding 2-series species, resulting in partial blockade of the FP receptor. Blocking FP receptor activity resulted in a reduction in neuronal injury in a rodent model of focal cerebral ischaemia, implying that this prostanoid receptor may play a role in ischaemia-reperfusion injury and be a possible pharmacological target in stroke therapy.

The changes in prostanoid composition in both cerebral cortex tissue as well as in plasma samples suggest that the effects of PUFA treatment are widespread, having both systemic and localised effects. The localised decrease in cerebral cortex TXA₂ may exert a neuroprotective effect by causing changes in cerebral blood flow or in modulation of the expression or activity of the TP receptor. However, the rise in plasma 8-iso-PGE₂ would appear to have a seemingly counter-productive effect on TP receptor activity. It would appear that changes in systemic bioactive lipid mediator production appear to provide more promising routes for development of a prophylactic stroke therapy. Increases in plasma PGE₂ and PGF_{3α}, both of which act on prostanoid receptors that have been shown to play a role in the development of ischaemia-reperfusion neuronal injury in rodent models of cerebral ischaemia, may provide potential pharmacological targets.

To conclude, the lipid profile changes observed in mice following intravenous PUFA treatment arise primarily from systemic effects, although a localised effect on one bioactive lipid mediator was also observed. Although subtle

differences in brain structural lipid composition was observed between PUFA treated animals and vehicle-injected or untreated mice, these changes were minor and discrete, suggesting that structural changes in the plasma membrane are not the cause of fatty acid-induced neuroprotection in mouse models of focal ischaemia.

Bibliography

Abumrad, N., Harmon, C. & Ibrahimi, A., 1998. Membrane transport of long-chain fatty acids: evidence for a facilitated process. *J Lipid Res*, 39(12), 2309-18.

Adibhatla, R.M. & Hatcher, J.F., 2007. Secretory phospholipase A2 IIA is up-regulated by TNF-alpha and IL-1alpha/beta after transient focal cerebral ischemia in rat. *Brain Research*, 1134(1), 199-205.

Ahmad, M. et al., 2009. Prolonged opportunity for neuroprotection in experimental stroke with selective blockade of cyclooxygenase-2 activity. *Brain Research*,

Albert, D. & Coniglio, J., 1977. Metabolism of eicosa-11,14-dienoic acid in rat testes. Evidence for delta8-desaturase activity. *Biochim. Biophys. Acta*, 489, 390-396.

Albert, D., Rhamy, R. & Coniglio, J., 1979. Desaturation of eicosa-11,14-dienoic acid in human testes. *Lipids*, 14, 498-500.

Allen, R.P. et al., 2001. MRI measurement of brain iron in patients with restless legs syndrome. *Neurology*, 56(2), 263-5.

Arita, M., Clish, C.B. & Serhan, C.N., 2005. The contributions of aspirin and microbial oxygenase to the biosynthesis of anti-inflammatory resolvins: novel oxygenase products from omega-3 polyunsaturated fatty acids. *Biochemical and Biophysical Research Communications*, 338(1), 149-157.

Azar, N.J. et al., 2008. Generalized tonic-clonic seizures after acute oxcarbazepine withdrawal. *Neurology*, 70(22 Pt 2), 2187-8.

Bagga, D. et al., 2003. Differential effects of prostaglandin derived from omega-6 and omega-3 polyunsaturated fatty acids on COX-2 expression and IL-6 secretion. *Proc Natl Acad Sci U S A* 100(4), 1751-1756.

Bang, D.Y., Ahn, E. & Moon, M.H., 2007. Shotgun analysis of phospholipids from mouse liver and brain by nanoflow liquid chromatography/tandem mass spectrometry. *J Chromatogr B Analyt Technol Biomed Life Sci*, 852(1-2), 268-77.

Bang, D.Y., Kang, D. & Moon, M.H., 2006. Nanoflow liquid chromatography-tandem mass spectrometry for the characterization of intact phosphatidylcholines from soybean, bovine brain, and liver. *J Chromatogr A*, 1104(1-2), 222-9.

Bannenberg, G.L. et al., 2005. Molecular circuits of resolution: formation and actions of resolvins and protectins. *J Immunol*, 174(7), 4345-55.

Barbosa-Sicard, E. et al., 2005. Eicosapentaenoic acid metabolism by cytochrome P450 enzymes of the CYP2C subfamily. *Biochem Biophys Res Comm*, 329(4), 1275-1281.

Barcelo-Coblijn, G., Hoggies, E. et al., 2003. Modification by docosahexaenoic acid of age-induced alterations in gene expression and molecular composition of rat brain phospholipids. *Proc Natl Acad Sci U S A*, 100(20), 11321-6.

Barcelo-Coblijn, G., Kitajka, K. et al., 2003. Gene expression and molecular composition of phospholipids in rat brain in relation to dietary n-6 to n-3 fatty acid ratio. *Biochim Biophys Acta*, 1632(1-3), 72-9.

Bazan, N.G., 2003. Synaptic lipid signaling: significance of polyunsaturated fatty acids and platelet-activating factor. *J Lipid Res*, 44(12), 2221-33.

Bazan, N.G., 1970. Effects of ischemia and electroconvulsive shock on free fatty acid pool in the brain. *Biochim Biophys Acta*, 218(1), 1-10.

Bazan, N.G., 2009. Cellular and molecular events mediated by docosahexaenoic acid-derived neuroprotectin D1 signaling in photoreceptor cell survival and brain protection. *Prostaglandins Leukot Essent Fatty Acids*, 81(2-3), 205-11.

Bear, M., 2001. *Neuroscience : exploring the brain* 2nd ed., Baltimore Md.: Lippincott Williams & Wilkins.

Beermann, C. et al., 2005. sn-position determination of phospholipid-linked fatty acids derived from erythrocytes by liquid chromatography electrospray ionization ion-trap mass spectrometry. *Lipids*, 40(2), 211-218.

Belayev, L. et al., 2005. Docosahexaenoic acid complexed to albumin elicits high-grade ischemic neuroprotection. *Stroke*, 36(1), 118-23.

Belayev, L. et al., 2009. LAU-0901, a novel platelet-activating factor receptor antagonist, confers enduring neuroprotection in experimental focal cerebral ischemia in the rat. *Brain Research*, 1253, 184-190.

Belayev, L. et al., 2008. LAU-0901, a novel platelet-activating factor antagonist, is highly neuroprotective in cerebral ischemia. *Experimental Neurology*, 214(2), 253-258.

Belayev, L. et al., 2009. Robust Docosahexaenoic Acid-Mediated Neuroprotection in a Rat Model of Transient, Focal Cerebral Ischemia. *Stroke*, 40, 3121-6

Bell-Parikh, L.C. et al., 2003. Biosynthesis of 15-deoxy-delta12,14-PGJ2 and the ligation of PPARgamma. *J Clin Invest*, 112(6), 945-955.

Berdeaux, O. et al., 2005. [Isoprostanes, biomarkers of lipid peroxidation in humans. Part 2: Quantification methods]. *Pathologie-Biologie*, 53(6), 356-363.

Berti, R. et al., 2002. Quantitative real-time RT-PCR analysis of inflammatory gene expression associated with ischemia-reperfusion brain injury. *J Cereb Blood Flow Metab*, 22(9), 1068-79.

Bible, E. et al., 2009. The support of neural stem cells transplanted into stroke-induced brain cavities by PLGA particles. *Biomaterials*, 30(16), 2985-94.

Bigler, J. et al., 2007. Polymorphisms predicted to alter function in prostaglandin E2 synthase and prostaglandin E2 receptors. *Pharmacogenet Genomics*, 17(3):221-7.

Birch, E.E. et al., 2010. The DIAMOND (DHA Intake And Measurement Of Neural Development) Study: a double-masked, randomized controlled clinical trial of the maturation of infant visual acuity as a function of the dietary level of docosahexaenoic acid. *Am J Clin Nutr*. 2010, 91 (4), 848-59

Birkle, D.L. & Bazan, N.G., 1988. Cerebral perfusion of metabolic inactivators: a new method for rapid fixation of labile lipid pools in brain. *Neurochem Res*, 13(9), 849-52.

Blondeau, N. et al., 2002. Polyunsaturated fatty acids induce ischemic and epileptic tolerance. *Neuroscience*, 109(2), 231-41.

Blondeau, N. et al. (2009) Subchronic Alpha-Linolenic Acid Treatment Enhances Brain Plasticity and Exerts an Antidepressant Effect: A Versatile Potential Therapy for Stroke. *Neuropsychopharmacology*, 34(11), 2548-2559.

Bosisio, E. et al., 1976. Correlation between release of free arachidonic acid and prostaglandin formation in brain cortex and cerebellum. *Prostaglandins*, 11 (5), 773-81.

Brash, A.R., 1999. Lipoxygenases: occurrence, functions, catalysis, and acquisition of substrate. *J Biol Chem*, 274(34), 23679-23682.

Brügger, B., et al. 1997. Quantitative analysis of biological membrane lipids at the low picomole level by nano-electrospray ionization tandem mass spectrometry. *Proc. Natl. Acad. Sci. USA* 94, 2339-44.

Burr, G.O. & Burr, M.M., 1929. A new deficiency disease produced by the rigid exclusion of fat from the diet. *J Biol Chem*, 82(345-367).

Cao, H. et al., 2008. An improved LC-MS/MS method for the quantification of prostaglandins E(2) and D(2) production in biological fluids. *Anal Biochem*, 372(1), 41-51.

Capdevila, J.H. & Falck, J.R., 2000. Biochemical and molecular characteristics of the cytochrome P450 arachidonic acid monooxygenase. *Prostaglandins Other Lipid Mediat*, 62(3), 271-92.

Capdevila, J.H. & Falck, J.R., 2002. Biochemical and molecular properties of the cytochrome P450 arachidonic acid monooxygenases. *Prostaglandins Other Lipid Mediat*, 68-69, 325-44.

Capdevila, J.H., Falck, J.R. & Harris, R.C., 2000. Cytochrome P450 and arachidonic acid bioactivation. Molecular and functional properties of the arachidonate monooxygenase. *J Lipid Res*, 41(2), 163-81.

Carrie, I. et al., 2000. Specific phospholipid fatty acid composition of brain regions in mice. Effects of n-3 polyunsaturated fatty acid deficiency and phospholipid supplementation. *J Lipid Res*, 41(3), 465-72.

Cenedella, R.J., Galli, C. & Paoletti, R., 1975. Brain free fatty levels in rats sacrificed by decapitation versus focused microwave irradiation. *Lipids*, 10(5), 290-3.

Chandrasekharan, N.V. et al., 2002. COX-3, a cyclooxygenase-1 variant inhibited by acetaminophen and other analgesic/antipyretic drugs: cloning, structure, and expression. *Proc Natl Acad Sci U S A*, 99(21), 13926-31.

Chen, C. & Bazan, N.G., 2005. Lipid signaling: sleep, synaptic plasticity, and neuroprotection. *Prostaglandins Other Lipid Mediat*, 77(1-4), 65-76.

Cheng, Q. et al., 2007. A population-based survey of multiple sclerosis in Shanghai, China. *Neurology*, 68(18), 1495-500.

Chiang, N., Arita, M. & Serhan, C.N., 2005. Anti-inflammatory circuitry: lipoxin, aspirin-triggered lipoxins and their receptor ALX. *Prostaglandins, Leukotrienes, and Essential Fatty Acids*, 73(3-4), 163-177.

Cho, H.P., Nakamura, M. & Clarke, S.D., 1999a. Cloning, expression, and fatty acid regulation of the human delta-5 desaturase. *J Biol Chem*, 274(52), 37335-9.

Cho, H.P., Nakamura, M.T. & Clarke, S.D., 1999b. Cloning, expression, and nutritional regulation of the mammalian Delta-6 desaturase. *J Biol Chem*, 274(1), 471-7.

Christie, W.W., 2003. *Lipid Analysis*, Bridgwater, UK: The Oily Press.

Christie, W.W., 2008. www.lipidlibrary.co.uk,

Claria, J. & Serhan, C.N., 1995. Aspirin triggers previously undescribed bioactive eicosanoids by human endothelial cell-leukocyte interactions. *Proc Natl Acad Sci U S A*, 92(21), 9475-9.

Cohen, M.V., Liu, G.S. & Downey, J.M., 1991. Preconditioning causes improved wall motion as well as smaller infarcts after transient coronary occlusion in rabbits. *Circulation*, 84(1), 341-9.

Comporti, M. et al., 2008. F2-isoprostanes are not just markers of oxidative stress. *Free Radic Biol Med*, 44(3), 247-56.

Cracowski, J., 2004. Isoprostanes: an emerging role in vascular physiology and disease? *Chemistry and Physics of Lipids*, 128(1-2), 75-83.

Cracowski, J., Berdeaux, O. & Durand, T., 2005. [Isoprostanes, biomarkers of lipid peroxidation in humans. Part 3: Biomarkers and mediators in vascular physiology and disease]. *Pathologie-Biologie*, 53(6), 364-368.

Deplanque, D. et al., 2003. Peroxisome proliferator-activated receptor-alpha activation as a mechanism of preventive neuroprotection induced by chronic fenofibrate treatment. *J Neurosci*, 23(15), 6264-71.

Dhodda, V.K. et al., 2004. Putative endogenous mediators of preconditioning-induced ischemic tolerance in rat brain identified by genomic and proteomic analysis. *J Neurochem*, 89(1), 73-89.

Diau, G. et al., 2003. Docosahexaenoic and Arachidonic Acid Influence on Preterm Baboon Retinal Composition and Function. *Investigative Ophthalmology and Visual Science*, 44, 4559-4566.

Duan, C. et al., 1999. Changes in phospholipids and free fatty acids in the brains of mice preconditioned by hypoxia. *Biol Signals Recept*, 8(4-5), 261-6.

Duffin, K. et al., 2000. Electrospray/tandem mass spectrometry for quantitative analysis of lipid remodeling in essential fatty acid deficient mice. *Anal Biochem*, 279(2), 179-88.

Durand, T., Cracowski, J. & Berdeaux, O., 2005. [Isoprostanes, biomarkers of lipid peroxidation in humans. Part 1. Nomenclature and synthesis]. *Pathologie-Biologie*, 53(6), 349-355.

Esch, S.W. et al., 2007. Rapid characterization of the fatty acyl composition of complex lipids by collision-induced dissociation time-of-flight spectrometry. *J Lipid Res*, 48(1), 235-41

Farias, S.E. et al., 2008. Formation of eicosanoids, E2/D2 isoprostanes, and docosanoids following decapitation-induced ischemia, measured in high-energy-microwaved rat brain. *J Lipid Res*, 49(9), 1990-2000.

Farooqui, A.A. & Horrocks, L.A., 2006. Phospholipase A2-generated lipid mediators in the brain: the good, the bad, and the ugly. *Neuroscientist*, 12(3), 245-60.

Fessel, J.P. et al., 2003. Isofurans, but not F2-isoprostanes, are increased in the substantia nigra of patients with Parkinson's disease and with dementia with Lewy body disease. *J Neurochem*, 85(3), 645-50.

Folch, J., Lees, M. & Sloane-Stanley, G.H., 1957. A simple method for the isolation and purification of total lipides from animal tissues. *J Biol Chem*, 226, 497-509.

Forman, B.M., Chen, J. & Evans, R.M., 1997. Hypolipidemic drugs, polyunsaturated fatty acids, and eicosanoids are ligands for peroxisome proliferator-activated receptors alpha and delta. *Proc Natl Acad Sci U S A*, 94(9), 4312-7.

Gao, L. et al., 2006. Formation of F-ring isoprostane-like compounds (F3-isoprostanes) in vivo from eicosapentaenoic acid. *J Biol Chem*, 281(20), 14092-14099.

Gele, P., 2004. *Stress Oxydant et Inflammation: Cibles Pharmacologiques de la Neuroprotection*. Universite de Lille II.

Gerbi, A. et al., 1999. Diet deficient in alpha-linolenic acid alters fatty acid composition and enzymatic properties of Na⁺, K⁺-ATPase isoenzymes of brain membranes in the adult rat. *J Nutr Biochem*, 10(4), 230-6.

Godukhin, O.V. & Obrenovitch, T.P., 2001. Asymmetric propagation of spreading depression along the anteroposterior axis of the cerebral cortex in mice. *J Neurophysiol*, 86(4), 2109-11.

Gora, S. et al., 2006 The proinflammatory mediator Platelet Activating Factor is an effective substrate for human group X secreted phospholipase A2. *Biochim Biophys Acta*. 2006, 1761(9), 1093-9.

Govolko, M.Y. & Murphy, E.J., 2008. An improved LC-MS/MS procedure for brain prostanoid analysis using brain fixation with head-focused microwave irradiation and liquid-liquid extraction. *J Lipid Res*, 49, 893-902.

Green, P. & Yavin, E., 1993. Elongation, desaturation, and esterification of essential fatty acids by fetal rat brain in vivo. *J Lipid Res*, 34(12), 2099-107.

Grotta, J. et al., 1995. Safety and tolerability of the glutamate antagonist CGS 19755 (Selfotel) in patients with acute ischemic stroke. Results of a phase IIa randomized trial. *Stroke*, 26(4), 602-5.

Gurr, M.I., Harwood, J.L. & Frayn, K.N., 2002. *Lipid Biochemistry: An Introduction*, Oxford, UK: Blackwell Science.

Hamilton, J.A., 1998. Fatty acid transport: difficult or easy? *J Lipid Res*, 39(3), 467-81.

Han, X. & Gross, R.W., 2005. Shotgun lipidomics: electrospray ionization mass spectrometric analysis and quantitation of cellular lipidomes directly from crude extracts of biological samples. *Mass Spectrom Rev*, 24(3), 367-412.

Harris, R.V. & James, A.T., 1965. Linoleic and alpha-linolenic acid biosynthesis in plant leaves and green alga. *Biochim Biophys Acta*, 106(3), 456-64.

Herskovitz, S. et al., 2005. Sensory symptoms in acquired neuromyotonia. *Neurology*, 65(8), 1330-1.

Heurteaux, C. et al. (2006) Alpha-linolenic acid and riluzole treatment confer cerebral protection and improve survival after focal brain ischemia. *Neuroscience*. 137, 247 - 251.

Hicks, A.M. et al., 2006. Unique molecular signatures of glycerophospholipid species in different rat tissues analyzed by tandem mass spectrometry. *Biochim Biophys Acta*, 1761(1022-1029).

Hirsch, D., Stahl, A. & Lodish, H.F., 1998. A family of fatty acid transporters conserved from mycobacterium to man. *Proc Natl Acad Sci U S A*, 95(15), 8625-9.

Hoffman, E. 2001. *Mass spectrometry: principles and applications*, Chichester, UK: John Wiley & Sons

Hong, S. et al., 2003. Novel docosatrienes and 17S-resolvins generated from docosahexaenoic acid in murine brain, human blood, and glial cells. Autacoids in anti-inflammation. *J Biol Chem*, 278(17), 14677-87.

Hong, S. et al., Resolvin D1, protectin D1, and related docosahexaenoic acid-derived products: Analysis via electrospray/low energy tandem mass spectrometry based on spectra and fragmentation mechanisms. *J Am Soc Mass Spectrom*.

Houjou, T. et al., 2005. A shotgun tandem mass spectrometric analysis of phospholipids with normal-phase and/or reverse-phase liquid chromatography/electrospray ionization mass spectrometry. *Rapid Commun Mass Spectrom*, 19(5), 654-66.

Igarashi, M. et al., 2007a. Docosahexaenoic acid synthesis from alpha-linolenic acid by rat brain is unaffected by dietary n-3 PUFA deprivation. *J Lipid Res*, 48(5), 1150-1158.

Igarashi, M., DeMar, J.C. et al., 2007b. Upregulated liver conversion of alpha-linolenic acid to docosahexaenoic acid in rats on a 15 week n-3 PUFA-deficient diet. *J Lipid Res*, 48(1), 152-164.

Igarashi, M., Ma, K. et al., 2007. Dietary n-3 PUFA deprivation for 15 weeks upregulates elongase and desaturase expression in rat liver but not brain. *J Lipid Res*, 48(11), 2463-2470.

Inoue, H. et al., 2003. Brain protection by resveratrol and fenofibrate against stroke requires peroxisome proliferator-activated receptor alpha in mice. *Neurosci Lett*, 352(3), 203-6.

James, A.T., 1963. The biosynthesis of long-chain saturated and unsaturated fatty acids in isolated plant leaves. *Biochim Biophys Acta*, 70, 9-19.

Jatana, M. et al., 2006. Inhibition of NF-kappaB activation by 5-lipoxygenase inhibitors protects brain against injury in a rat model of focal cerebral ischemia. *Journal of Neuroinflammation*, 3, 12.

Jisaka, M. et al., 2005. Double dioxygenation by mouse 8S-lipoxygenase: specific formation of a potent peroxisome proliferator-activated receptor alpha agonist. *Biochem Biophys Res Comm*, 338(1), 136-143.

Jump, D.B. et al., 2005. Fatty acid regulation of hepatic gene transcription. *J Nutr*, 135(11), 2503-2506.

Kerwin, J.L., Tuininga, A.R. & Ericsson, L.H., 1994. Identification of molecular species of glycerophospholipids and sphingomyelin using electrospray mass spectrometry. *J Lipid Res*, 35(6), 1102-14.

Kis, B. et al., 2004. Regional distribution of cyclooxygenase-3 mRNA in the rat central nervous system. *Brain Research. Molecular Brain Research*, 126(1), 78-80.

Kitagawa, K. et al., 1991. 'Ischemic tolerance' phenomenon detected in various brain regions. *Brain Research*, 561(2), 203-11.

Kitagawa, K. et al., 1990. 'Ischemic tolerance' phenomenon found in the brain. *Brain Research*, 528(1), 21-4.

Kitajka, K. et al., 2002. The role of n-3 polyunsaturated fatty acids in brain: modulation of rat brain gene expression by dietary n-3 fatty acids. *Proc Natl Acad Sci U S A*, 99(5), 2619-24.

Kitajka, K. et al., 2004. Effects of dietary omega-3 polyunsaturated fatty acids on brain gene expression. *Proc Natl Acad Sci U S A*, 101(30), 10931-6.

Kuhn, H., Walther, M. & Kuban, R.J., 2002. Mammalian arachidonate 15-lipoxygenases structure, function, and biological implications. *Prostaglandins & Other Lipid Mediators*, 68-69, 263-290.

Lagarde, M., 2003. [Metabolism of bioactive lipids]. *Pathologie-Biologie*, 51(5), 241-243.

Lai, B. et al., 2008. Electrophysiological neurodifferentiation of subventricular zone-derived precursor cells following stroke. *Neuroscience Letters*, 442(3), 305-308.

Lauritzen, I. et al., 2000. Polyunsaturated fatty acids are potent neuroprotectors. *Embo J*, 19(8), 1784-93.

Lee, C.H. & Hajra, A.K., 1991. Molecular species of diacylglycerols and phosphoglycerides and the postmortem changes in the molecular species of diacylglycerols in rat brains. *J Neurochem*, 56(2), 370-9.

Lee, S.H. et al., 2008. Acute ophthalmoplegia (without ataxia) associated with anti-GQ1b antibody. *Neurology*, 71(6), 426-9.

Lee, S.T. et al., 2008. Decreased number and function of endothelial progenitor cells in patients with migraine. *Neurology*, 70(17), 1510-7.

Lees, K.R. et al., 2000. Glycine antagonist (gavestinel) in neuroprotection (GAIN International) in patients with acute stroke: a randomised controlled trial. GAIN International Investigators. *Lancet*, 355(9219), 1949-54.

Lenoir, G., Williamson, P. & Holthuis, J.C., 2007. On the origin of lipid asymmetry: the flip side of ion transport. *Curr Opin Chem Biol*, 11(6), 654-61.

Leray, C., 2008. www.cyberlipid.org,

Levin, G. et al., 2002. Differential metabolism of dihomo-gamma-linolenic acid and arachidonic acid by cyclo-oxygenase-1 and cyclo-oxygenase-2: implications for cellular synthesis of prostaglandin E1 and prostaglandin E2. *Biochem J*, 365(Pt 2), 489-96.

Levin, H.S. et al., 2000. Reduction of corpus callosum growth after severe traumatic brain injury in children. *Neurology*, 54(3), 647-53.

Lieberman, M., Marks, A. & Smith, C., *Marks' Essentials of Medical Biochemistry: A Clinical Approach* 2nd ed., Lippincott Williams and Wilkins.

Lin, Y.H. & Salem, N., 2007. Whole body distribution of deuterated linoleic and alpha-linolenic acids and their metabolites in the rat. *J Lipid Res*, 48(12), 2709-24.

Little, S.J. et al., 2007. Docosahexaenoic acid-induced changes in phospholipids in cortex of young and aged rats: a lipidomic analysis. *Prostaglandins Leukot Essent Fatty Acids*, 77(3-4), 155-62.

Liu, Y. et al., 1992. Protection of rat hippocampus against ischemic neuronal damage by pretreatment with sublethal ischemia. *Brain Res*, 586(1), 121-4.

Longmire, A.W., Roberts, L.J. & Morrow, J.D., 1994. Actions of the E2-isoprostane, 8-ISO-PGE2, on the platelet thromboxane/endoperoxide receptor in humans and rats: additional evidence for the existence of a unique isoprostane receptor. *Prostaglandins*, 48(4), 247-256.

Lopez-Garcia, E. et al., 2004. Major dietary patterns are related to plasma concentrations of markers of inflammation and endothelial dysfunction. *Am J Clin Nutr*, 80(4), 1029-35.

Lukiw, W.J. et al., 2005. A role for docosahexaenoic acid-derived neuroprotectin D1 in neural cell survival and Alzheimer disease. *J Clin Invest*, 115(10), 2774-83.

Ma, Y.C. & Kim, H.Y., 1995. Development of the on-line high-performance liquid chromatography/thermospray mass spectrometry method for the analysis of phospholipid molecular species in rat brain. *Anal Biochem*, 226(2), 293-301.

Malerba, G. et al., 2008. SNPs of the FADS gene cluster are associated with polyunsaturated fatty acids in a cohort of patients with cardiovascular disease. *Lipids*, 43(4), 289-299.

Malow, B.A. et al., 2008. Treating obstructive sleep apnea in adults with epilepsy: a randomized pilot trial. *Neurology*, 71(8), 572-7.

Marcheselli, V.L. et al., 2003. Novel docosanoids inhibit brain ischemia-reperfusion-mediated leukocyte infiltration and pro-inflammatory gene expression. *J Biol Chem*, 278(44), 43807-17.

Martin, S.J. et al., 1995. Early Redistribution of Plasma Membrane Phosphatidylserine Is a General Feature of Apoptosis Regardless of the Initiating Stimulus: Inhibition by Overexpression of Bcl-2 and Abl. *J Exp Med*, 182 (5): 1545-56.

Martinez, M. & Mougan, I., 2004, Fatty Acid Composition of Human Brain Phospholipids During Normal Development. *J Neurochem*, 71(6), 2528-2533.

Masoodi, M. et al., 2008. Simultaneous lipidomic analysis of three families of bioactive lipid mediators leukotrienes, resolvins, protectins and related hydroxy-fatty acids by liquid chromatography/electrospray ionisation tandem mass spectrometry. *Rapid Commun Mass Spectrom*, 22(2), 75-83.

Masoodi, M. & Nicolaou, A., 2006. Lipidomic analysis of twenty-seven prostanoids and isoprostanes by liquid chromatography/electrospray tandem mass spectrometry. *Rapid Commun Mass Spectrom*, 20(20), 3023-9.

Matsushima, K. & Hakim, A.M., 1995. Transient forebrain ischemia protects against subsequent focal cerebral ischemia without changing cerebral perfusion. *Stroke*, 26(6), 1047-52.

Matsuzaka, T. et al., 2002. Cloning and characterization of a mammalian fatty acyl-CoA elongase as a lipogenic enzyme regulated by SREBPs. *J Lipid Res*, 43(6), 911-920.

McMahon, A. et al., 2007. A Stargardt disease-3 mutation in the mouse Elov14 gene causes retinal deficiency of C32-C36 acyl phosphatidylcholines. *FEBS Letters*, 581(28), 5459-5463.

McMaster, M. 2005. *LC/MS: a practical user's guide*. Chichester, UK: John Wiley & Sons.

McMurry, J.E. & Begley, T.P., 2005. *The organic chemistry of biological pathways*, Englewood, CO: Roberts and Co. Publishers.

McNair, H.M. & Miller, J.M., 1998. *Basic Gas Chromatography*, New York, NY: John Wiley & Sons Inc.

Milne, G.L. et al., 2007. Quantification of F2-isoprostanes as a biomarker of oxidative stress. *Nature Protocols*, 2(1), 221-226.

Mishra, A., Chaudhary, A. & Sethi, S., 2004. Oxidized omega-3 fatty acids inhibit NF-kappaB activation via a PPARalpha-dependent pathway. *Arterioscler Thromb Vasc Biol*, 24(9), 1621-7.

Montuschi, P., Barnes, P.J. & Roberts, L.J., 2004. Isoprostanes: markers and mediators of oxidative stress. *Faseb J*, 18(15), 1791-800.

Moriguchi, T. et al., 2004. Effects of an n-3-deficient diet on brain, retina, and liver fatty acyl composition in artificially reared rats. *J Lipid Res*, 45(8), 1437-1445.

Morrow, J.D. et al., 1990. A series of prostaglandin F2-like compounds are produced in vivo in humans by a non-cyclooxygenase, free radical-catalyzed mechanism. *Proc Natl Acad Sci U S A*, 87(23), 9383-7.

Mukherjee, P.K. et al., 2004. Neuroprotectin D1: a docosahexaenoic acid-derived docosatriene protects human retinal pigment epithelial cells from oxidative stress. *Proc Natl Acad Sci U S A*, 101(22), 8491-6.

Murry, C.E., Jennings, R.B. & Reimer, K.A., 1986. Preconditioning with ischemia: a delay of lethal cell injury in ischemic myocardium. *Circulation*, 74(5), 1124-36.

Nakamura, M.T. & Nara, T.Y., 2003. Essential fatty acid synthesis and its regulation in mammals. *Prostaglandins Leukot Essent Fatty Acids*, 68(2), 145-50.

Natarajan, R. & Nadler, J.L., 2004. Lipid inflammatory mediators in diabetic vascular disease. *Arteriosclerosis, Thrombosis, and Vascular Biology*, 24(9), 1542-1548.

Nicolaou, A.E. & Kokotos, G.E. eds., 2004. *Bioactive Lipids*, Bridgwater, UK: The Oily Press.

Nicolaou, A., Masoodi, M. & Mir, A., 2009. Lipidomic analysis of prostanoids by liquid chromatography-electrospray tandem mass spectrometry. *Methods in Molecular Biology (Clifton, N.J.)*, 579, 271-286.

Nourooz-Zadeh, J. et al., 1999. F4-isoprostanes as specific marker of docosahexaenoic acid peroxidation in Alzheimer's disease. *Journal of Neurochemistry*, 72(2), 734-740.

Obrenovitch, T.P. et al., 1988. In situ freezing of the brain for metabolic studies: evaluation of the "box" method for large experimental animals. *J Cereb Blood Flow Metab*, 8(5), 742-749.

O'Brien, J.S., Fillerup, D.L. & Mead, J.F., 1964. Quantification and fatty acid and fatty aldehyde composition of ethanolamine, choline, and serine glycerophosphatides in human cerebral grey and white matter. *J Lipid Res*, 5(3), 329-38.

Ogiso, H., Suzuki, T. & Taguchi, R., 2008. Development of a reverse-phase liquid chromatography electrospray ionization mass spectrometry method for lipidomics, improving detection of phosphatidic acid and phosphatidylserine. *Anal Biochem*, 375(1), 124-31.

Oliw, E.H., 1989. Biosynthesis of 18(RD)-hydroxyeicosatetraenoic acid from arachidonic acid by microsomes of monkey seminal vesicles. Some properties of a novel fatty acid omega 3-hydroxylase and omega 3-epoxygenase. *J Biol Chem*, 264(30), 17845-17853.

Ottani, F. et al., 1995. Prodromal angina limits infarct size. A role for ischemic preconditioning. *Circulation*, 91(2), 291-7.

Park, W.J. et al., 2009. An alternate pathway to long-chain polyunsaturates: the FADS2 gene product Delta8-desaturates 20:2n-6 and 20:3n-3. *J Lipid Res*, 50(6), 1195-1202.

Parker-Barnes, J.M. et al., 2000. Identification and characterization of an enzyme involved in the elongation of n-6 and n-3 polyunsaturated fatty acids. *Proc Natl Acad Sci U S A*, 97(15), 8284-9.

Pawlosky, R.J. et al., 2001. Physiological compartmental analysis of alpha-linolenic acid metabolism in adult humans. *J Lipid Res*, 42(8), 1257-65.

Petasis, N.A. et al., 2005. Design, synthesis and bioactions of novel stable mimetics of lipoxins and aspirin-triggered lipoxins. *Prostaglandins, Leukotrienes, and Essential Fatty Acids*, 73(3-4), 301-321.

Petkov, P.M. et al., 2004. An efficient SNP system for mouse genome scanning and elucidating strain relationships. *Genome Research*, 14(9), 1806-1811.

Phillis, J.W., Horrocks, L.A. & Farooqui, A.A., 2006. Cyclooxygenases, lipoxygenases, and epoxygenases in CNS: their role and involvement in neurological disorders. *Brain Res Rev*, 52(2), 201-43.

Ponten, U. et al., 1973. Optimal freezing conditions for cerebral metabolites in rats. *J Neurochem*, 21(5), 1127-38.

Powell, W.S., 2003. 15-Deoxy-delta12,14-PGJ2: endogenous PPARgamma ligand or minor eicosanoid degradation product? *J Clin Invest*, 112(6), 828-830.

Pulfer, M. & Murphy, R.C., 2003. Electrospray mass spectrometry of phospholipids. *Mass Spectrom Rev*, 22(5), 332-64.

Pulliam, L., Berens, M.E. & Rosenblum, M.L., 1988. A normal human brain cell aggregate model for neurobiological studies. *Journal of Neuroscience Research*, 21(2-4), 521-530.

Rapoport, S.I., Chang, M.C. & Spector, A.A., 2001. Delivery and turnover of plasma-derived essential PUFAs in mammalian brain. *J Lipid Res*, 42(5), 678-85.

Rehncrona, S. et al., 1982. Brain cortical fatty acids and phospholipids during and following complete and severe incomplete ischemia. *J Neurochem*, 38(1), 84-93.

Roberts, L.J. et al., 1998. Formation of isoprostane-like compounds (neuroprostanes) in vivo from docosahexaenoic acid. *Journal Biol Chem*, 273(22), 13605-13612.

Roberts, L.J. & Morrow, J.D., 1997. The generation and actions of isoprostanes. *Biochim Biophys Acta*, 1345(2), 121-135.

Roberts, L.J. & Fessel, J.P., 2004. The biochemistry of the isoprostane, neuroprostane, and isofuran pathways of lipid peroxidation. *Chemistry and Physics of Lipids*, 128(1-2), 173-186.

Roberts, L.J. & Morrow, J.D., 1997. The generation and actions of isoprostanes. *Biochim Biophys Acta*, 1345(2), 121-35.

Rodriguez de Turco, E.B. et al., 2002. Systemic fatty acid responses to transient focal cerebral ischemia: influence of neuroprotectant therapy with human albumin. *J Neurochem*, 83(3), 515-24.

Rogaeva, E.A. et al., 2001. Screening for PS1 mutations in a referral-based series of AD cases: 21 novel mutations. *Neurology*, 57(4), 621-5.

Rouzer, C.A. & Marnett, L.J., 2005. Structural and functional differences between cyclooxygenases: fatty acid oxygenases with a critical role in cell signaling. *Biochem Biophys Res Commun*, 338(1), 34-44.

Samuelsson, B. et al., 1987. Leukotrienes and lipoxins: structures, biosynthesis, and biological effects. *Science (New York, N.Y.)*, 237(4819), 1171-1176.

Schaffer, J.E. & Lodish, H.F., 1994. Expression cloning and characterization of a novel adipocyte long chain fatty acid transport protein. *Cell*, 79(3), 427-36.

Schott, R.J. et al., 1990. Ischemic preconditioning reduces infarct size in swine myocardium. *Circ Res*, 66(4), 1133-42.

Scott, B.L. & Bazan, N.G., 1989. Membrane docosahexaenoate is supplied to the developing brain and retina by the liver. *Proc Natl Acad Sci U S A*, 86(8), 2903-7.

Seeds, N.W., 1971. Biochemical differentiation in reaggregating brain cell culture. *Proc Natl Acad Sci U S A* 68(8), 1858-1861.

Serhan, C.N. & Chiang, N., 2008. Endogenous pro-resolving and anti-inflammatory lipid mediators: a new pharmacologic genus. *British Journal of Pharmacology*, 153 Suppl 1, S200-215.

Serhan, C.N., Hamberg, M. & Samuelsson, B., 1984. Lipoxins: novel series of biologically active compounds formed from arachidonic acid in human leukocytes. *Proc Natl Acad Sci U S A*, 81(17), 5335-5339.

Serhan, C.N., 2005. Mediator lipidomics. *Prostaglandins Other Lipid Mediat*, 77(1-4), 4-14.

Serhan, C.N. et al., 2000. Novel functional sets of lipid-derived mediators with antiinflammatory actions generated from omega-3 fatty acids via cyclooxygenase 2-nonsteroidal antiinflammatory drugs and transcellular processing. *J Exp Med*, 192(8), 1197-204.

Serhan, C.N. et al., 2004. Resolvins, docosatrienes, and neuroprotectins, novel omega-3-derived mediators, and their aspirin-triggered endogenous epimers: an overview of their protective roles in catabasis. *Prostaglandins Other Lipid Mediat*, 73(3-4), 155-72.

Serhan, C.N. et al., 2006. Anti-inflammatory actions of neuroprotectin D1/protectin D1 and its natural stereoisomers: assignments of dihydroxy-containing docosatrienes. *J Immunol*, 176(3), 1848-59.

Shaffel, S.S. et al., 2003. COX-3: a splice variant of cyclooxygenase-1 in mouse neural tissue and cells. *Brain Res Mol Brain Res*, 119(2), 213-5.

Simopoulos, A.P., 1991. Omega-3 fatty acids in health and disease and in growth and development. *Am J Clin Nutr*, 54(3), 438-63.

Sinclair, A. & Weisinger, R., 2004. Omega 3 fatty acids and the brain. *Chemistry in Australia*, 71, 6-10.

Song, Y.M. et al., 2007. Teaching neuroimage: sensory level in parietal lobe lesion. *Neurology*, 68(24), E38-9.

Spagnuolo, C. et al. PGF2 alpha, thromboxane B2 and HETE levels in gerbil brain cortex after ligation of common carotid arteries and decapitation *Prostaglandins*. 18 (1), 53-61

Sprecher, H. et al., 1995. Reevaluation of the pathways for the biosynthesis of polyunsaturated fatty acids. *J Lipid Res*, 36(12), 2471-7.

Suh, M. & Clandinin, M.T. 2005. 20:5n-3 but not 22:6n-3 is a preferred substrate for synthesis of n-3 very-long- chain fatty acids (C24-C36) in retina. *Curr Eye Res*, 30(11):959-68.

Swaab, D.F., 1971. Pitfalls in the use of rapid freezing for stopping brain and spinal cord metabolism in rat and mouse. *J Neurochem*, 18(11), 2085-92.

Taber, D.F., Morrow, J.D. & Roberts, L.J., 1997. A nomenclature system for the isoprostanes. *Prostaglandins*, 53(2), 63-7.

Taber, D.F., Fessel, J.P. & Roberts, L.J., 2004. A nomenclature system for isofurans. *Prostaglandins & Other Lipid Mediators*, 73(1-2), 47-50.

Taguchi, R. et al., 2005. Focused lipidomics by tandem mass spectrometry. *J Chromatogr B Analyt Technol Biomed Life Sci*, 823(1), 26-36.

Tapiero, H. et al., 2002. Polyunsaturated fatty acids (PUFA) and eicosanoids in human health and pathologies. *Biomed Pharmacother*, 56(5), 215-22.

Tasaki, K. et al., 1997. Lipopolysaccharide pre-treatment induces resistance against subsequent focal cerebral ischemic damage in spontaneously hypertensive rats. *Brain Res*, 748(1-2), 267-70.

Tvrdik, P. et al., 2000. Role of a new mammalian gene family in the biosynthesis of very long chain fatty acids and sphingolipids. *J Cell Biol*, 149(3), 707-718.

Uauy, R., Mena, P. & Rojas, C., 2000. Essential fatty acids in early life: structural and functional role. *Proc Nutr Soc*, 59(1), 3-15.

Ursin, V.M., 2003. Modification of plant lipids for human health: development of functional land-based omega-3 fatty acids. *J Nutr*, 133(12), 4271-4274.

Vance, D.E. & Vance, J.E., 2009. Physiological consequences of disruption of mammalian phospholipid biosynthetic genes. *J Lipid Res*, 50 Suppl, S132-137.

VanRollins, M. & Murphy, R.C., 1984. Autooxidation of docosahexaenoic acid: analysis of ten isomers of hydroxydocosahexaenoate. *J Lipid Res*, 25(5), 507-517.

Veech, R.L. et al., 1973. Freeze-blowing: a new technique for the study of brain in vivo. *J Neurochem*, 20(1), 183-188.

- Wada, M. et al., 2007. Enzymes and receptors of prostaglandin pathways with arachidonic acid-derived versus eicosapentaenoic acid-derived substrates and products. *J Biol Chem*, 282(31), 22254-22266.
- Wada, T., Kondoh, T. & Tamaki, N., 1999. Ischemic "cross" tolerance in hypoxic ischemia of immature rat brain. *Brain Research*, 847(2), 299-307.
- Wainwright, P.E., 2002. Dietary essential fatty acids and brain function: a developmental perspective on mechanisms. *Proc Nutr Soc*, 61(1), 61-9.
- Wang, Y. et al., 2005. Tissue-specific, nutritional, and developmental regulation of rat fatty acid elongases. *J Lipid Res*, 46(4), 706-715.
- Wassall, S.R. & Stillwell, W., 2008. Docosahexaenoic acid domains: the ultimate non-raft membrane domain. *Chem Phys Lipids*, 153(1), 57-63.
- Watson, A.D., 2006. Thematic review series: systems biology approaches to metabolic and cardiovascular disorders. Lipidomics: a global approach to lipid analysis in biological systems. *J Lipid Res*, 47(10), 2101-11.
- Wegener, S. et al., 2004. Transient ischemic attacks before ischemic stroke: preconditioning the human brain? A multicenter magnetic resonance imaging study. *Stroke*, 35(3), 616-621.
- Weih, M. et al., 1999. Attenuated stroke severity after prodromal TIA: a role for ischemic tolerance in the brain? *Stroke*, 30(9), 1851-1854.
- Wenk, M.R. 2003. Phosphoinositide profiling in complex lipid mixtures using electrospray ionization mass spectrometry. *Nat Biotechnol*, 21 (7), 813-7.
- Wenk, M.R., 2005. The emerging field of lipidomics. *Nat Rev Drug Discov*, 4(7), 594-610.
- Westerberg, R. et al., 2006. ELOVL3 is an important component for early onset of lipid recruitment in brown adipose tissue. *J Biol Chem*, 281(8), 4958-4968.
- Weylandt, K.H. & Kang, J.X., 2005. Rethinking lipid mediators. *Lancet*, 366(9486), 618-20.
- Williard, D.E. et al., 2001. Docosahexaenoic acid synthesis from n-3 polyunsaturated fatty acids in differentiated rat brain astrocytes. *J Lipid Res*, 42(9), 1368-76.

Wilson, R. & Sargent, J.R., 1993. Lipid and fatty acid composition of brain tissue from adrenoleukodystrophy patients. *J Neurochem*, 61(1), 290-297.

Xiao, Y., Huang, Y. & Chen, Z.Y., 2005. Distribution, depletion and recovery of docosahexaenoic acid are region-specific in rat brain. *Br J Nutr*, 94(4), 544-50.

Yang, M.S. et al., 1983. An improved method for in situ freezing of cat brain for metabolic studies. *J Neurochem*, 41(5), 1393-1397.

Yehuda, S. et al., 1998. Fatty acids and brain peptides. *Peptides*, 19(2), 407-19.

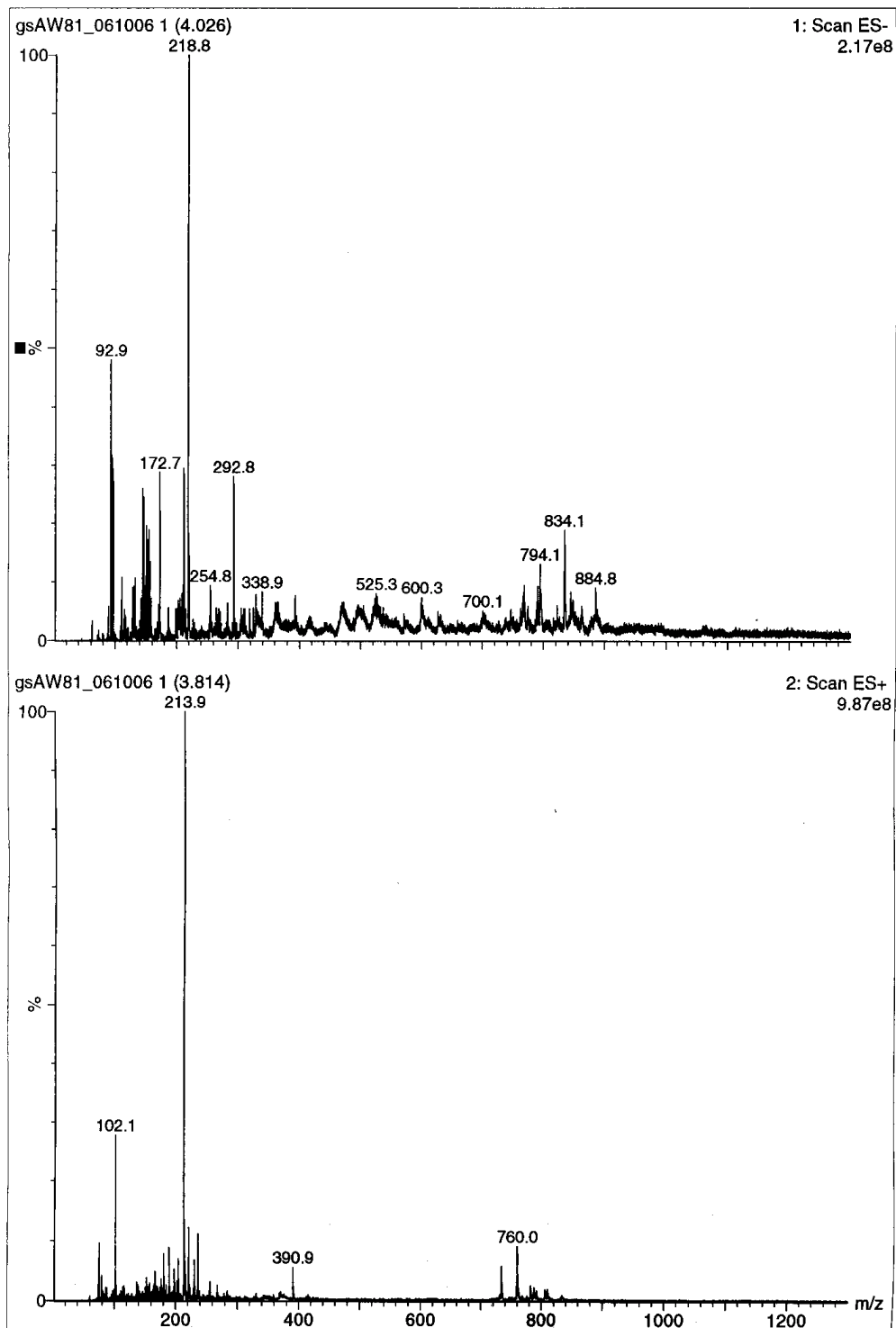
Yokomizo, T. et al., 1997. A G-protein-coupled receptor for leukotriene B₄ that mediates chemotaxis. *Nature*, 387(6633), 620-4.

Zhou, L. & Nilsson, A., 2001. Sources of eicosanoid precursor fatty acid pools in tissues. *J Lipid Res*, 42(10), 1521-1542.

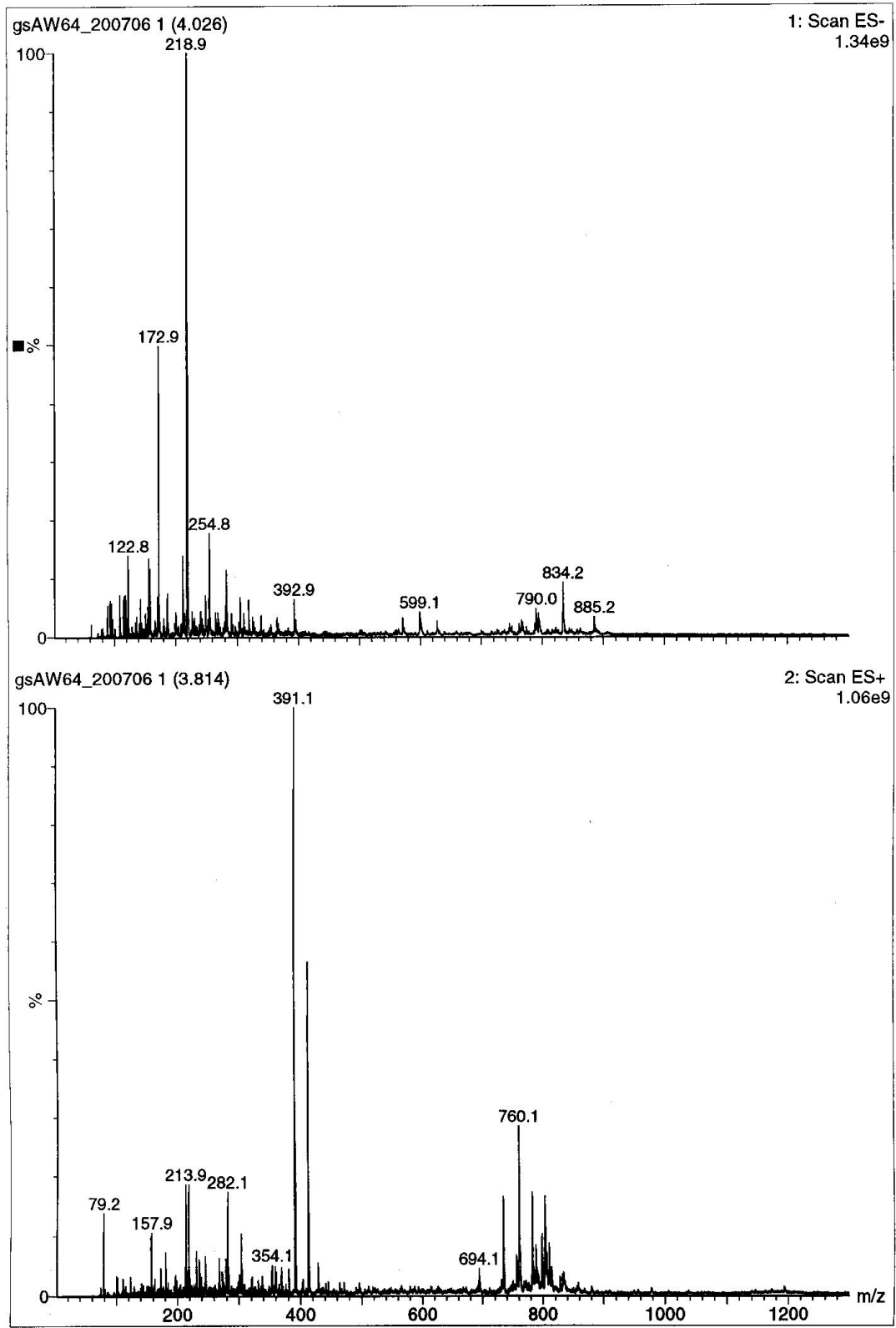
<http://www.differentstrokes.co.uk>

Appendix 1.1 Phospholipid analysis in mouse cerebral cortex using MS

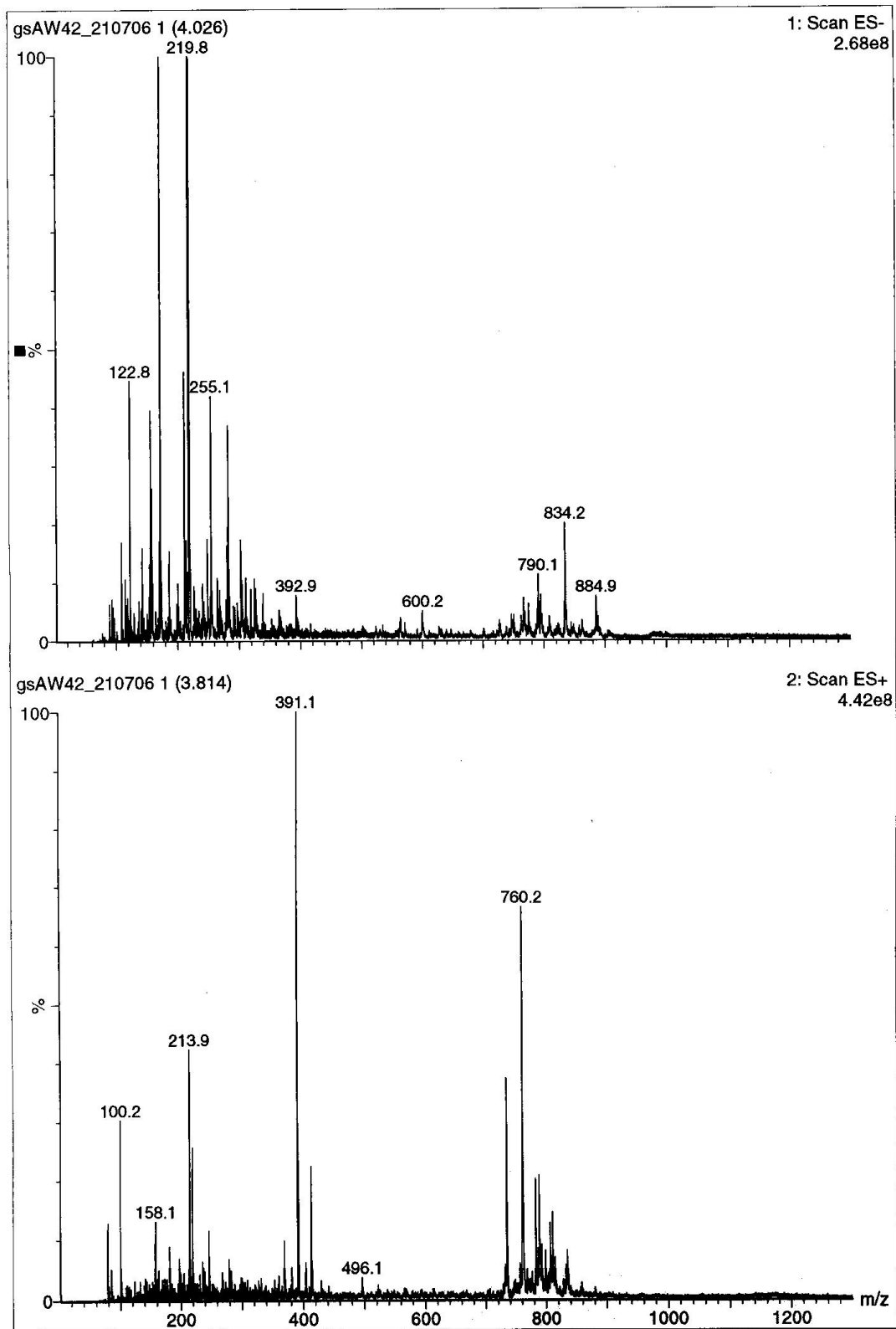
Representative general scan mass spectrum of mouse cerebral cortex in VEH3 group



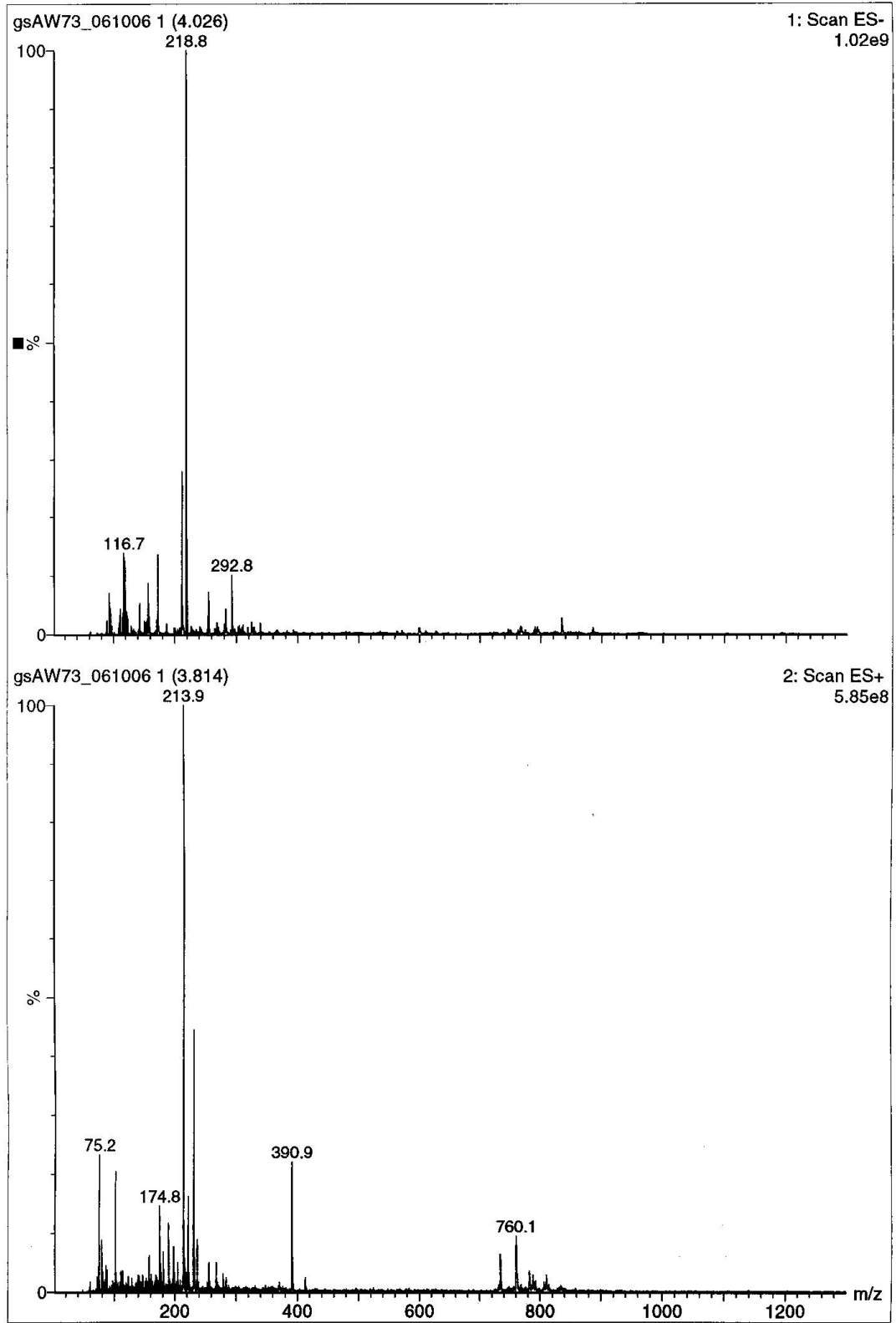
Representative general scan mass spectrum of mouse cerebral cortex in VEH24 group



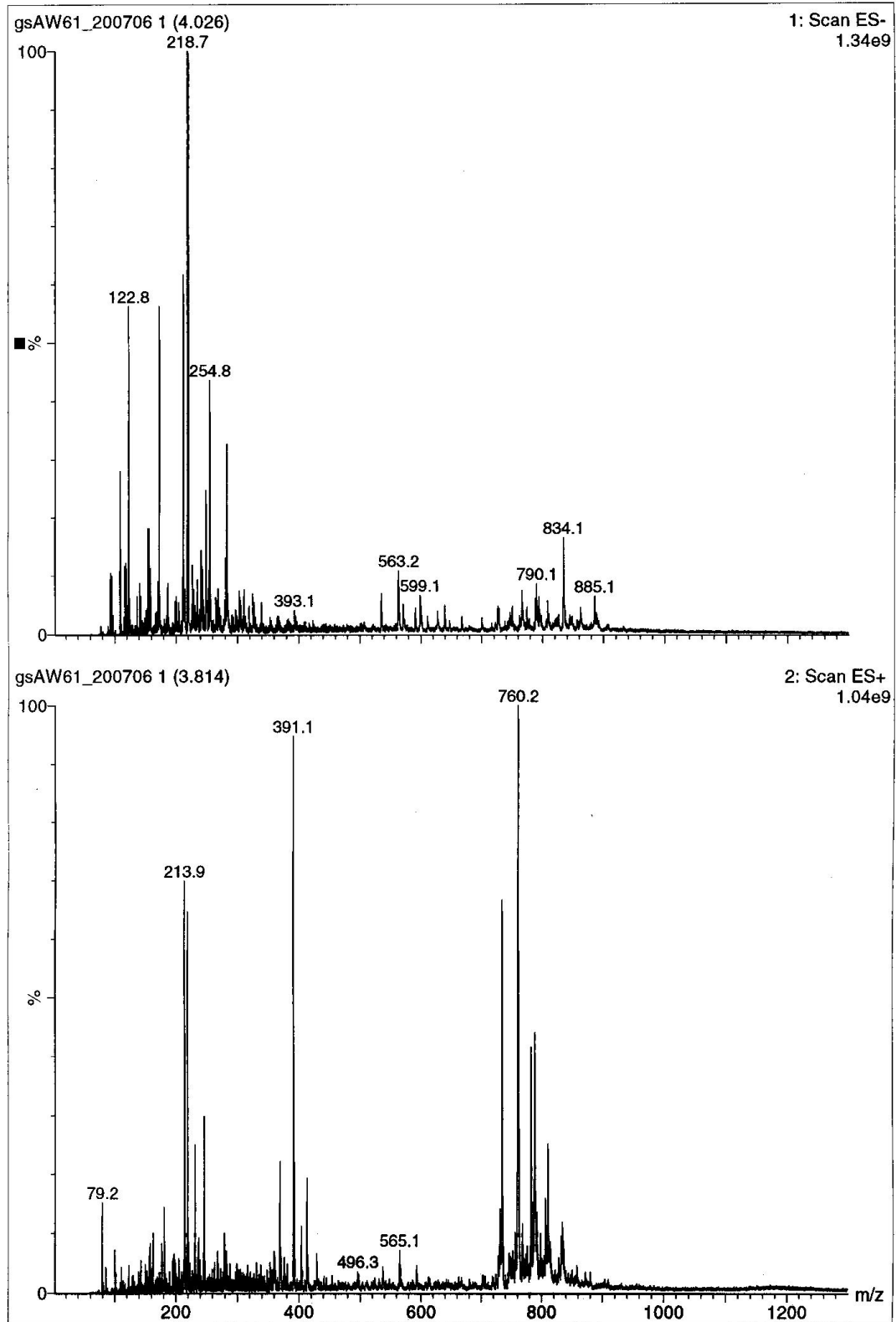
Representative general scan mass spectrum of mouse cerebral cortex in VEH72 group



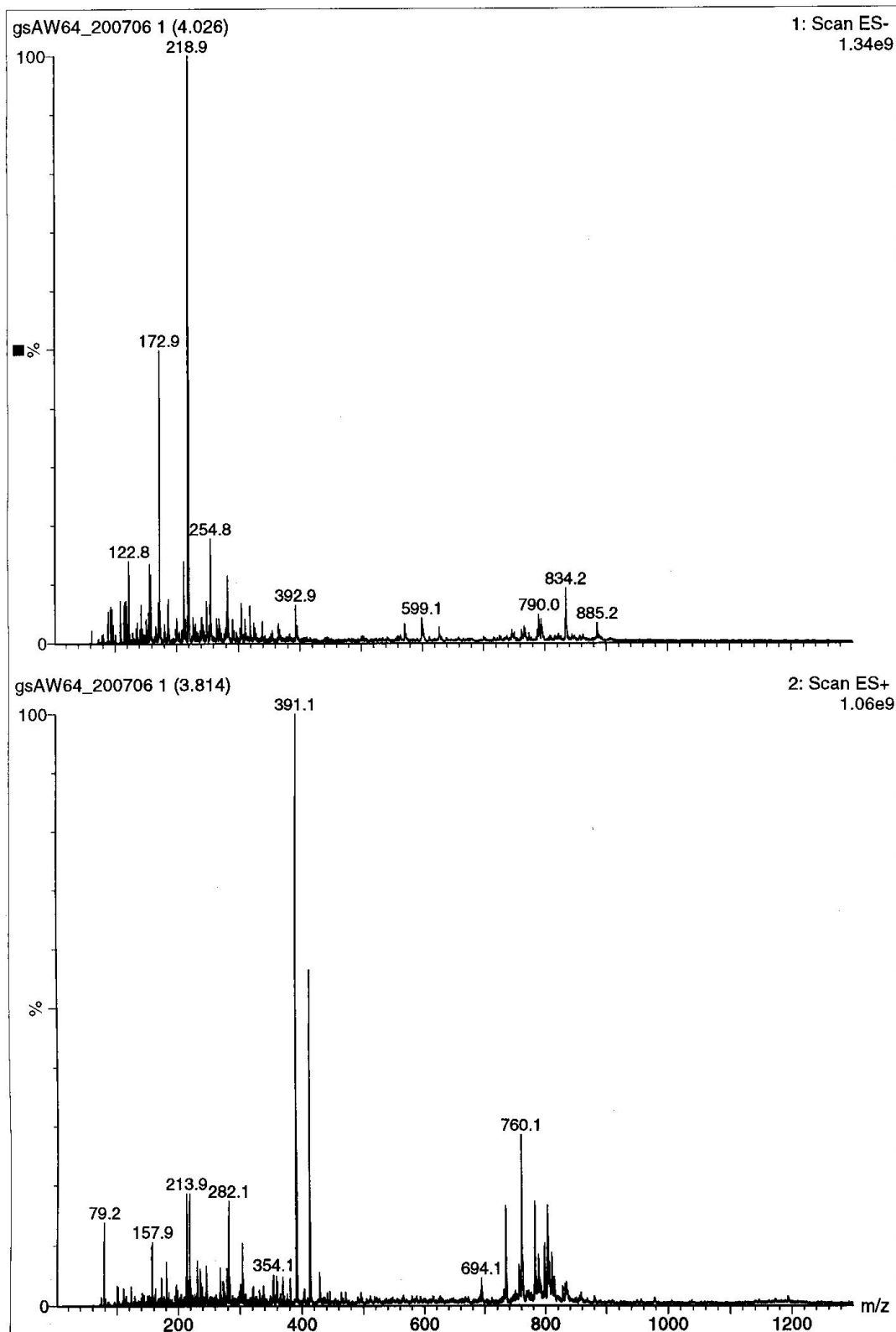
Representative general scan mass spectrum of mouse cerebral cortex in VEH168 group



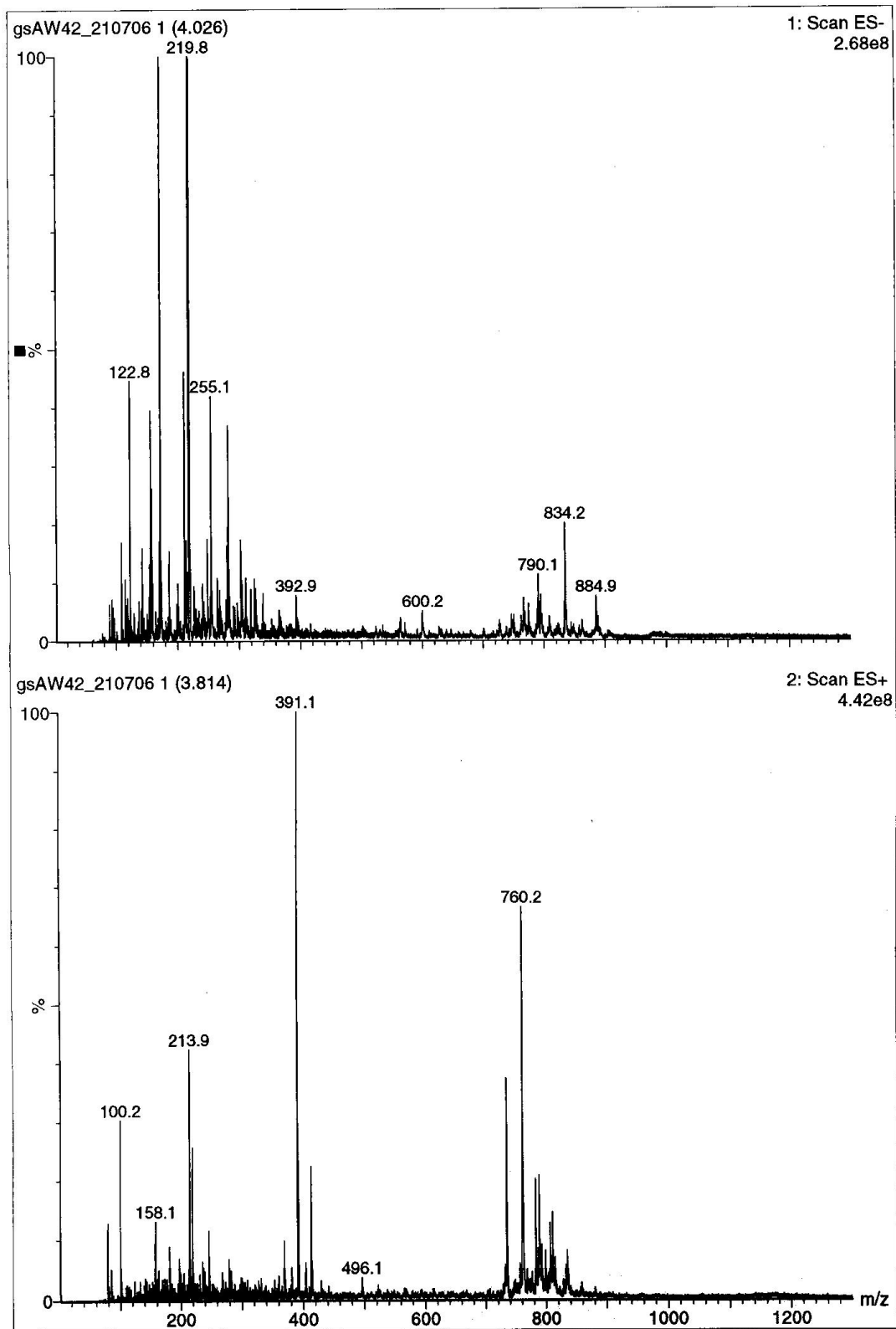
Representative general scan mass spectrum of mouse cerebral cortex in ALA3 group



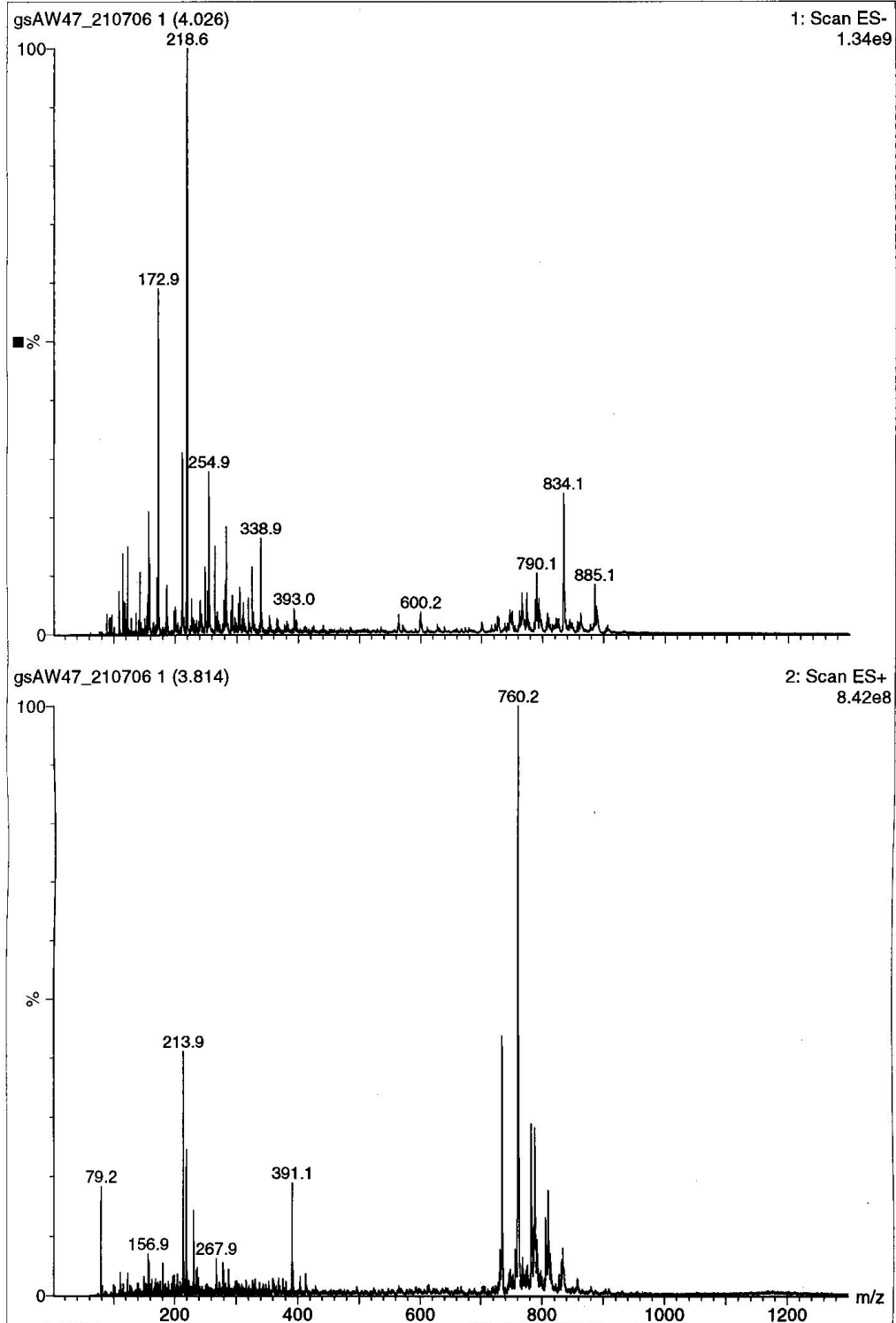
Representative general scan mass spectrum of mouse cerebral cortex in ALA24 group



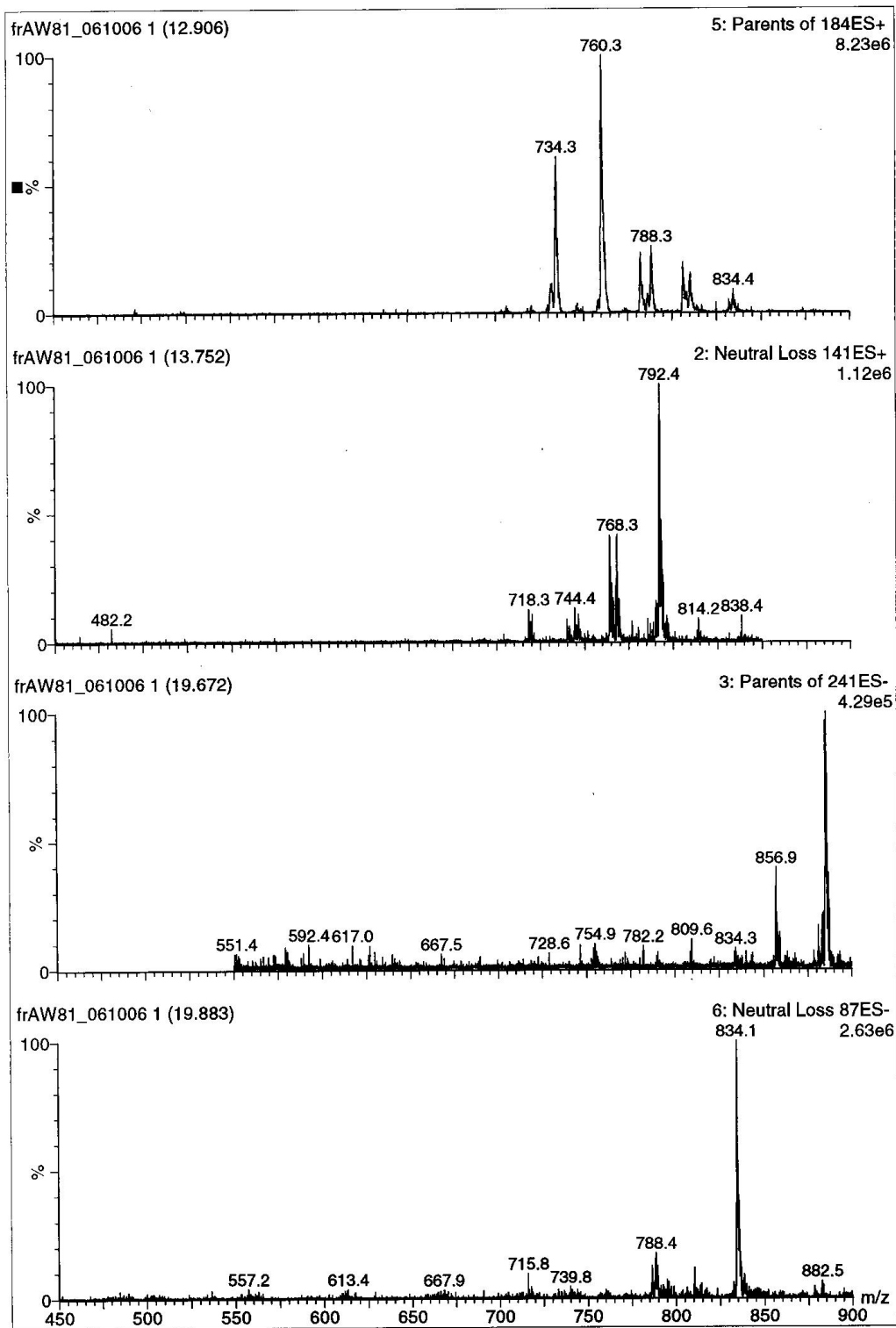
Representative general scan mass spectrum of mouse cerebral cortex in ALA72 group



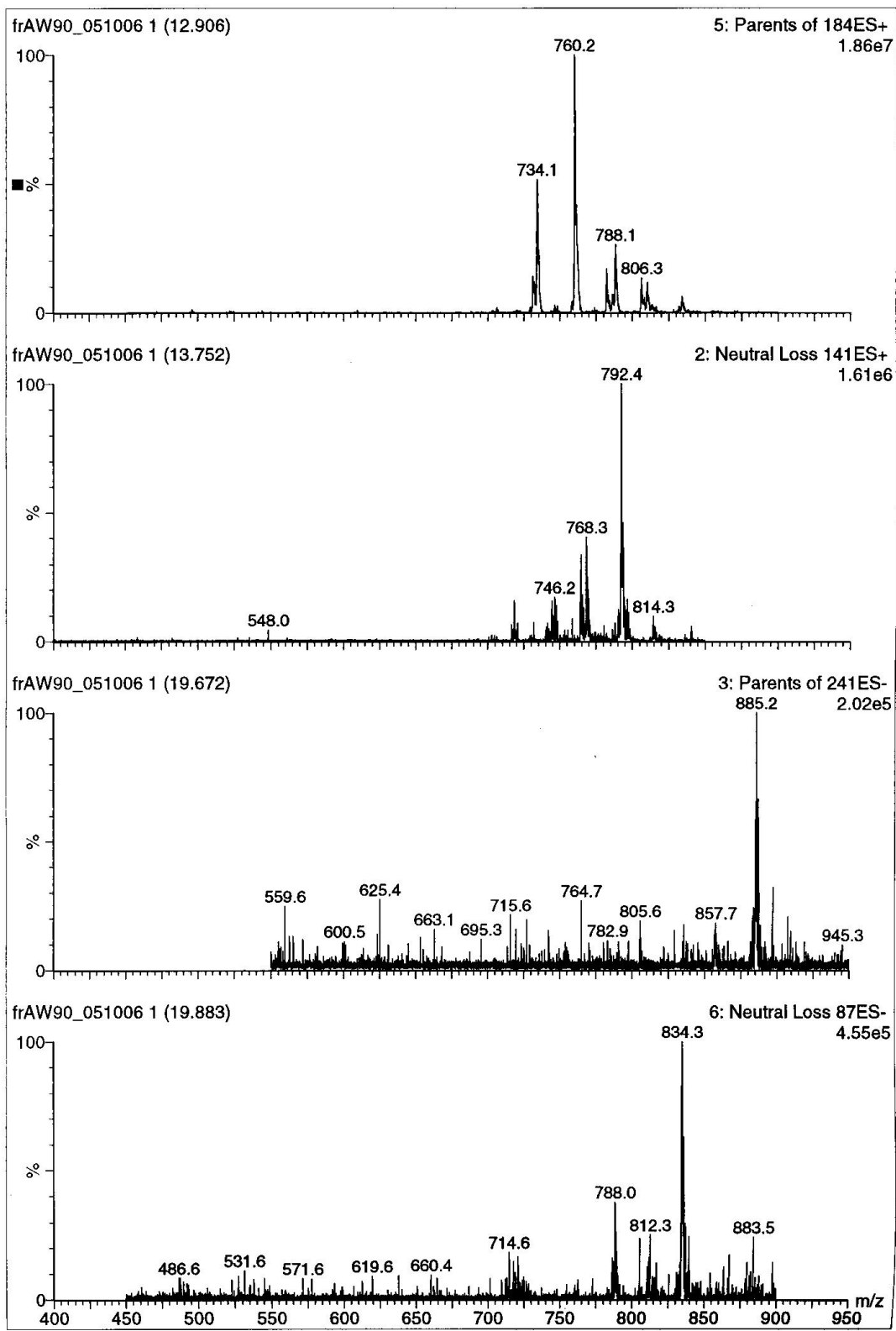
Representative general scan mass spectrum of mouse cerebral cortex in ALA168 group



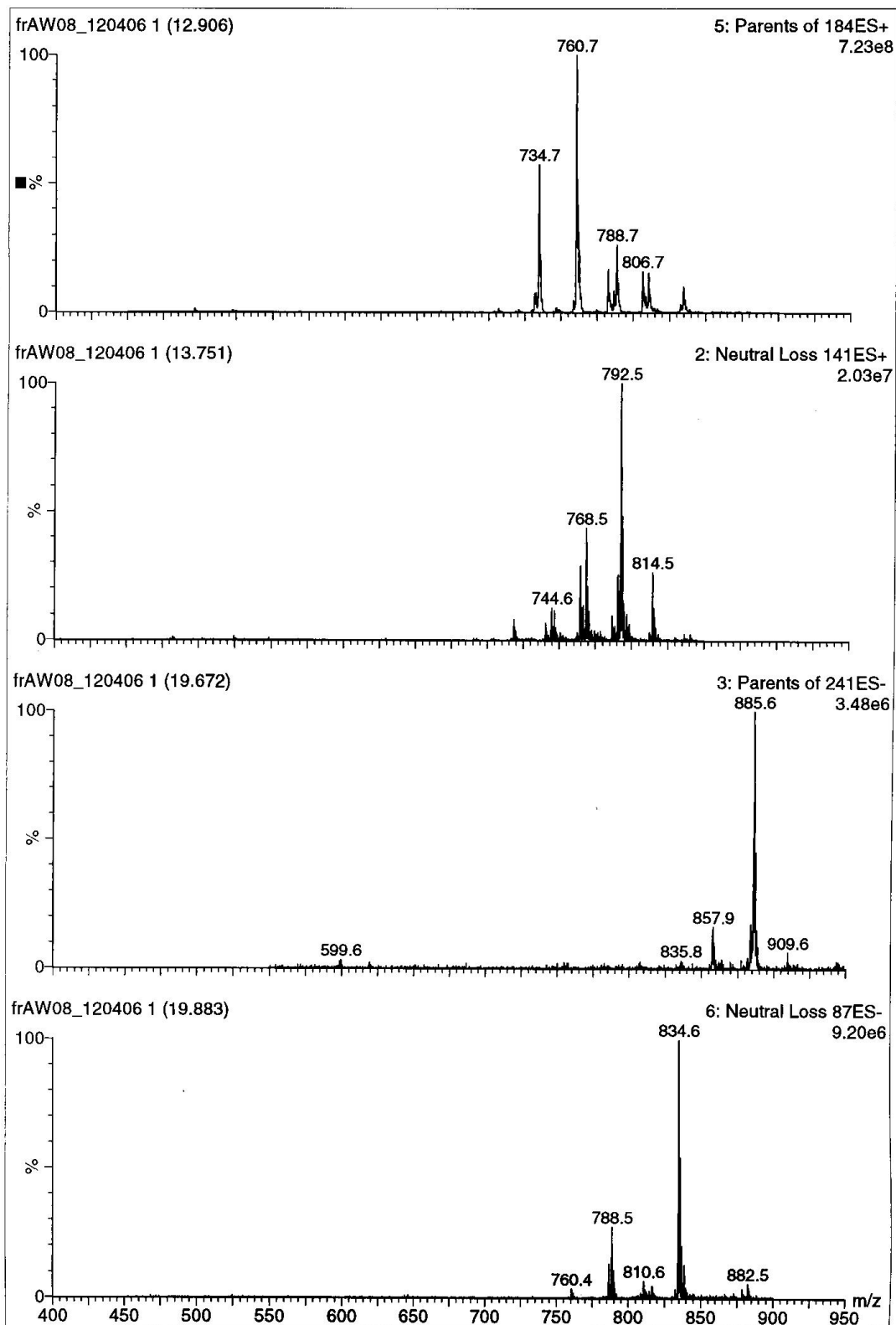
Representative neutral loss and precursor ion scanning mass spectra of cerebral cortex in VEH3 group mouse



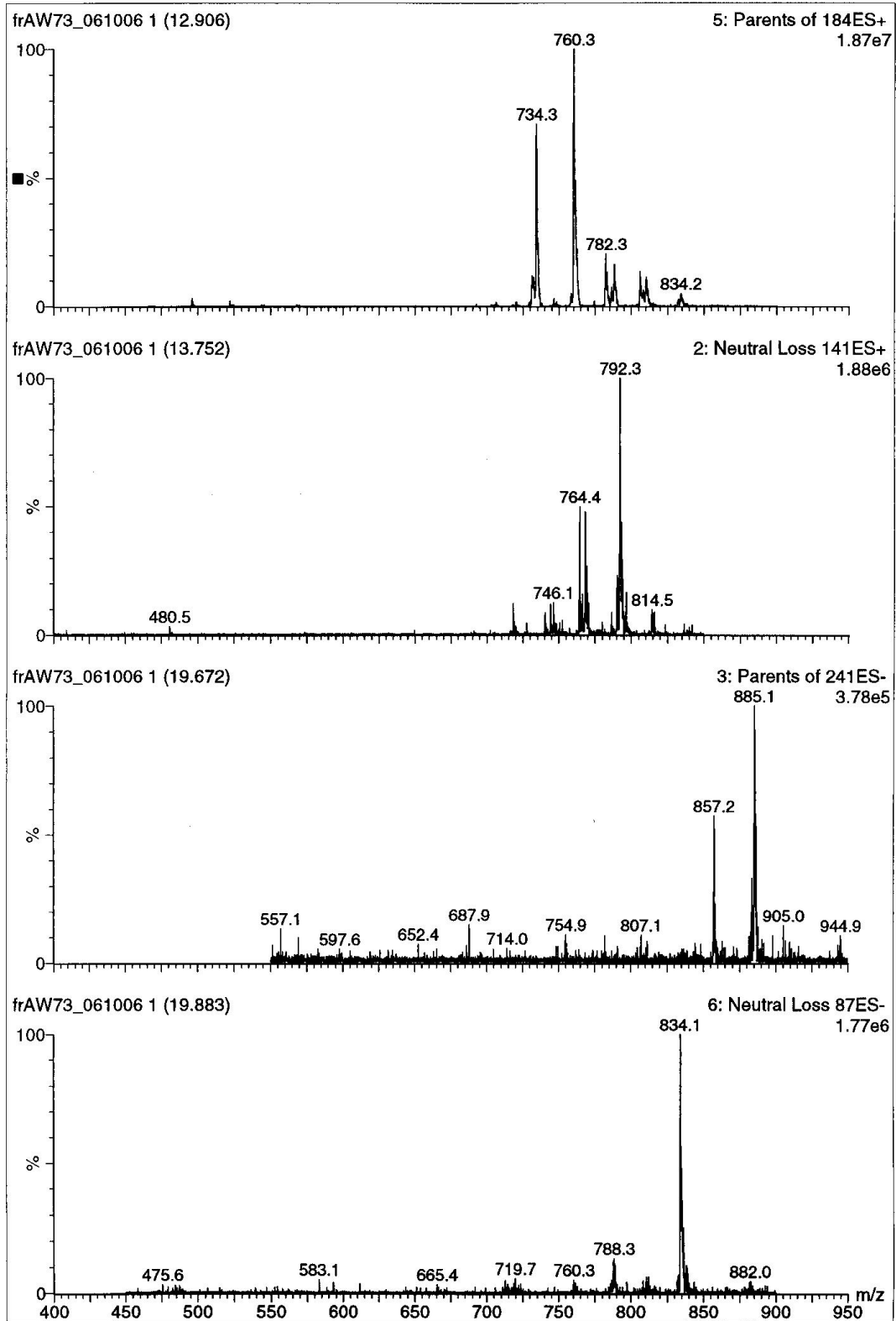
Representative neutral loss and precursor ion scanning mass spectra of cerebral cortex in VEH24 group mouse



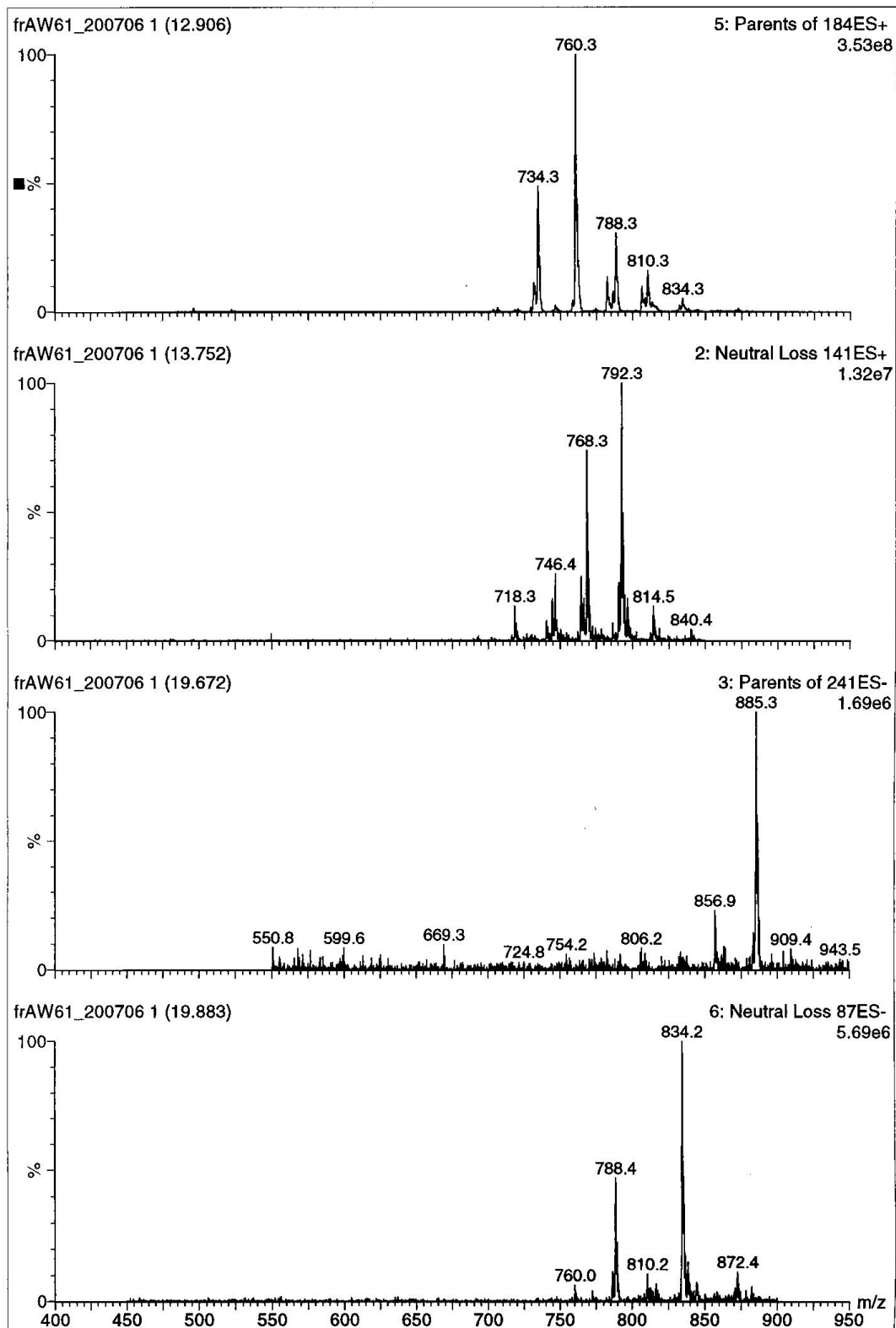
Representative neutral loss and precursor ion scanning mass spectra of cerebral cortex in VEH72 group mouse



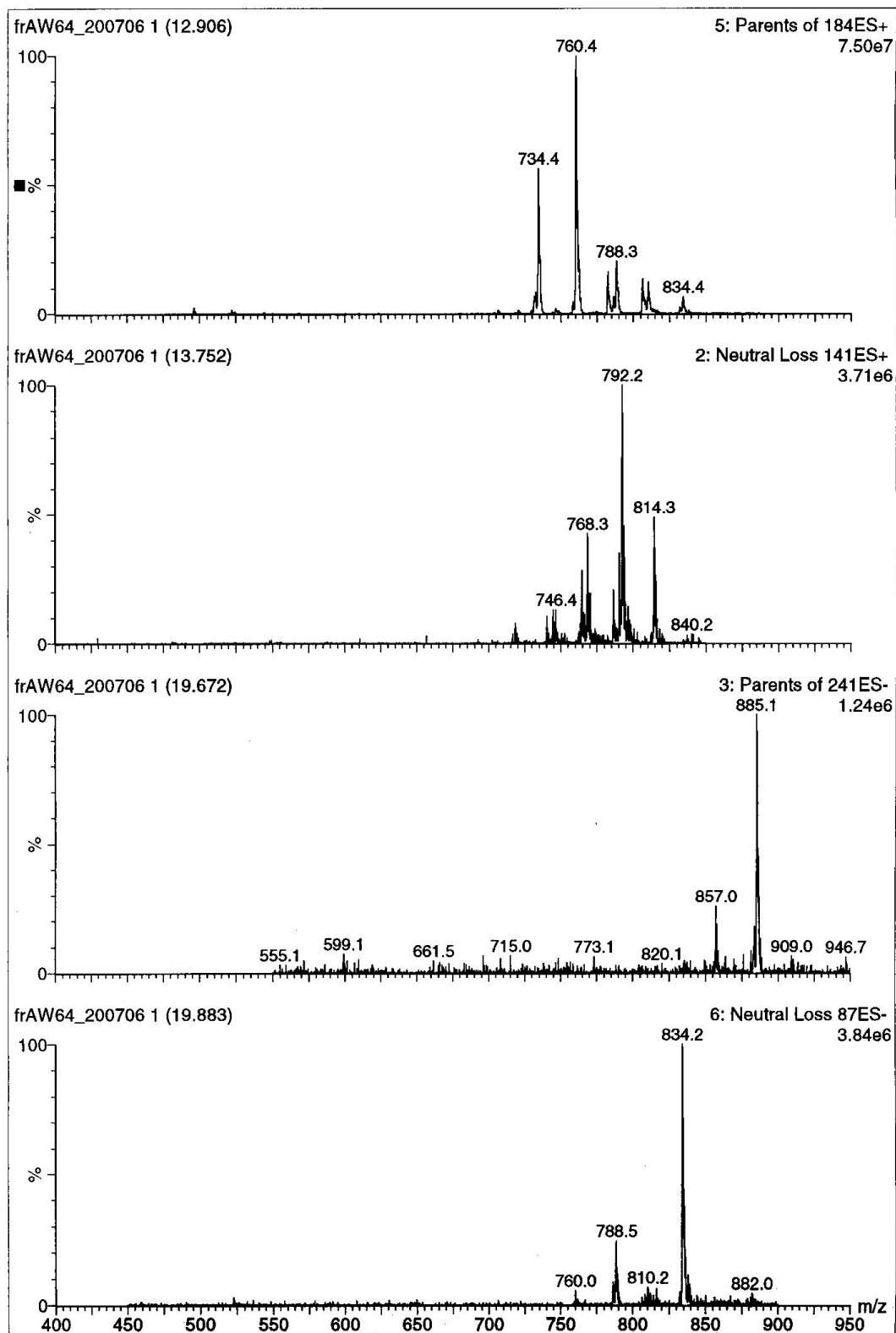
Representative neutral loss and precursor ion scanning mass spectra of cerebral cortex in VEH168 group mouse



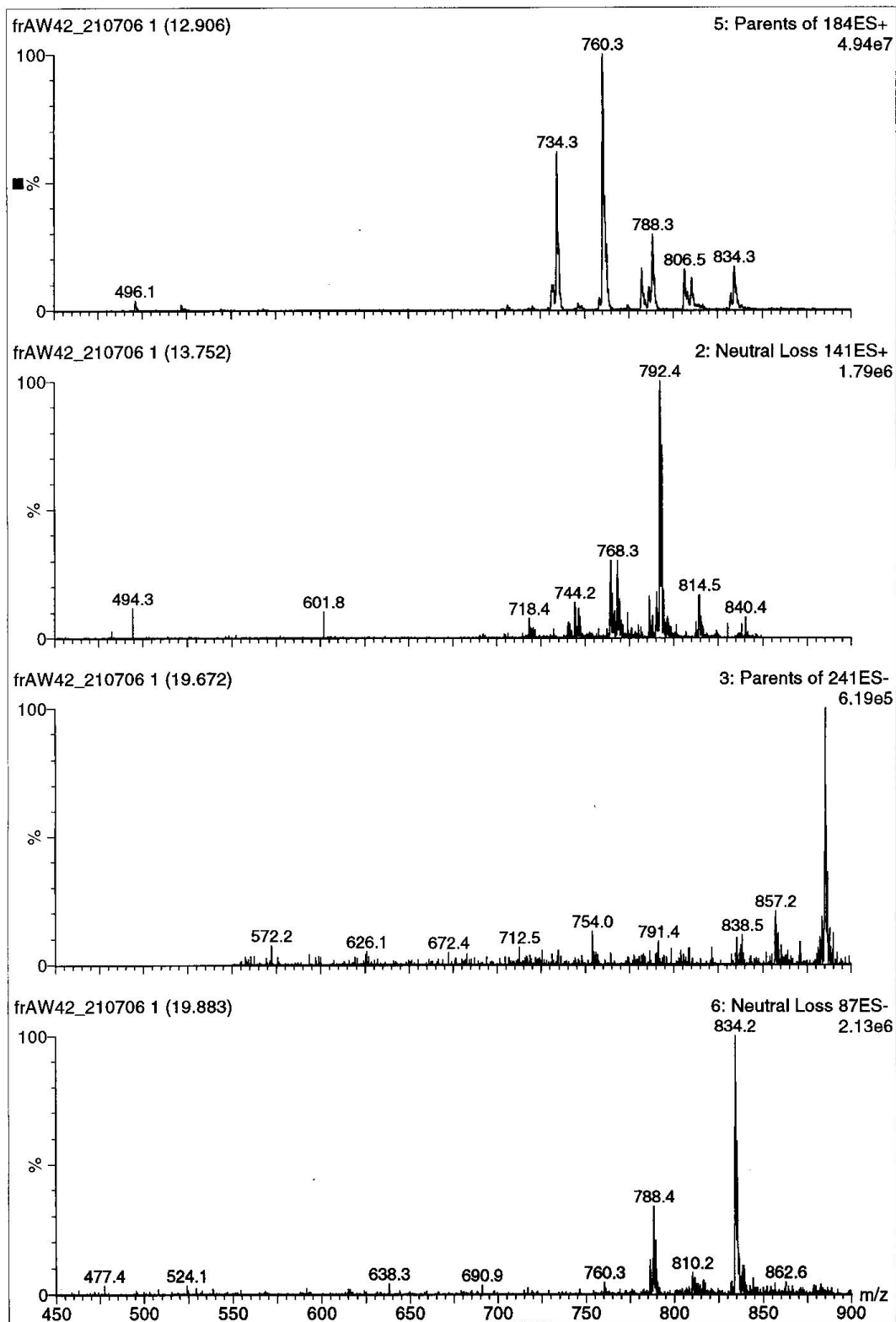
Representative neutral loss and precursor ion scanning mass spectra of cerebral cortex in ALA3 group mouse



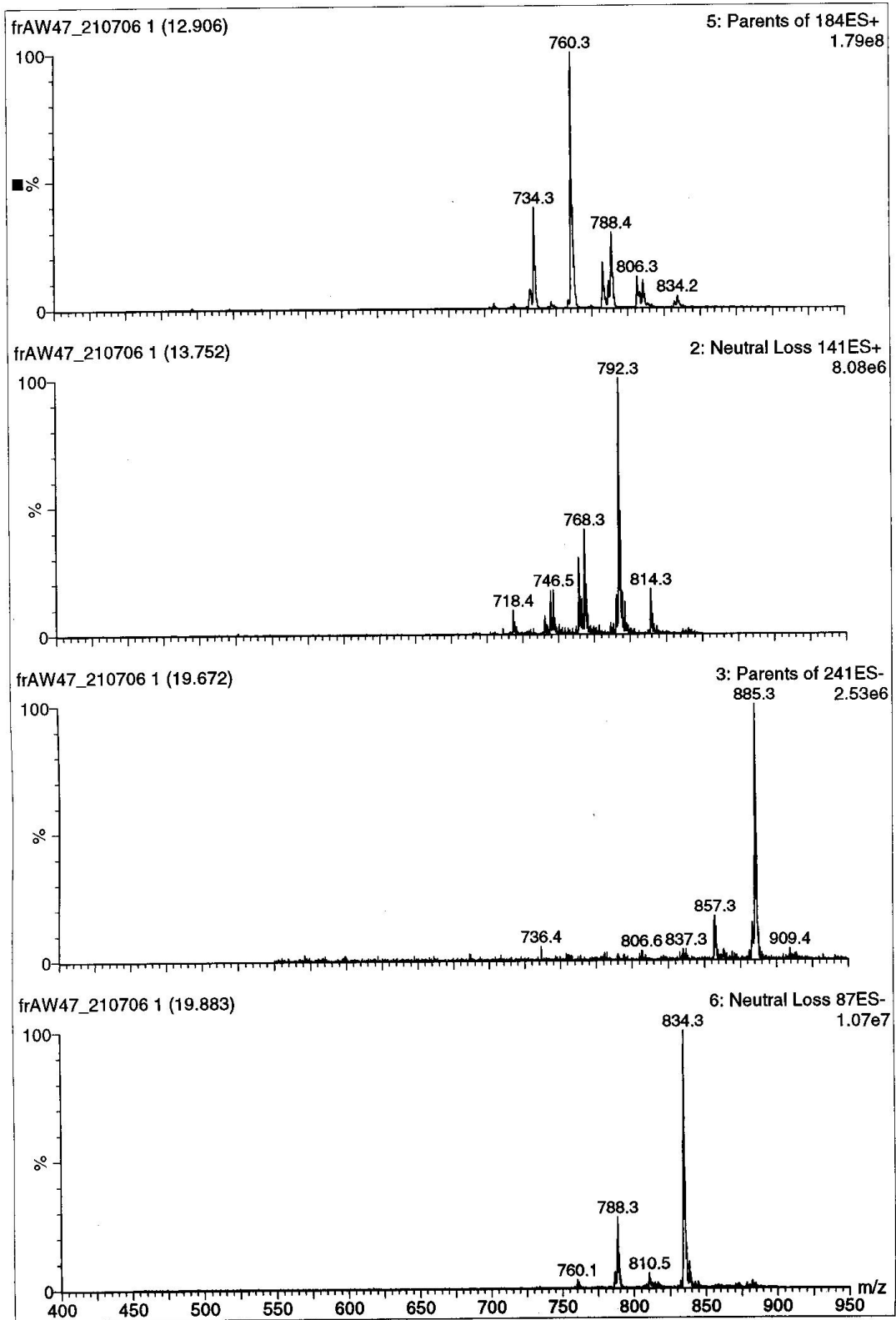
Representative neutral loss and precursor ion scanning mass spectra of cerebral cortex in ALA24 group mouse



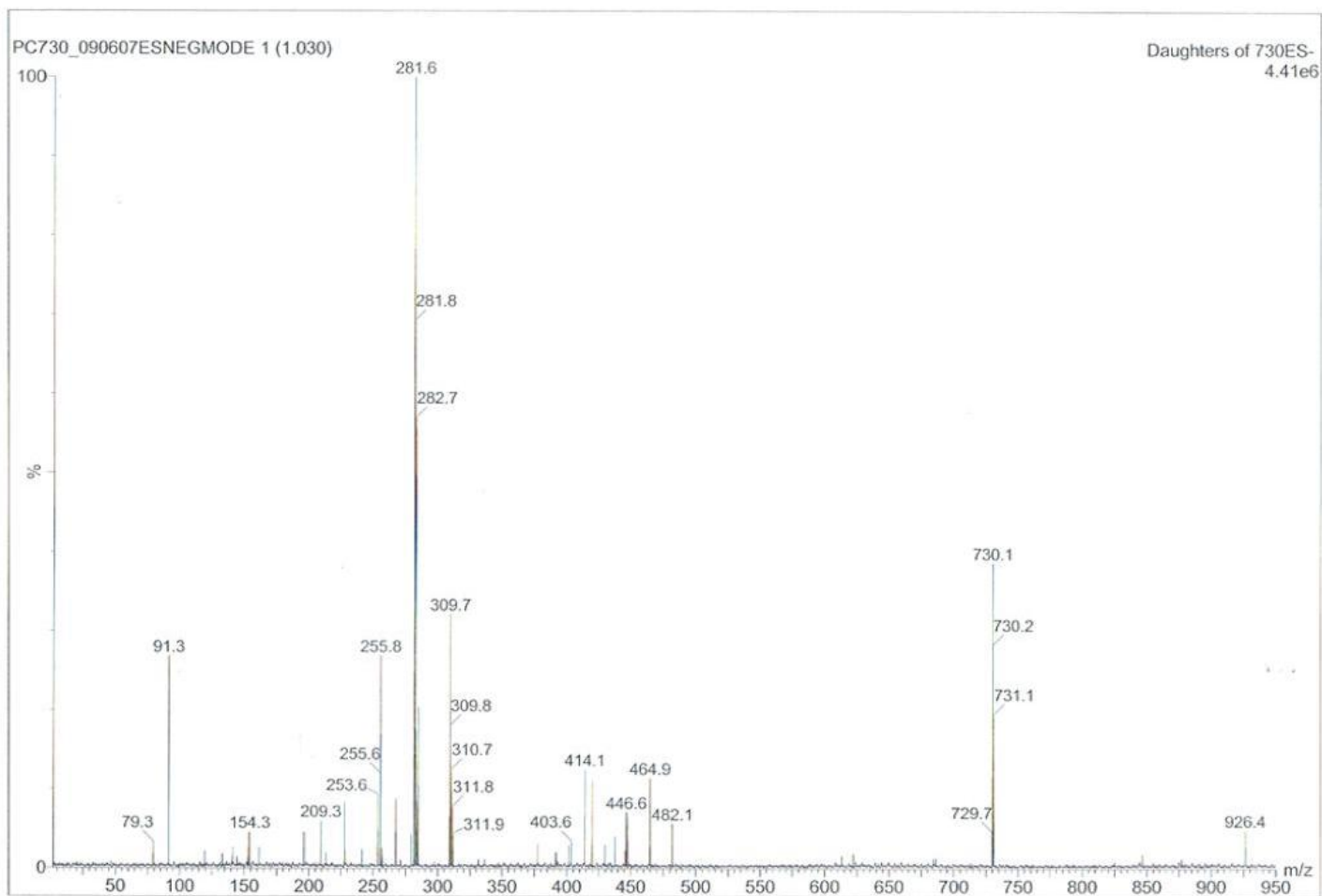
Representative neutral loss and precursor ion scanning mass spectra of cerebral cortex in ALA72 group mouse



Representative neutral loss and precursor ion scanning mass spectra of cerebral cortex in ALA168 group mouse

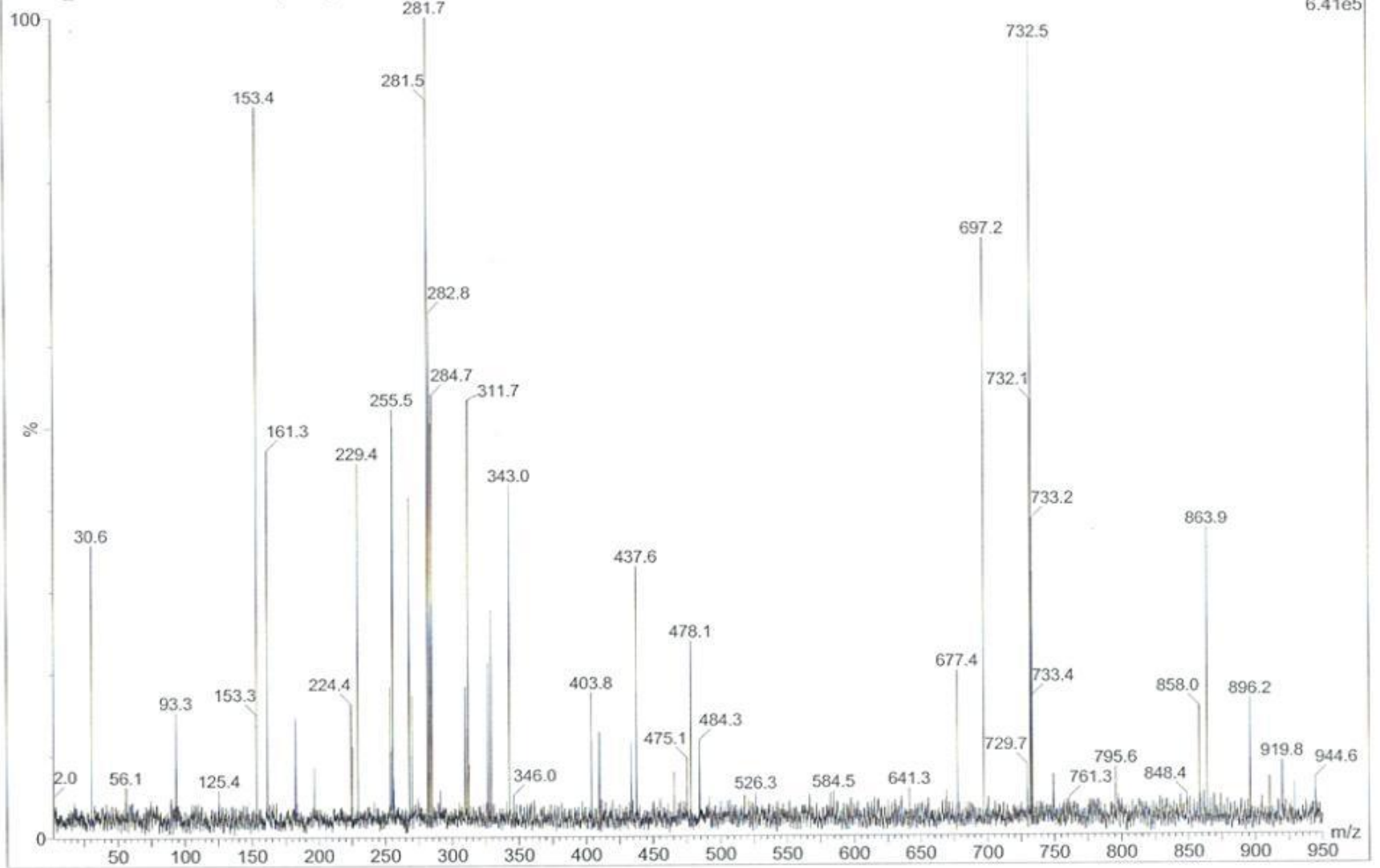


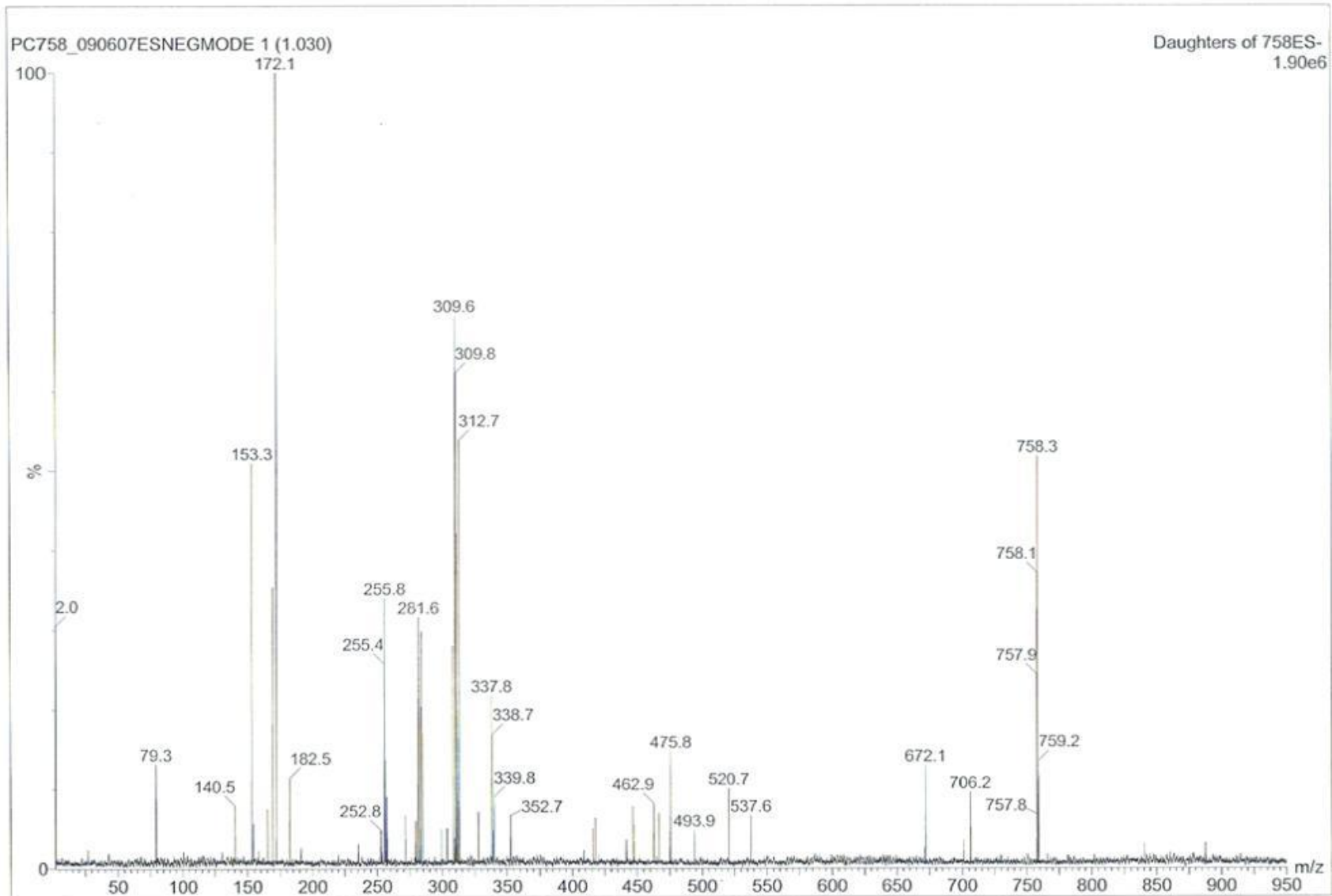
Appendix 1.2 – MS/MS scans of phospholipid species in mouse cerebral cortex

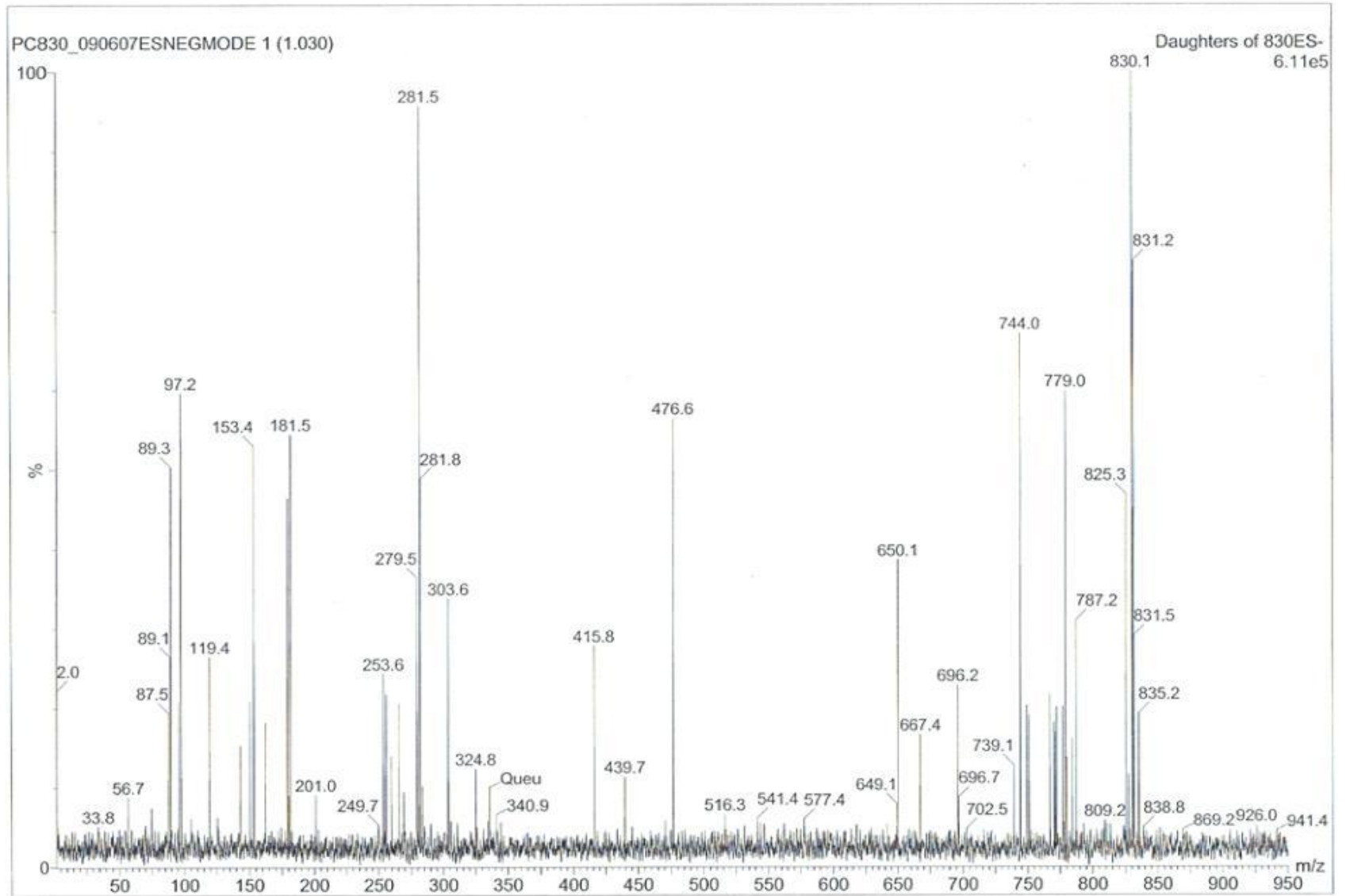


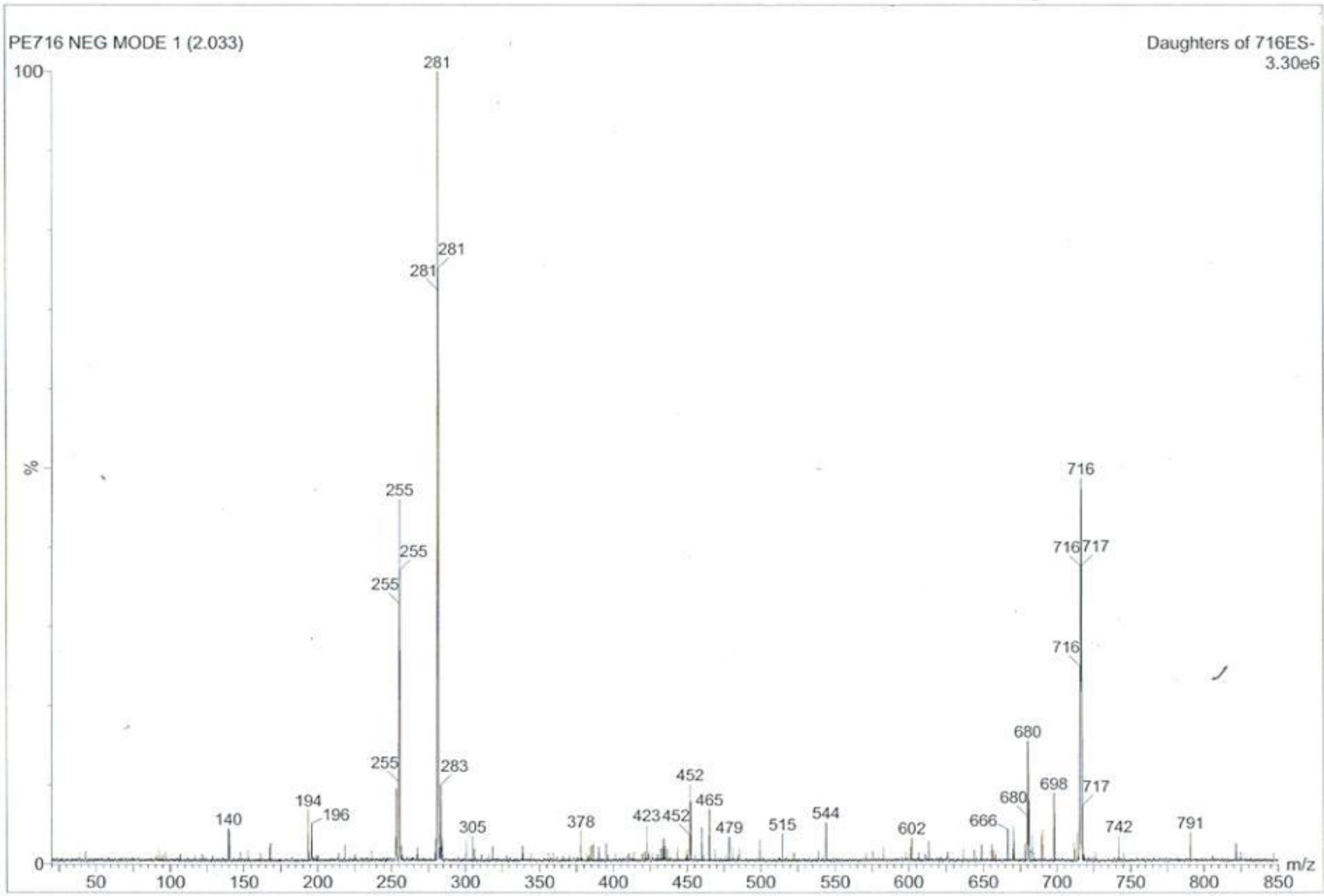
PC732_090607ESNEGMODE 1 (1.030)

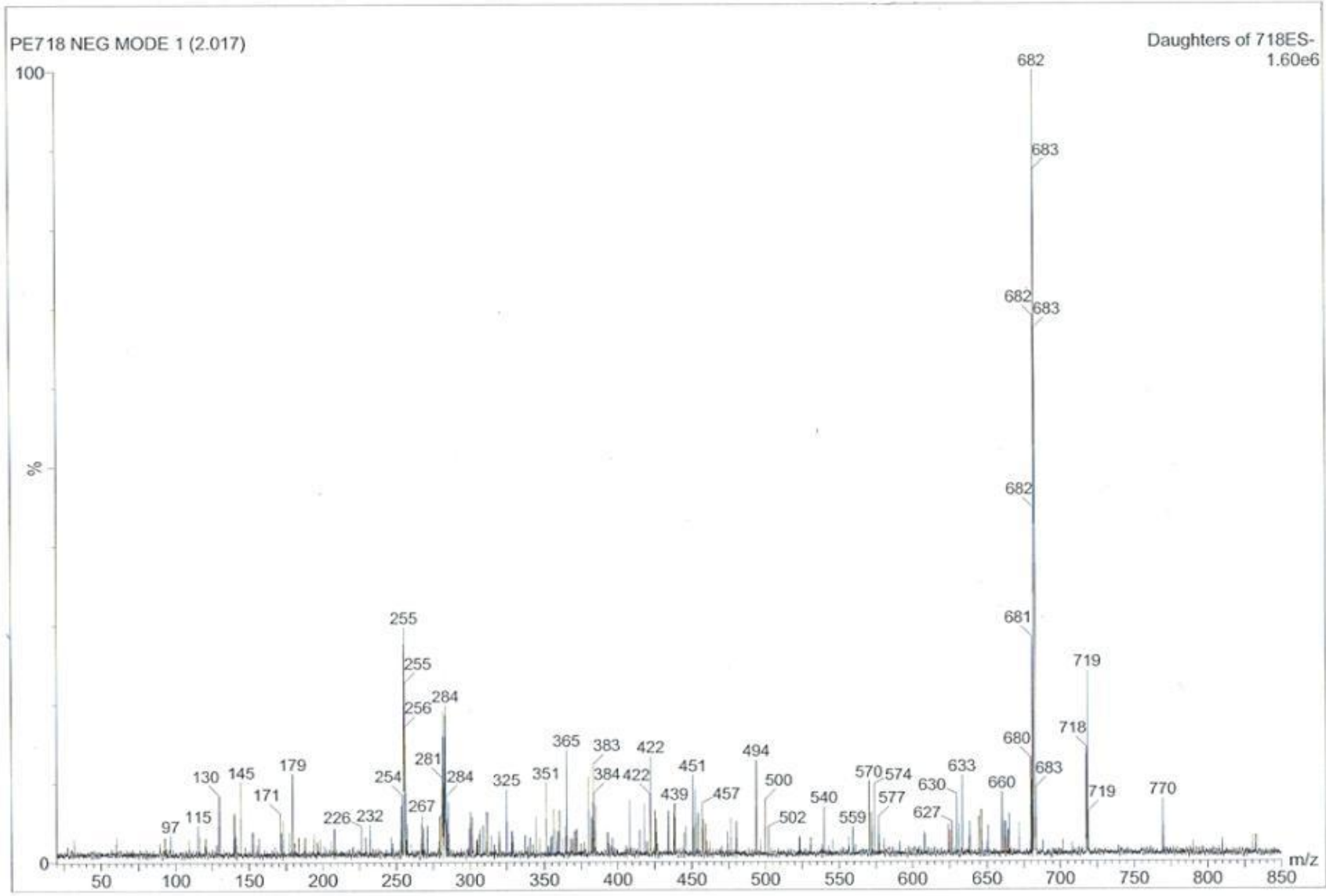
Daughters of 732ES-
6.41e5

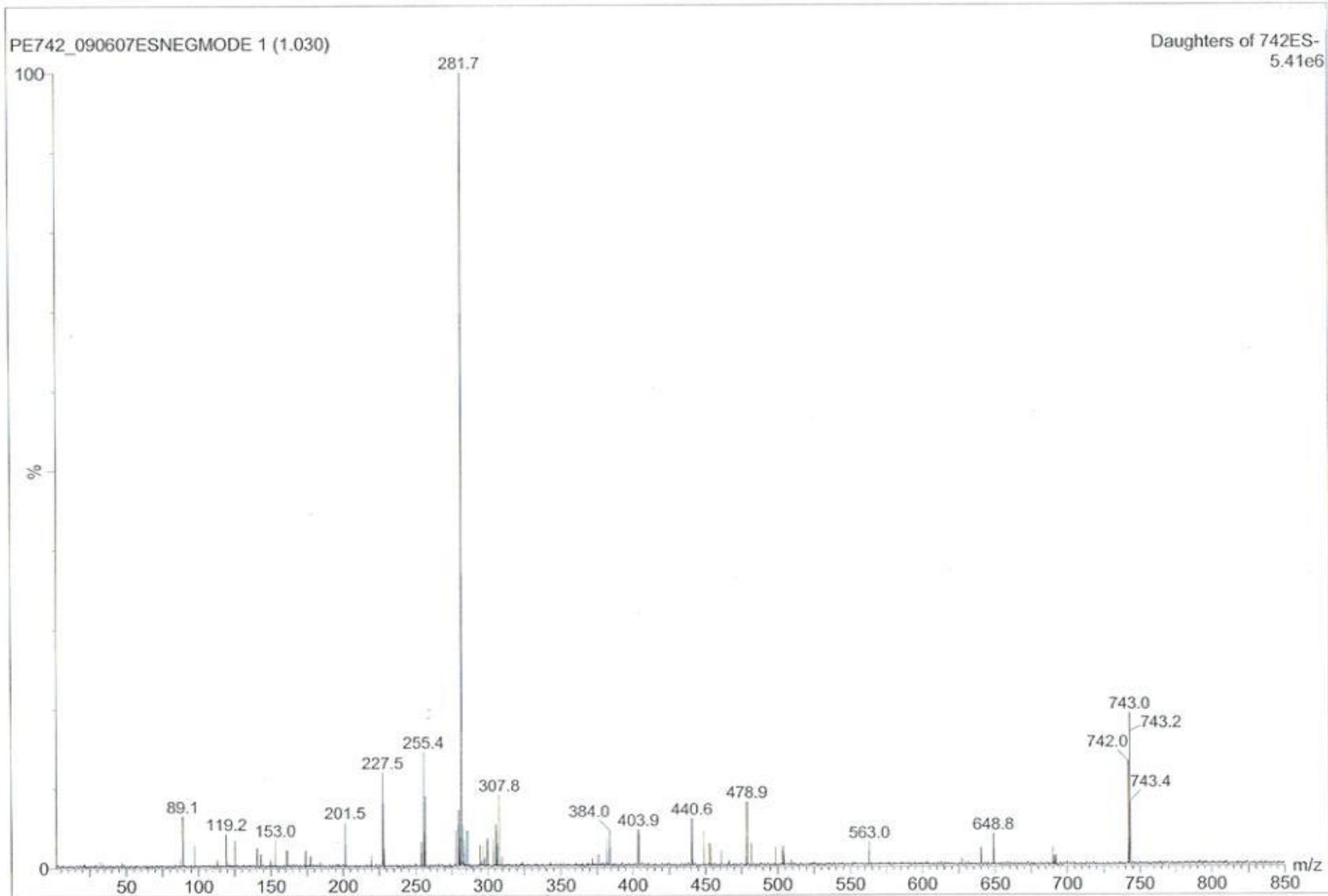


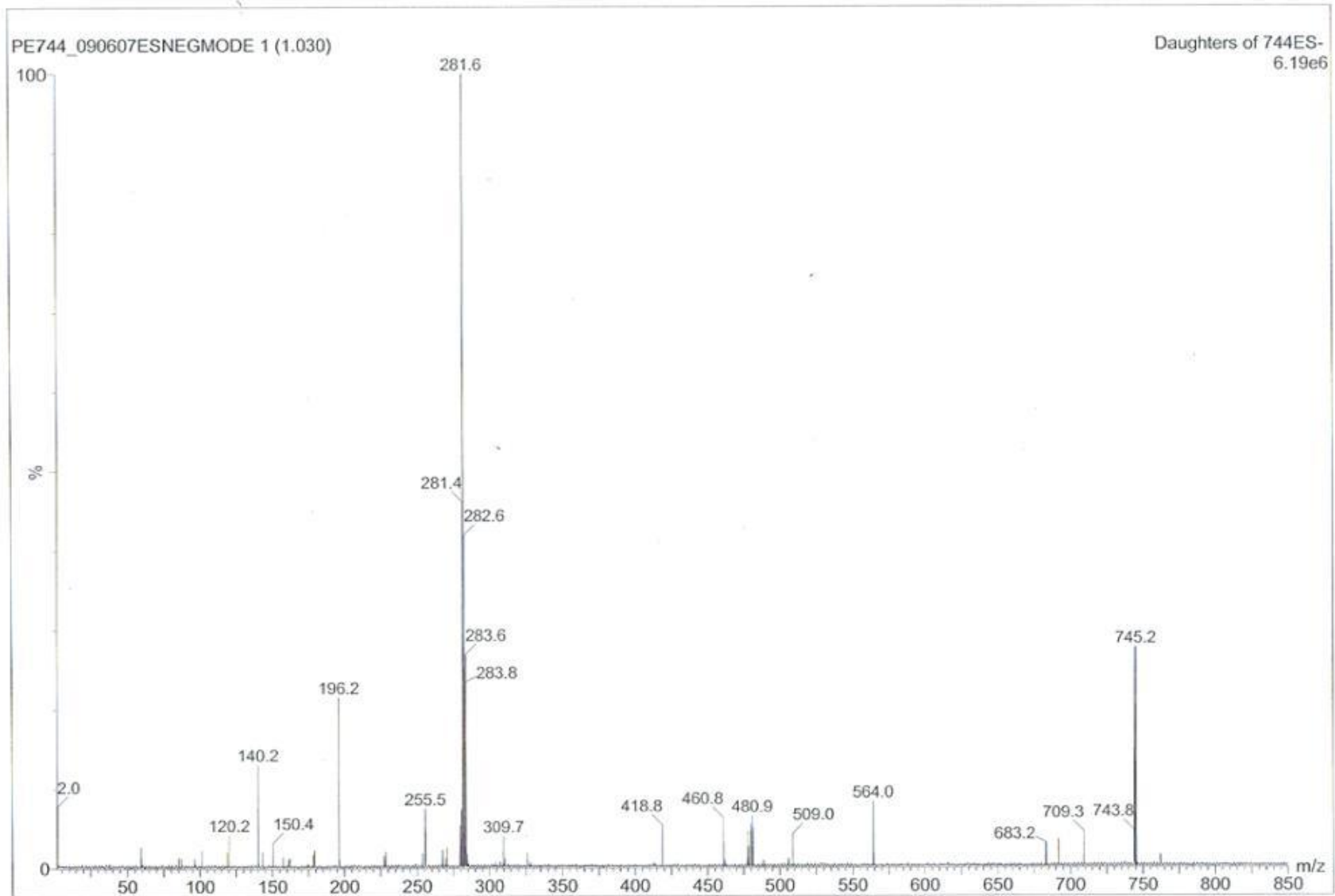


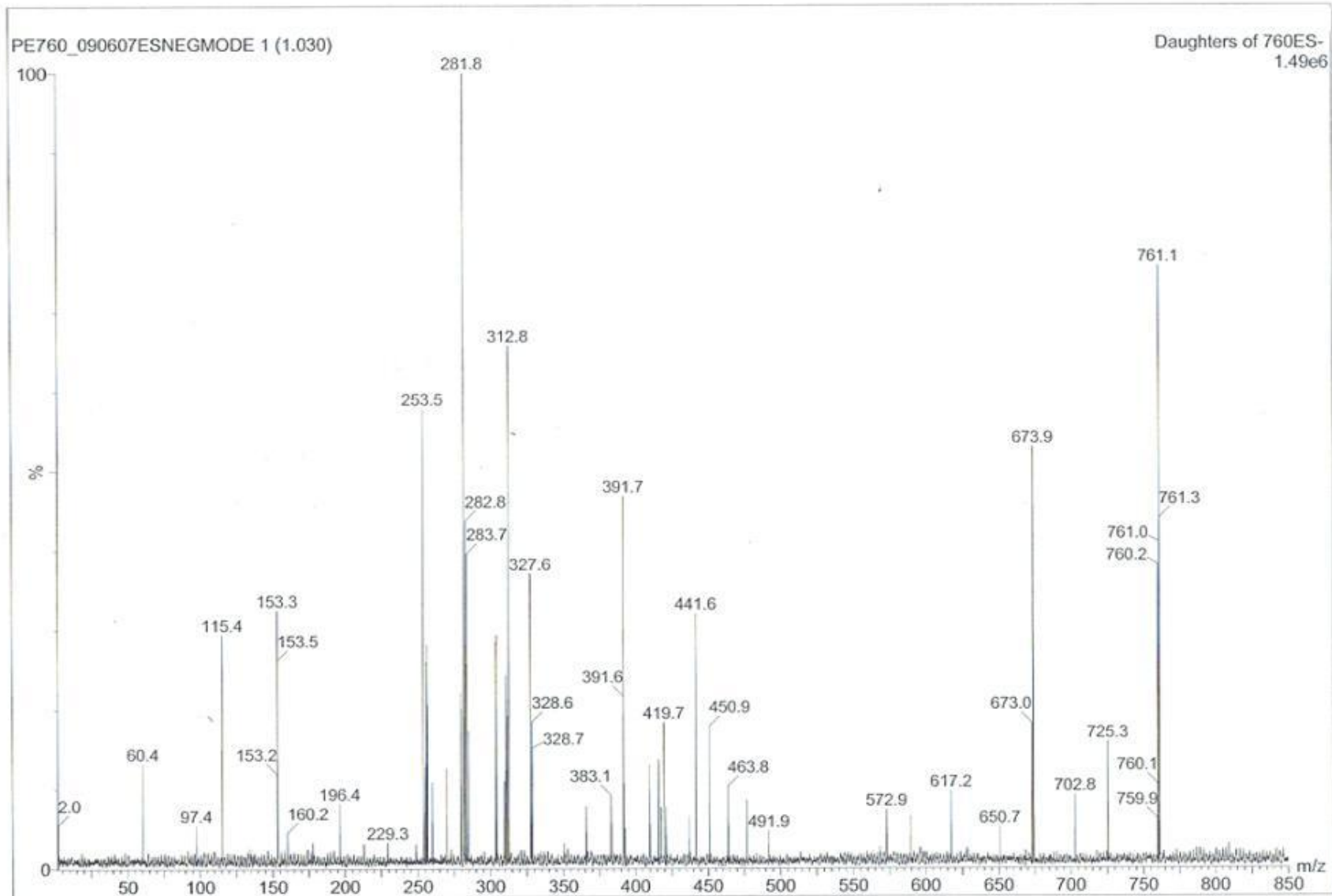


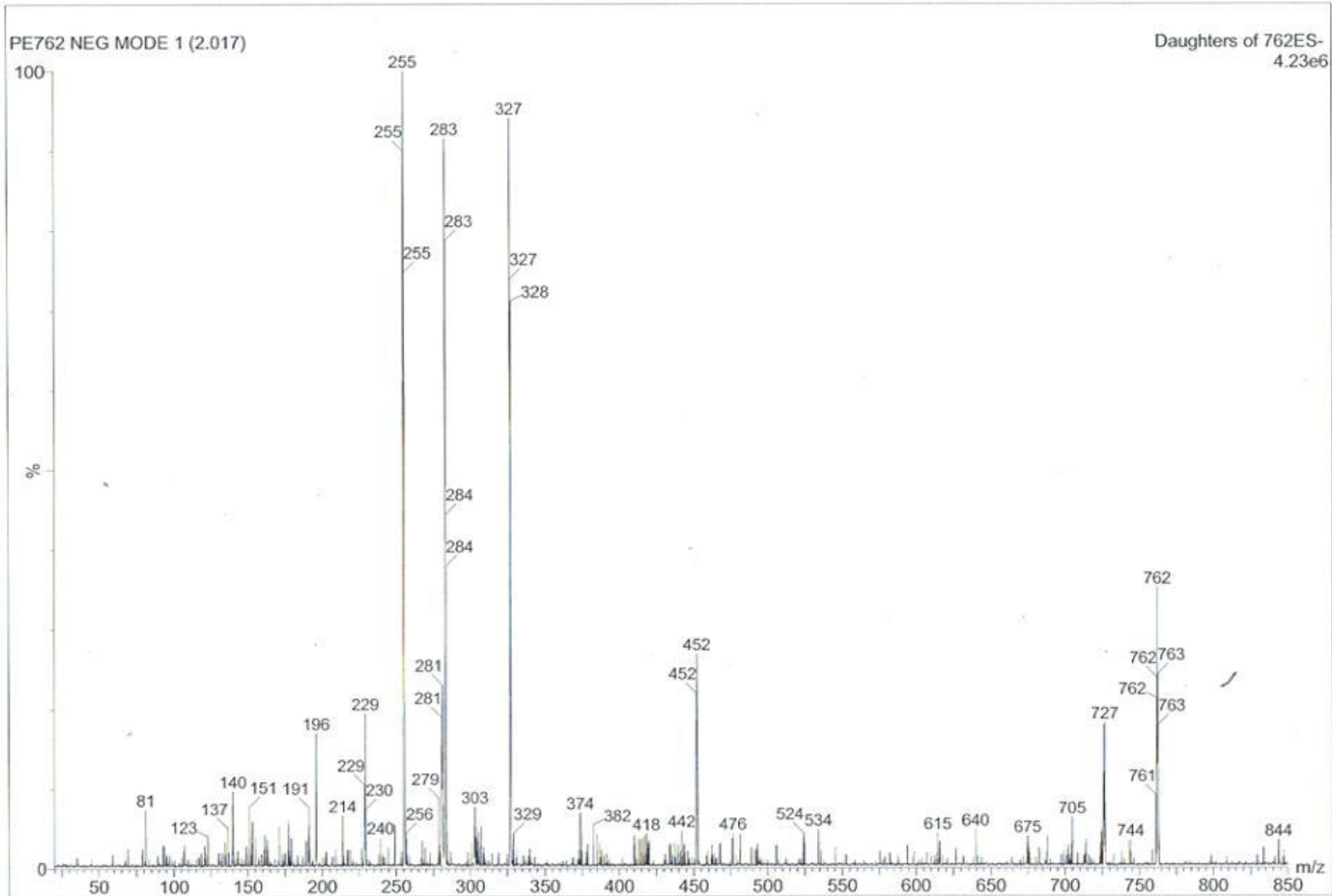


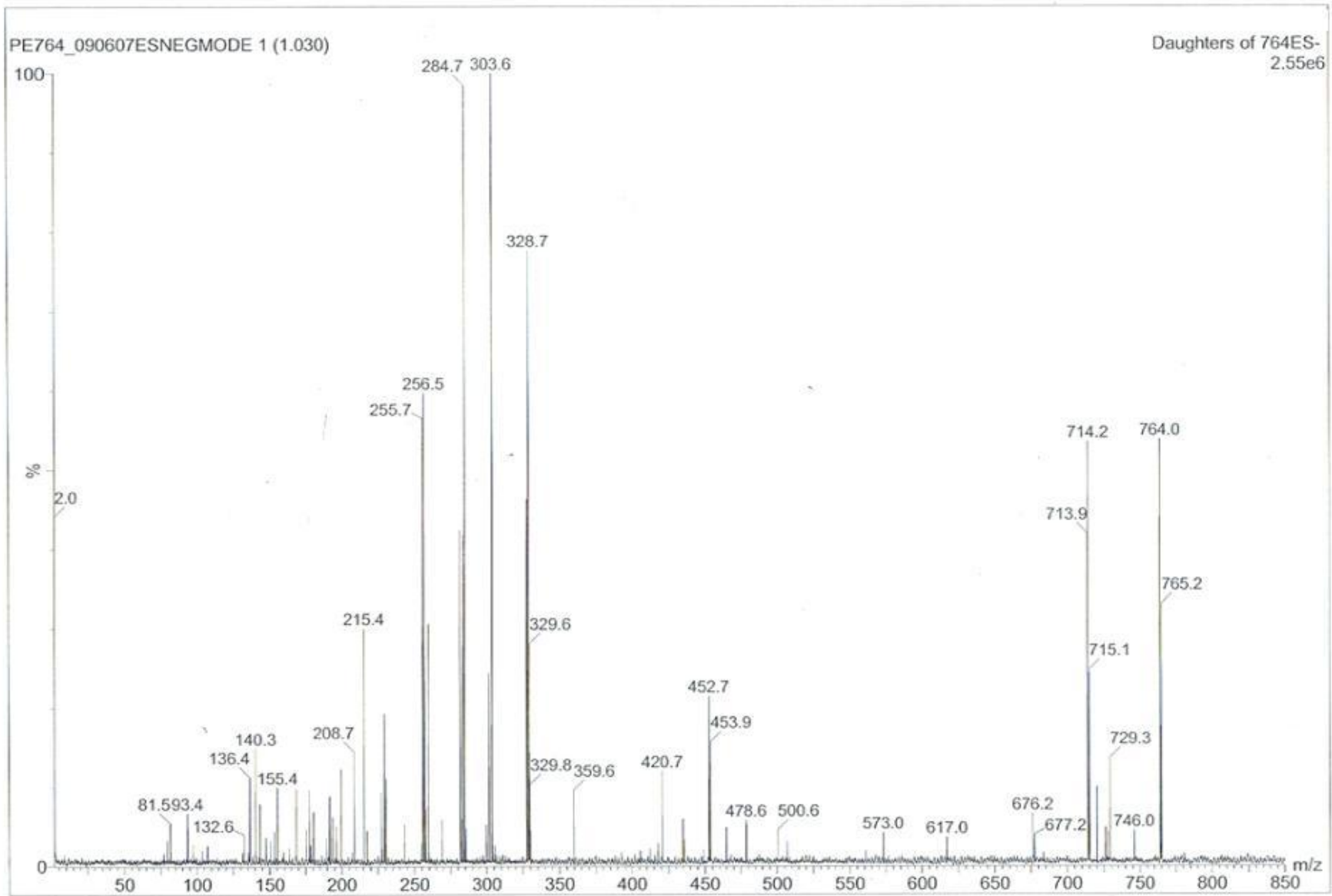






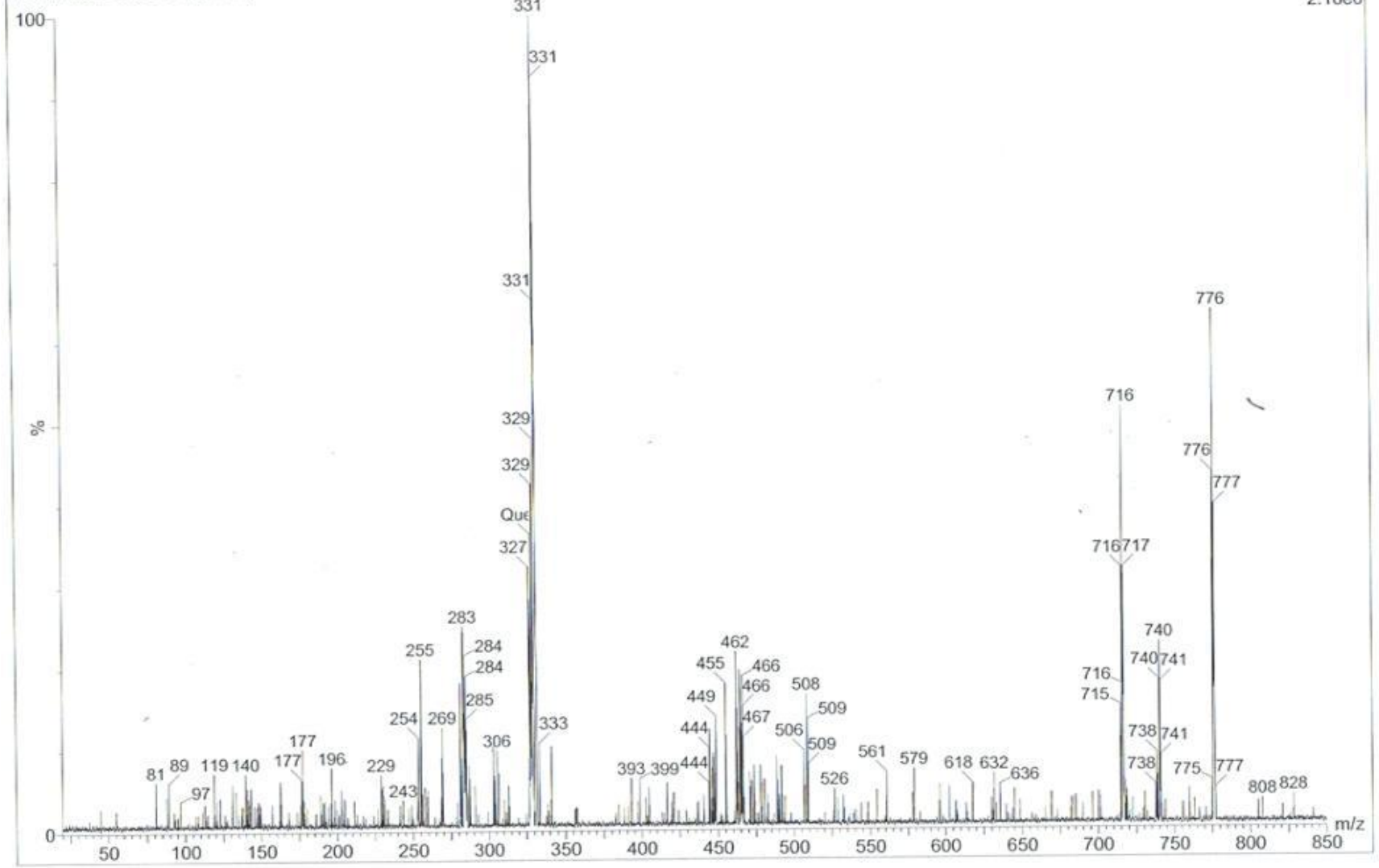


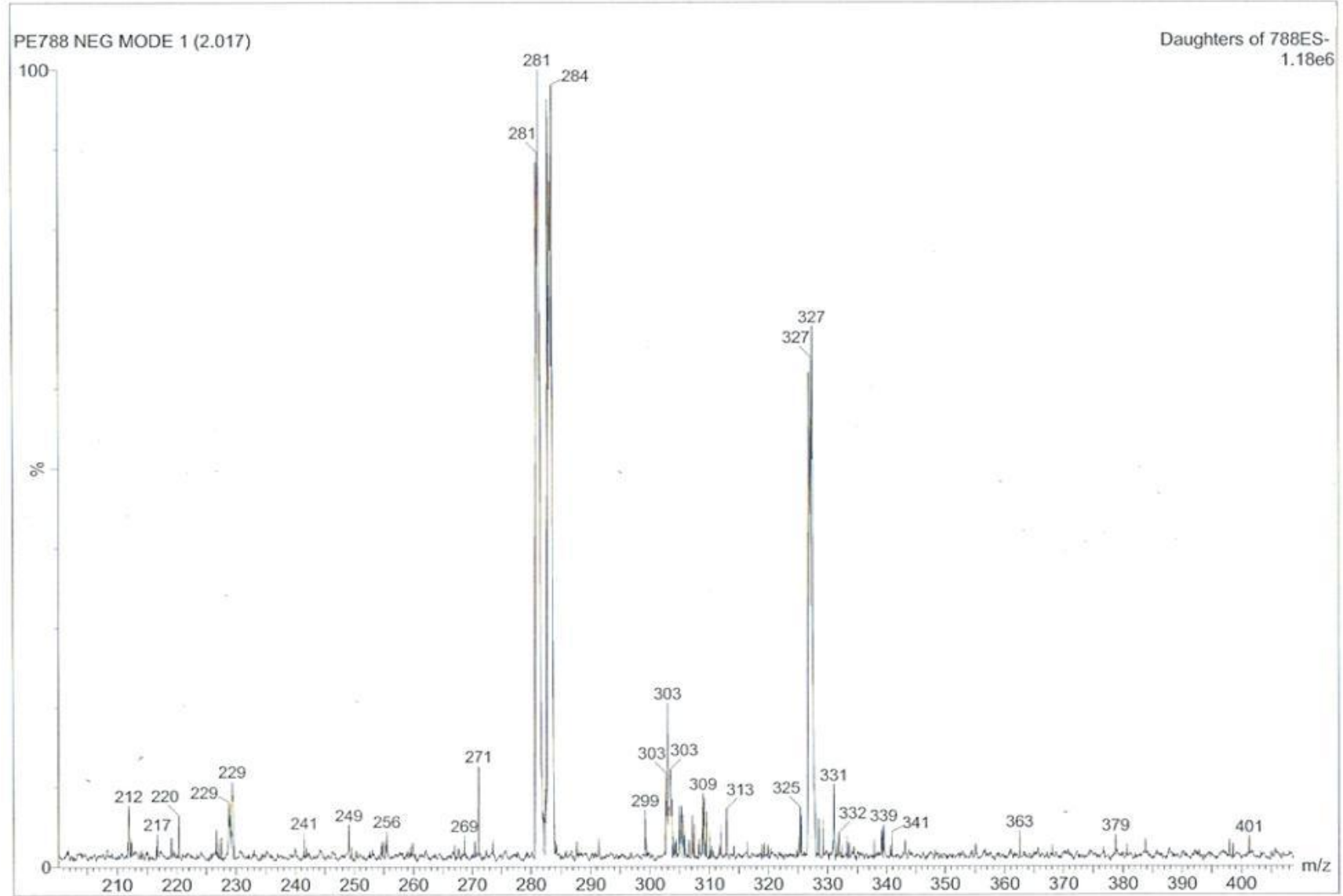




PE776 NEG MODE 1 (2.017)

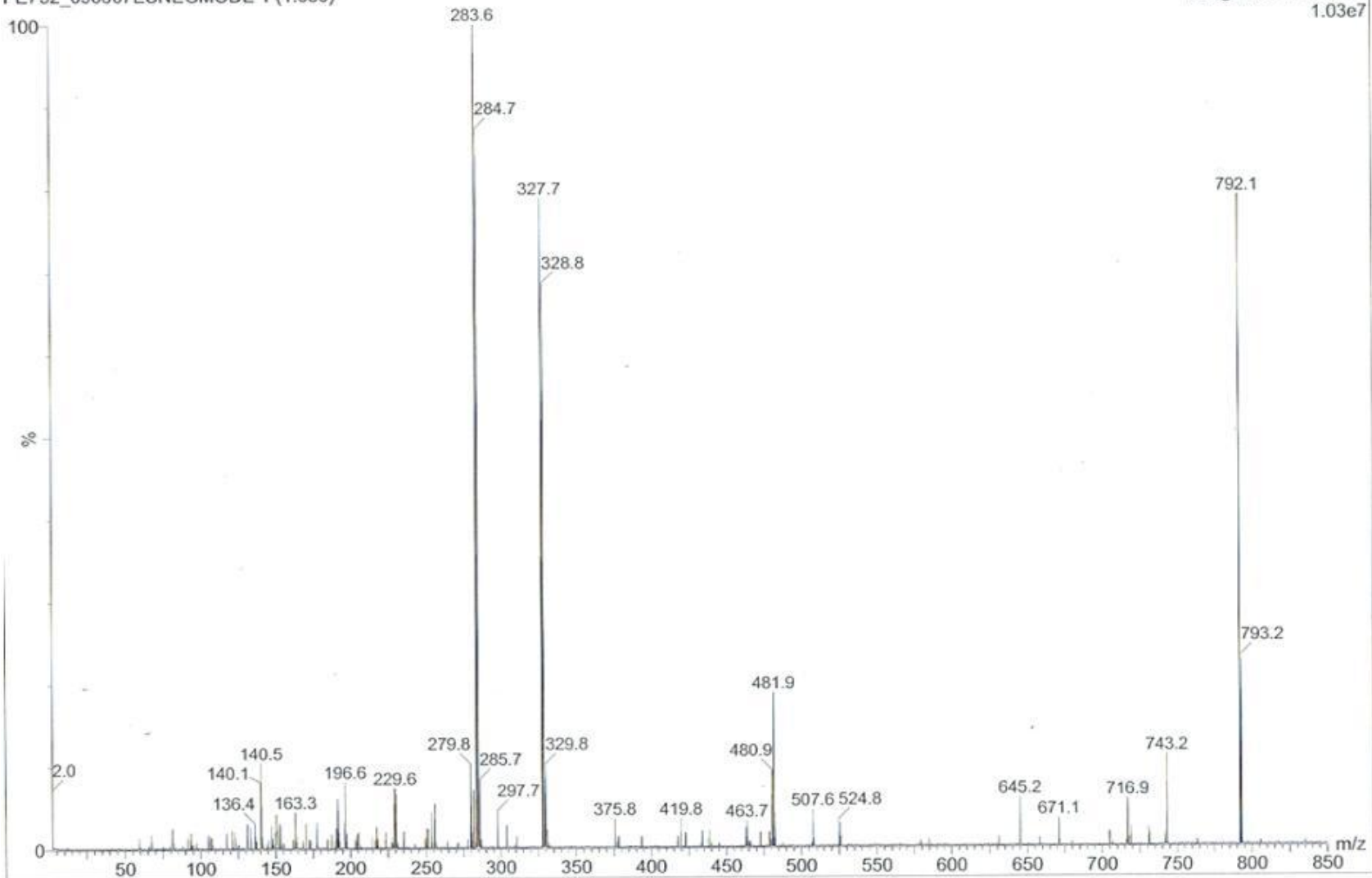
Daughters of 776ES-
2.18e6

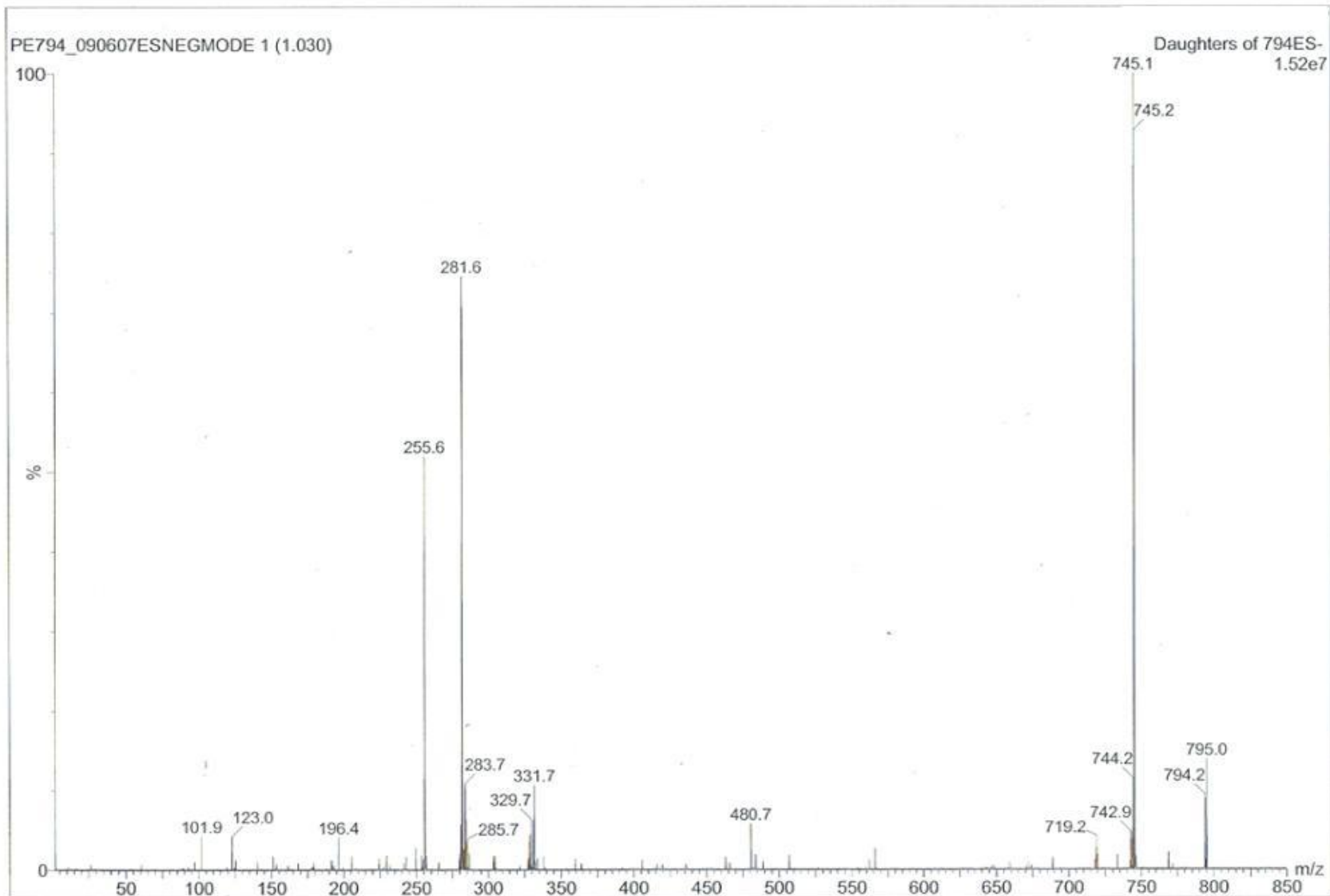


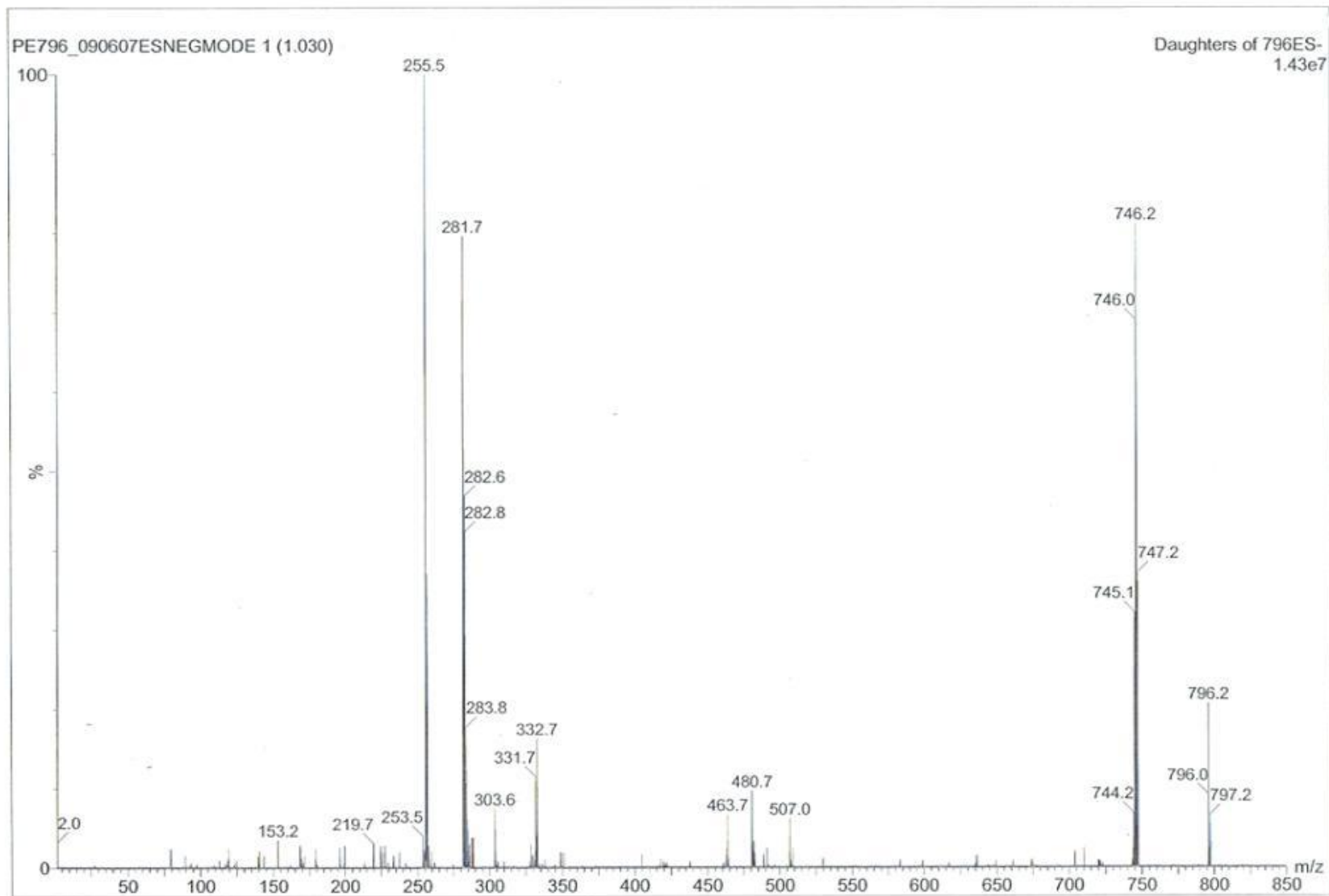


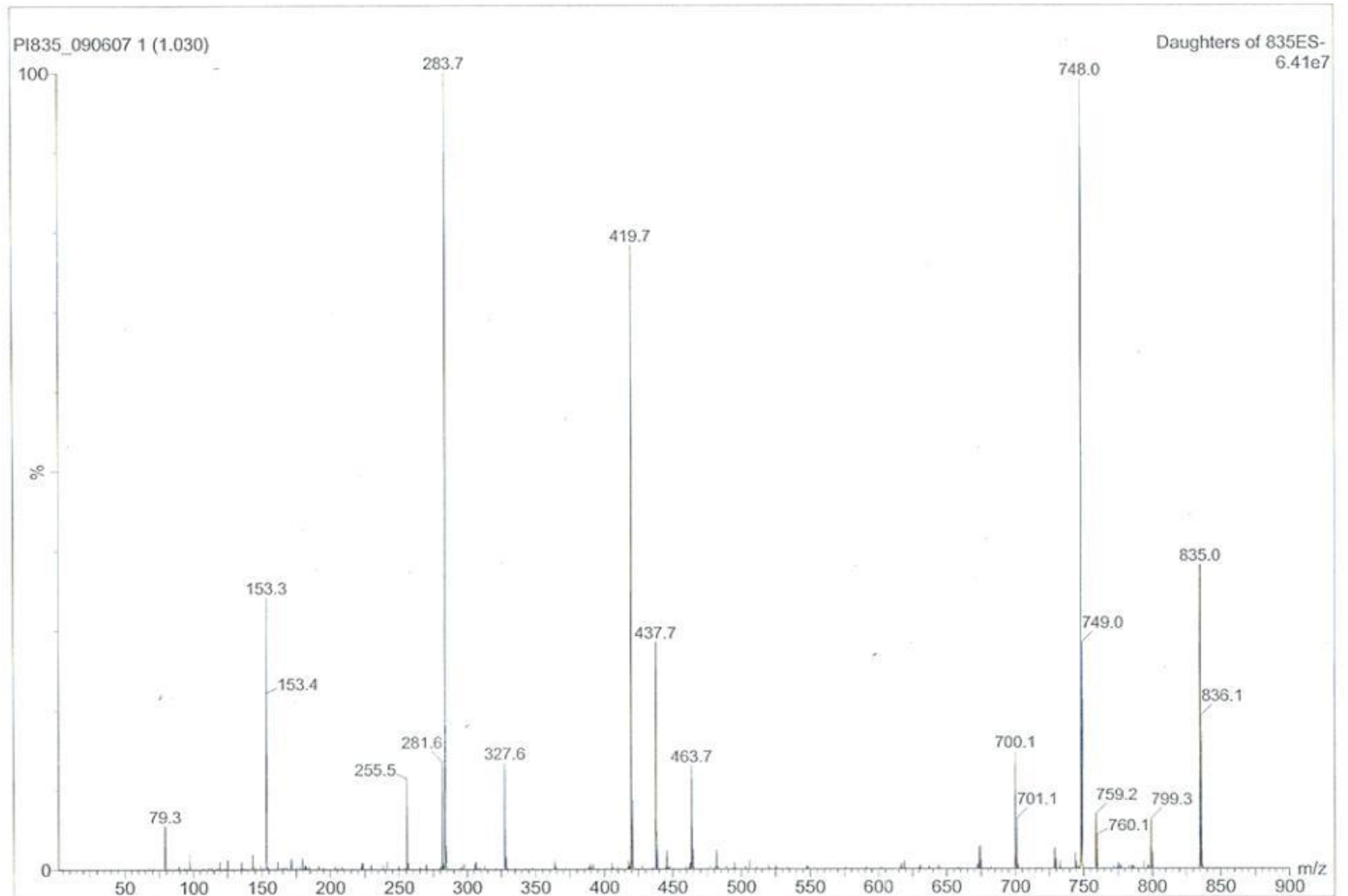
PE792_090607ESNEGMODE 1 (1.030)

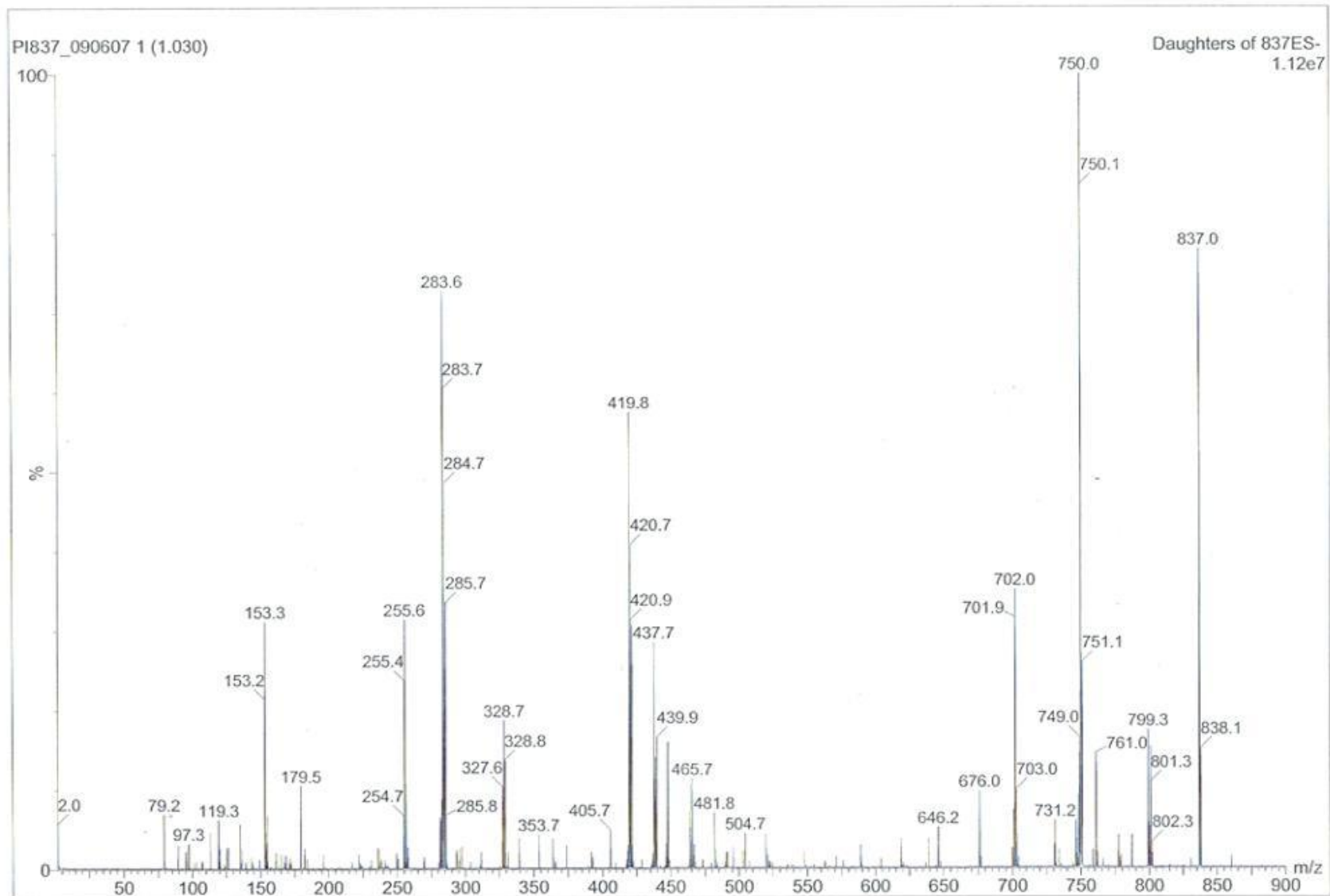
Daughters of 792ES-
1.03e7

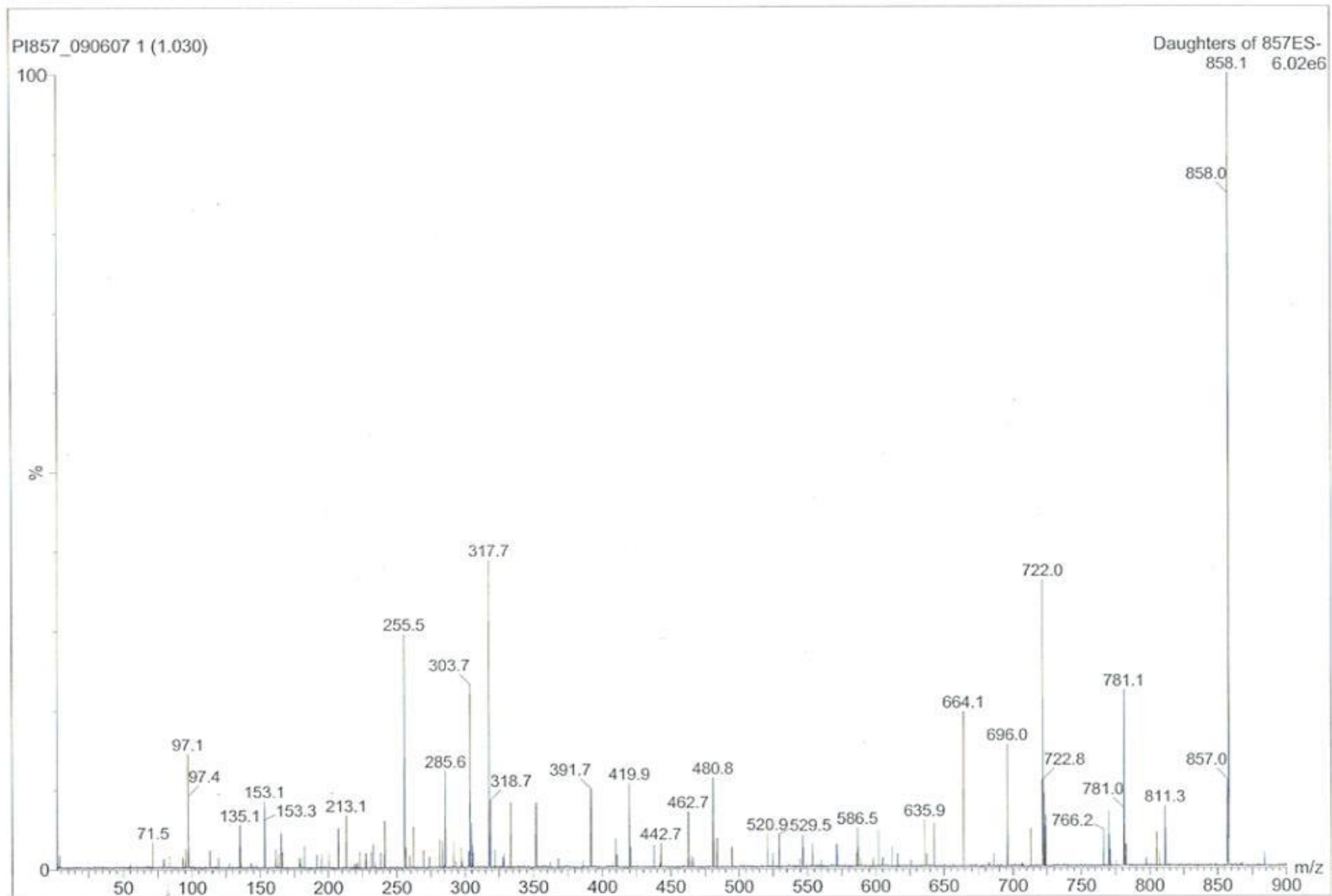


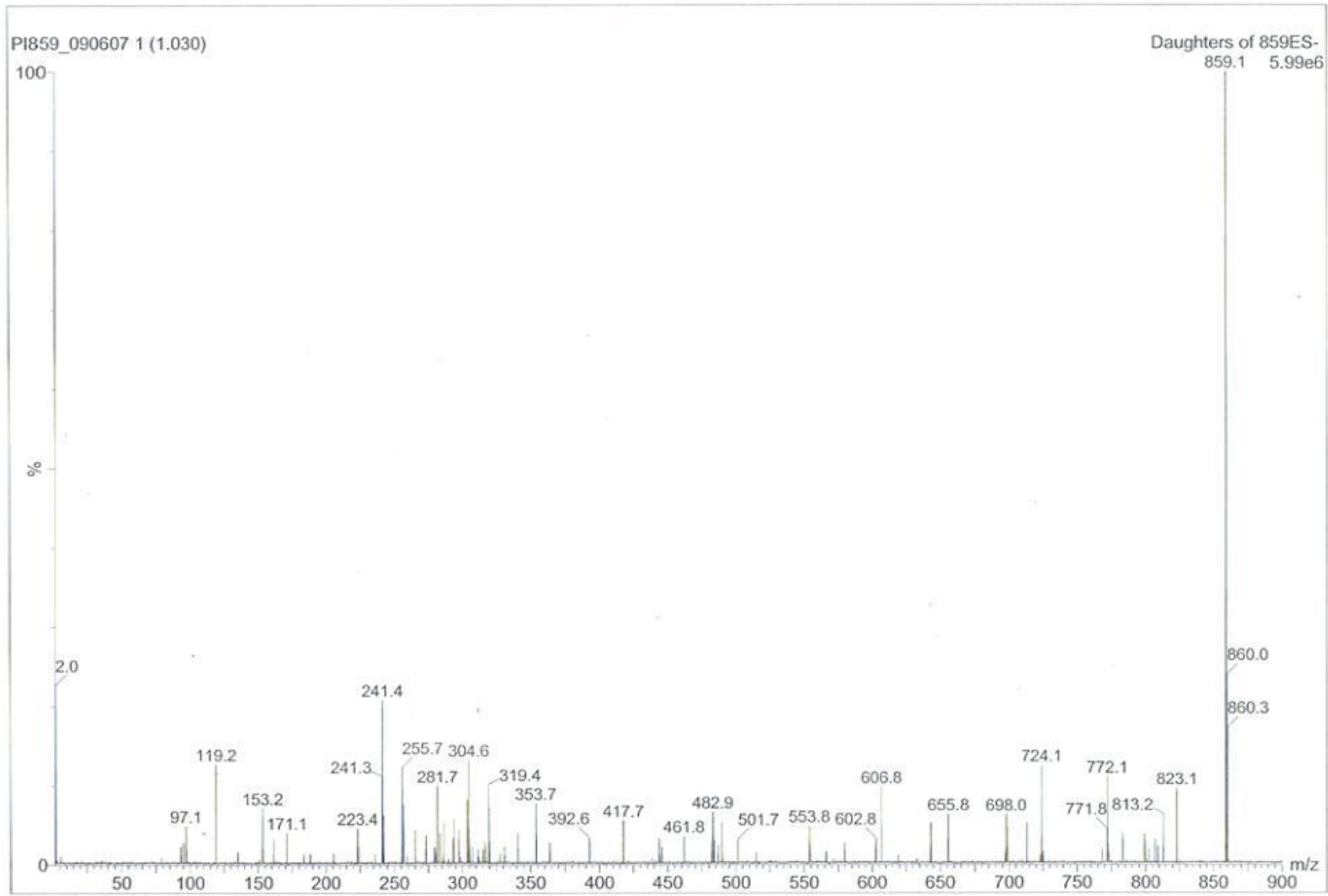


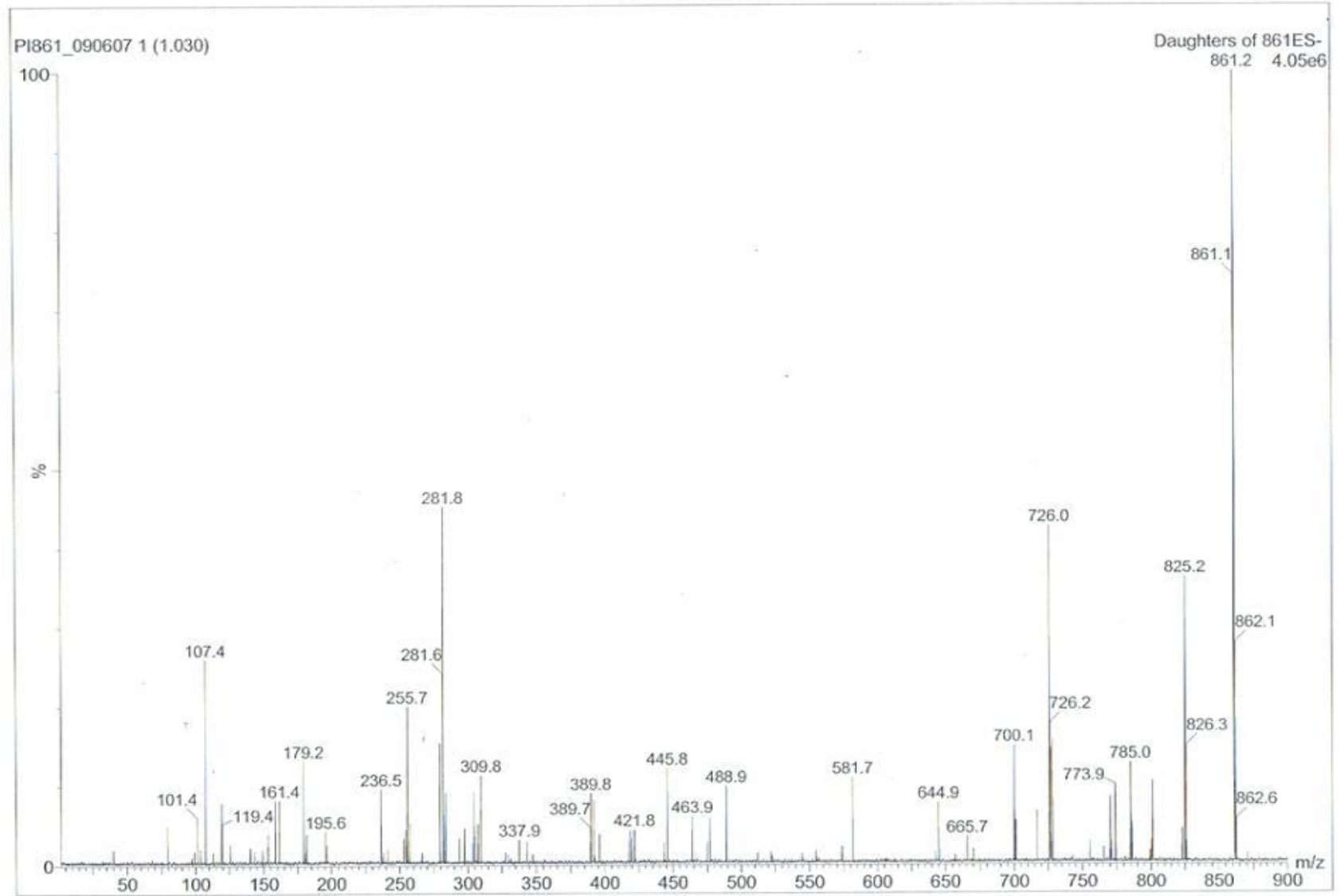


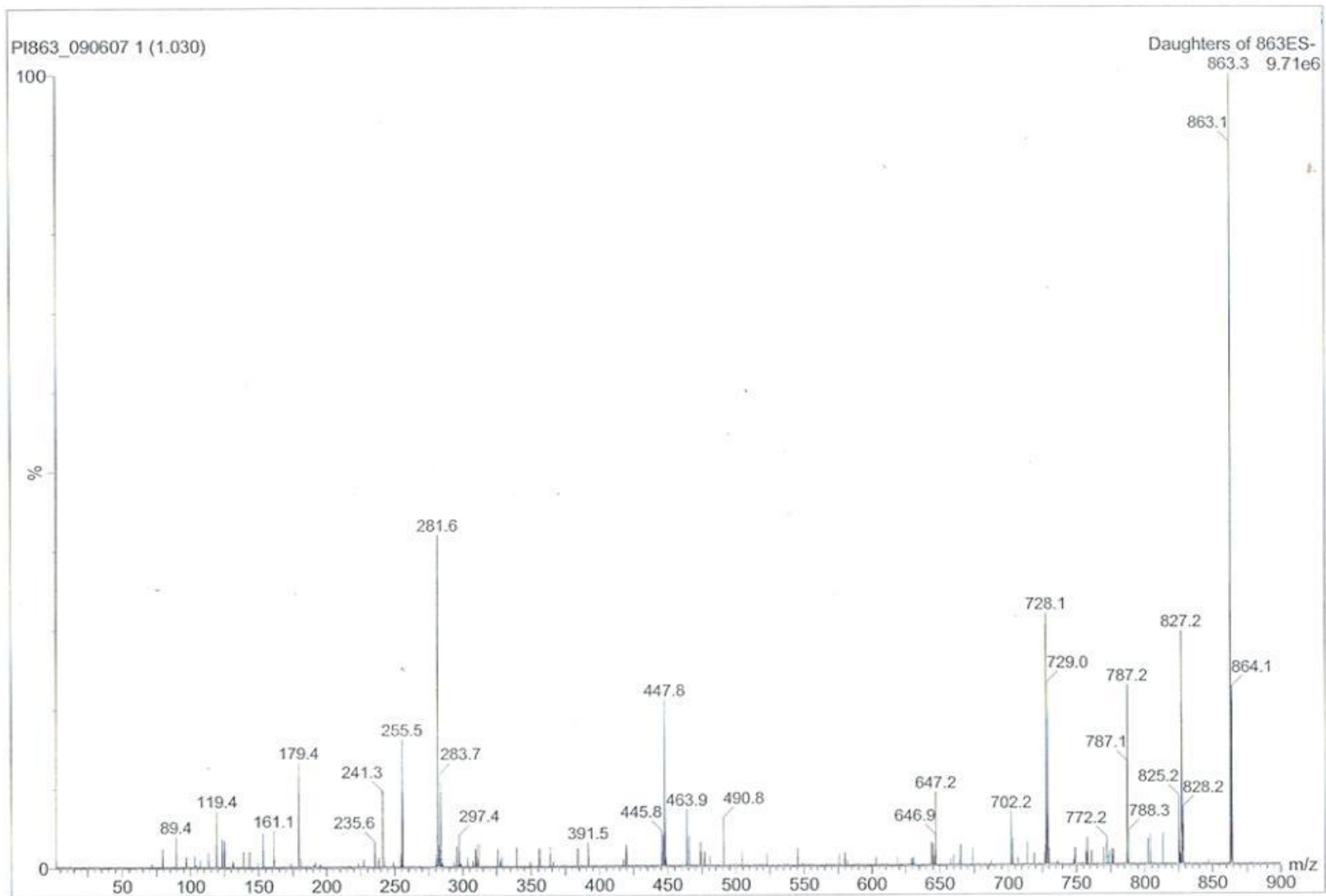


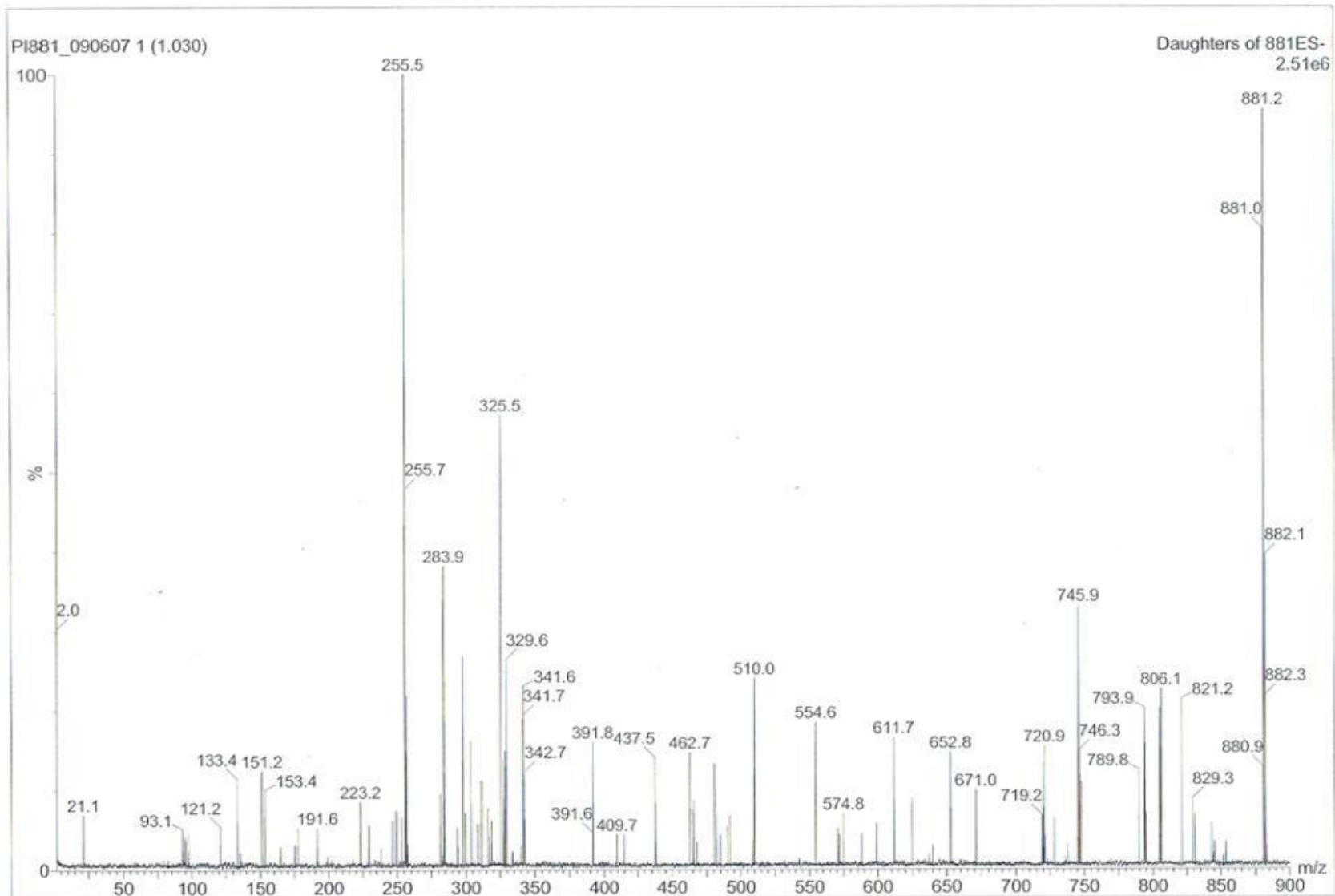


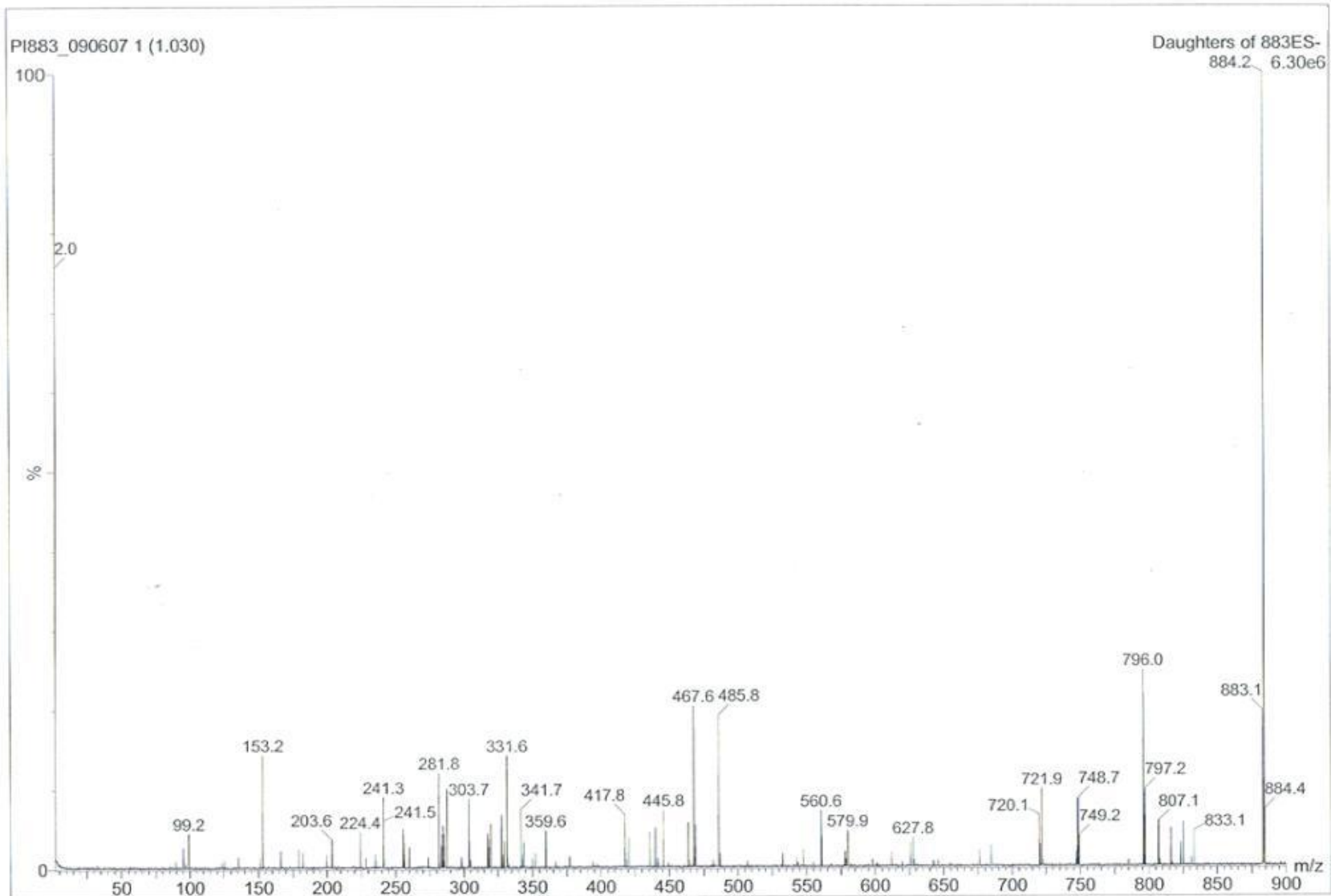






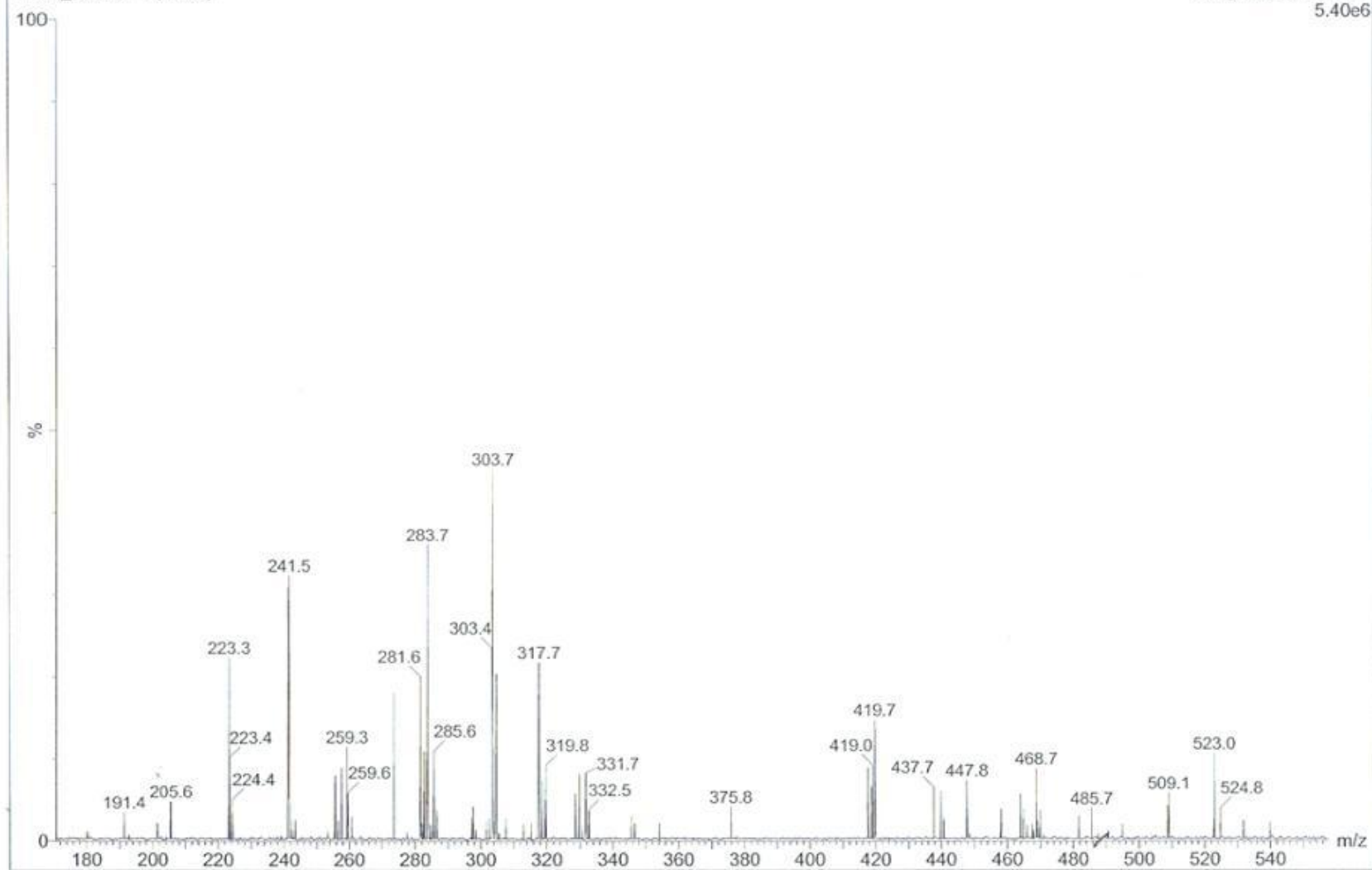


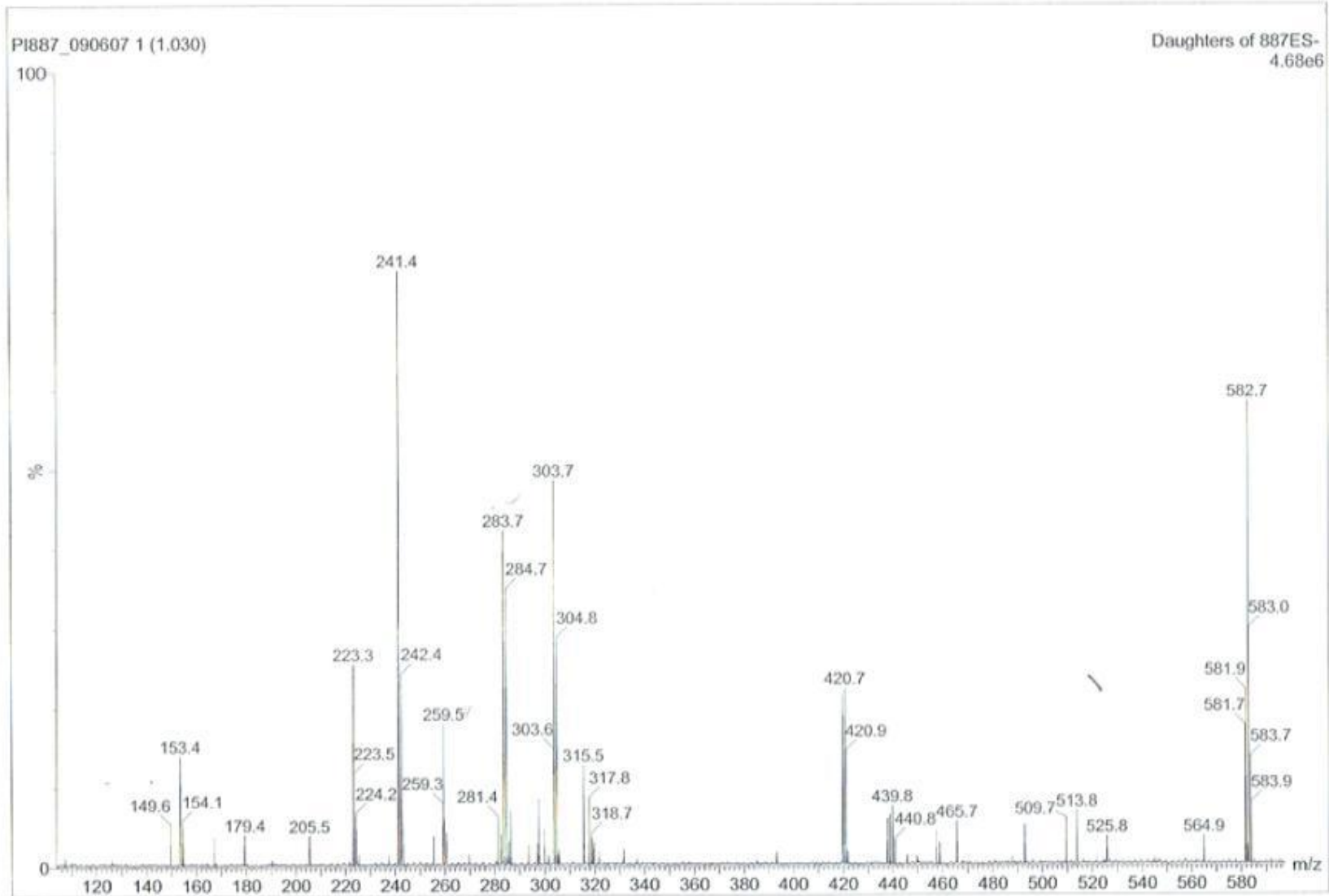


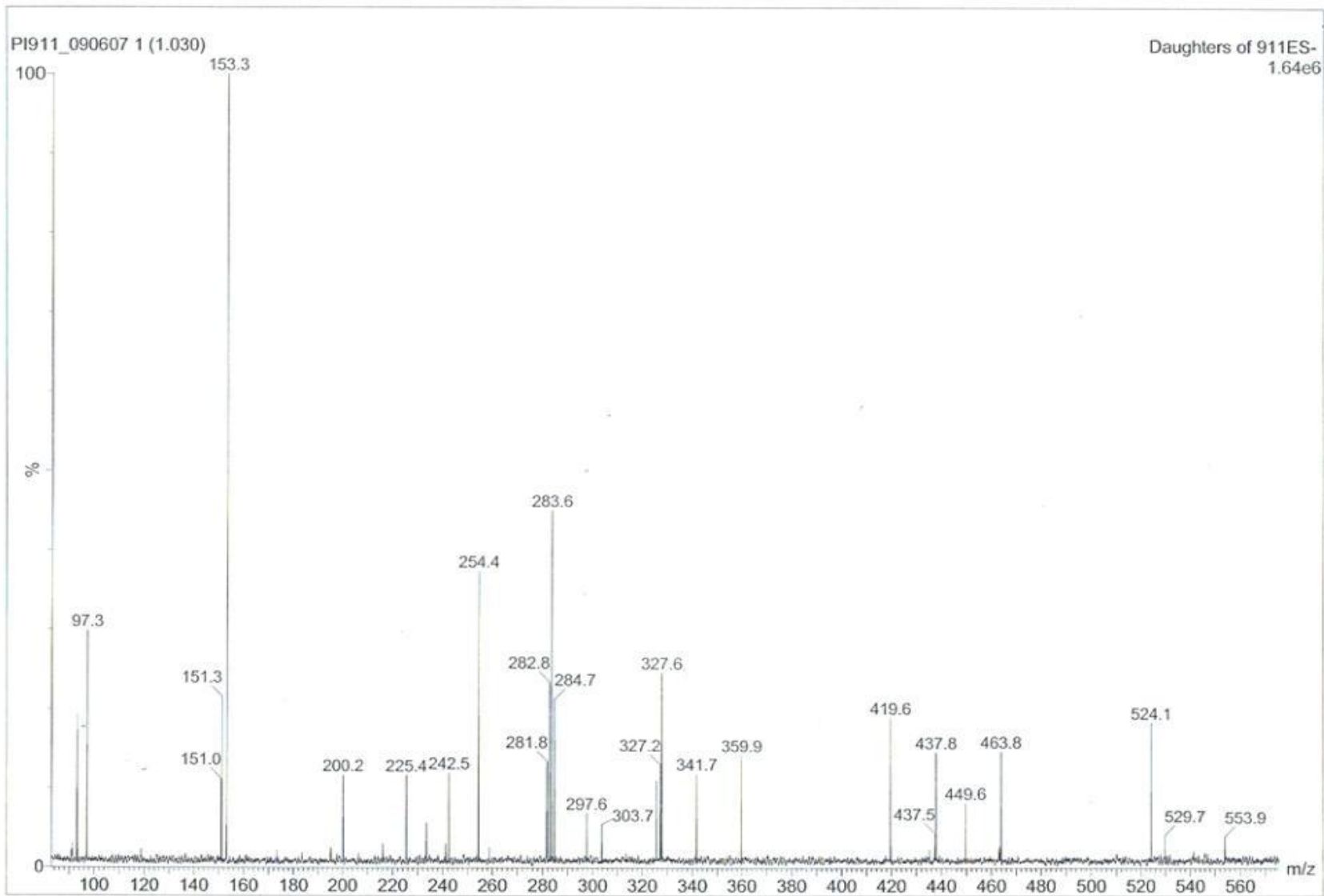


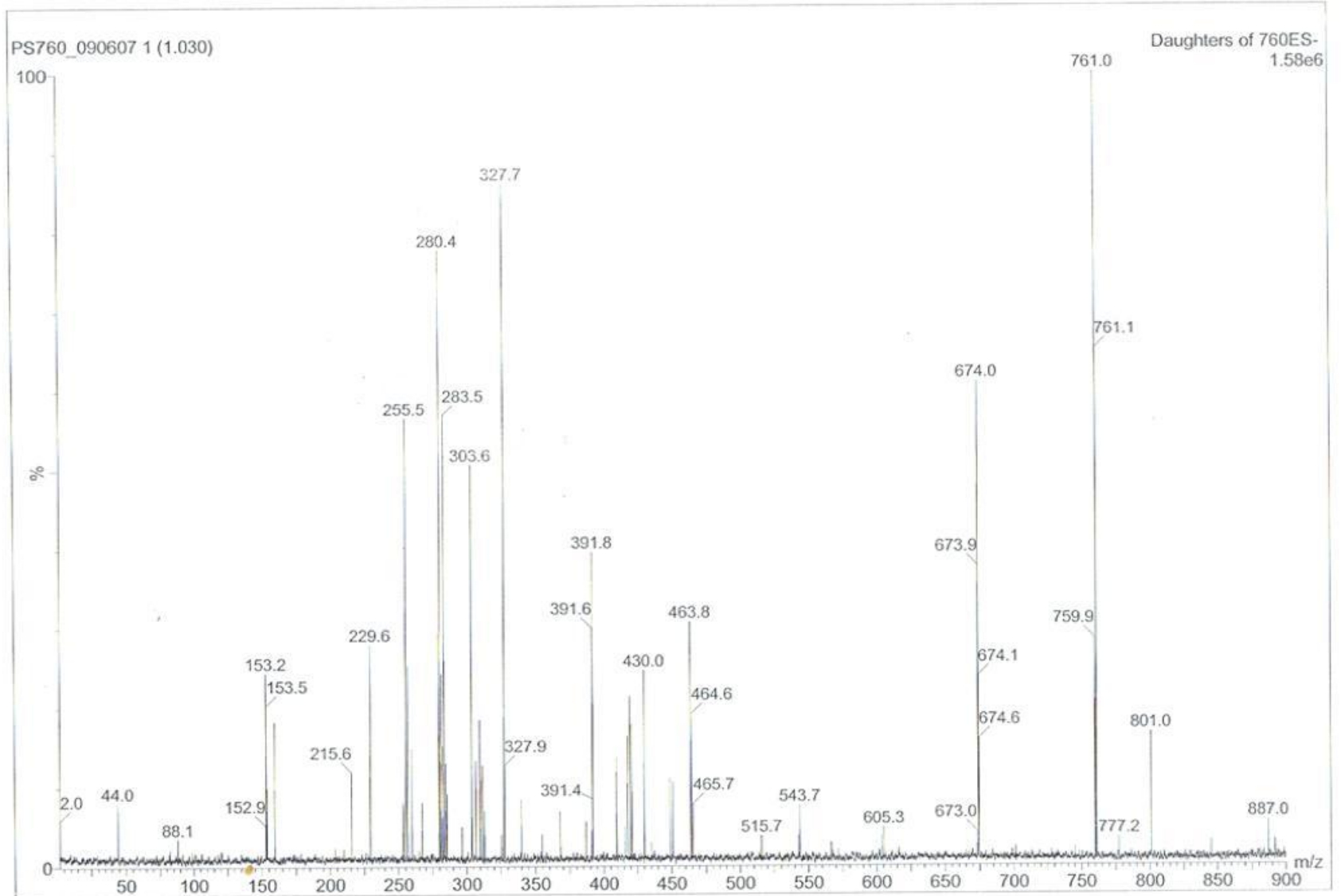
PI885_090607 1 (1.030)

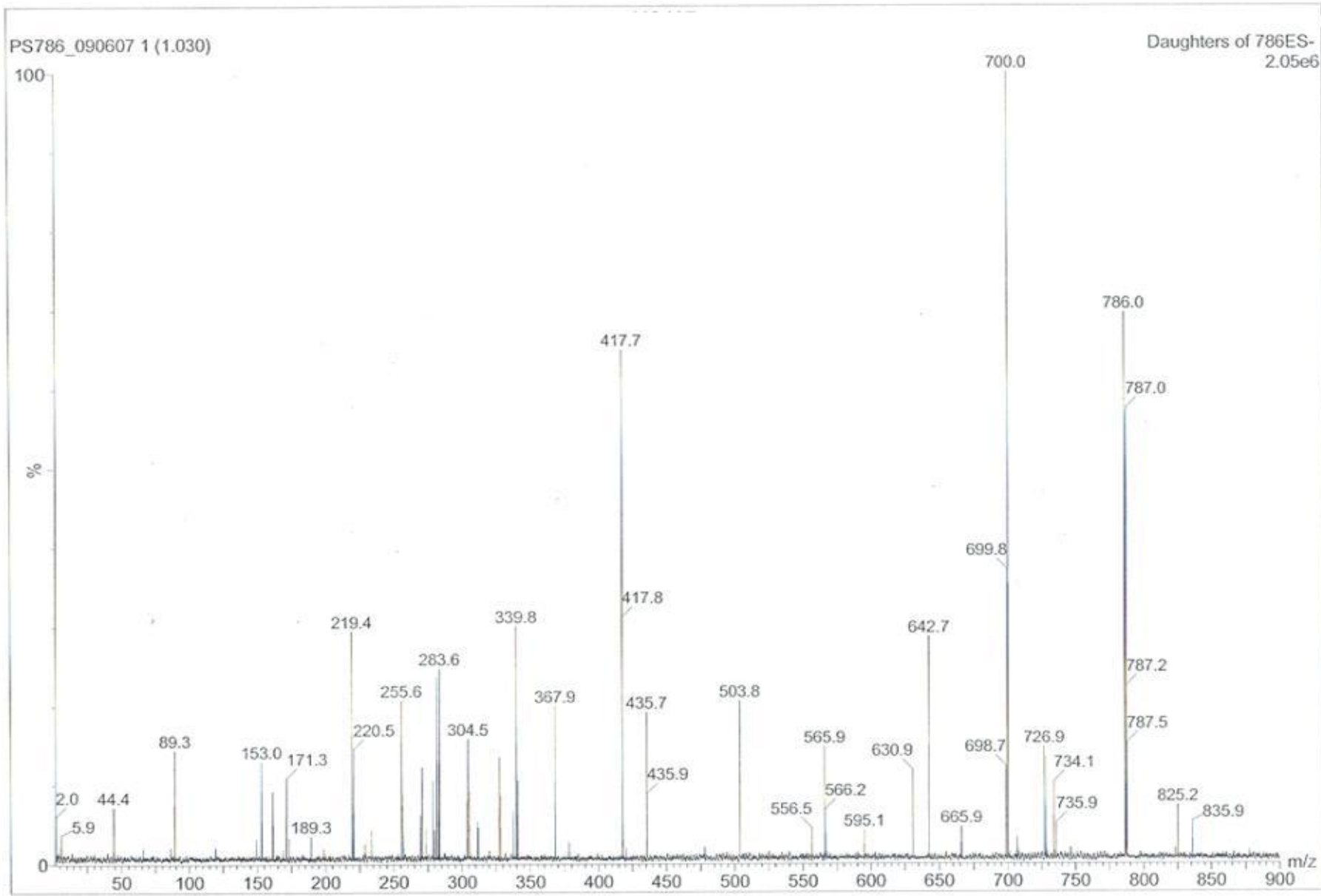
Daughters of 885ES-
5.40e6

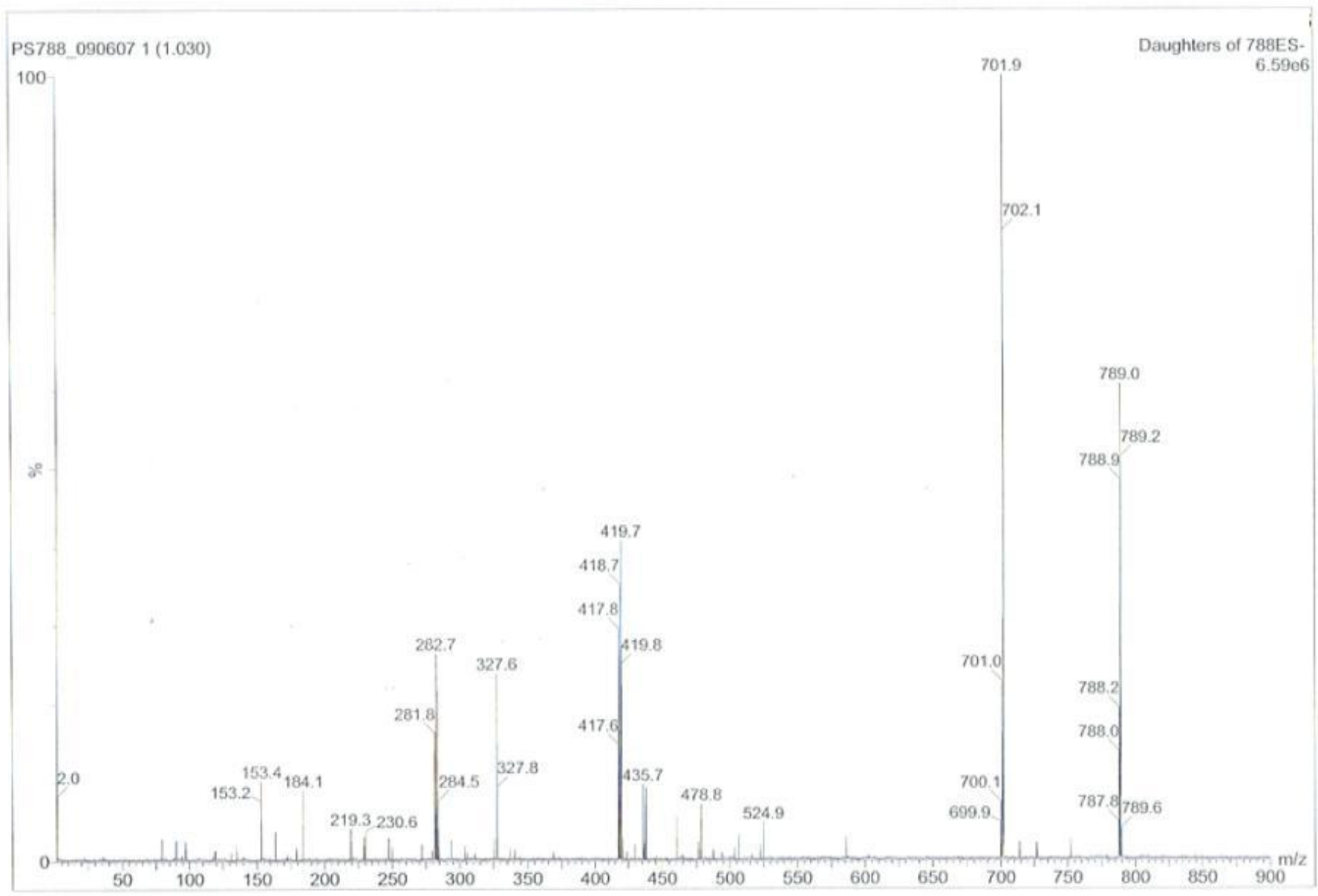


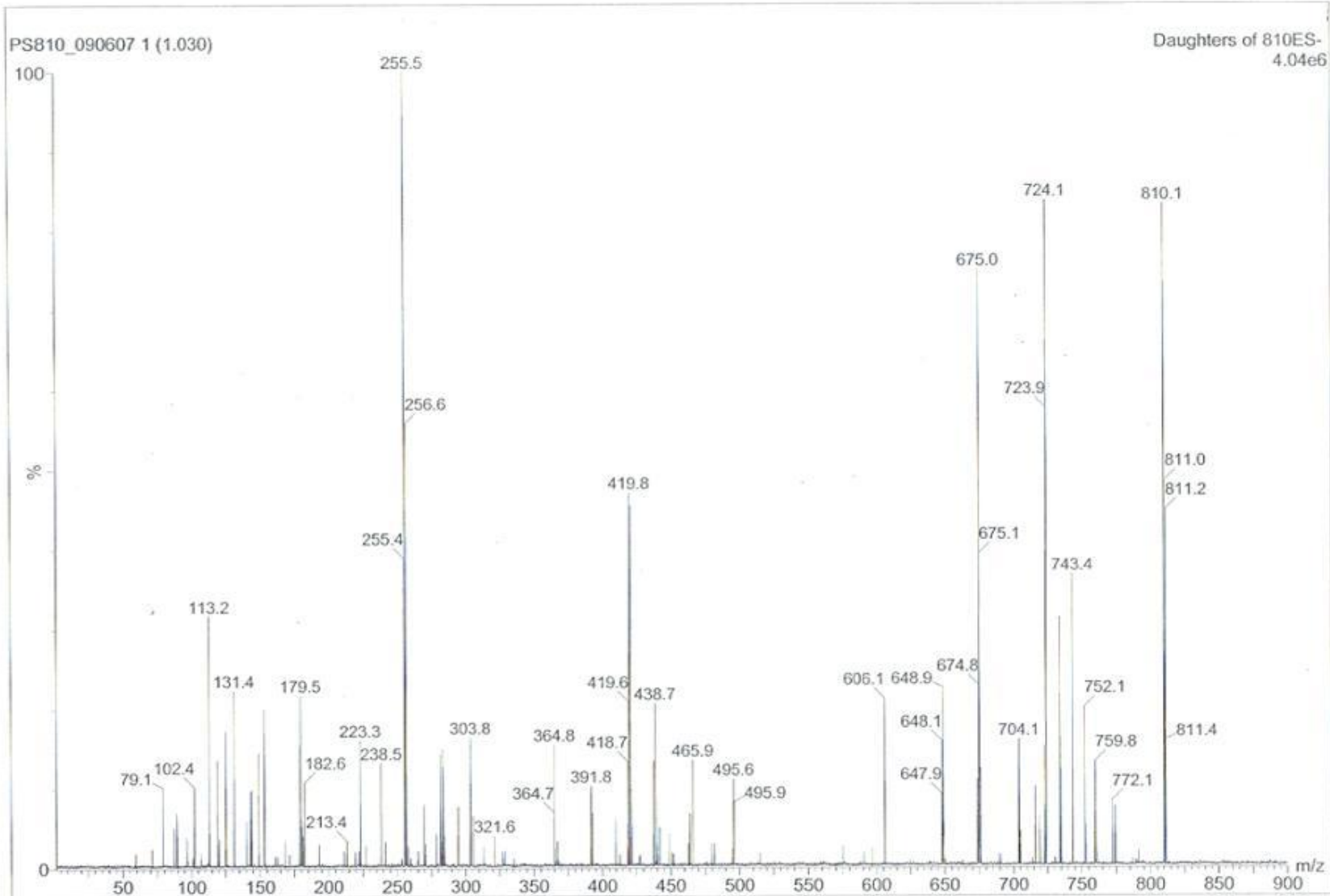


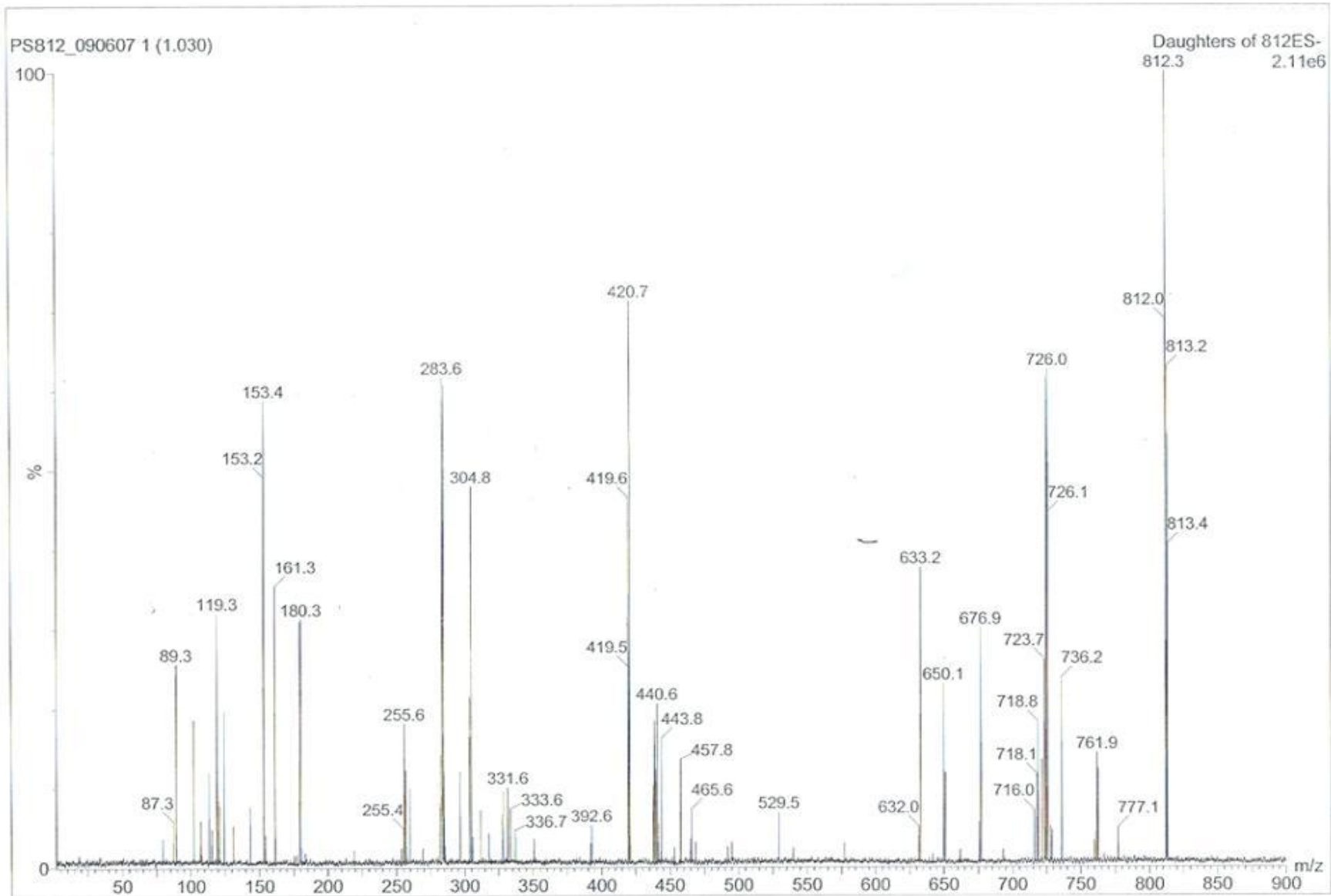


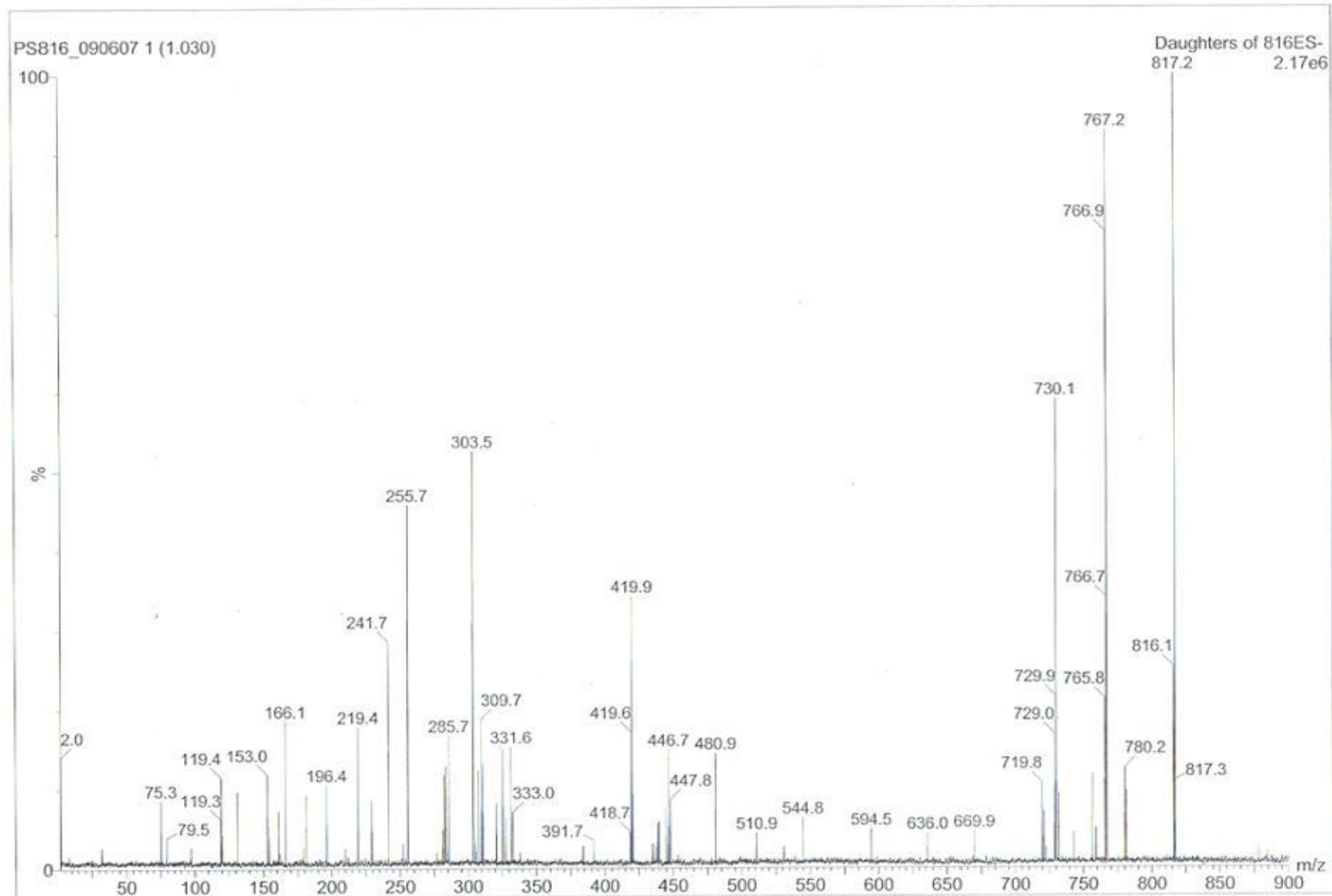






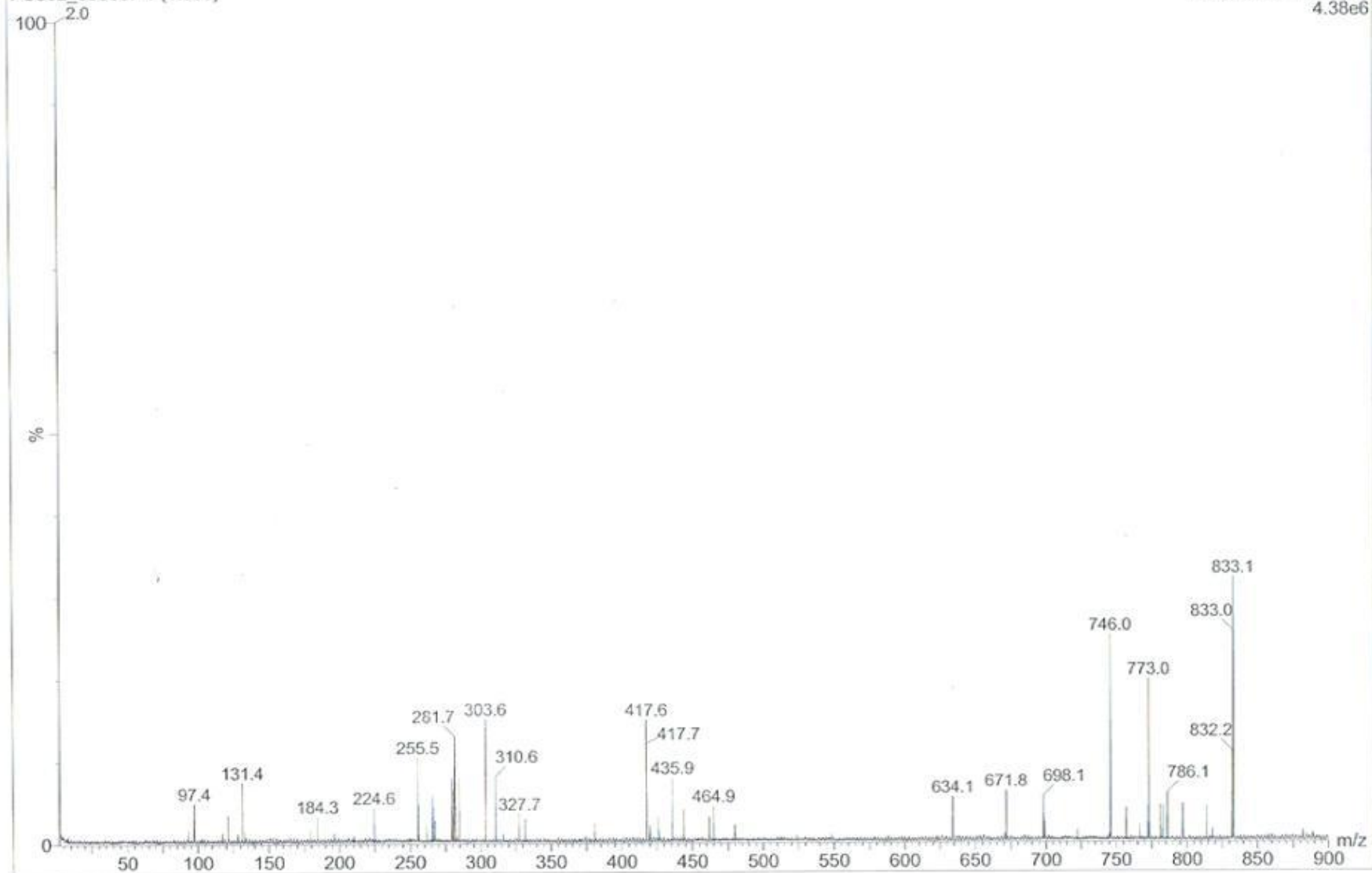


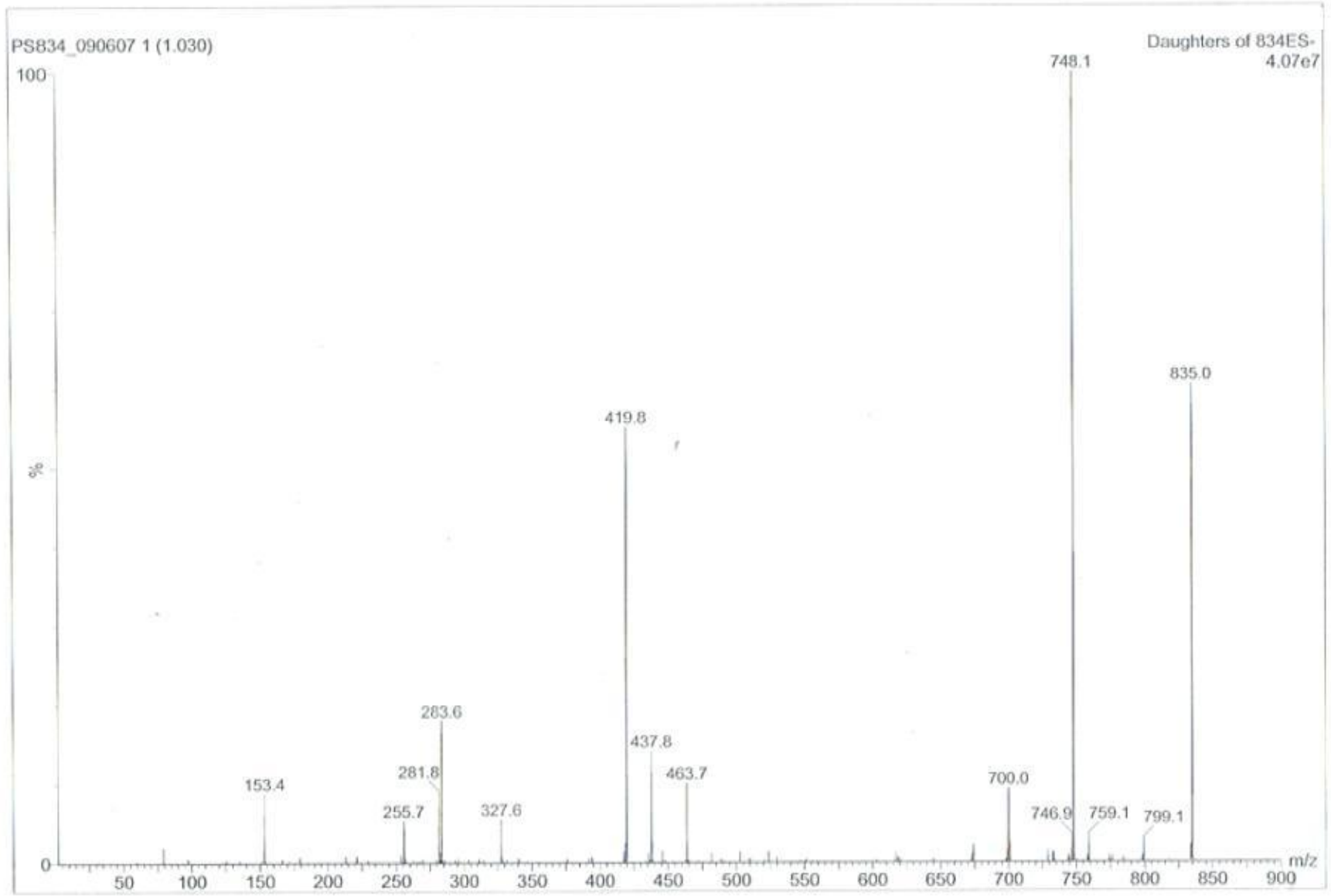


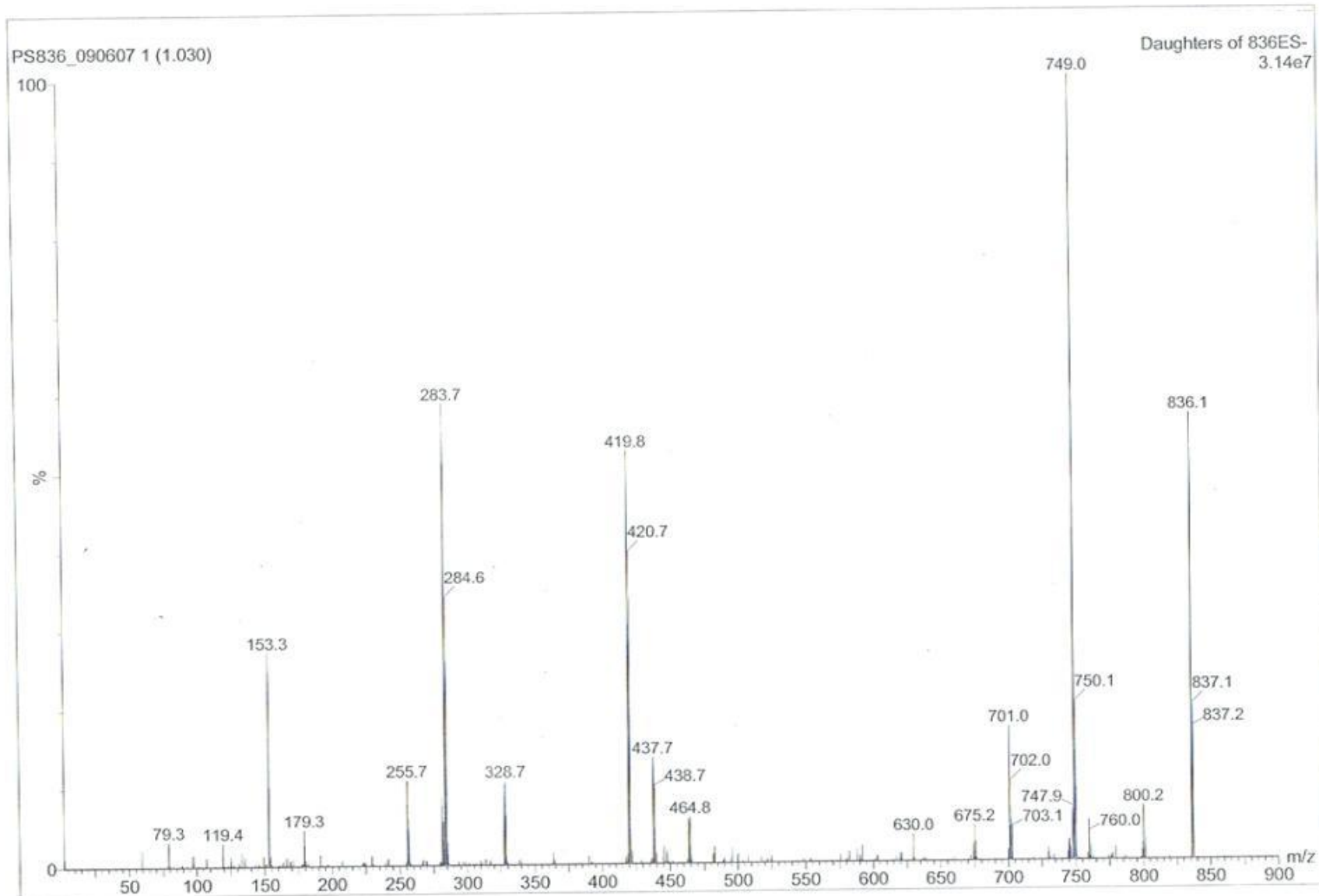


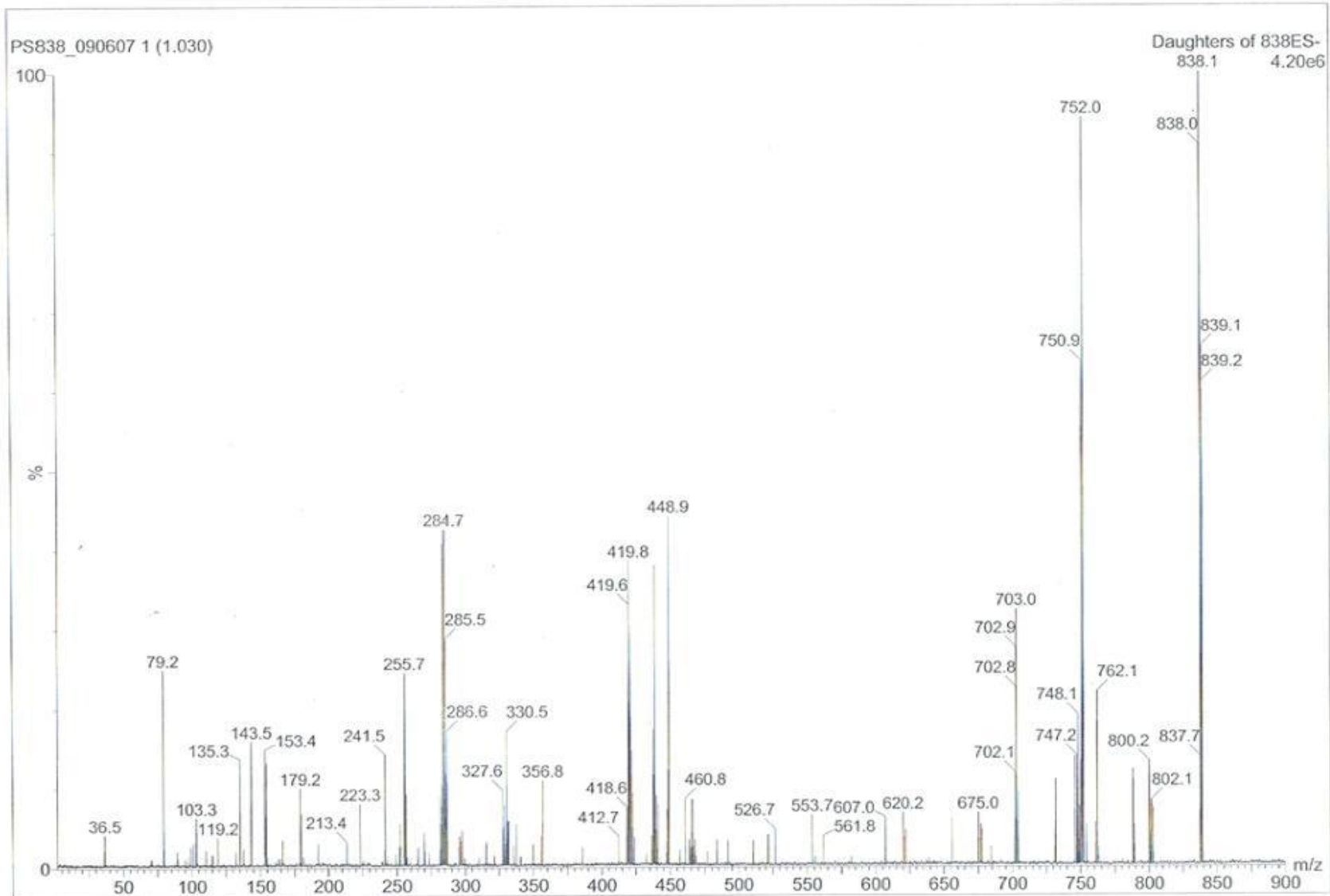
PS832_090607 1 (1.030)

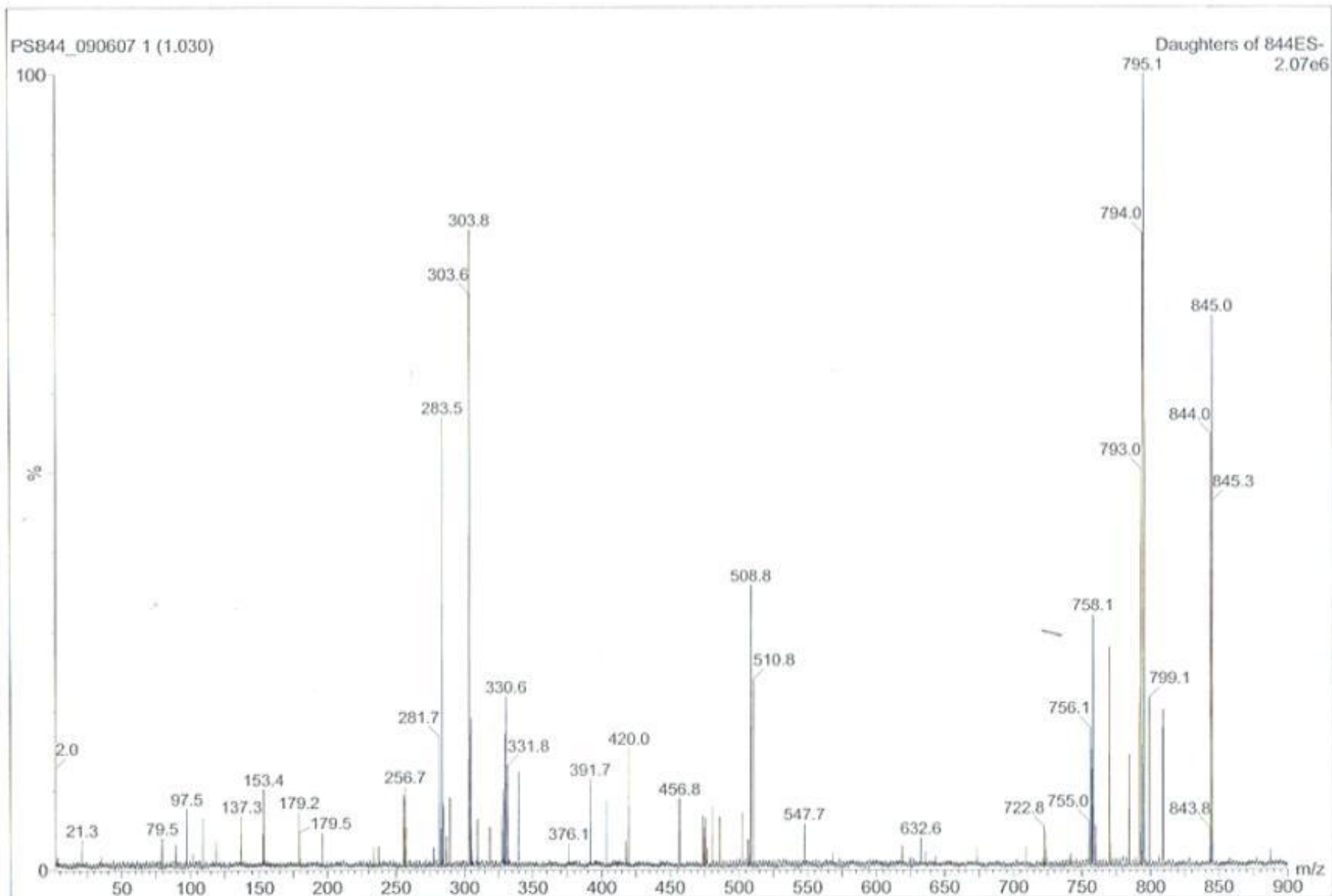
Daughters of 832ES-
4.38e6





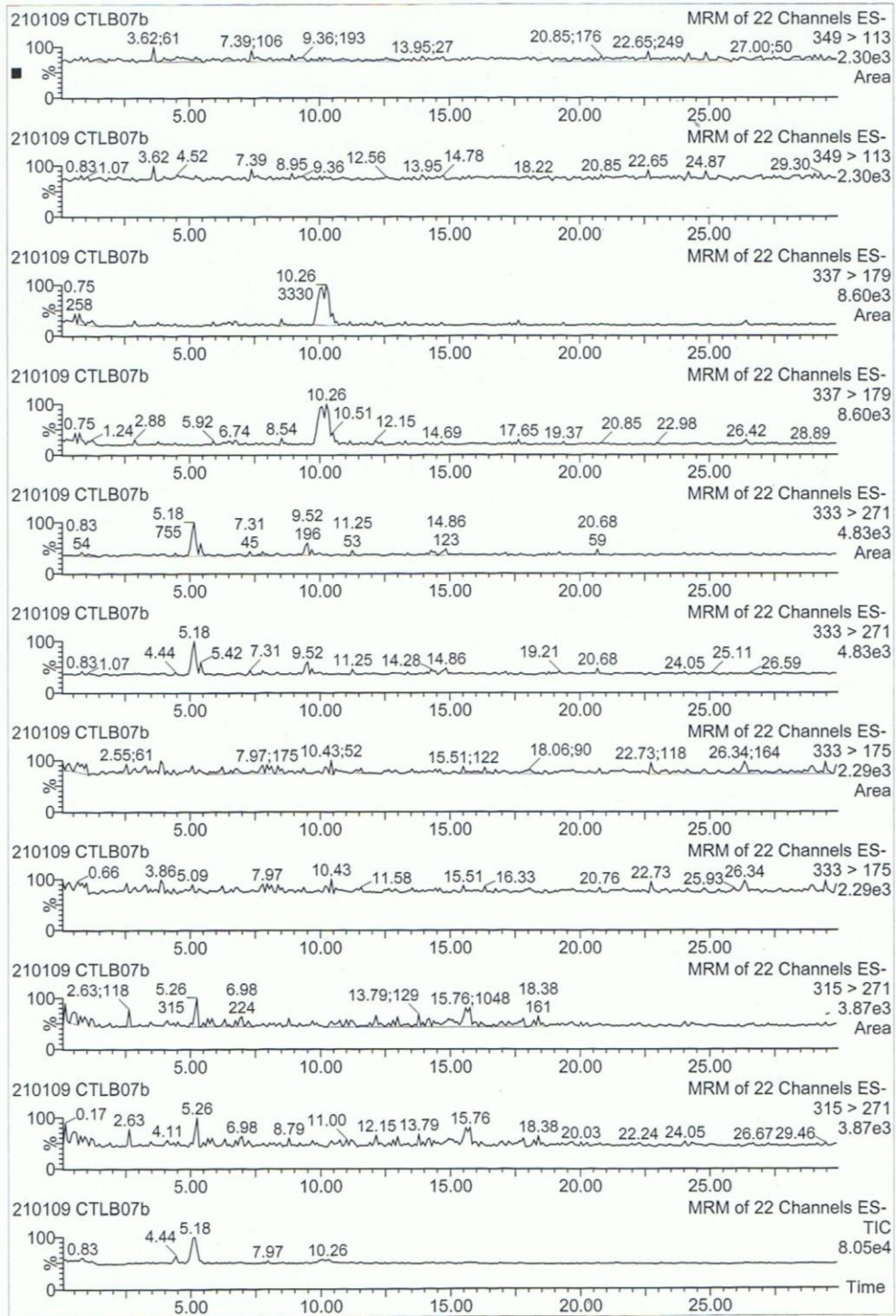


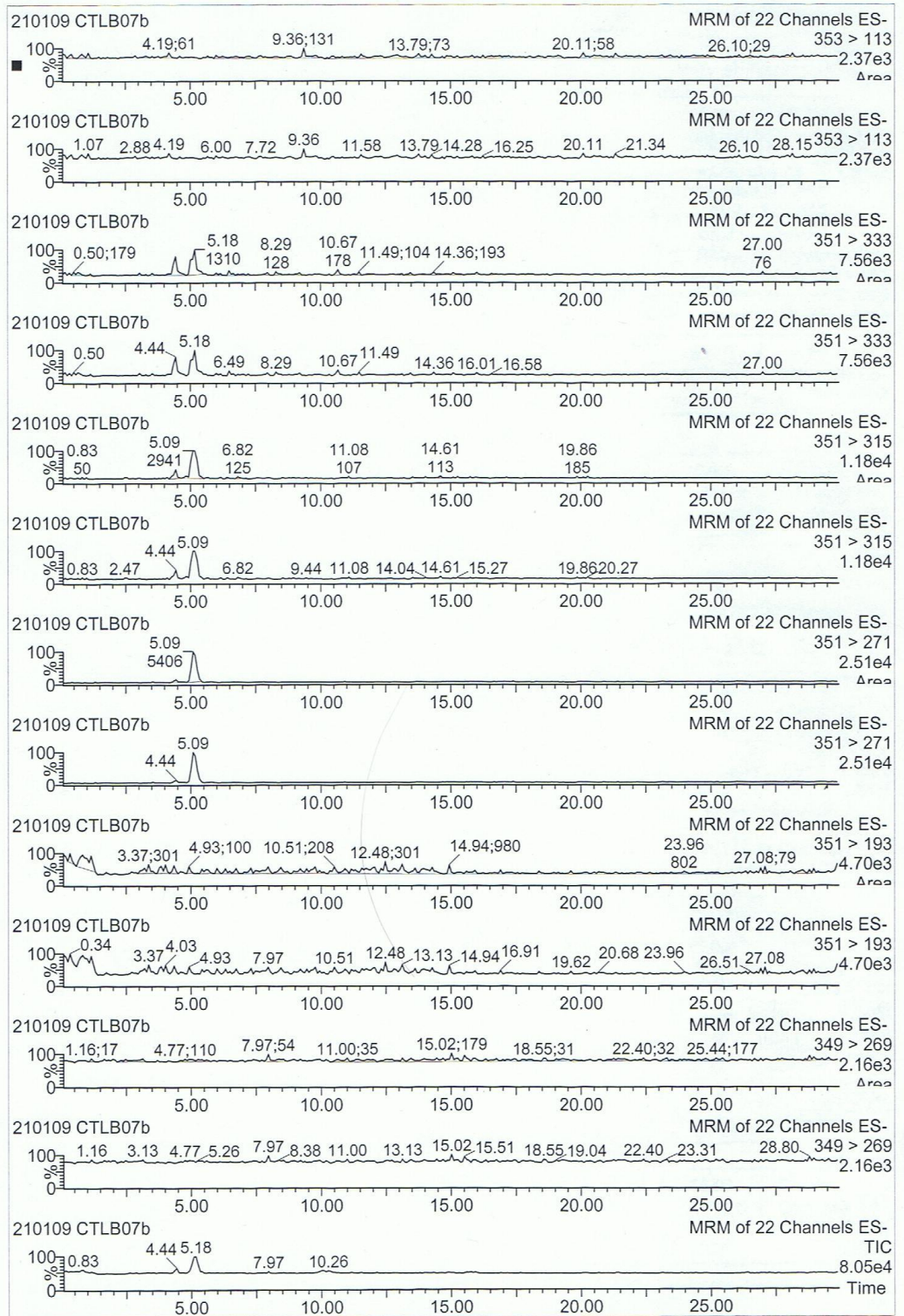


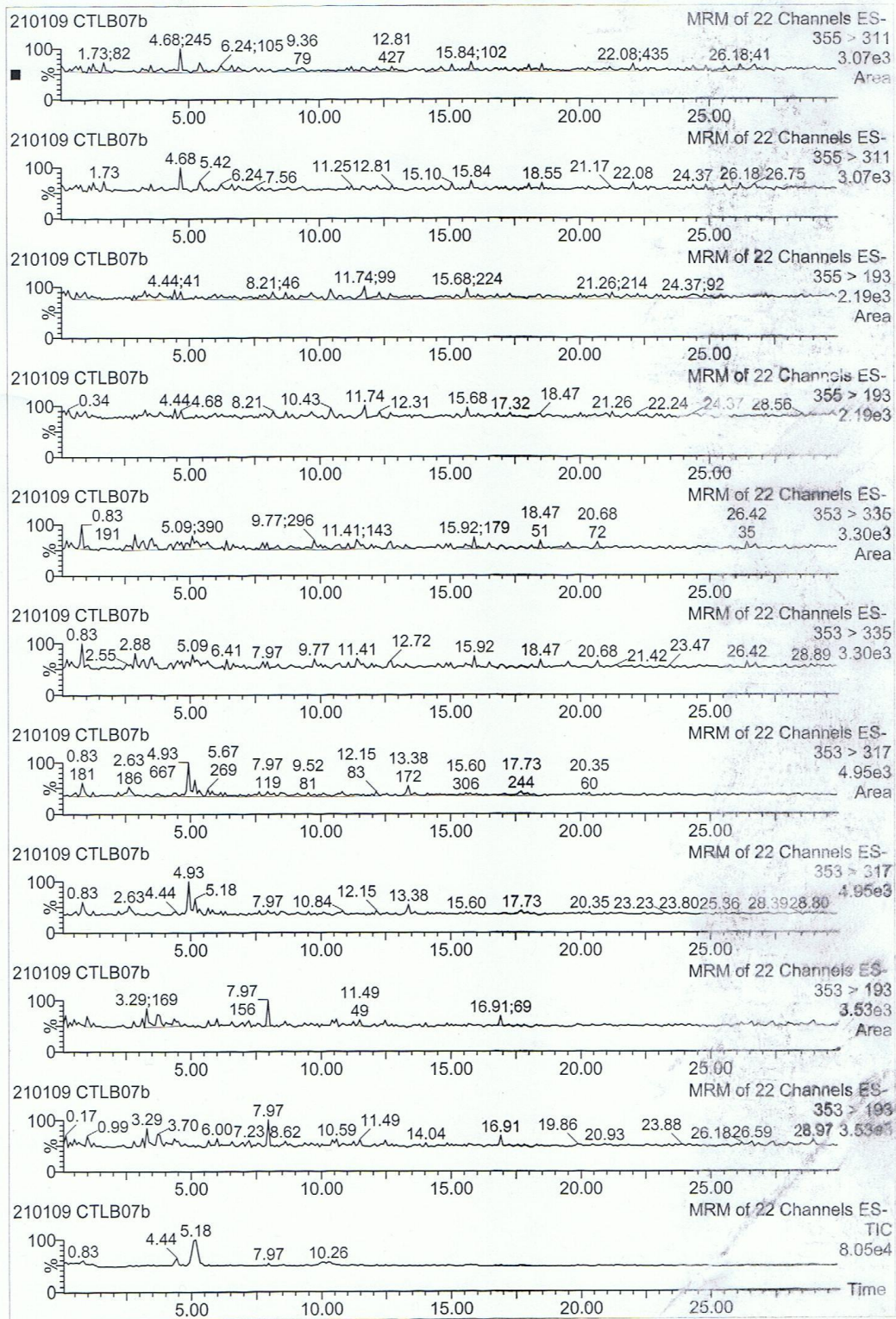


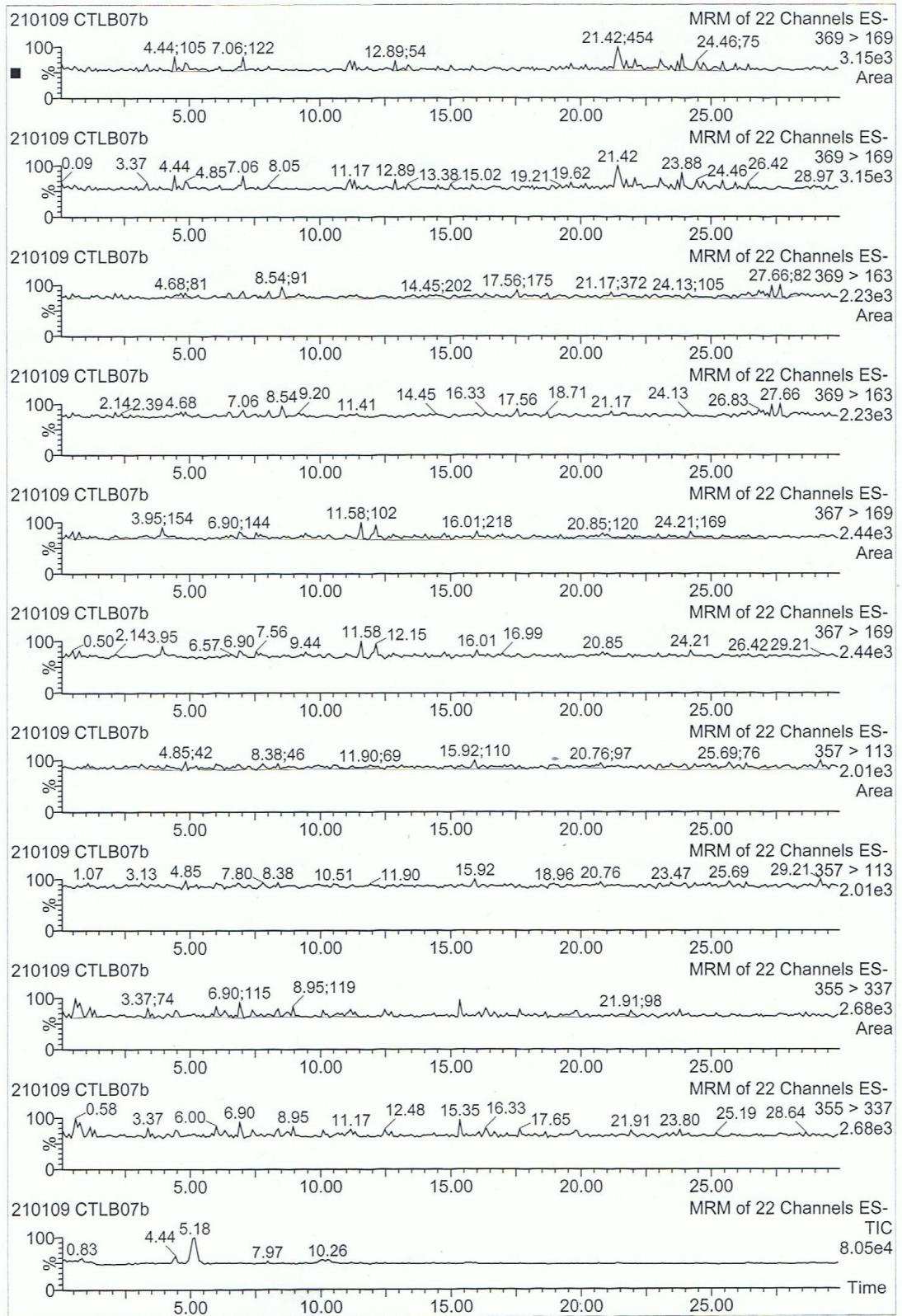
Appendix 2 - Lipid mediator analysis in mouse cerebral cortex using LC-MS/MS

Representative chromatograms of 22 MRM channels for naïve mouse cerebral cortex









Representative chromatograms of 22 MRM channels for naïve mouse cerebral plasma

